The oncogenic role of ATP-sensitive potassium ion (K_{ATP}) channels in human papillomavirus (HPV)-positive cancer cells

James Alexander Scarth

Submitted in accordance with the requirements for the degree of

Doctor of Philosophy

The University of Leeds

School of Molecular and Cellular Biology

Astbury Centre for Structural Molecular Biology

September 2022

The candidate confirms that the work submitted is his own and that appropriate credit has been given where reference has been made to the work of others.

Acknowledgements

'If a potato can become vodka, then I can become a doctor.'

I would like to express my upmost gratitude to my supervisor Prof Andrew Macdonald for his support and guidance throughout this PhD. He took a risk in taking on a naïve young scientist who had never before stepped foot in a tissue culture laboratory and wasn't quite sure what he was getting himself in for! His constant advice has helped shaped me and allowed me to grow as a researcher, ensuring I am appropriately prepared for a career in academia. I would also like to thank my co-supervisor Dr Adel Samson for his support, proofreading, and for co-ordinating the *in vivo* experiments. Thank you too to the University of Leeds for PhD scholarship funding, allowing me to undertake this research.

Thank you to all of the people I have worked with in Garstang 8.54, and latterly the Garstang 9 mega-lab, for creating an enjoyable and productive environment. Particular thanks to all present members of the Macdonald group: Molly Patterson, Corinna Brockhaus, Joe Cogan, Kate Wang, Dr Yigen Li and Diego Barba Moreno, for making the lab an enjoyable place to be. A specific mention must go to Molly and Corinna: going through this four-year process alongside you has significantly eased the stress and torment caused! I know you will both go on to achieve great things and I wish you the best in your chosen careers. Thanks also to past members of the group, including Dr Michaella Antoni, Dr Ethan Morgan and Dr Chris Wasson, for many useful discussions and fun times in the pub! Ethan – you displayed immeasurable (and sometimes undeserved) patience when teaching me how to be a functioning researcher in the first year and I continue to look to you for guidance and advice.

Finally, I must thank all my family and friends for their support over the years. Particular thanks to my parents, Ian and Christine, for always being proud of me and without whom, none of this would have been possible.

Abstract

Persistent infection with high-risk human papillomaviruses (HPVs) is the causal factor in multiple human malignancies, including >99% of cervical cancers and a growing proportion of oropharyngeal cancers. Prolonged expression of the viral oncoproteins E6 and E7 is necessary for transformation to occur. Although some of the mechanisms by which these oncoproteins contribute to carcinogenesis are well-characterised, a comprehensive understanding of the signalling pathways manipulated by HPV is lacking.

This study demonstrates that the targeting of a host ion channel by HPV can contribute to cervical carcinogenesis. Through the use of pharmacological activators and inhibitors of ATP-sensitive potassium ion (K_{ATP}) channels, we reveal that these channels are active in HPV-positive cells and that this activity is necessary for HPV oncoprotein expression. Further, expression of SUR1, which forms the regulatory subunit of the multimeric channel complex, was found to be upregulated in a manner dependent on the E7 oncoprotein and likely involving the host transcription factor SP1. Importantly, knockdown of K_{ATP} channel subunits significantly impeded cell proliferation via induction of a G1 phase cell cycle arrest. This was confirmed both *in vitro* and in *in vivo* tumourigenicity assays. However, K_{ATP} channel activity was not found to be critical for the survival of HPV+ cancer cells. Mechanistically, it is proposed that the pro-proliferative effect of K_{ATP} channels is mediated via the activation of a MAPK/AP-1 signalling axis. Finally, the significance of K_{ATP} channels in HPV+ oropharyngeal cancers was assessed. Surprisingly, it was discovered that, in contrast to cervical cancer, depletion of K_{ATP} channel subunits had little impact on HPV gene expression or cell proliferation.

Further research to undertake a complete characterisation of the role of K_{ATP} channels in all HPV-associated diseases is now warranted in order to determine whether the clinically available inhibitors of these channels could represent an effective therapeutic option.

Table of Contents

List of Figures

List of Tables

Abbreviations

%	Percent
~	Approximately
°C	Degrees Celsius
µg	Microgram
µL	Microlitre
µM	Micromolar
3'	3 prime
5'	5 prime
ABC	ATP-binding cassette
ADP	Adenosine diphosphate
ANO1/TMEM16A	Anoctamin-1/Transmembrane protein 16A
AP-1	Activator protein-1
APS	Ammonium persulphate
ASCC	Anal squamous cell carcinoma
ATF	cAMP-dependent transcription factor
ATM	Ataxia telangiectasia mutated
ATP	Adenosine triphosphate
ATR	Ataxia telangiectasia and Rad3-related
BAP31	B-cell-associated protein 31
BCA	Bicinchoninic acid
bHLH	Basic helix-loop-helix
BLAST	Basic local alignment search tool
bp	Base pairs
BPV	Bovine papillomavirus
BRCA1	Breast cancer type 1 susceptibility protein
BRD4	Bromodomain-containing protein 4
BSA	Bovine serum albumin
Ca^{2+}	Calcium ion
$CaCl_2$	Calcium chloride
cAMP	Cyclic adenosine monophosphate
CBM	Cyclin binding motif

CBP	CREB-binding protein
c-CBL	Casitas B-lineage lymphoma
CDK	Cyclin dependent kinase
CFTR	Cystic fibrosis transmembrane conductance regulator
cGAS	Cyclic GMP-AMP synthase
CHI	Congenital hyperinsulinism
ChIP	Chromatin immunoprecipitation
CIN	Cervical intraepithelial neoplasia
CKII	Casein kinase II
CO_2	Carbon dioxide
CR	Conserved region
CREB	cAMP response element-binding protein
CRISPR	Clustered regularly interspaced short palindromic repeats
cryo-EM	Cryogenic electron microscopy
CS	Cantu syndrome
CUL2	Cullin 2
CXCL14	Chemokine (C-X-C motif) ligand 14
ddH_2O	Double distilled water
DDR	DNA damage response
$DiBAC_4(3)$	Bis-(1,3-Dibutylbarbituric Acid) Trimethine Oxonol
DLG1	Discs large homolog 1
DMEM	Dulbecco’s Modified Eagle's Medium
DMSO	Dimethyl sulfoxide
DNA	Deoxyribonucleic acid
dNTP	Deoxyribonucleoside triphosphate
DREAM	Dimerization partner, pRb-like, E2F and multi-vulval class B
DUSP	Dual specificity protein phosphatase
E6AP	E6-associated protein
Eag	Ether-a-go-go
ECL	Enhanced chemiluminescence
ECM	Extracellular matrix
EDTA	Ethylenediaminetetraacetic acid
EF-1α	Elongation factor 1-alpha

eGFP	Enhanced green fluorescent protein
EGFR	Epidermal growth factor receptor
EMEM	Eagle's Minimum Essential Medium
EMT	Epithelial to mesenchymal transition
EMT-TF	EMT-activating transcription factor
ER	Endoplasmatic reticulum
ERK1/2	Extracellular signal-regulated kinase 1/2
EV	Epidermodysplasia verruciformis
FACS	Fluorescence-activated cell sorting
FADD	Fas-associated protein with death domain
FBS	Foetal bovine serum
FDA	Food and Drug Administration
FEH	Focal epithelial hyperplasia
FHV	Flock house virus
FITC	Fluorescein isothiocyanate
FOXA2	Forkhead box protein A2
FOXM1	Forkhead box protein M1
g	Gram
GAPDH	Glyceraldehyde 3-phosphate dehydrogenase
GEO	Gene Expression Omnibus
GFP	Green fluorescent protein
GLUT1	Glucose transporter 1
GPCR	G protein-coupled receptor
H_2O_2	Hydrogen peroxide
HA	Haemagglutinin
HDAC	Histone deacetylase
HEPES	4-(2-hydroxyethyl)-1-piperazineethanesulfonic acid
HIF-1α	Hypoxia-inducible factor 1-alpha
HLA	Human leukocyte antigen
HNSCC	Head and neck squamous cell carcinoma
HOK	Human oral keratinocyte
HPV	Human papillomavirus
HPV-	HPV negative

HPV+	HPV positive
HPV16+	HPV16 positive
HRE	Hypoxia response element
HR-HPV	High-risk HPV
H-score	Histology score
HSIL	High-grade squamous intraepithelial lesion
HSPG	Heparin sulphate proteoglycan
ICTV	International Committee on Taxonomy of Viruses
IFN	Interferon
IgG	Immunoglobulin G
IHC	Immunohistochemistry
IL6	Interleukin 6
IP	Immunoprecipitation
IRF	Interferon regulatory factor
ISG	Interferon-stimulated gene
JAK	Janus kinase
JNK1/2	cJun N-terminal kinase 1/2
K^+	Potassium ion
K2P	Two-pore domain potassium ion channel
K_2SO_4	Potassium sulphate
K_{ATP}	ATP-sensitive potassium ion channel
kb	Kilobase pairs
K_{Ca}	Calcium-activated potassium ion channel
KCl	Potassium chloride
KDM	Lysine-specific demethylase
KGFR	Keratinocyte growth factor receptor
Kir	Inward-rectifying potassium ion channel
KLK8	Kallikrein-8
L	Litre
LB	Luria-Bertani
LLETZ	Large loop excision of the transformation zone
LMIC	Low- and middle-income countries
LSIL	Low-grade squamous intraepithelial lesion

M	Molar
MAPK	Mitogen-activated protein kinase
MEK1/2	Mitogen-activated protein kinase kinase 1/2
mg	Milligram
Mg^{2+}	Magnesium ion
MHC	Major histocompatibility complex
min	Minutes
miRNA	MicroRNA
mL	Millilitre
mM	Millimolar
mm	Millimetre
MMP	Matrix metalloproteinase
mRNA	Messenger RNA
MSK1/2	Mitogen- and stress-activated protein kinase 1/2
mTORC1	Mammalian target of rapamycin complex 1
MTT	3-(4,5-dimethylthiazol-2-yl)-2,5-diphenyltetrazolium bromide
NaCl	Sodium chloride
NBD	Nucleotide binding domain
NBS	Nucleotide binding site
NDM	Neonatal diabetes mellitus
NEAA	Non-essential amino acids solution
NES	Nuclear export signal
NF1	Neurofibromin 1
NF-κB	Nuclear factor kappa-light-chain-enhancer of activated B cells
ng	Nanogram
NLS	Nuclear localisation signal
nM	Nanomolar
nm	Nanometre
NSCLC	Non-small cell lung cancer
Oct1	Octamer transcription factor 1
OD	Optical density
ORF	Open reading frame

ori	Origin of replication
PAE	Polyadenylation site (early)
PAL	Polyadenylation site (late)
Pap	Papanicolaou
PARP	Poly (ADP-ribose) polymerase
PBM	PDZ binding motif
PBS	Phosphate-buffered saline
PcG	Polycomb group
PCR	Polymerase chain reaction
PDZ	PSD-95/DLG/ZO-1
PI	Propidium iodide
PI3K	Phosphoinositide 3-kinase
PIP_2	Phosphatidyl-inositol 4,5-bisphosphate
PIPES	Piperazine-N,N′-bis(2-ethanesulfonic acid)
PKA	Protein kinase A
PKC	Protein kinase C
PLC	Phospholipase C
PML	Promyelocytic leukaemia
PMSF	Phenylmethylsulphonyl fluoride
pRb	Retinoblastoma protein
PRR	Pattern recognition receptor
PS	Phosphatidylserine
p-TEFb	Positive transcription elongation factor
PTPN14	Protein tyrosine phosphatase non-receptor type 14
PV	Papillomavirus
qPCR	Quantitative PCR
RIG-I	Retinoic acid-inducible gene I
RIPA	Radioimmunoprecipitation assay
RNA	Ribonucleic acid
ROS	Reactive oxygen species
RRM2	Ribonucleoside-diphosphate reductase subunit M2
RRP	Recurrent respiratory papillomatosis
RSEM	RNA-Seq by Expectation-Maximization

RT	Room temperature
RT-qPCR	Reverse transcription-quantitative PCR
SCC	Squamous cell carcinoma
SCID	Severe combined immunodeficient
SD	Standard deviation
SDS	Sodium dodecyl sulphate
SDS-PAGE	SDS polyacrylamide gel electrophoresis
sec	Seconds
shNTC	Non-targetting control shRNA
shRNA	Short hairpin RNA
SIAH1	Seven in absentia homologue 1
siRNA	Small interfering RNA
SKCa	Small conductance calcium-activated potassium ion channel
SNX	Sorting nexin
SP1	Specificity protein 1
STAT	Signal transducer and activator of transcription
STING	Stimulator of interferon genes
STK4	Serine/threonine kinase 4
STS	Staurosporine
SUR	Sulfonylurea receptor
SV40	Simian virus 40
TAE	Tris-acetate-EDTA
TBP	TATA-binding protein
TBS-T	Tris-buffered saline - Tween20
TCGA	The Cancer Genome Atlas
TEA	Tetraethylammonium
TEMED	Tetramethylethylenediamine
TERT	Telomerase reverse transcriptase
TGN	*trans*-Golgi network
TIF	Tagged image file
TLR9	Toll-like receptor 9
TMC	Transmembrane channel-like protein
TMD	Transmembrane domain

TNFR1	Tumour necrosis factor receptor 1
TopBP1	DNA topoisomerase II binding protein 1
TRAIL	TNF-related apoptosis-inducing ligand
TSS	Transcription start site
TWIST1	Twist-related protein 1
TYK2	Non-receptor tyrosine kinase 2
UK	United Kingdom
URR	Upstream regulatory region
USF	Upstream stimulatory factor
USP	Ubiquitin specific peptidase
UV	Ultraviolet
V	Volt
v/v	volume/volume
VLP	Virus-like particle
w/v	weight/volume
WT	Wildtype
YAP1	Yes-associated protein 1
YY1	Yin Yang 1
ZEB1	Zinc finger E-box-binding homeobox 1
α	Alpha
β	Beta
γ	Gamma
μ	Mu
ν	Nu

Chapter 1 Introduction

1.1 Papillomaviridae

The *Papillomaviridae* is an ancient family of non-enveloped viruses consisting of a double-stranded DNA genome [1]. To date, over 400 papillomavirus (PV) isolates have been reported in a wide variety of fish, reptiles, birds and mammals, including over 200 different human papillomaviruses (HPVs) [1, 2]. Classification of PVs is based upon comparisons of the nucleotide sequence of the *L1* gene, encoding the major capsid protein, as this is the most well-conserved between types. A genome-based classification system, which differs from that of the International Committee on Taxonomy of Viruses (ICTV), is used for PVs due to the difficulties in establishing culture systems to propagate the viruses. Further, PVs fail to induce a robust antibody response, thus precluding a serology-based classification [3]. Within the *Papillomaviridae*, PVs are first classified into genera (of which there are over 50) and then into species groups which share similar biological properties. To be classified as a new 'type', the DNA sequence of a new L1 ORF must differ by at least 10% from any other PV type [3, 4]. In comparison, types from different genera within the *Papillomaviridae* share <60% *L1* sequence identity, whilst types in different species within the same genus can display up to 70% sequence similarity [4, 5].

The PVs which infect humans are classified into five different genera: Alpha (α), Beta (β), Gamma (γ), Mu (μ) and Nu (ν) (**Fig 1.1**). Of these, the γ-genus is the largest (containing 98 HPV types), whilst both the α- and β-genera contain over 50 types [5]. HPV types of the α-genus are the most well-studied as they have the highest clinical significance. These viruses mainly infect mucosal epithelial sites and include the 15 virus types (such as HPV16, 18 and 31) associated with a risk of developing anogenital and oropharyngeal cancers [6]. These viruses are

therefore designated as ‘high-risk’. The genus also contains ‘low-risk’ viruses (such as HPV6 and 11, members of the αPV-10 species) that are associated with benign hyperproliferative lesions in the mucosal epithelium [7]. HPVs of the β-genus typically infect cutaneous epithelia and are linked to the development of benign warts, although are suspected to be associated with the development of non-melanoma skin carcinoma in combination with ultraviolet (UV) radiation [8]. HPVs of the remaining three genera generally only cause benign disease.

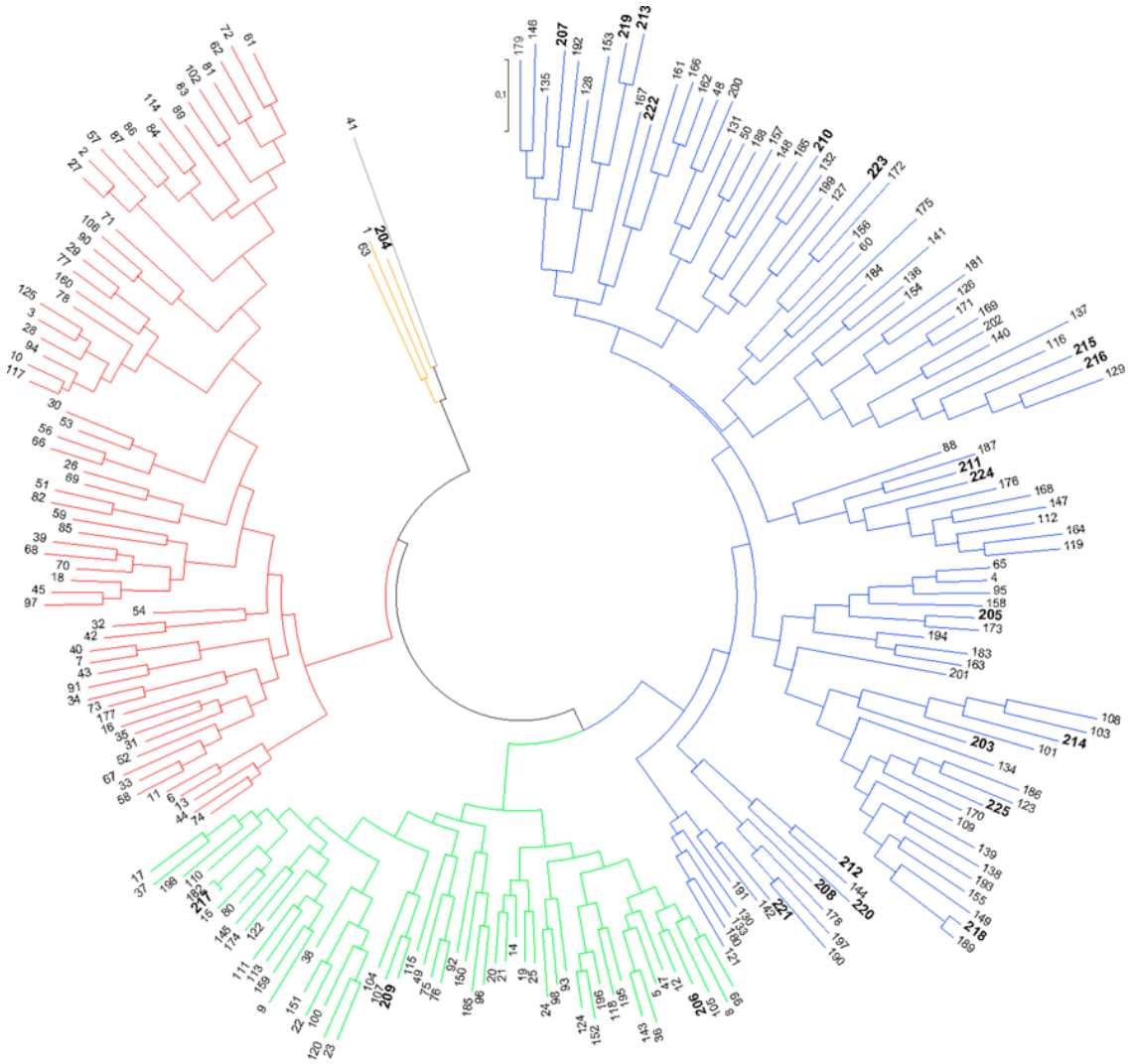

Figure 1.1 Phylogenetic tree displaying the currently-recognised HPV types. Alpha, beta, gamma, mu and nu papillomaviruses are presented in red, green, blue, orange and grey colours respectively. Phylogeny is based upon sequence identity of the L1 gene. Taken from [5].

1.2 HPV transmission

HPV is one of the most common sexually transmitted infections in the world [9]. The primary route of mucosal infection is via sexual intercourse. Direct skin-to-skin contact is required, although penetration is not necessarily a prerequisite [7]. The use of condoms is thought to reduce the risk of infection, although transmission can still occur via contact with unprotected genital skin areas [10]. Further, indirect transmission has also been reported, such as that caused by sharing towels with infected individuals [11]. Indeed, non-sexual transmission can also occur by kissing or genital scratching [12]. Vertical transmission of HPV from mother to child, either *in utero* via the placenta or perinatally during delivery, is also possible [12]. For an infection to then be established, the virus must gain access to the basal layer of the epithelium via microlesions [13].

Transmission of cutaneous HPV occurs via shedding of the virus with desquamated epithelial cells. For a new infection to be established, either direct person-to-person contact or indirect contact with contaminated surfaces such as flooring, socks and shoes is required [14]. Transmission is particularly common in children and adolescents, perhaps due to increased physical contact and poorer handwashing practice [11]. The presence of rough surfaces, such as those near swimming pools, can increase shedding of infected keratinocytes and thus promote transmission [11]. As with mucosal HPVs, the virus must gain access to the basal epithelial layer in order to establish an infection.

1.3 HPV-associated disease

1.3.1 Cutaneous infections

The majority of cutaneous infections are caused by HPVs of the β- and γ-genera which are widely present on the skin of normal individuals [11]. Some HPVs from

the α-genus (such as HPV2, 3 and 10) have also been shown to infect the cutaneous epithelium. Infections with these viruses can result in the development of benign warts, particularly in young children and immunosuppressed individuals [13]. The warts are characterised by hypertrophy of all layers of the epithelium, which results in thickening (acanthosis) and folding (papillomatosis) of the skin as well as an increased thickness of the cornified layer (hyperkeratosis) [11].

Common warts can occur at multiple sites but are most often found on fingers and on the back of hands. They are most commonly caused by HPV types 2, 4 and 7. In contrast, flat warts (caused by infection with HPV3, 10 and 28) are much smaller and most often occur on the face and the backs of hands. Plantar warts (also known as verrucas) are frequently caused by HPV1, 2 and 4 and are located on the sole of the foot. As with other cutaneous infections, plantar warts are most commonly found in children and adolescents, with infection often occurring after barefoot activities. In the majority of cases, cutaneous warts only prove to be a minor inconvenience with spontaneous regression seen in 80% of cases within two years [15].

Interestingly, the rare autosomal recessive disorder epidermodysplasia verruciformis (EV) results in an increased susceptibility to infection with a subset of β-HPVs, particularly HPV5 and HPV8 [8]. The disease is characterised by cutaneous lesions resembling pityriasis versicolor which can progress to squamous cell carcinoma (SCC) at sites exposed to sunlight in a large proportion of individuals [8]. 75% of patients with the condition possess loss-of-function mutations in one of two genes (*EVER1* and *EVER2*, also known as *TMC6* and *TMC8* respectively) located on chromosome 17q25 [16]. The genes encode transmembrane channel-like proteins which are localised to the endoplasmic reticulum (ER) [17]. The exact function of the EVER proteins remains unclear,

although it has been suggested that they may aid in the regulation of intracellular zinc homeostasis, with the excess cytoplasmic zinc resulting from non-functional EVER proteins leading to the activation of the transcription factor AP-1 and increased viral replication [16]. Further, EV patients commonly display impaired T cell responses, perhaps indicating the *EVER* genes have additional immune-related functions.

Recent studies have also identified a potential role of β-HPVs in the development of SCC in non-EV individuals. Indeed, multiple studies have shown that viral DNA and antibodies specific for the L1 capsid protein are more frequently present in SCC patients compared to the general population [8]. Further, a meta-analysis demonstrated a significant association between the presence of five β-HPVs, including HPV5 and HPV8, and the development of SCC [18]. It is thought that β-HPVs act during the early stages of skin carcinogenesis, as HPV DNA is not always found in SCC lesions but is relatively common in actinic keratosis, the precursor lesion of SCC [19]. The current hypothesis is therefore that the actions of the E6 and E7 oncoproteins in promoting cell cycle progression during a productive infection in order to achieve viral DNA replication permits the accumulation of UV-induced DNA damage, thus leading to the inactivation of tumour suppressors or activation of host oncoproteins [8].

1.3.2 Mucosal infections

Infections at mucosal epithelial sites with α-HPVs are significantly more common than those at cutaneous sites, yet the majority are asymptomatic [11]. Anogenital warts (also known as condyloma acuminata) are the most common manifestation of a mucosal infection, over 90% of which are caused by HPV types 6 and 11 [20]. Indeed, it is estimated that 1% of the sexually active population present with clinically-apparent warts [21]. Productive virus replication is less efficient than in

cutaneous HPV infections but the virus is still highly transmissible, with the transmission rate between sexual partners estimated to be as high as 60% [11]. Spontaneous resolution of warts is common, with around 30% showing complete regression within four months but in cases of persistence, surgical removal of warts is often necessary [21].

HPV types 6 and 11 are also associated with the majority of recurrent respiratory papillomatosis (RRP) cases. This is a chronic disease characterised by the presence of benign lesions within the aerodigestive tract (most commonly in the larynx) which can occur in both adults and children [22]. The clinical course of the disease is unpredictable, varying from spontaneous regression to multiple cycles of recurrence. Infections in children and those with HPV11 are associated with increased disease severity and are more likely to require repeated rounds of surgery to remove lesions and prevent obstruction of the airway [22]. In rare cases, malignant transformation of the papillomas can occur [23].

Focal epithelial hyperplasia (FEH, also known as Heck's disease) is a similarly rare HPV-associated disorder found most frequently in women and children. It is thought that over 90% of cases are due to infection with either HPV13 or 32. The disease is characterised by the presence of multiple benign lesions on the oral mucosa, tongue or lips, with most cases displaying spontaneous regression in an average of 18 months [24].

In contrast, infection with a high-risk mucosal HPV can result in the development of malignant neoplasms at several anatomical sites. Indeed, HPV infection has been shown to be the contributing factor in almost all cancers of the cervix, anus and vagina; a subset of cancers of the vulva, penis and oropharynx; and a small proportion of laryngeal and oral cavity cancers (**Fig 1.2**) [6]. Currently, there are

15 HPV types considered to be high-risk – HPV16, 18, 31, 33, 35, 39, 45, 51, 52, 56, 58, 59, 68, 73, 82 – although HPV types 16 and 18 are responsible for the majority of malignancies [25]. Of the HPV-attributable cancers, cervical cancer has been by far the most widely-studied, with the causal link between HPV and cervical cancer first being established almost 40 years ago by Prof Harald zur Hausen, for which he was awarded the Nobel Prize in Physiology or Medicine [26]. Over 99% of cervical cancer cases are associated with high-risk HPV infection, with HPV16 responsible for ~55%, HPV18 for ~15%, and the remainder caused by the other high-risk HPVs [6].

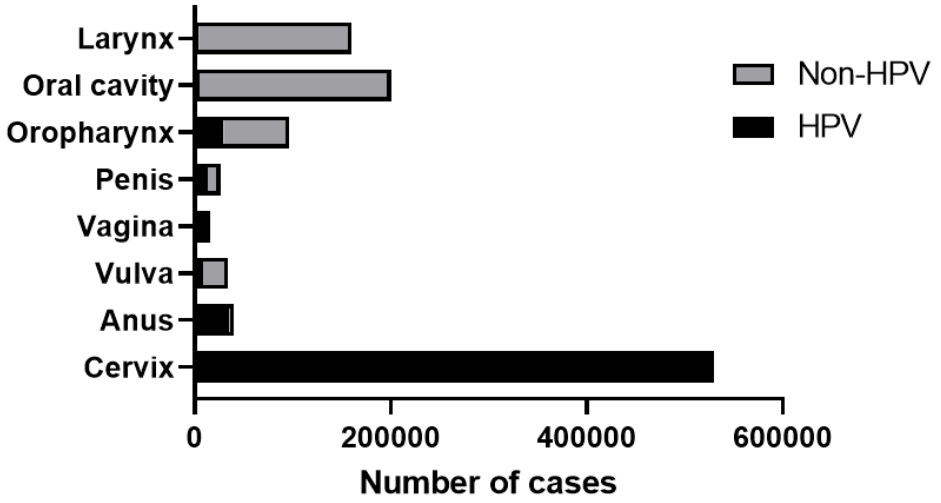

Figure 1.2 Number of HPV-attributable cancer cases worldwide per annum. Data is taken from [27] and listed by anatomical site.

However, carcinogenesis is not the default result of a high-risk HPV infection. In the vast majority of cases (~85%), high-risk HPVs will only cause a subclinical transient infection which is cleared over a period of a few months by the immune system [7]. Only in the event of a persistent infection, where the host immune response fails to detect and clear the virus efficiently, can transformation take place. Although even in this situation, cancer is a rare event and takes several years to occur.

Cervical disease, termed cervical intraepithelial neoplasia (CIN), is classified using a three-stage system based on the proportion of epithelium displaying abnormalities. More rarely, a two-stage system, consisting of low-grade and high-grade squamous intraepithelial lesions (LSIL and HSIL respectively), is also used. CIN1 (or LSIL) represents mild cervical dysplasia and indicates a transient HPV infection with a very low risk of progression [11]. In contrast, CIN2 and CIN3 (corresponding to HSIL) represent a persistent, abortive HPV infection with abnormal cells present more widely or throughout the cervical epithelium. Although some CIN3 lesions may still regress spontaneously, this represents the precursor to an invasive carcinoma [6].

Cervical cancers can also be classified by the anatomical site from which they arise. Around 80% of cervical cancers are SCCs and arise from cells within the transformation zone, whilst those associated with endocervical glands are known as adenocarcinomas and make up ~20%. Interestingly, HPV16 is more closely associated with SCC and HPV18 with adenocarcinomas, although the reasons for this apparent type-specific tropisms are poorly understood [28].

As stated above, high-risk HPVs can also cause cancers at other anogenital sites. This includes 25% of vulvar, almost 80% of vaginal, half of penile and close to 90% of anal cancers [27]. Compared to cervical cancer, a greater proportion of all of these anogenital malignancies are due to infection with HPV16.

HPV infection is also associated with the development of head and neck squamous cell carcinomas (HNSCCs). HNSCCs are a diverse group of tumours, and those which occur in the oropharynx, oral cavity and larynx can be linked to HPV infection. The proportion of HNSCCs attributable to HPV varies with anatomic site however, with over 30% of oropharyngeal cancers attributable to

HPV, but only ~2% of laryngeal and oral cavity cancers [27]. The other major aetiological agents of HNSCCs are smoking and excessive alcohol consumption, although the overall proportion of HPV-negative (HPV-) HNSCCs has decreased in recent years. The overwhelming majority (>95%) of HPV-positive (HPV+) HNSCCs are due to HPV16 infection, but HPV types 18, 31, 33 and 35 can also be detected [29].

1.4 HPV epidemiology

The global prevalence of HPV infection at any one time is considered to be approximately 11-12%, although there is significant regional variation [30]. In general, less well-developed countries display higher rates of HPV infection, with particularly high prevalence observed in Eastern Africa and the Caribbean where infection rates can exceed 30%. Furthermore, it is thought that over 80% of both men and women will contract HPV during their lifetimes [31]. As such, HPV-associated diseases have a high impact worldwide. Indeed, it has been estimated that 4.5% of all cancers worldwide can be attributed to HPV [27].

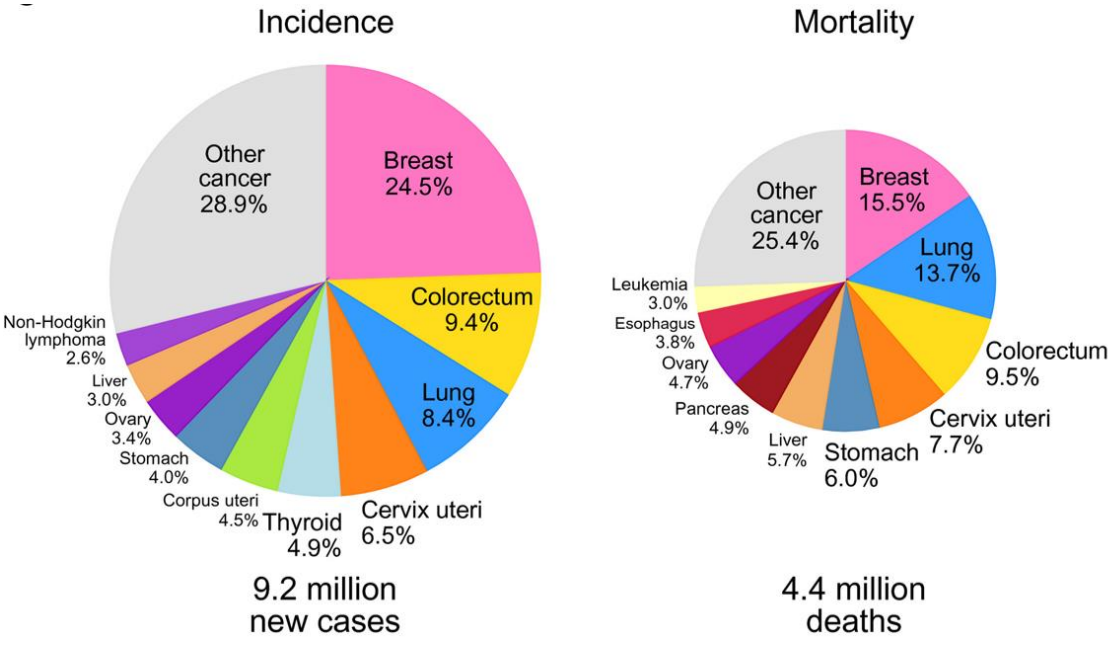

Figure 1.3 Estimated global incidence and mortality of cancers in females. Taken from [32].

Of the cancers associated with HPV infection, cervical cancer is by far the most prevalent. Cancer of the cervix is the fourth most common malignancy in women worldwide and the fourth leading cause of cancer-related deaths in women (**Fig 1.3**) [32]. As such, it represents a major global health challenge. In 2020, it is estimated that in excess of 600,000 people were diagnosed with cervical cancer and almost 350,000 deaths worldwide could be attributed to the malignancy [32]. Indeed, cervical cancer is the leading cause of cancer death in 36 countries [32]. The vast majority of both cases and deaths occur in sub-Saharan Africa and Southeast Asia (**Fig 1.4**), likely due to the lack of vaccination and screening programmes. Additionally, the high incidence of HIV infections in sub-Saharan Africa further contributes to the number of cervical cancer cases as infection has been shown to increase the risk of both HPV infection and cervical cancer [33]. In contrast, incidence and mortality rates in many other populations worldwide have decreased in recent decades due to the advent of highly effective screening and vaccination programmes [32].

In addition to cervical cancer, a significant proportion of other anogenital cancers are attributable to HPV. Of these, cancer of the anus is most frequent, with approximately 35,000 HPV-attributable cases per annum which are split equitably between the sexes [27]. Cancers of the vulva, vagina and penis are rarer, with only around 10,000 HPV-associated cases per annum [27]. Whilst the incidence of these cancers is still relatively high in sub-Saharan Africa, many countries in the Americas and western Europe also have high numbers of cases [27].

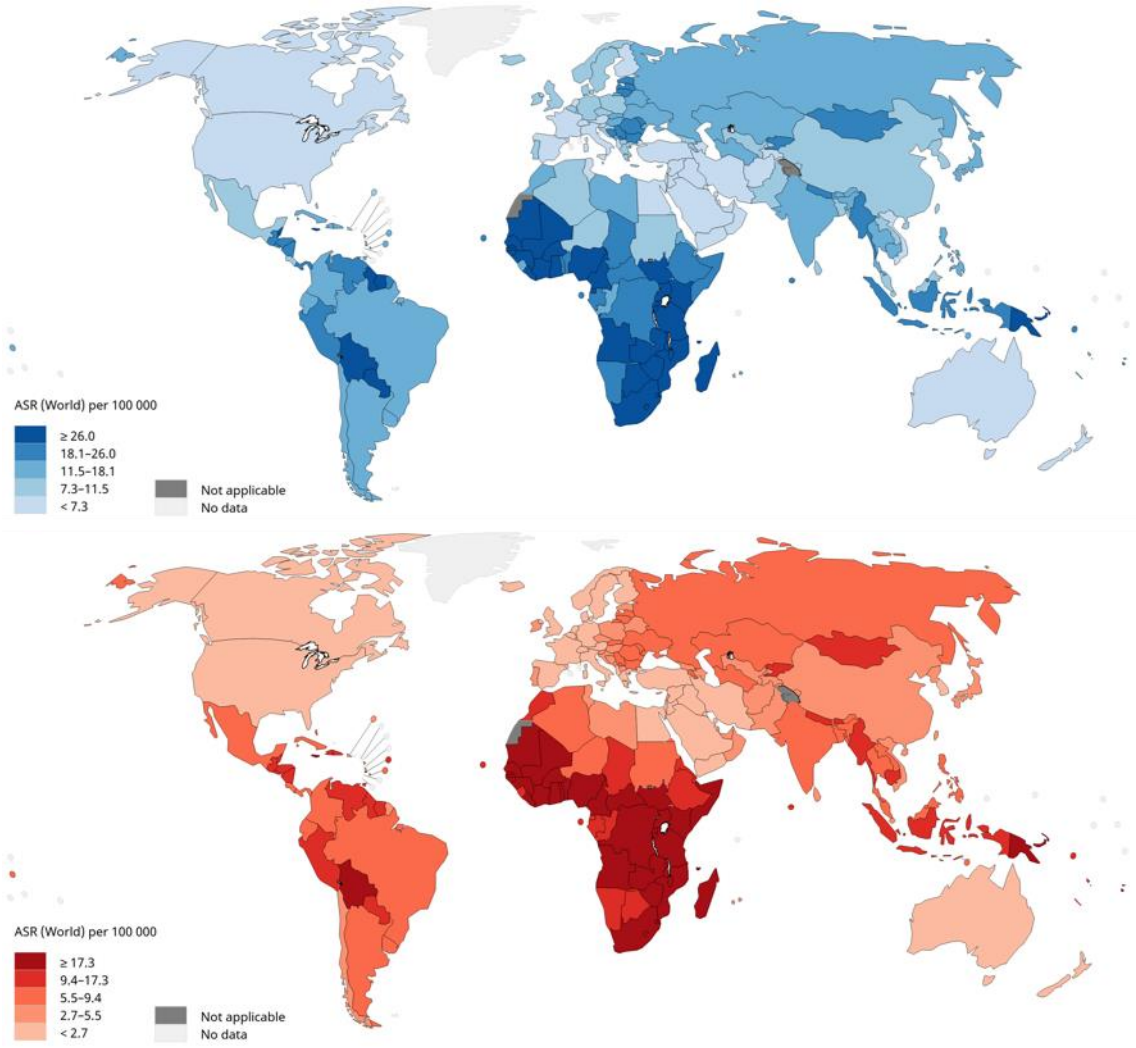

Figure 1.4 Age-standardised incidence and mortality rates of cervical cancer. Incidence (blue), mortality (red). Data shown includes females of all ages. Data taken from [34].

Collectively, HNSCCs are the sixth most common malignancy worldwide and the seventh leading cause of cancer-related deaths [34]. Historically, HNSCC prevalence has been highest in countries in Asia, Eastern Europe and South America associated with high tobacco use [35]. Whilst the overall incidence of HNSCC has decreased in most countries (consistent with declines in tobacco use), the incidence of oropharyngeal cancers has rapidly increased in the last 20 years, which has been attributed to HPV [35]. Indeed, the prevalence of HPV in oropharyngeal cancers has been reported to exceed 70% in some countries currently [29]. The increase in HPV+ oropharyngeal cancers has primarily

occurred in the developed countries of Europe and North America, with HPV-HNSCCs still predominating in Asian countries.

1.5 Prevention and treatment of HPV-associated diseases

1.5.1 Prevention

The primary method of preventing HPV-associated disease is via prophylactic vaccination. Three vaccines are currently available, all of which consist of recombinant self-assembling L1 virus-like particles (VLPs) which induce a strong neutralising antibody response [36]. The first, Cervarix, is bivalent and offers protection against the most common causes of HPV-associated malignancy, HPV types 16 and 18. Gardasil is quadrivalent and is effective in preventing infection with HPV types 6 and 11, the causal factors in ~90% of genital warts, in addition to HPV16 and 18 [20, 37]. Both of these vaccines display near 100% efficacy levels in preventing HPV infection and associated disease [36]. More recently, a 9-valent vaccine has been developed to cover five additional oncogenic types (HPV31, 33, 45, 52 and 58) which together account for ~20% of cervical cancer cases, whilst maintaining the high efficacy of the other vaccines [38].

As a result of this, around 100 countries worldwide have introduced HPV vaccination programmes to date [39]. For example, in the UK girls aged 12-13 have been receiving the vaccine since 2008 and this has been extended to include boys of the same age in recent years. A recent meta-analysis has demonstrated that, as a result of these vaccination programmes, HPV16/18 prevalence and diagnoses of anogenital warts and CIN2+ lesions have significantly decreased in girls and young women by up to 80% in multiple high-income countries [39]. Interestingly, anogenital wart diagnoses in boys and young

men have also decreased significantly in recent years, likely due to substantial population-level herd effects limiting HPV transmission [39]. This trend is expected to continue in future years as vaccination programmes are more widely extended to include boys.

Despite the widespread introduction of HPV vaccination in developed countries, a significant lag exists in its introduction in low- and middle-income countries (LMICs) [40]. This is important as ~90% of cervical cancer-related deaths occur in LMICs [34]. Significant challenges in the implementation of vaccination in these countries exist, such as the difficulties in reaching girls for multiple doses where school attendance may be low, as well as logistical issues and the need for cold storage [40]. The prohibitively high cost of vaccination has been overcome somewhat with the introduction of novel financing mechanisms [41]. Promisingly however, significant progress is being made, with over 20 LMICs expected to introduce HPV vaccination programmes in the next four years [42].

As the vaccines are ineffective in older individuals already infected with HPV and there is an absence of effective anti-viral drugs targeting the virus, screening methods to identify cervical disease prior to progression to cancer is necessary. Cervical screening was introduced in the UK in 1988, whereby a Papanicolaou (Pap) smear was used to collect cells of the cervical epithelium and examine them for the presence of CIN. Since 2003, liquid-based cytology screening has been performed due to reported increases in sensitivity and a reduction in the number of inadequate samples [11]. The current guidance in the UK states that screening should be performed every three years for women aged 25-49 and every five years for women aged 50-64 [43]. The impact of cervical screening has been profound: an estimated 70% of cervical cancer-related deaths have been prevented as a result of the programme in the UK [44]. However, the efficacy of

high-risk HPV-based screening has been found to significantly exceed that of conventional cytology-based cervical screening in detecting CIN2+ lesions, resulting in a gradual transition worldwide to this method for women aged over 30 where the probability of transient HPV infection is lower [45, 46]. In the UK, this was expected to be completed by the end of 2019 [47]. A potential side-effect of this is an increase in false-positive rates, whereby HPV is present yet the individual displays normal cervical cytology, which could cause significant psychological and physical harm if unnecessary treatment is undertaken [48]. Liquid-based cytology triage is therefore still recommended in the case of a positive HPV test [47].

1.5.2 Treatment

Treatment of cutaneous HPV lesions is not usually necessary due to their tendency to resolve spontaneously. In the event of persistence, the application of salicylic acid solutions at home is effective in the majority of cases. Cryotherapy with dry ice or liquid nitrogen should be reserved for the most recalcitrant of lesions [11].

Multiple treatment possibilities exist for anogenital warts which predominantly focus on removal of the wart rather than the underlying viral infection. Application of creams containing either podophyllotoxin or imiquimod, which induce necrosis of the wart and an inflammatory immune response respectively, can be performed easily in the home [21]. Both treatments have been demonstrated to have moderate clearance rates. Alternatively, cryotherapy or surgical excision may be used to remove the abnormal tissue [21].

The treatment method used for cervical disease will depend on the CIN grade assigned. CIN1 lesions present a very low risk of progression to cancer and so

no treatment is necessary [11]. As CIN2/3 lesions present a higher risk of progression, removal of the abnormal cells is normally recommended. This is most commonly performed by large loop excision of the transformation zone (LLETZ), whereby cells are removed using a thin wire loop heated with an electric current. In more severe cases or those of recurrent cervical disease, hysterectomy may be necessary. If, however, screening identifies evidence of cancerous tissue, hysterectomy with concomitant radiotherapy or chemotherapy will be required [49].

1.6 Papillomavirus virology

1.6.1 Genome organisation

Papillomaviruses possess a circular double-stranded DNA genome of approximately 8 kb in size which is packaged into non-enveloped, icosahedral virions of ~60 nm in size (**Fig 1.5**) [50]. The genome can be organised into three major regions: an upstream regulatory region (URR), an early region, and a late region. These are separated by two polyadenylation sites: early (PAE) and late (PAL) [6]. The URR contains the virus origin of replication (*ori*) as well as multiple binding sites for host transcription factors such as SP1, Oct1 and YY1, as well as viral early proteins, and as such plays an important role in regulating viral gene expression [51]. The early region encompasses over half of the viral genome and harbours six open reading frames (ORFs) for the E1, E2, E4, E5, E6 and E7 proteins. Some papillomaviruses, such as HPV16, HPV31 and bovine papillomavirus 1 (BPV1), have an additional E8 ORF resulting in the production of a spliced E8^E2 transcript [52]. The late region lies downstream of the early region and consists of the L1 and L2 ORFs encoding the major and minor structural proteins respectively. The genome contains two well-characterised

promoters: the early promoter (p97 for HPV16, p105 for HPV18) located within the URR which regulates almost all early gene expression, and a late differentiation-dependent promoter (p670 for HPV16, p811 for HPV18) found in the E7 ORF that controls expression of the structural proteins [53].

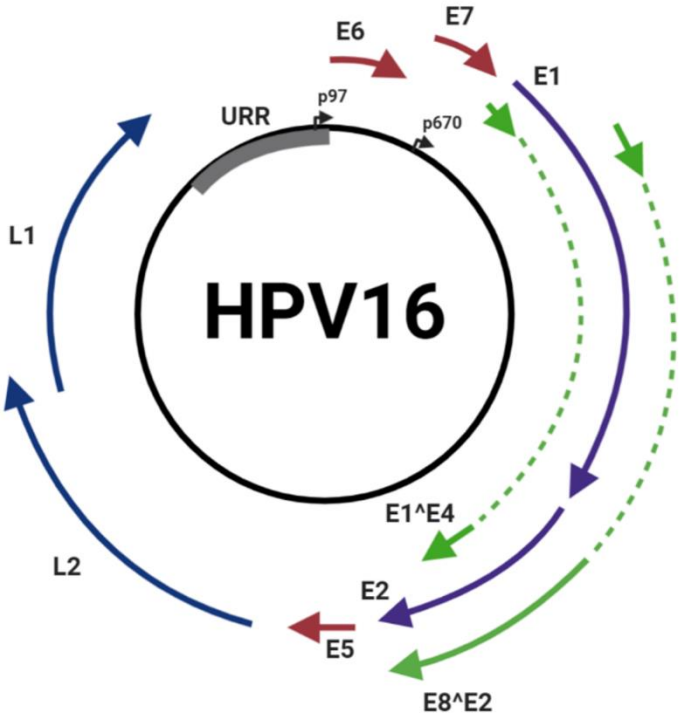

Figure 1.5 HPV genome organisation. The genome of the high-risk α-PV HPV16 is displayed, although other high-risk HPVs have highly similar genomes. The position of each ORF is indicated around the genome. The locations of the early and late promoters (p97 and p670 respectively) are marked with arrowheads. URR, upstream regulatory region. Adapted from [50].

1.6.2 Life cycle

The most widely studied HPV subtypes are those that can cause cervical cancer, and as such the events that occur during an α-PV infection are best understood (**Fig 1.6**). Far less is known about infections involving other HPV types and at other epithelial sites, although it is reasonable to assume that the same broad principles will apply. For a productive viral infection to be established, virions must gain access to the basal lamina of the stratified epithelium via microlesions [13] or, in the case of high-risk HPV types, by entering cells at the squamo-columnar junction [54].

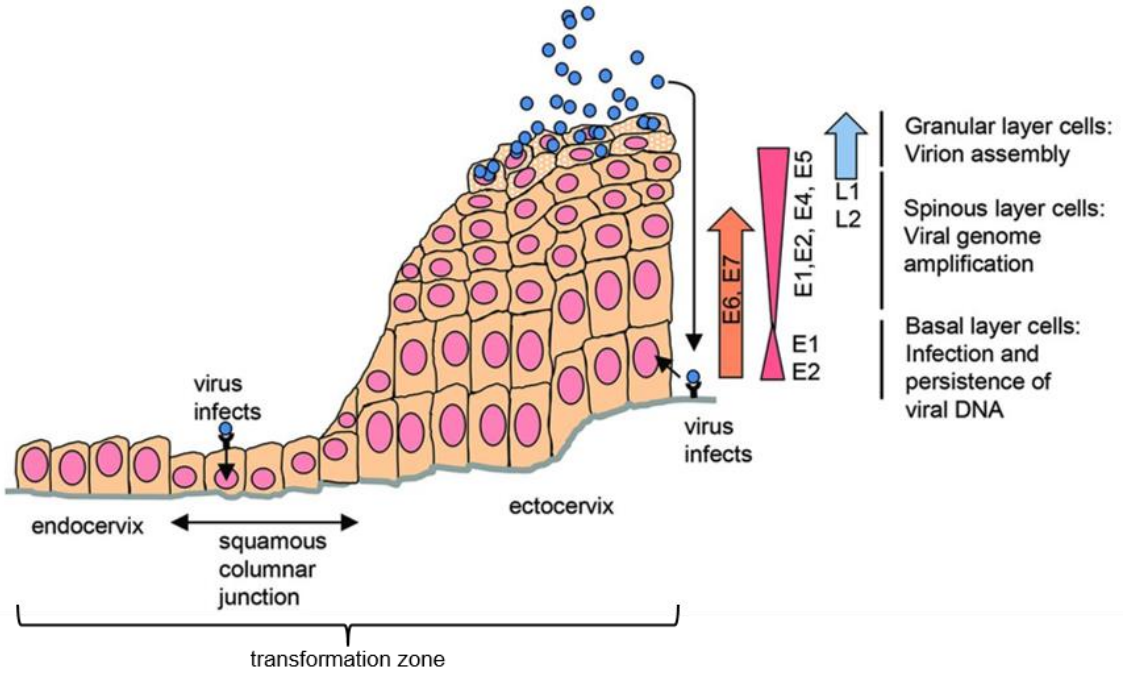

Figure 1.6 HPV replication in the cervical epithelium. Stages of the life cycle and temporal regulation of viral gene expression are outlined. The majority of cervical cancers arise from infections within the transformation zone. Adapted from [6].

The first stage in establishment of infection is host cell entry, which is mediated by interactions between the viral L1 capsid protein and multiple cellular proteins (discussed further in 1.7.2). Briefly, primary attachment involves binding to heparin sulphate proteoglycans (HSPGs) on the basement membrane or on the surface of basal keratinocytes [55]. This induces conformational changes in the capsid structure, resulting in the exposure of the minor capsid protein L2 and binding to secondary receptors. Subsequently, endocytosis is triggered. In the case of HPV16, endocytosis occurs via a clathrin-, caveolin-, cholesterol-, lipid raft- and dynamin-independent mechanism [56]. Rather, a novel ligand-induced pathway similar to micropinocytosis is used by the virus.

After internalisation, HPV virions are trafficked via the endosomal pathway where acidification in the late endosome triggers capsid disassembly. During this, the majority of L1 dissociates from the L2/viral DNA complex and remains within the late endosome to be subsequently targeted for degradation. The L2/viral DNA

complex, alongside the remaining L1, traffics first towards the *trans*-Golgi network (TGN) and then to the nucleus in a microtubule-dependent manner [57]. This ensures evasion of immune detection by cyclic GMP-AMP synthase (cGAS) and stimulator of interferon genes (STING) [58]. Nuclear entry is critically dependent upon breakdown of the nuclear membrane which occurs upon mitotic onset [59].

Following nuclear entry, the virus genome undergoes an initial phase of amplification and is subsequently maintained as an episome, with around 50-100 copies per cell [6]. HPV does not encode a polymerase and therefore must rely upon host factors for genome replication. The infected basal cells then acts as a viral episome reservoir: after cell division one daughter cell remains in the basal layer whilst the other begins to migrate up through the epithelial layers. As suprabasal cells begin to differentiate, expression of the viral early proteins E5, E6 and E7 prevents cell cycle exit, providing a suitable environment for further genome amplification to take place using the host replication machinery in concert with the viral E1 and E2 proteins. As such, the virus is said to uncouple proliferation from differentiation. The E5, E6 and E7 proteins do not possess any intrinsic enzymatic activity, so this must be achieved by interacting with and modulating the activity of host cellular factors.

The virus life cycle is completed in the upper epithelial layers after cell cycle exit has occurred and requires expression of the viral capsid proteins L1 and L2 from the late promoter. The mechanism associated with the switch from early to late promoter use is poorly understood, but likely involves the differentiation-dependent increase in expression of host transcription factors such as c-MYB and NF1 [60]. Virion assembly requires recruitment of the capsid proteins by E2 to the site of genome replication – PML (promyelocytic leukaemia) bodies [61, 62]. Virus maturation occurs in the uppermost layer of keratinocytes, where

oxidisation of the cellular environment allows formation of disulphide bonds between adjacent L1 proteins, producing stable and infectious virions [63]. Finally, virus particles are shed from the epithelial surface to permit infection of nearby cells.

1.7 HPV proteins

1.7.1 E1 and E2 regulatory proteins

The E1 protein is the one of the most conserved proteins encoded by PVs and functions as a hexameric DNA helicase [64]. As such, it is the only PV protein which possesses enzymatic activity. E1 proteins are ~600 amino acids in size and consist of three distinct regions: a regulatory region at the N-terminus; a central DNA-binding domain; and a C-terminal enzymatic domain [64]. The N-terminal region is dispensable for *in vitro* DNA replication but is essential *in vivo* [65]. The region contains multiple sequence motifs including nuclear localisation and export signals (NLS and NES respectively) and a cyclin binding motif (CBM). The DNA-binding domain permits association of E1 with the viral *ori* located within the URR. The *ori* contains six E1 binding sites; association with which permits the assembly of E1 double-trimers, an important intermediate in the formation of replication-competent double-hexamers [66, 67]. The C-terminal enzymatic domain can be divided into three subdomains (an oligomerisation region, an AAA+ ATP-binding site and a C-terminal brace) which together cooperate to form an active helicase [64]. The flexible C-terminal brace is thought to aid in maintaining E1 oligomer stability during conformational changes induced by DNA unwinding and ATP hydrolysis [68].

E1 is required throughout the virus life cycle, firstly in order to increase the copy number of viral episomes in proliferating basal cells, and subsequently for

genome amplification in differentiating keratinocytes. Surprisingly however, maintenance of episomes in suprabasal keratinocytes is thought to be E1-independent [69]. The switch in activities of E1 is thought to be regulated in part by HPV-induced host caspase cleavage, given that mutations to remove cleavage motifs in E1 prevent episome amplification in differentiated keratinocytes [70]. E1 is also tightly regulated by other post-translational modifications, including phosphorylation, ubiquitination and SUMOylation [64]. For example, phosphorylation of E1 by extracellular signal-regulated kinase 1 (ERK1), JNK2 and CDK2 at sites within the N-terminus promote its nuclear retention and thus viral replication [71, 72].

The E2 protein is encoded by all PVs and has essential roles in the regulation of viral transcription, DNA replication and episome maintenance [73]. The protein forms stable dimers which display primarily nuclear organisation. All E2 proteins consist of an N-terminal transactivation domain and a C-terminal DNA binding/dimerisation domain separated by a flexible hinge region which varies in length between PV types. This hinge region possesses various auxiliary functions: α-PV E2s contain a motif which promotes nuclear localisation, whilst the β-PV E2 hinge region can be phosphorylated by protein kinase A (PKA) thus stabilising the protein and permitting binding to host chromatin [74, 75]. E2 proteins bind to conserved $ACCN_6GGT$ sequence motifs found within the URR, of which α-PVs possess four [76].

A key function of E2 is in regulating the assembly of DNA replication machinery at the PV *ori*. E2 firstly acts as a molecular tether by binding to the *ori* and E1 simultaneously in order to recruit E1 [77]. This permits the formation of E1 double-trimers and the ATP-dependent local unwinding of DNA [78]. The binding and hydrolysis of ATP leads to the dissociation of E2 and the assembly of E1 double-

hexamers, permitting further unwinding. Host factors required for DNA synthesis, including topoisomerase I and replication protein A, are then co-opted via direct interactions with E1 [79, 80].

Additionally, E2 is required for genome maintenance by ensuring the faithful segregation of viral episomes into daughter cells after mitotic cell division. This is achieved by simultaneous binding of E2 to the viral genome and host chromatin [81, 82]. The identity of the host chromatin-associated protein required for this remains controversial: evidence indicates that whilst BRD4 is essential for BPV1 tethering, it does not colocalise with the E2 proteins of α-PVs on mitotic chromatin [83-85]. Rather, recent evidence indicates that TopBP1 may be the elusive tethering agent for high-risk HPV types: it does colocalise with E2 on mitotic chromatin and was found to be critical for E2-mediated segregation [86, 87].

E2 proteins also have a major role in regulating the transcription of viral genes [73]. This is achieved via the recruitment of cellular transcriptional machinery to the viral promoter in order to either activate or suppress gene expression. The effect on transcription is thought to reflect the occupancy of different E2 binding sites: association of E2 with its promoter-proximal binding sites was shown to sterically hinder the binding of cellular factors such as SP1 and TBP, resulting in transcriptional silencing [88]. An interaction between E2 and BRD4 (shared by all PVs) is essential for this transcriptional repression, highlighting the numerous roles BRD4 has during the virus life cycle [84]. Binding of E2 to BRD4 abrogates recruitment of the transcriptional elongation factor p-TEFb, thus inhibiting transcription [89, 90]. In contrast, occupation of distal binding sites by E2 has been shown to activate early gene expression [91]. The shorter forms of E2 encoded by some PVs, such as E8^E2, invariably act as transcriptional repressors [52].

Importantly, the E2 ORF is often disrupted during integration of the viral genome into host DNA. This is a common event during carcinogenesis; indeed the majority of HPV16-associated cervical cancer cases and almost all HPV18-associated cases contain an integrated genome, as do 70% of HPV+ HNSCC cases [13, 92]. Integration prevents E2 acting as a negative regulator of early gene expression and therefore leads to increased oncoprotein expression and hence a growth advantage [93].

1.7.2 L1 and L2 structural proteins

PV capsids consist of two proteins, the major capsid protein L1 and the minor capsid protein L2. The capsid structure consists of 360 L1 monomers arranged into 72 pentameric capsomeres [13]. The number of L2 proteins within capsids is ill-defined, although up to 72 have been reported [94]. Disulphide bonds connect neighbouring L1 capsomeres, formation of which occurs during desquamation and is essential for virion stability [63]. L2 is only minimally exposed on the surface of virions.

As L1 is the only major surface-exposed capsid protein, it plays a vital role in mediating cell entry. Initial attachment of PV virions involves interactions between the L1 protein and HSPGs on the extracellular basement membrane and cell surface [55]. This interaction is mediated by two lysine residues on the top of L1 pentamers [95]. Virions may also bind to laminin-332 in the extracellular matrix, although this interaction is currently unconfirmed *in vivo* [96]. Binding to HSPGs induces a conformational change in the capsid which facilitates cleavage of L1 by the trypsin-like serine protease kallikrein-8 (KLK8) [97]. Subsequently, the capsid undergoes a cyclophilin B-dependent conformational change. Together, these act to expose the N-terminus of the minor capsid protein L2 [98]. This allows L2 to be cleaved by the host protease furin which, although dispensable

for viral entry, is required for L2-mediated endosome escape after initial endocytosis [99]. These cleavage events permit association of HPV capsids with a secondary receptor, which is essential for infectious uptake. However, the identity of the secondary receptor remains elusive. Multiple host proteins have been proposed, including α6 and β4 integrins, the tetraspanins CD63 and CD151, as well as annexin A2 [100].

After endocytic entry and capsid disassembly in the late endosome, the viral genome must be trafficked towards the nucleus, a process absolutely dependent on L2. However, viral DNA is firstly trafficked in complex with L2 towards the TGN [101]. Critically, L2 possesses a C-terminal cell-penetrating peptide and a transmembrane-like domain, conferring the ability to span the endocytic membrane [102, 103]. This permits direct interactions with components of the retrograde transport machinery, including the retromer complex, SNX17 and SNX27, to ensure appropriate sorting [104]. Indeed, mutation of the retromer binding sites within L2 abrogates binding and results in the accumulation of L2/viral DNA complexes in early endosomes [105]. Onward trafficking to the nucleus is critically dependent upon nuclear envelope breakdown associated with mitosis [59]. Fragmentation of the TGN during the early stages of mitosis allows L2/viral DNA complexes to associate with microtubules and migrate towards condensed chromosomes [106]. A central chromosome-binding region of L2 allows complexes to remain attached to chromatin throughout mitosis before moving to PML bodies during G1 phase [107].

The capsid proteins are then required during the latter stages of the life cycle for the assembly of progeny virions within the nucleus. Restriction of capsid protein expression to the uppermost layers of the epithelium has been hypothesised to aid in immune evasion by preventing contact between the highly immunogenic

virion and immune cells. L1 proteins assemble into pentameric capsomeres in the cytoplasm before undergoing karyopherin-dependent nuclear import [108]. Karyopherin binding has also been implicated in restricting virion assembly to the nucleus by preventing premature association of pentamers in the cytoplasm [109]. Import of L2 meanwhile requires complex formation with the chaperone protein Hsc70 in addition to karyopherins [110]. However, the mechanisms regulating assembly of L1 and L2 once in the nucleus and those ensuring appropriate incorporation of viral genomes into capsids are poorly understood. The SUMOylation of L2, as well as binding of L2 to nucleophosmin may play a role [111, 112]. Ultimately, capsid maturation is achieved via formation of disulphide bonds between L1 proteins due to the oxidising environment in the uppermost epithelial layer [63].

1.7.3 E4 protein

In comparison to other PV proteins, the role of E4 in the infectious life cycle of the virus is less well understood. In HPVs, the E4 gene product is produced from a spliced mRNA in which the initiation codon and the first five amino acids are derived from the E1 ORF, and as such is often termed E1^E4 [113]. Although historically *E4* was classified as an early gene as the ORF lies entirely within the early region of the genome (**Fig 1.5**), no function of E4 during the early stages of the virus life cycle have yet been identified. Rather, E4 has been found to be expressed highly in the middle and upper layers of the epithelium during a productive infection, coinciding with the onset of genome amplification and prior to the induction of L1 and L2 expression [114]. Indeed, organotypic raft cultures have confirmed that the absence of a functional E4 ORF prevents efficient genome amplification and late gene expression [115]. Interestingly however, HPV16 is thought to have a greater dependence on E4 functionality than HPV18

[116]. The importance of E4 for genome amplification is likely associated with its ability to induce a G2 arrest via binding CDK1/cyclin B complexes and sequestering them in the cytoplasm [117]. E4 may also modulate the activity of cellular mitogen-activated protein kinases (MAPKs) in order to facilitate E1 nuclear translocation and hence viral DNA replication [116].

The activities of E4 are tightly regulated by phosphorylation: members of the MAPK family as well as PKA have been shown to target the protein [113]. Phosphorylation of E4 by ERK1/2 is thought to increase its stability and ability to bind cellular keratin filaments [118]. This leads to a reorganisation of the cytokeratin network towards the cell periphery. Additionally, cleavage of the N-terminus of E4 by calpain in the uppermost epithelial layers promotes its self-association and the formation of amyloid-like fibres, further disrupting the cytoskeleton [119]. The significance of this is as yet uncertain, although it has been hypothesised to facilitate the transmission of newly-synthesised virions.

1.7.4 E5 protein

In contrast to the well-characterised E6 and E7 oncoproteins (discussed in 1.7.5 and 1.7.6 respectively), the functions of E5 remain to be fully elucidated. This is likely to be in part because, to date, only two E5 proteins have been studied in detail (those encoded by BPV1 and HPV16), although the lack of available antibody reagents and difficulties in achieving recombinant expression have prevented us from gaining a more thorough understanding of the roles of E5 in the life cycle of HPV and carcinogenesis [120]. Despite sharing little sequence similarity, the E5 proteins of BPV1 and HPV16 display highly overlapping cellular targets, suggesting that the functions of E5 proteins may be conserved between papillomaviruses and play a significant role in the replicative cycle [120].

E5 is a small, highly hydrophobic, membrane-associated protein which possesses three transmembrane domains (TMDs) and localises to the ER and Golgi apparatus [121]. Like the other oncoproteins, E5 possesses no enzymatic activity and must therefore manipulate the cellular environment by binding host factors and modulating their activity. Interestingly, sequence analysis reveals that several HPV types (β, γ and μ) lack a recognisable E5 ORF, perhaps suggesting that the functions of E5 are carried out by other viral proteins in these types [121]. Significantly however, all high-risk mucosal HPVs possess a conserved E5 oncoprotein which is termed E5α [121]. Indeed, HPV16 E5 has been demonstrated *in vivo* to contribute to carcinogenesis, both alone or in combination with another HPV oncoprotein [122]. In contrast, low-risk HPV types encode two E5 proteins (termed E5A and E5B), but these show little sequence conservation with E5α and are only weakly transforming [120].

An important characteristic of HPV16 E5 is its ability to oligomerise both *in vitro* and *in vivo*, resulting in the formation of hexameric channel structures [123]. The protein has therefore been added to a growing group of virus-encoded membrane proteins known as ‘viroporins’ [124]. Viroporin activity of E5 can be inhibited through the use of both rimantadine and alkyl-imino sugars [123, 125]. Blockade of channel activity prevents E5-mediatied activation of MAPK signalling and reduces cyclin B1 expression, indicating that E5 may be a potential drug target in the treatment of HPV infection [125].

In order to understand the role of E5 in the life cycle of HPV, organotypic raft cultures using keratinocytes containing the genomes of HPV16, 18 and 31 which lack a functional E5 ORF have been used [126-128]. These studies have shown that E5 is not required for genome establishment in undifferentiated cells, but rather plays a key role in the differentiation-dependent stages later in the HPV life

cycle. Indeed, loss of E5 expression prevents the cell cycle re-entry in differentiating suprabasal cells which is required for a productive HPV infection, as demonstrated by a reduction in cyclin B1 expression and host DNA synthesis [126-128]. Despite this, E5 is thought not to be required for the expression of late viral proteins, as no changes in the levels of L1 or E4 could be detected [126, 128].

One of the most important functions of the E5 oncoprotein is in targeting the epidermal growth factor receptor (EGFR) signalling pathway. Indeed, the majority of cervical cancers demonstrate increased EGFR expression, perhaps indicating that E5 modulation of this pathway is necessary for transformation [121]. Indeed, studies in mice have shown that the transforming ability of E5 is attenuated by the expression of a dominant-negative EGFR [129]. However, the mechanism by which E5 targets EGFR remains unclear. Initial studies suggested that an interaction between E5 and the 16K subunit of the vacuolar H^+-ATPase (v-ATPase) was key. This would decrease the rate of EGFR degradation by inhibiting the endosomal acidification process; rather the receptors would be recycled back to the plasma membrane. However, more recent evidence indicates that the level of E5 binding to v-ATPases would be insufficient to induce the observed changes in endosome acidification [130]. It is now thought that E5 prevents EGFR degradation by inhibiting the membrane fusion required for endosomal maturation. Additionally, E5 has been show to promote EGFR signalling in other ways. These include binding to EGFR directly, promoting the phosphorylation of EGFR and also preventing its degradation by disrupting the interaction between EGFR and the E3 ubiquitin ligase c-CBL (casitas B-lineage lymphoma) [121].

Activation of EGFR-mediated signalling results in increased keratinocyte proliferation, but HPV E5 also manipulates host differentiation by modulating the activity of the keratinocyte growth factor receptor (KGFR). In uninfected keratinocytes, KGFR protein levels increase in the suprabasal layers of the stratified epithelium, suggesting that KGFR-driven signalling may promote the transition from proliferation to differentiation. However, HPV16 E5 has been shown to reduce the expression of KGFR (via an unknown mechanism), resulting in a delay in differentiation [131]. However, recent studies of the HPV18 life cycle have revealed an unexpected interplay between the EGFR and KGFR pathways and identified a potential mechanism for KGFR downregulation. The activation of EGFR by E5 and the ensuing MAPK activity was shown to contribute towards the suppression of KGFR expression and downstream AKT signalling, thus impairing keratinocyte differentiation [128].

E5 proteins have also been shown to be capable of modulating the immune response to infection. The E5 oncoprotein does this by interfering with antigen presentation to cytotoxic T lymphocytes by the host major histocompatibility (MHC) class I protein complex. This is achieved by preventing the trafficking of MHC class I complexes to the plasma membrane, resulting in them being retained within the Golgi apparatus [132]. Indeed, a reduction in surface expression of MHC class I complexes can be observed in cervical carcinomas [133, 134]. This intracellular retention is achieved through a direct interaction between E5 and the heavy chain of MHC class I [135]. An association between E5 and the chaperone B-cell-associated protein 31 (BAP31) as well as its binding partner A4 is also thought to play a role [136, 137]. Interestingly, only the human leukocyte antigen (HLA)-A and HLA-B MHC class I complexes are targeted as these are associated with T-cell activation; the alternative HLA-C and HLA-E

molecules are not affected by E5. HPV16 E5 is also able to modulate MHC class II expression by inhibiting endosomal processing of the invariant chain chaperone and hence blocking the loading of peptides and trafficking to the plasma membrane [138]. The evolution of multiple mechanisms to interfere with antigen presentation perhaps reflects the importance of evading the host immune response during a productive infection. Indeed, cells expressing HPV16 E5 are poorly-recognised and able to evade killing by CD8+ T cells [139].

1.7.5 E6 protein

The E6 ORF is located immediately downstream of the URR which when transcribed results in the production of a protein ~150 amino acids in length [140]. Interestingly, a small number of PVs which lack a recognisable E6 ORF have been identified, including BPV types 3, 4 and 6 as well as HPV types 101 and 103; presumably the functions of E6 are either not required by these viruses or are performed by an alternative viral or host protein [141]. Unlike the E7 oncoprotein, expression of E6 alone does not result in immortalisation of keratinocytes, but co-expression of both is highly efficient in immortalising cells [142]. E6 has been reported to localise to both the nuclear and cytoplasmic compartments of the cell [140]. Alternative splicing of high-risk HPV E6 transcripts can result in the production of a truncated protein termed E6*, but the functions of this protein remain poorly understood. E6 proteins do not possess any enzymatic activities and thus all of its functions must be mediated by protein-protein interactions (summarised in **Fig 1.7**).

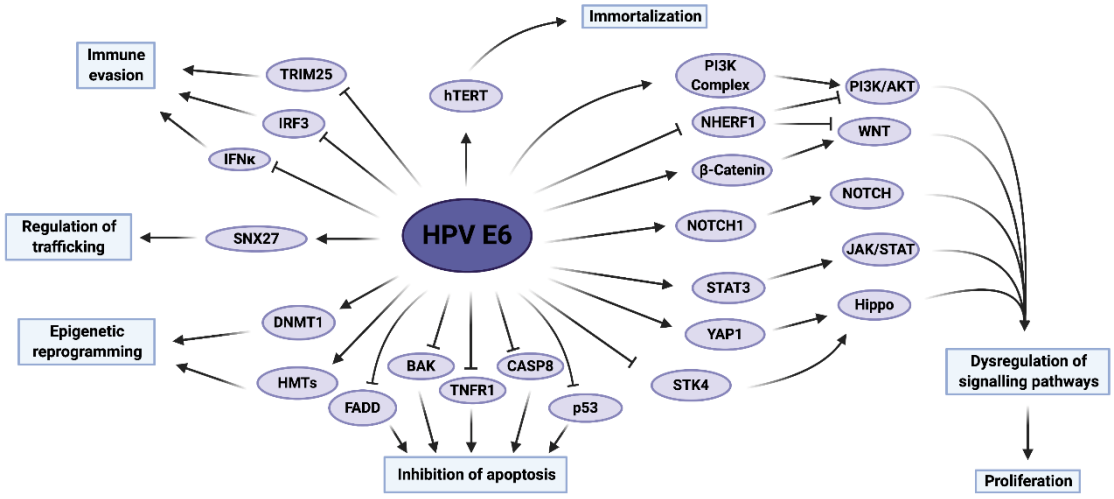

Figure 1.7 Summary of HPV E6 activities which contribute towards host-cell transformation. The host proteins and pathways reported to be modulated by HPV E6 are displayed, as well as the functional impact these have on the host cell. Taken from [50].

One of the best-studied functions of the E6 is in blocking pro-apoptotic signalling mediated by p53 (**Fig 1.8**). This is necessary to protect cells from apoptosis and/or growth arrest in response to HPV oncoprotein-mediated cell cycle re-entry in suprabasal cells. HPV possesses multiple mechanisms of interfering with p53 function [143]. Firstly, high-risk HPV E6 is able to interact with the host E6-associated protein (E6AP), a HECT domain-containing E3 ubiquitin ligase, by binding to its leucine-rich LXXLL consensus sequence [144, 145]. The resulting E6-E6AP complex recruits and ubiquitinates p53, subsequently leading to its degradation via the proteasome. This however does not totally deplete the host cell of p53 and low-risk and β HPVs do not demonstrate any ability to degrade p53. E6 proteins have therefore evolved additional degradation-independent mechanisms to inhibit p53 signalling. Indeed, E6 proteins interact with p53 directly and thus inhibit its DNA-binding activity, hence preventing it from transactivating the transcription of target genes [146]. Further, E6 has the ability to inhibit the acetylation of p53 by the related acetyltransferases p300 and CBP (CREB-binding protein) via the formation of a p53-E6-p300/CBP complex; an

activity common to both high-risk and low-risk E6 proteins [147, 148]. E6 also inhibits the function of ADA3, which similarly promotes p53 acetylation and thus stabilisation; although in contrast to p300/CBP, this is achieved via degradation [149]. Together, this prevents the transcriptional activation of pro-apoptotic p53 target genes. Finally, E6 proteins of both high-risk and low-risk HPVs are also able to sequester p53 in the cytoplasm via binding to its C-terminus and masking its NLS [140]. Whilst the primary aim of this is to abrogate pro-apoptotic signalling, in the context of a persistent infection, the prolonged loss of p53 function will allow the accumulation of genetic mutations and thus contribute to cancer progression.

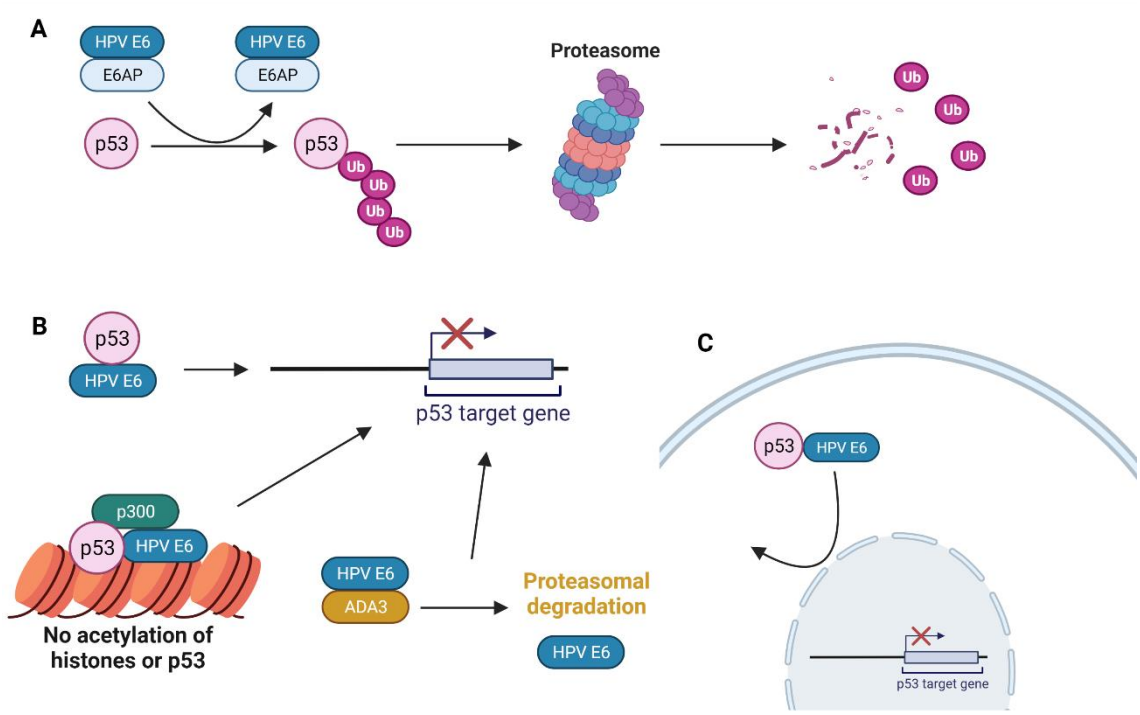

Figure 1.8 Regulation of p53 by HPV E6. A) HPV E6 in complex with E6AP targets p53 for proteasomal degradation. B) Association of E6 inhibits the DNA-binding of p53. E6 inhibits the acetylation of p53 and neighbouring histones and induces the degradation of the coactivator ADA3. C) E6 binding to the C terminus of p53 leads to sequestration in the cytoplasm. Figure created using BioRENDER.com.

E6 is also able to inhibit apoptosis via other mechanisms. The intrinsic pathway, whereby intracellular stimuli induce apoptotic signalling, can be blocked by both high-risk and low-risk HPV E6 proteins. This is primarily achieved through binding to the host pro-apoptotic protein Bak, leading to its degradation by the

proteasome [150, 151]. This in turn prevents the release of cytochrome c from the mitochondria and hence cleavage of effector caspases cannot occur. In contrast, blocking of the extrinsic pathway, which transmits extracellular apoptotic stimuli from the cell surface, can occur at multiple stages. Firstly, HPV16 E6 has been shown to be capable of binding directly to the C-terminus of tumour necrosis factor receptor 1 (TNFR1), a cell surface transmembrane death receptor, thus preventing the formation of the death-inducing signalling complex and transduction of pro-apoptotic signalling [152]. Additionally, HPV16 E6 is able to bind to the adaptor protein Fas-associated protein with death domain (FADD) and the effector caspase caspase-8 and induce their degradation [153, 154]. As these proteins are required to potentiate signalling from all death receptors, this allows the virus to inhibit extrinsic signalling from multiple receptors at once, including Fas and TNF-related apoptosis-inducing ligand (TRAIL).

A property unique to the E6 oncoproteins of high-risk HPVs is the presence of a C-terminal PDZ (PSD-95/DLG/ZO-1) binding motif (PBM). This motif permits binding to a range of host proteins which possess PDZ domains of ~90 amino acids in length. An interaction with E6 has been confirmed for at least 19 PDZ proteins to date, although this represents only a small fraction of the ~200 host PDZ proteins [155]. Despite this, the range of proteins possessing PDZ domains clearly allows E6 to target multiple aspects of the host cell environment. Significantly, p53 degradation-defective high-risk E6 proteins are still capable of immortalising cells, but those defective in binding PDZ partners are unable to induce epithelial hyperplasia, underlining the importance of modulating the activity of host PDZ proteins [156, 157]. Interestingly, several of the PDZ proteins confirmed to bind HPV E6, including SCRIB, DLG1 and the MAGI family of proteins, are regulators of cell polarity and cell-cell contacts [158-161]. The

interaction with E6 results in the proteasomal degradation and/or mislocalisation of the PDZ proteins, hence disrupting cell polarity, a common characteristic of malignant cells. E6 also targets the host factor sorting nexin 27 (SNX27) utilising its PDZ domain, this results in dysregulation of trafficking of proteins such as glucose transporter 1 (GLUT1), essential for glucose uptake and hence cellular homeostasis and proliferation [162]. Furthermore, it was recently demonstrated that high-risk E6 proteins promote host cell proliferation and survival in a PBM-dependent manner via the activation of cJun N-terminal kinase 1/2 (JNK1/2) signalling [163]. Taken together, these observations have led to the hypothesis that targeting of PDZ proteins contributes significantly to HPV-induced transformation [164]. Indeed, the number of PDZ proteins bound by E6 correlates strikingly with the potential for oncogenicity: although binding to DLG1 is shared by all high-risk E6 proteins, only those of HPV16 and 18 are capable of binding SCRIB [165]. Binding of E6 to PDZ proteins is abrogated by phosphorylation of a threonine residue within the PBM [166]. Surprisingly however, there is the potential for subtle differences in the regulation mechanisms between HPV types: HPV16 E6 displays a higher susceptibility to phosphorylation by AKT, whilst HPV18 E6 is more readily phosphorylated by PKA [166].

In addition to its activities in regulating p53 and PDZ protein activity, recent evidence suggests E6 is capable of modulating a multitude of host signalling pathways regulating cell proliferation and survival. For example, E6-induced increased STAT3 phosphorylation has been reported to be required for both episomal maintenance in undifferentiated keratinocytes and the continued proliferation of suprabasal cells in the context of the HPV life cycle [167]. Further, STAT3 phosphorylation is also increased in HPV+ cervical cancer; this is achieved via E6-dependent upregulation of NFκB signalling and subsequent

autocrine/paracrine activation of STAT3 by IL6 [168]. Importantly, this STAT3 activity, as well as that of the upstream kinase JAK2, is essential for the proliferation and survival of HPV+ cancer cells [169]. Additionally, HPV16 E6 is capable of inducing the prolonged phosphorylation of receptor tyrosine kinases such as EGFR, resulting in activation of downstream mitogenic signalling via the PI3K and MAPK pathways [170]. Induction of Wnt signalling by HPV E6 has also been reported in HPV+ cancer cells: the combined effect of upregulated forkhead box protein M1 (FOXM1) expression, which promotes the nuclear translocation of β-catenin, and a decrease in seven in absentia homologue 1 (SIAH1) expression, a β-catenin-targeting E3 ubiquitin ligase, leads to increased expression of Wnt-dependent genes [171, 172]. Finally, dysregulation of the Hippo pathway has also been reported. E6 prevents proteasomal degradation of the transcription factor yes-associated protein 1 (YAP1), the major downstream effector of the Hippo pathway, whilst E6 and E7 coordinate in downregulating expression of the upstream serine/threonine-protein kinase 4 (STK4) via a novel miRNA-mediated mechanism [173, 174].

A key target of high-risk E6 proteins which contributes towards host cell immortalisation is the telomerase enzyme [175]. Activation of telomerase allows replication of host telomeric DNA, thus preventing excessive shortening of telomeres at the 3’ end of chromosomes during DNA replication and the subsequent induction of senescence. Activation is achieved by promoting transcription of *TERT* (*telomerase reverse transcriptase*), which encodes the catalytic subunit of telomerase, although the mechanisms involved are complex and yet to be fully understood [140]. It is thought that binding of c-MYC and SP1 to the *TERT* promoter mediates the E6-induced increases in expression, but formation of the E6/E6AP complex was also found to be critical for the activation

of TERT expression [176, 177]. It was later discovered that E6/E6AP induces the proteasomal degradation of the transcriptional repressor NFX1-91, and that the increased c-MYC binding is due to E6-mediated dissociation of the transcriptional repressors USF1 and USF2 from the *TERT* promoter [178, 179].

Evidence also suggests that E6 is capable of modulating the immune response to infection. High-risk E6 proteins interact with a component of the innate immune response: interferon regulatory factor 3 (IRF3) [180]. This interaction is thought to prevent the transactivation of IFN-β expression and hence the induction of interferon-stimulated genes (ISGs). Further, HPV18 E6 has been demonstrated to directly interact with and impair activation of the non-receptor tyrosine kinase 2 (TYK2), thus inhibiting the induction of JAK-STAT signalling [156]. Disruption of the immune response can also be achieved via disruption of the RIG-I pathway: E6 proteins from several high-risk types bind to TRIM25 and USP15, two key activators of RIG-I, promoting the ubiquitination and degradation of TRIM25 and ultimately inhibiting the activation of RIG-I signalling [181]. Finally, E6 silences expression of the keratinocyte-specific interferon IFNκ to prevent activation of antiviral ISGs and pattern recognition receptors (PRRs) [182].

1.7.6 E7 protein

The E7 protein is the major transforming protein of high-risk HPVs and its continued expression is essential for carcinogenesis [2, 50, 183, 184]. The protein is ~100 amino acids long and possesses two conserved regions (CR1 and CR2) in its N-terminus which show significant similarity to other oncoproteins encoded by DNA viruses including adenovirus E1A and simian virus 40 (SV40) T antigen [50]. The C-terminus of E7 is less well-conserved except for two CXXC zinc-binding motifs [184]. E7 possesses both an NLS and an NES, suggesting that it

shuttles between the cytoplasm and nucleus and has functions in both compartments [185]. These functions are summarised in **Fig 1.9**.

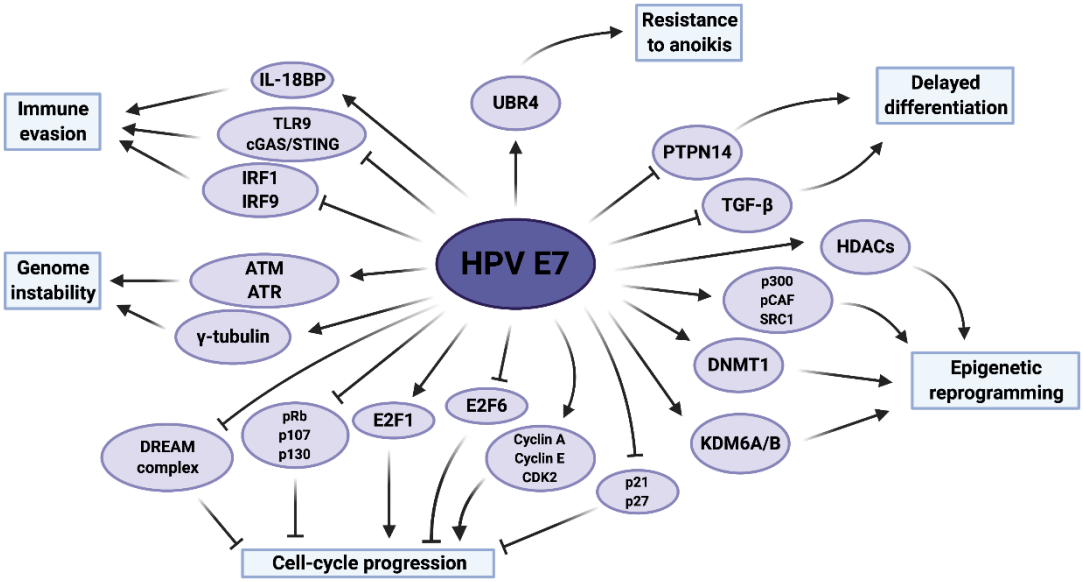

Figure 1.9 Summary of HPV E7 activities which contribute towards host-cell transformation. The host proteins and pathways reported to be modulated by HPV E7 are displayed, as well as the functional impact these have on the host cell. Taken from [50].

The most well-characterised function of E7 is in regulating the G1/S phase transition in order to promote increased proliferation through disruption of E2F transcription factor activity (**Fig 1.10**). This is achieved via binding of E7 to the retinoblastoma protein (pRb) and the related pocket proteins p107 and p130 [186-188]. Evidence suggests that the binding of E7 to p130, which is highly expressed in differentiated keratinocytes, is the most important of these interactions for triggering S phase re-entry in the squamous epithelium [189]. A conserved LXCXE motif located within the CR2 domain of E7 is necessary for its interaction with the pocket proteins [187]. Some evidence indicates that sequences within the C-terminus of E7 may also be required for pRb binding [190]. Binding of E7 disrupts complexes formed between pRb and E2F transcription factors, the release of which permits expression of E2F-dependent genes associated with cell cycle progression such as cyclins A and E, contributing towards S phase re-

entry in differentiating subrabasal keratinocytes [143]. Concurrently, binding of HPV E7 to p107 and p130 leads to disruption of the dimerization partner, pRb-like, E2F and multi-vulval class B (DREAM) repressor complex, permitting a further enhancement in the expression of proliferative genes [191, 192]. E7-pocket protein binding and S phase entry is significantly enhanced by casein kinase II phosphorylation of serine-32 and -34 residues within the CR2 domain [189, 193]. Additionally, high-risk E7 proteins can target Rb family members for proteasomal degradation via a mechanism that requires binding to the cullin 2 ubiquitin ligase complex by E7 [194-196]. E7-induced degradation also requires cleavage of pRb by the protease calpain-1; this unmasks a C-terminal unstructured region of pRb which acts as an efficient initiation region for degradation by the proteasome [197, 198]. In contrast, low-risk E7 proteins have a significantly weaker affinity for the pocket proteins and only p130 is targeted for degradation, which perhaps contributes to their lack of transforming activity [187, 199].

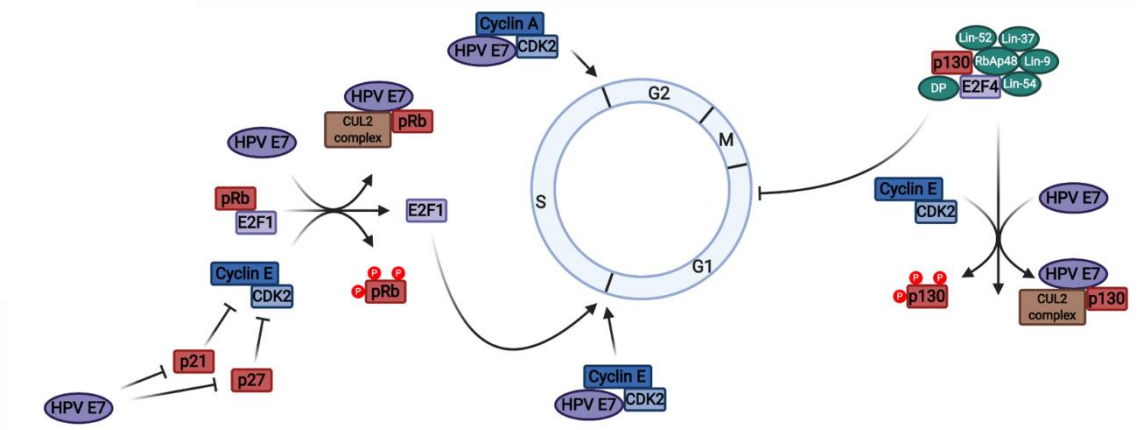

Figure 1.10 Dysregulation of cell-cycle checkpoints by HPV E7. E7 binds to and induces the degradation of the retinoblastoma protein (pRb) in a cullin 2 (CUL2) ubiquitin ligase-dependent manner. This releases the E2F1 transcription factor from inhibitory complexes, permitting the expression of genes associated with S-phase progression. Degradation of the related pocket proteins p107 and p130 prevents inhibition of G1 progression by the DREAM complex. HPV E7 also binds directly to cyclins A and E, potentiating cyclin-dependent kinase 2 (CDK2) activity. Further, HPV E7 can suppress the activity of the CDK inhibitors p21 and p27, allowing increased cyclin/CDK phosphorylation of pRb and enhanced E2F1-dependent transcription. Adapted from [50].

E7 proteins are also able to dysregulate the G1/S phase checkpoint in other ways. A direct interaction between E7 and E2F1 has been reported, leading to a further increase in E2F-dependent gene expression [200]. Further, HPV16 E7 is capable of binding and inactivating the non-canonical E2F family member E2F6, which acts as a transcriptional repressor of E2F-responsive promoters via the recruitment of polycomb group (PcG) complexes [201]. Similarly, the activity of CDK2, a kinase crucial for S phase entry and progression, is maintained via an interaction between its cognate cyclins (cyclin E and cyclin A) and E7 [202]. Additionally, the activities of the CDK2 inhibitors $p21^{CIP1}$ and $p27^{KIP1}$, which are implicated in mediating keratinocyte differentiation via inducing a G1 cell cycle arrest, are suppressed by E7 binding [203-205]. Together these mechanisms act to ensure the efficient S phase re-entry of differentiating suprabasal epithelial cells.

In addition to its roles in driving proliferation, emerging evidence indicates that E7 may also play a role in impairing cellular differentiation. A diverse range of E7 proteins possess the ability to bind the non-receptor protein tyrosine phosphatase PTPN14, with high-risk E7 proteins additionally able to target it for proteasomal degradation using the UBR4 ubiquitin ligase [206, 207]. This loss of PTPN14 is critical in both delaying the epithelial differentiation programme and for cellular transformation, although evidence that this is achieved via modulation of Hippo pathway signalling remains controversial [208, 209]. Interestingly, mutational analyses indicate that this constitutes one of the as yet poorly-defined pRb-independent functions of E7: regions in both CR1 and the C-terminus are necessary for formation of the E7/PTPN14/UBR4 complex. Additionally, high-risk E7 proteins are able to suppress the differentiation-dependent increase in expression of the microRNA miR-203 [210]. This, in turn, contributes to increased protein levels of ΔNp63, a key driver of proliferation in epithelial tissue which is commonly overexpressed in SCCs of the head and neck and cervix.

The E7 oncoprotein also plays a role in immune evasion by HPV. Indeed, recent evidence suggests that expression of both E6 and E7 is necessary to repress the host innate immune response [211]. A key target for HPV is the host PRRs: direct binding of HPV18 E7 to STING, in a manner dependent on its LXCXE pRb-binding motif, results in inhibition of the cGAS-STING signalling axis, a major pathway involved in the recognition of exogenous DNA [212]. Signalling is further repressed in HPV+ cervical cancer cells via E7-induced upregulation of the H3K9-specific DNA methyltransferase SUV39H1, leading to the suppression of cGAS and STING expression [213]. The histone demethylases KDM5B and KDM5C also participate in STING silencing by promoting removal of the activatory histone marker H3K4me3 [214]. Indeed, expression of KDM5B and

STING are negatively correlated in HPV+ cancers [214]. Additionally, HPV16 E7 is able to promote the epigenetic silencing of the dsDNA sensor Toll-like receptor 9 (TLR9) [215]. Together, these measures act to prevent production of type I interferons. The interferon response is also suppressed via binding of E7 to IRF9, abrogating the expression of ISGs [216]. Further, mouse models have demonstrated that HPV16 E7 expression results in a locally immunosuppressive environment where cytotoxic T lymphocyte function is significantly suppressed [217]. Mechanistically, this could be associated with reduced expression of the chemokine CXCL14, observed in both cervical cancer and HPV+ HNSCC tissue, due to E7-dependent promoter hypermethylation. Importantly, reintroduction of CXCL14 results in increased immune cell infiltration and suppresses tumour growth [218]. HPV E7 may also interfere with MHC class I surface expression, in addition to the role played by E5, in order to prevent NK cell-mediated killing [219].

The E7 oncoprotein likely has an additional key function in modulating DNA damage response (DDR) signalling. Activation of both the ATM (Ataxia telangiectasia mutated) and ATR (Ataxia telangiectasia and Rad3-related) kinases, crucial regulators of the DDR, is necessary for productive viral replication which occurs in a G2-arrested environment of differentiated epithelial cells [220-223]. In uninfected cells, the ATM and ATR kinases become activated in response to DNA double-strand breaks and replication stress respectively resulting in a cell cycle arrest, suggesting that activation of these pathways by HPV may contribute towards the observed G2 arrest. It has been postulated that arrest in a G2-like environment, following host DNA replication, permits exclusive access to the cellular factors and DNA replication machinery required for genome amplification. What remains unclear however, is whether DDR activation is simply

a result of the replication stress caused by E7-induced unscheduled proliferation which the virus has grown to tolerate [224, 225], or rather whether the virus has evolved specific strategies to target DDR signalling. Some mechanistic details have been proposed: ATM activation is thought to be accomplished via a non-canonical route involving E7-driven STAT5 signalling and the acetyltransferase Tip60 [226, 227]. STAT5 is also implicated in driving the ATR-DDR response: high-risk E7-induced constitutive STAT5 phosphorylation drives transcription of TopBP1, which subsequently binds and stimulates the kinase activity of ATR [223]. Whilst the exact mechanism by which the DNA repair machinery contributes towards virus replication also remains unknown, it is clear that inhibition of either ATM or ATR signalling suppresses HPV genome amplification [222, 223]. Viral hijacking of ATR signalling is hypothesised to be associated with ensuring a sufficient supply of dNTPs for productive replication, which would otherwise be in short supply in a G2 environment of differentiated cells. Expression of RRM2, the small subunit of the ribonucleotide reductase complex required for *de novo* synthesis of nucleotides and a key downstream target of ATR-DDR signalling, is significantly upregulated in HPV+ cells [228]. Intriguingly, a recent study suggests that DNA repair factors may be recruited away from host DNA towards viral genomes [229]. Indeed, several ATM signalling components, including ATM, γH2AX, Chk2 and BRCA1, are localised to the sites of viral replication during an infection [230]. This has led to the hypothesis that HPV episomes are shielded from the DNA damage ensuing from oncogene-induced replication stress, and that this may contribute to DNA lesions and genetic instability in the host genome necessary for progression to cancer [229].

1.8 ATP-sensitive potassium ion (K_{ATP}) channels

1.8.1 Overview of potassium ion (K^+) channels

Potassium ion (K^+) channels are cell membrane-localised protein complexes that facilitate movement of K^+ both into and out of cells and across intracellular membranes. Over 70 mammalian K^+ channels have been identified to date which can be broadly categorised into three major classes: voltage-gated, inward-rectifying (Kir) and two-pore domain (K2P) channels (**Fig 1.11**) [231]. These classes of channel differ in both their structure and their functions within the cell. The voltage-gated family, consisting of the Kv, KCNQ and ether-a-go-go (Eag) subfamilies, is by far the largest group of K^+ channels with around 40 members, all of which possess six TMDs and a single pore-forming domain. Kir family subunits possess two TMDs flanking their pore-forming domain and assemble into tetramers to produce a functional channel. The K2P family of channels differs from others in that the subunits possess four TMDs and assemble into dimers. A smaller fourth group of a further eight channels has been described: the calcium (Ca^{2+})-activated K^+ channels (K_{Ca}). This class can be subdivided into two subfamilies: the six TMD small conductance Ca^{2+} -activated (SKCa) channels, and the four members of the Slo channel family which possess either six or seven TMDs [232]. All K^+ channels can be broadly divided into two parts: a pore-forming domain to permit ion flux, which varies little between the classes; and a regulatory domain to control channel gating. All K^+ channels share a signature sequence: a conserved eight amino acid motif (TXGXG) which confers exclusive conductance to K^+ ions [233].

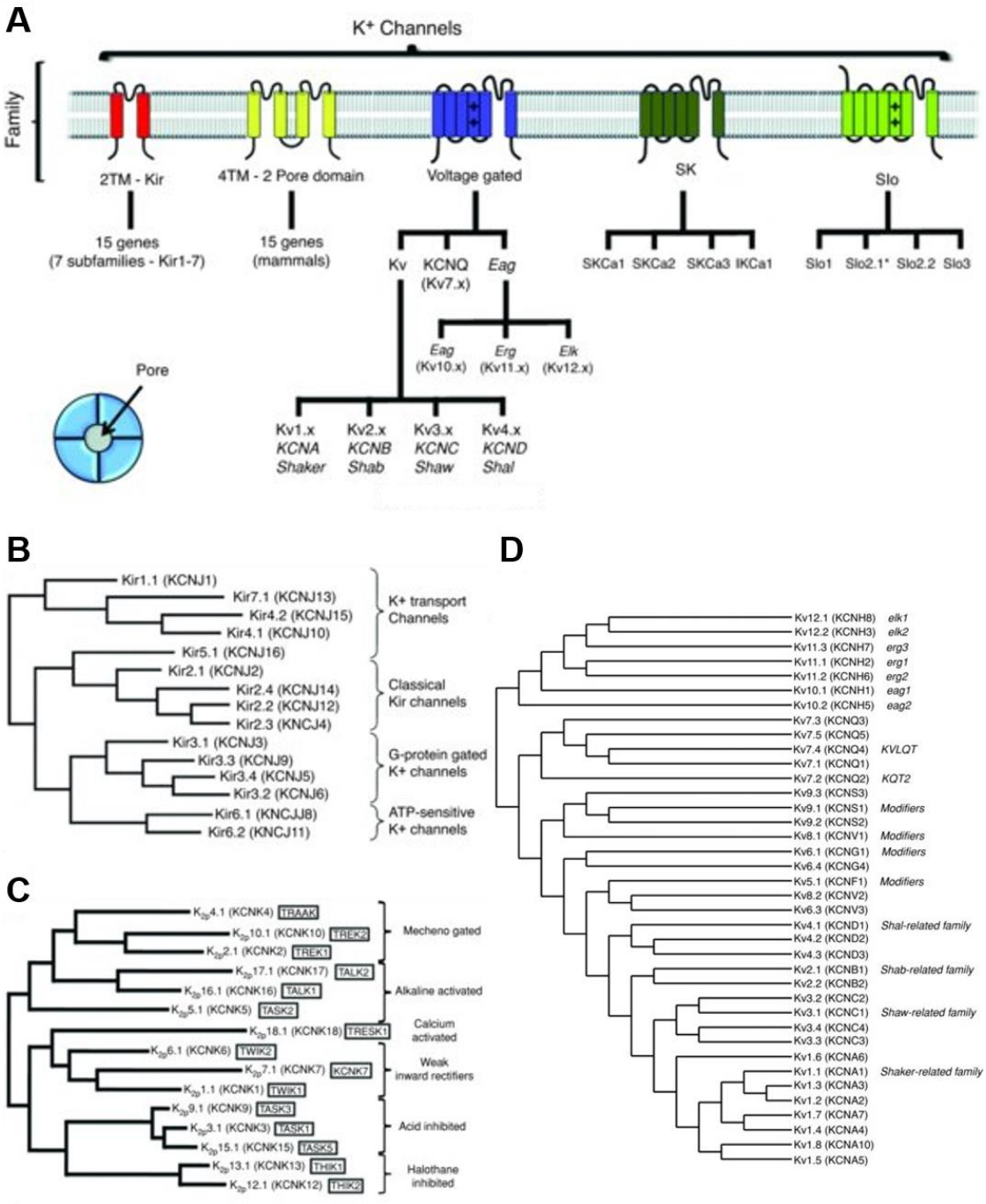

Figure 1.11 Diversity of mammalian potassium ion (K^+) channels. A) K^+ channel families arranged by subunit structure. B-D) Expanded phylogenetic trees displaying members of the inward-rectifying (Kir), two-pore domain (K2P) and voltage-gated families respectively constructed using sequence alignment tools. Adapted from [231].

1.8.2 K_{ATP} channel structure, assembly and tissue expression

ATP-sensitive K^+ (K_{ATP}) channels are hetero-octameric plasma membrane complexes consisting of four inwardly-rectifying pore-forming subunits (either Kir6.1 or Kir6.2) surrounded by four regulatory sulphonylurea receptor (SUR)

subunits [234-236]. As such, they are unlike many other K^+ channels in that the pore-forming and regulatory functions are split between different subunits. Multiple isoforms of the sulphonylurea receptor exist: SUR1 (encoded by *ABCC8*), and SUR2A and SUR2B, which are produced via alternative splicing of the *ABCC9* transcript [237]. The existence of analogous K_{ATP} channels in the mitochondrial membrane remained controversial until the recent unequivocal identification of the genes encoding the mitoK_{ATP}, termed *MITOK* and *MITOSUR* [238]. Despite being encoded by different genes, these channels are similarly composed of pore-forming and regulatory subunits.

The Kir6.x subunits are typical of the inward-rectifying family of channels in that they possess intracellular N- and C-termini and two TMDs (referred to as M1 and M2) separated by a pore-forming hairpin loop containing the K^+ signature sequence (**Fig 1.12**) [236]. Cloning techniques led to the identification of two Kir6.x isoforms, Kir6.1 and Kir6.2, which display ~71% amino acid conservation [239, 240]. The SURs are unusual in that they are members of a subgroup of the ATP-binding cassette (ABC) superfamily of transporters (ABCC) which lack any intrinsic transport activity [241]. SURs possess 17 membrane-spanning helices grouped into three domains comprising five (TMD0) or six (TMD1 and TMD2) helices respectively (**Fig 1.12**) [236]. The extracellular N-terminus and TMD0 are connected to the other domains via an intracellular loop L0. Additionally, L0 provides the physical interaction with Kir6.x. Two nucleotide binding domains (NBD1 and NBD2) containing Walker A and Walker B motifs are located on the cytosolic side of the plasma membrane in the TMD1-TMD2 linker region and C-terminal region respectively. These Walker motifs confer the ability to bind and hydrolyse ATP. Importantly, only when Kir6.x subunits are co-expressed with an SUR subunit can the properties of the K_{ATP} channel be fully recapitulated [240,

242]. The recent advancement in cryo-electron microscopy (cryo-EM) has led to the publication of multiple K_{ATP} channel structures in recent years and these promise to allow a greater understanding of the molecular details of K_{ATP} channel assembly, gating and pharmacological inhibition [243-251].

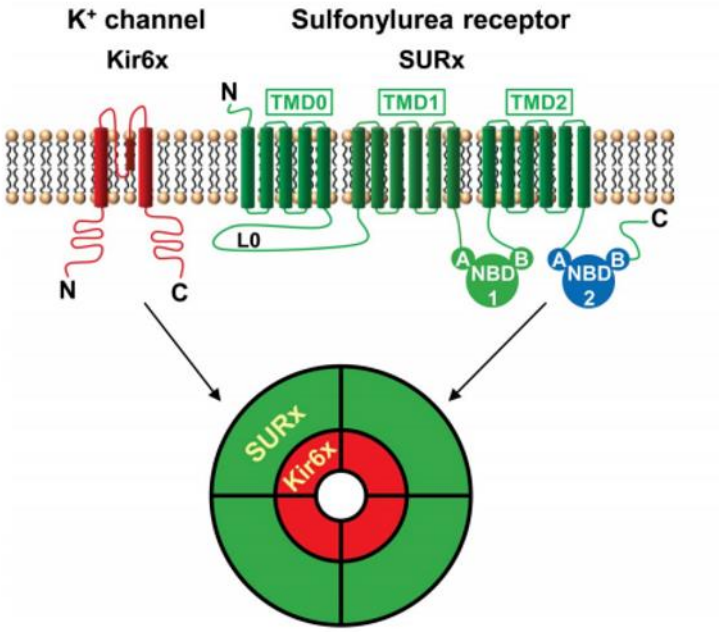

Figure 1.12 Structure of the ATP-sensitive potassium ion (K_{ATP}) channel. Hetero-octameric channels consist of four pore-forming subunits (Kir6.x) and four sulphonylurea receptor subunits (SURx). TMD, transmembrane domain; NBD, nucleotide binding domain; L0, linker region; A and B represent Walker A and B motifs respectively. Taken from [236].

K_{ATP} channels have been found to be expressed in multiple tissues, including cardiac myocytes, pancreatic β cells, skeletal muscle and epithelial cells [236]. Interestingly, the composition of K_{ATP} channels varies between tissue types: the pancreatic β cell channel consists of Kir6.2 and SUR1, whilst Kir6.1 and SUR2B constitute the smooth muscle K_{ATP} channel [236, 252]. Indeed, this structural heterogeneity is likely responsible for the diverse range of functions displayed by K_{ATP} channels (discussed in 1.8.4).

Surprisingly little is known surrounding the mechanisms by which K_{ATP} channel gene expression is controlled. Regulation of *KCNJ11* (Kir6.2) and *ABCC8*

(SUR1) is perhaps best understood; these genes encode pancreatic β cell K_{ATP} channel and their promoters were successfully cloned and analysed in 1998 [253]. Both putative promoters were found to contain several SP1 binding sites and enhancer (E)-box motifs, regions which permit binding of basic helix-loop-helix (bHLH) transcription factors such as c-Myc and HIF1α, perhaps indicating a degree of transcriptional co-regulation. Subsequent cloning of the mouse *ABCC8* promoter confirmed that SP1 was able to bind and activate its transcription, and the pancreatic β cell-expressed transcription factors NeuroD/Beta2 and FOXA2 may also participate in its regulation [254-256]. Interestingly, *ABCC8* expression has been shown to be upregulated in response to hypoxia via a mechanism in which HIF1 drives expression of SP1 [257]. FOXA2 has also been demonstrated to participate in the activation of *KCNJ11* transcription, further supporting the hypothesis of overlapping transcription regulatory networks [256]. Whilst data regarding transcriptional regulation of the other K_{ATP} channel genes (*KCNJ8* and *ABCC9*) is scarce, there is some indication that, at least in the context of cardiac myocytes, Forkhead family transcription factors may have a significant role [258].

Functional expression of K_{ATP} channels requires trafficking to the plasma membrane, a process which can only occur upon correct assembly of the hetero-octameric complexes within the ER. Indeed, when either subunit is expressed alone, ER exit is prevented by arginine-based localisation motifs (RKR) which are present in both subunits and act as ER retention/retrieval signals due to recognition by COPI vesicle coat protein complexes [259, 260]. Truncation of the C-terminus of Kir6.2 can enable the formation of functional channels in the absence of SURx subunits, illustrating that the Kir6.2 RKR motif is located within this portion of the protein [261]. Appropriate channel assembly results in the masking of these signals, thus it is thought to be a mechanism to ensure only

appropriately assembled channels can progress through the secretory pathway [259]. Other cellular proteins have also been reported to be associated with K_{ATP} channel trafficking. Whilst the Kir6.2 RKR motif is fully masked by binding of SUR1, the corresponding motif possessed by SUR1 remains partially exposed in the fully assembled octamer. Complete masking of these RKR motifs requires the recruitment of cytosolic 14-3-3 proteins to the K_{ATP} complex [260, 262]. Indeed, many ion channels and plasma membrane proteins have subsequently been found to possess COPI interaction motifs and require 14-3-3 proteins for efficient trafficking, indicating that this is a key cellular control mechanism [263]. Further, onward trafficking of K_{ATP} channels can be promoted by phosphorylation of the Kir6.2 C-terminus by PKA, at least in the context of cardiac myocytes, which leads to decreased COPI binding and hence silencing of the RKR motif [264]. Other cellular factors associated with the progress of K_{ATP} channels through the secretory system include the heat-shock protein Hsp90, which promotes the efficient folding of SURx subunits, and Derlin-1, a protein involved in ER-associated degradation of misfolded proteins including Kir6.x and SURx [265, 266].

1.8.3 K_{ATP} channel regulation

The mechanisms regulating K_{ATP} channel gating are numerous and highly complex (**Fig 1.13**). A defining property of K_{ATP} channels is that they link the metabolic activity of cells to their membrane potential: a fall in cytoplasmic ATP leads to increased channel opening and thus K^+ efflux. Expression of a C-terminally truncated Kir6.2 which is able to form functional channels in the absence of SURx subunits revealed that sensitivity to ATP is conferred by the Kir6.x subunit [261]. However, co-expression with SUR1 markedly enhanced ATP inhibition, indicating that the SURx subunits also contribute towards ATP

sensitivity possibly due to allosteric effects [261]. Further mutagenesis studies subsequently identified key amino acids within both the N- and C-termini of Kir6.2 that are required for ATP binding [267, 268]. More recent cryo-EM crystal structures have confirmed that residues 182-185 and 332-335 of Kir6.2 form positively-charged binding pockets for ATP, whilst the N48 and R50 residues of the neighbouring Kir6.2 subunit form hydrogen bonds with the adenine base [243, 244, 246]. Each Kir6.x subunit possesses one ATP binding site, thus creating a total of four potential binding sites per channel, although binding of one ATP molecule has been shown to be sufficient to induce channel closure [269, 270].

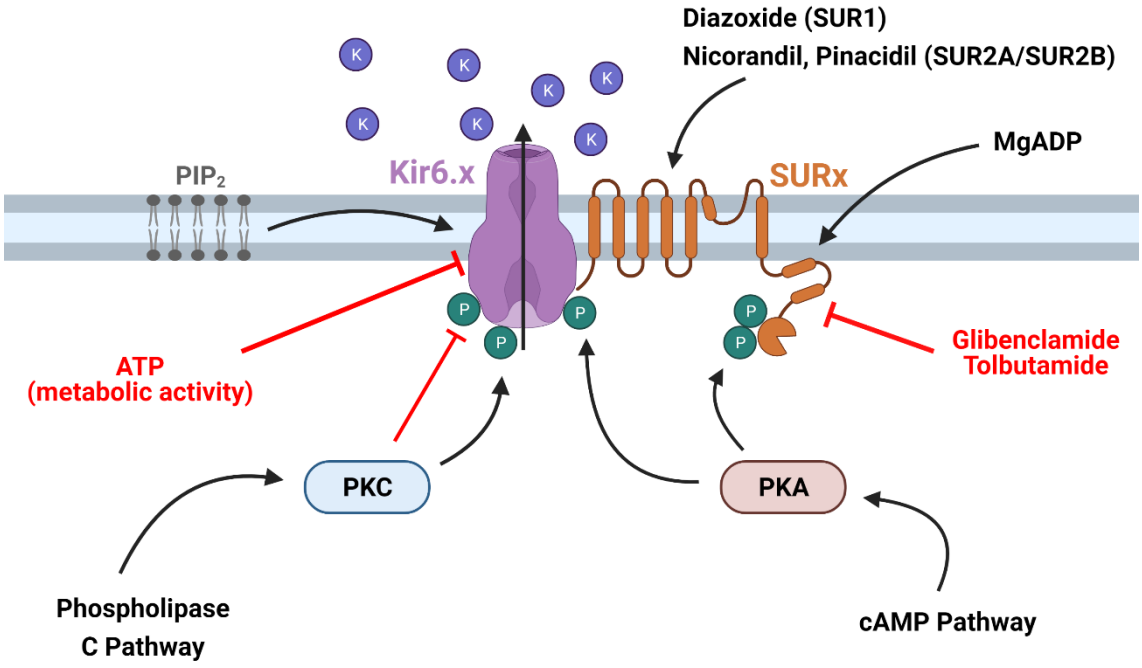

Figure 1.13 Mechanisms regulating the gating of K_{ATP} channels. A defining property of K_{ATP} channels is their inhibition by ATP, thus linking cellular metabolism to membrane potential. Conversely, channel opening is promoted via binding of ADP, in complex with Mg^{2+} ions, to SURx subunits. Membrane lipid composition also regulates gating: the presence of phosphatidyl-inositol 4,5-bisphosphate (PIP_2) promotes K^+ flux. Kinase activity is an important regulator of K_{ATP} activity: phosphorylation of Kir6.1 by protein kinase C (PKC) can inhibit channel activity, but phosphorylation of Kir6.2 subunits promotes channel opening. Phosphorylation by protein kinase A (PKA) promotes channel activity. Multiple pharmacological activators (diazoxide, nicorandil, pinacidil) and inhibitors (glibenclamide, tolbutamide) have also been described. Figure created using BioRENDER.com.

Conversely, binding of ADP to K_{ATP} channels has a stimulatory effect on gating. Sensitivity to ADP is conferred by the SURx subunit, and activation by ADP required complex formation with Mg^{2+} [261, 271, 272]. In the absence of either Mg^{2+} or SURx subunits, ADP has an inhibitory effect presumably due to binding to the ATP-binding pocket present in Kir6.x subunits [261, 273]. MgADP binds to Walker A and B motifs located within the NBDs of SUR subunits [274, 275]. Although MgATP is also able to stimulate K_{ATP} channel activity via binding to the SUR NBDs, it is ~10 fold less efficient than MgADP and this ability is normally masked by the potent inhibitory effects of ATP discussed above [268, 276]. Like many members of the ABC transporter family, SUR subunits possess one catalytically active (i.e. capable of ATP hydrolysis) nucleotide binding site (NBS2) and one unable to hydrolyse ATP (NBS1, the degenerate site); these are formed upon dimerisation of the NBDs, giving a total of eight NBSs per fully-assembled channel [277]. The dimers are antiparallel in nature and as such each NBS contains the Walker A and B motifs of one NBD and the so-called ABC signature sequence (typically LSGGQ) of the other NBD. Given that MgADP is able to activate K_{ATP} channels, it is clear that the hydrolytic activity of NBS2 is not required for channel opening; yet it remains possible that MgATP must first be hydrolysed to MgADP in order to activate the channels [277]. More recently, fluorescence resonance energy transfer has been used to measure in real time the binding of nucleotides to SUR1, revealing that whilst Mg^{2+} is not required for initial binding of ADP, it is necessary for SUR1 conformational changes, NBD dimerisation and channel activation [278].

In addition to nucleotides, it is clear that K_{ATP} channel gating is also dependent on the lipid composition of the plasma membrane. Application of phosphatidyl-inositol 4,5-bisphosphate (PIP_2) has been shown to result in increased K^+ flux

and can even overcome channel inhibition by high ATP concentrations [279]. Despite PIP_2 only being a minor phospholipid component of cell membranes, it has been shown to activate all inward-rectifying K^+ channels [280]. Mutagenesis studies have identified potential residues within the C-terminus of Kir6.2 that may be required for PIP_2 binding [280], although the significance and mechanism of regulation by PIP_2 remain unclear. One possibility is that it may ensure K_{ATP} channels remain inactive until they reach the cell surface as intracellular membrane compartments possess much lower concentrations of PIP_2 [281]. Recent cryo-EM structures indicate that the inhibitory ATP binding site may be located adjacent to the putative PIP_2 binding site on Kir6.2, leading to the hypothesis that binding of these molecules may at least in part be mutually exclusive [246]. Moreover, a recent study has implicated S-palmitoylation, the covalent attachment of fatty acids to cysteine residues, in the regulation of K_{ATP} channel opening [282]. It was discovered that Kir6.2, but not SUR1, was palmitoylated at a conserved C166 residue found in several Kir channels. Palmitoylation was found to positively regulate K_{ATP} channels by increasing their sensitivity to PIP_2.

Furthermore, K_{ATP} channel opening is also regulated by kinase activity. The K_{ATP} channels found in smooth muscle cells of the vasculature, composed of Kir6.1 and SUR2B, can be phosphorylated by PKA [283, 284]. This is the mechanism by which vasodilators such as adrenaline promote relaxation of vascular smooth muscle; PKA acts downstream of the classical cAMP-dependent pathway induced upon binding of a vasodilator to its cognate G protein-coupled receptor (GPCR). Evidence indicates that direct phosphorylation at residues S385 of Kir6.1 and T633, S1387 and S1465 in SUR2B by PKA significantly enhances channel opening [285, 286]. Given that the phosphorylation sites on SUR2B are

situated adjacent to the NBDs, it is conceivable that phosphorylation promotes channel opening via enhancing MgADP binding. PKA phosphorylation sites have also been identified in other K_{ATP} subunits, S372 and T224 of Kir6.2 and S1571 of SUR1, indicating this is likely a general method of K_{ATP} channel regulation [287, 288]. Conversely, binding of vasoconstrictors such as noradrenaline to their GPCRs leads to the closure of K_{ATP} channels via the induction of the phospholipase C (PLC) – protein kinase C (PKC) pathway [289]. Whilst this signalling pathway involves the hydrolysis of PIP_2, this is not thought to significantly affect channel gating [236]. Rather, PKC phosphorylates a cluster of residues in the C-terminus of Kir6.1 in order to promote channel closure [290]. Mechanistically, PKC phosphorylation likely inhibits K_{ATP} channels by facilitating their internalisation in a caveolin-1-dependent manner [291]. Paradoxically, phosphorylation by PKC has been shown to activate the cardiac K_{ATP} channel [292]. These channels consist of Kir6.2 subunits which lack the inhibitory phospho-sites of Kir6.1; rather phosphorylation occurs at an alternative threonine residue, indicating tissue-specific modes regulation exist [293]. However, under conditions of prolonged PKC activation, these Kir6.2-containing K_{ATP} channels may undergo internalisation; suggesting the presence of a negative feedback mechanism that likely evolved to prevent excessive K_{ATP} channel activity [294]. Clearly, the regulation of K_{ATP} channels by PKC is highly complex and warrants further investigation.

Numerous pharmacological inhibitors and activators of K_{ATP} channels have been described. One such group is the sulphonylurea class of drugs, which act to inhibit K_{ATP} channel activity. Multiple compounds in this class have been developed, including tolbutamide and glibenclamide, a second-generation drug which displays increased binding affinity [236]. These compounds have been

used widely for the treatment of type two diabetes mellitus since the 1960s [295], but it was not until much later that their mechanism of action was elucidated [296]. Sulphonylureas induce K_{ATP} channel closure by binding to SURx subunits which, in the context of pancreatic β cells, promotes insulin release. Improvements in electron microscopy have permitted further understanding of this mechanism: it is now thought that the glibenclamide binding pocket is formed from residues in both TMD1 and TMD2 of SUR1 [245]. Functional confirmation was provided by mutagenesis of the residues lining the binding pocket; this diminished glibenclamide-induced channel inhibition [245]. Two of these residues are not conserved in SUR2A, which may account for slight differences in the binding affinities of sulphonylureas [297]. Further, in structures in which the SUR1 NBDs are bound by nucleotides, the pocket becomes too small to accommodate glibenclamide, leading to the hypothesis that association of glibenclamide interferes with conformational changes occurring upon MgADP stimulation [247]. Other agents are also able to inhibit K_{ATP} channel opening, such as the broadly-acting K^+ channel modulator tetraethylammonium [298].

Additionally, a diverse range of pharmacological agents, including diazoxide, nicorandil and pinacidil, are able to activate K_{ATP} channels. Significantly, some of these compounds (e.g. nicorandil, pinacidil) are selective for SUR2A/SUR2B-containing channels, whilst others (e.g. diazoxide) are more specific for SUR1-containing channels [236]. Given the structural diversity of K_{ATP} openers, it is highly likely that multiple binding sites on the SURx subunits exist. Studies indicate that regions within TMD1 of SUR1 and TMD2 of SUR2A/SUR2B may be necessary for binding of channel openers [299]. It is thought that channel activation may be induced by promoting and stabilising the NBD dimers formed upon MgADP binding to SUR1 [278]. The first cryo-EM structure of SUR1 in

complex with NN414, a diazoxide-type channel opener, was recently published; this confirmed the interaction of channel activators with both TMD1 and TMD2 of SUR1 [251].

1.8.4 Biological functions of K_{ATP} channels

The most well-understood function of K_{ATP} channels is in regulating insulin secretion by pancreatic β cells (**Fig 1.14A**) [236]. Insulin promotes the uptake of glucose by skeletal muscle, the liver and adipose tissue and is therefore crucial in maintaining blood glucose homeostasis. After increases in the blood glucose concentration, glucose uptake and subsequent oxidative metabolism leads to an increase in the cellular ATP concentration. K_{ATP} channel activity is hence reduced, resulting in a depolarisation of the plasma membrane and the opening of voltage-dependent Ca^{2+} channels. This then leads to the secretion of insulin-containing vesicles from the cells. An update to this 'canonical' signalling mechanism has recently been proposed whereby the initial increase in cellular ATP that drives K_{ATP} channel closure is instead driven by plasma membrane-localised pyruvate kinase, with oxidative metabolism-derived ATP subsequently ensuring the maintenance of signalling [300, 301]. Paradoxically, K_{ATP} channels are also implicated in the regulation of glucagon secretion by pancreatic α cells, although this is less well characterised [302].

K_{ATP} channels also have important functions in the heart (**Fig 1.14B**). Interestingly, whilst the ventricular K_{ATP} channel is composed of Kir6.2 and SUR2A subunits, the atrial channel instead contains the SUR1 regulatory subunit [303]. Although the role of K_{ATP} channels in the heart is less well understood than in the pancreas, mouse studies indicate that channels may be required for adaptation to stress since Kir6.2$^{(-/-)}$ mice have reduced tolerance to high-intensity exercise [304]. Further, cardiac K_{ATP} channels are implicated in protection from

ischaemia-induced injury [236]. Opening of channels in response to ischaemia is thought to stabilise the plasma membrane potential and shorten action potentials, thus reducing cell contractility and hence the energy demands of myocytes. Indeed, overexpression of SUR2A in mice renders them resistant to both hypoxia- and ischaemia-induced injury [305]. Similarly, Kir6.2-containing K_{ATP} channels in skeletal muscle cells are implicated in preventing muscle damage during strenuous or prolonged exercise [236]. Though the mechanism is unknown, it is reasonable to assume it would be analogous to that described in cardiac muscle.

Biological functions of K_{ATP} channels in smooth muscle cells of the vasculature, composed of Kir6.1 and SUR2B subunits, have also been described (**Fig 1.14C**). Evidence indicates that the channels may be necessary in blood pressure regulation: both $SUR2^{(-/-)}$ and $Kir6.1^{(-/-)}$ mice demonstrate significant hypertension [306, 307]. Mechanistically, as in pancreatic β cells, K_{ATP} channel closure results in membrane depolarisation and influx of Ca^{2+} via voltage-dependent channels. This ultimately causes contraction and hence increased blood pressure. K_{ATP} channels are also expressed in non-vascular smooth muscle cells of the gastrointestinal tract, bladder and respiratory tract. The role of these channels is poorly understood, but application of K_{ATP} channel inhibitors can induce contraction, thus pointing towards mechanistic similarities with vascular smooth muscle cells [236].

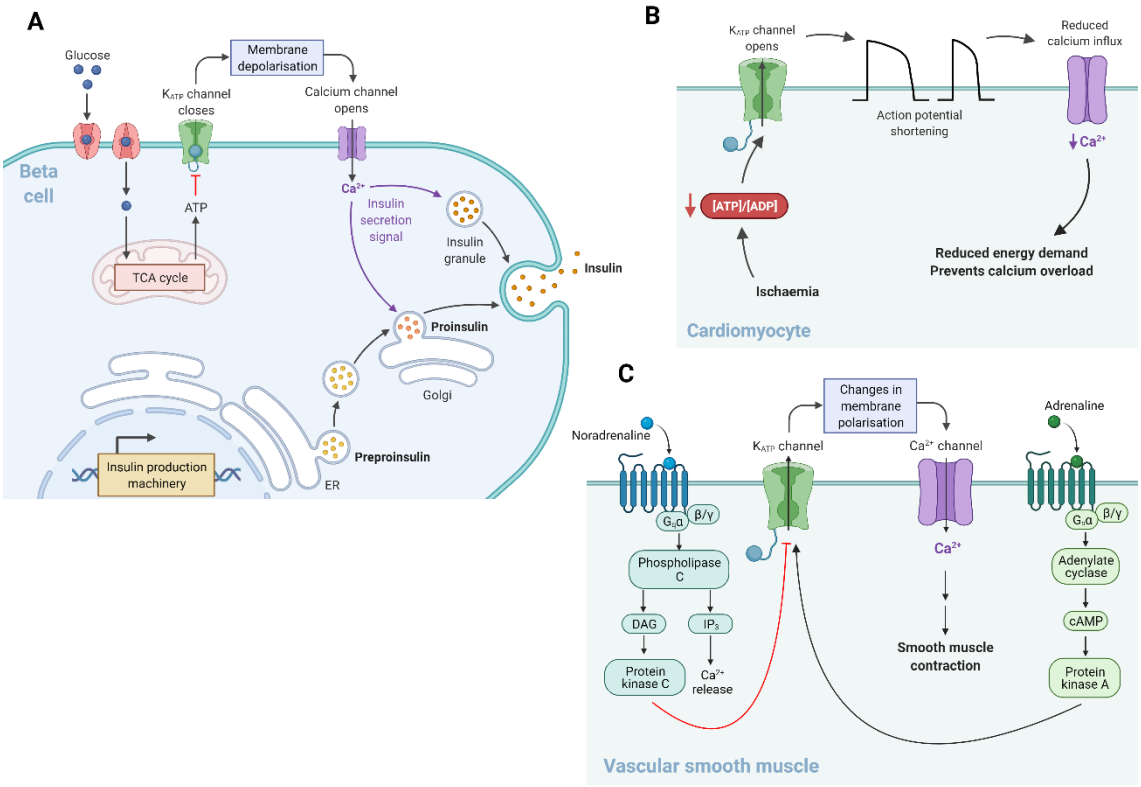

Figure 1.14 Biological functions of K_{ATP} channels. A) Glucose uptake into pancreatic beta cells promotes oxidative metabolism and hence an increase in cellular ATP levels. This results in K_{ATP} closure and membrane depolarisation. Opening of voltage-gated Ca^{2+} channels and Ca^{2+} influx leads to insulin secretion. B) Cardiac K_{ATP} channels provide protection from ischaemia. In response to metabolic insult, K_{ATP} channels open. This stabilises the membrane potential, shortens action potentials and reduces Ca^{2+} influx, hence conserving energy stores and preventing calcium overload. C) K_{ATP} channels in the vascular smooth muscle are implicated in vascular tone and blood pressure regulation. Binding of vasodilators (e.g. adrenaline) to cognate receptors induces activatory protein kinase A signalling. This causes membrane hyperpolarisation, Ca^{2+} channel closure and ultimately smooth muscle relaxation. Conversely, vasoconstrictors (e.g. noradrenaline) induce inhibitory protein kinase C signalling, resulting in K_{ATP} channel closure. Membrane depolarisation, Ca^{2+} channel opening and smooth muscle contraction ensues. Figure created using BioRENDER.com.

1.8.5 K_{ATP} channelopathies

The importance of K_{ATP} channels in a wide variety of tissues, and indeed the diverse range of functions associated with the channels, is reflected in the multiple diseases linked to improper K_{ATP} channel activity (so-called channelopathies). Given the crucial role of K_{ATP} channels in regulating insulin release, it is unsurprising that many of these pathologies are associated with

impaired pancreatic β cell function [308]. One such channelopathy is congenital hyperinsulinism (CHI), a disease in which inappropriately high levels of insulin secretion from pancreatic β cells result in low blood glucose and ultimately a potential loss of consciousness and neurological damage. Whilst a variety of genetic causes have been reported, loss-of-function mutations in either *ABCC8* or *KCNJ11* (Kir6.2) inherited in a recessive manner are the most common cause [309]. Loss of K_{ATP} channel activity can occur due to trafficking mutations in *ABCC8* which reduce cell surface expression, likely due to misfolding, an inability to associate with Kir6.x subunits or indeed rapid endocytosis upon reaching the plasma membrane [236]. Alternatively, the channel may be trafficked correctly but mutations render the SUR1 subunit insensitive to MgADP stimulation [310]. Promisingly, pharmacological chaperones have recently been shown to be able to rescue trafficking mutations and restore K_{ATP} channel surface expression [311].

Conversely, mutations in *ABCC8* and *KCNJ11* that lead to K_{ATP} channel hyperactivity can result in the rare disorder neonatal diabetes mellitus (NDM) [312, 313]. As with CHI, although mutations in several genes can be the cause of NDM, those in K_{ATP} channel genes are the most common. Whilst mechanistically the mutations can act in a variety of ways, all are activating mutations which prevent channel closure in the presence of elevated ATP:ADP ratios and hence result in insufficient insulin secretion by pancreatic β cells [314]. Interestingly, a remarkable genotype-phenotype correlation exists between the degree to which ATP sensitivity of the channel is reduced and the clinical severity presented in the patient [314]. Furthermore, a common polymorphism in *KCNJ11*, which results in a modest reduction in ATP sensitivity, has been linked with the development of type two diabetes mellitus in later life [315]. Management of NDM

typically involves oral sulphonylurea therapy which greatly improves quality of life [308].

Another such channelopathy is Cantu syndrome (CS), a very rare disease first described in 1982 characterised by gain-of-function mutations in *ABCC9* or, less commonly, in *KCNJ8* (Kir6.1) [316-320]. The disorder is typically diagnosed in childhood and a multitude of disease manifestations have been reported: hypertrichosis (excessive hair growth) and facial dysmorphology are present in all individuals, with many additionally suffering from several heart and cardiovascular abnormalities as well as migraines [321]. However, a mechanistic understanding of how K_{ATP} channel over-activity leads to such diverse phenotypes remains to be elucidated. Of particular interest is a recent study demonstrating, using a mouse model of CS, that many of the cardiovascular phenotypes CS patients present with can be reversed through administration of the K_{ATP} channel inhibitor glibenclamide, opening up a potential new avenue for therapeutic intervention [322].

1.8.6 Role of K_{ATP} channels in the control of cell proliferation

The importance of ion channels in the regulation of the cell cycle and cell proliferation has become increasingly recognised in recent years [323-325]. A model has been proposed in which the plasma membrane potential of cells undergoes a rapid hyperpolarisation during progression through the G1-S phase checkpoint, followed by a more prolonged period of depolarisation during G2 and mitosis [325]. It is thought that K^+ channels are particularly important for the initial hyperpolarisation as a number of K^+ efflux channels have been observed to be increased in expression and activity during G1 [324, 325]. Interestingly, observations in a variety of cell types indicate that K^+ channel expression may

increase in response to mitogens, opening up the possibility of bidirectional signalling networks [324].

Given the number of ion channel genes reportedly dysregulated during carcinogenesis, it has been argued that cancer could be classified as a channelopathy [326]. Significantly, ion channels may represent ideal candidates for novel cancer therapeutics given the abundance of licensed and clinically available drugs targeting the complexes which could be repurposed if demonstrated to be effective [327]. K^+ channel activity has been observed in a wide variety of cancer cells [323], and K_{ATP} channels are no exception to this: expression in multiple neoplasms has been reported, including breast, gastric and cervical cancer, as well as hepatocellular carcinoma and glioma cells [328-332]. Not unsurprisingly, channel inhibition using the pharmacological inhibitors glibenclamide or tolbutamide was shown to result in a G1 phase arrest, consistent with the hypothesis that K_{ATP} channels are required for the G1/S-phase associated hyperpolarisation of the plasma membrane potential [329, 330, 333]. Additionally, some reports indicate K_{ATP} channel inhibition in cancer cells can lead to the induction of apoptosis [328, 330, 331], although other investigations have found no evidence of this [329, 332]. This may potentially reflect the cell type-specific roles K_{ATP} channels, or perhaps may be a result of differing subunit compositions in the cell types analysed. Despite this, the mechanism by which K_{ATP} channel activity promotes proliferation remains to be elucidated. One study has suggested that signalling may proceed via the MAPK-ERK1/2 pathway: stimulation of K_{ATP} channels using diazoxide promoted ERK1/2 phosphorylation, whilst treatment with the MEK1/2 inhibitor U0126 prevented any diazoxide-induced increase in cell proliferation [333]. However, this remains an area of active research.

Interestingly, two recent studies have suggested that the SUR1 subunit may have additional oncogenic functions in cancer independent of K_{ATP} channels. A direct interaction between SUR1 and the p70S6K kinase was reported, which subsequently led to increased activation of the mammalian target of rapamycin complex 1 (mTORC1) signalling pathway [334, 335]. However, given the lack of supporting evidence for channel-independent SURx functions and the current paradigm for K_{ATP} channel assembly, in which neither subunit is trafficked beyond the ER in the absence of the other, these findings remain highly controversial.

1.9 Aims of the project

Despite the availability of highly effective vaccines against HPV, there are currently no specific anti-viral therapies for the treatment of HPV infection or HPV-induced malignancies. Therefore, a greater understanding of the mechanisms by which HPV modulates the host cell environment in order to drive transformation is required such that novel therapies can be identified. Preliminary studies in the Macdonald lab have recently identified a potentially key role for host K_{ATP} channels in regulating oncogene expression in primary keratinocytes harbouring the HPV18 genome. Host ion channels represent excellent candidates for novel therapies given the abundance of licensed and clinically available drugs targeting the complexes which could be repurposed if shown to be effective. This PhD will build upon these initial findings, aiming to undertake a complete assessment of the role of K_{ATP} channels in HPV+ cervical cancer cells, before extending this to reveal the impact of inhibiting K_{ATP} channels in HPV16+ HNSCC cells.

Specifically, the aims of this thesis are:

1) To reveal the importance of host K_{ATP} channel activity for HPV gene expression in cervical cancer cells.

2) To understand the role of K_{ATP} channels in key cellular phenotypes including proliferation, cell cycle progression, epithelial to mesenchymal transition (EMT) and apoptosis.
3) To investigate the importance of K_{ATP} channels in HPV+ and HPV- HNSCC cell lines.

Chapter 2 Materials and Methods

2.1 Bacterial cell culture

2.1.1 Preparation of chemically competent bacteria

DH5α *Escherichia coli* cells were streaked out onto Luria-Bertani (LB) agar plates (10 g tryptone, 10 g NaCl, 5 g yeast extract, 15 g agar, ddH_2O up to 1 L, pH 7.0) in the absence of antibiotics and incubated at 37°C overnight. A single colony was selected and inoculated into 20 mL 2xYT media (16 g tryptone, 10 g yeast extract, 5 g NaCl, ddH_2O up to 1 L, pH 7.0) and grown with shaking for 6 hours. The starter culture was then used to inoculate 200 mL 2xYT media, which was grown at 18°C with shaking until the OD reached 0.6-0.8. The culture was incubated on ice for 10 min, then centrifuged at 2500 x g for 10 min at 4°C to pellet cells. Cells were resuspended in 80 mL ice-cold transformation buffer (10 mM PIPES-KOH pH 6.7, 15 mM $CaCl_2$, 250 mM KCl, 55 mM $MnCl_2$) and incubated on ice for 10 min. Cells were centrifuged as above and the resulting pellet resuspended in 18.6 mL ice-cold transformation buffer. 1.4 mL DMSO was then added slowly with gentle stirring, followed by a further incubation period on ice for 10 min. Cells were aliquoted and snap frozen in dry ice before storing at -80°C. Preparation of chemically competent bacteria was performed by Mr Diego Barba Moreno.

2.1.2 Bacterial cell growth

Chemically competent DH5α *E.coli* cells (see 2.1.1) were used to prepare plasmid DNA. Cells were grown in LB liquid medium (10 g tryptone, 10 g NaCl, 5 g yeast extract, ddH_2O up to 1 L, pH 7.0) with shaking or on solid LB agar at 37°C overnight. The appropriate antibiotics were added to the media to allow for selection (100 µg/mL ampicillin or 50 µg/mL kanamycin).

2.1.3 Transformation of bacteria

50 µL chemically competent DH5α cells were thawed on ice before incubating with 1 µL plasmid DNA for 20 min on ice. Cells were heat-shocked at 42°C for 45 sec before returning to ice for 5 min. 950 µL LB media was added and cells incubated at 37°C with shaking for 1 hour. Transformed cells were spread onto LB agar plates containing the appropriate antibiotic and incubated overnight at 37°C. The plasmids used in this thesis are detailed in **Appendix Table 1**.

2.1.4 Plasmid DNA preparation

For small-scale preparation of plasmid DNA, 10 mL LB media containing the appropriate antibiotic was inoculated with a single colony from an LB agar plate and incubated overnight at 37°C with shaking. Cells were harvested by centrifugation (4000 x g, 30 min, 4°C) and plasmid DNA purified using the Monarch® Plasmid Miniprep Kit (T1010, New England Biolabs (NEB)). DNA was eluted in 30 µL nuclease-free water.

To prepare plasmid DNA on a larger scale, a starter culture of 20 mL LB media containing the appropriate antibiotic was inoculated with a single colony from an LB agar plate and incubated at 37°C for 8 hours with shaking. This culture was added to 80 mL LB media containing appropriate antibiotic and grown at 37°C overnight with shaking. Cells were harvested by centrifugation (4000 x g, 30 min, 4°C) and plasmid DNA purified using the QIAGEN Plasmid Maxi Kit (12163, Qiagen) following the provided protocol. DNA was eluted in 200 – 600 µL nuclease-free water as appropriate.

Plasmid DNA concentration was determined using a NanoDrop™ One Microvolume UV-Vis Spectrophotometer (ND-ONE-W, ThermoFisher Scientific).

2.1.5 Preparation of glycerol stocks

For long-term storage of transformed bacteria, 500 µL of 50% (v/v) glycerol solution was added to 500 µL of an overnight bacterial culture and mixed by pipetting. Glycerol stocks were frozen immediately at -80°C.

2.2 Site-directed mutagenesis

Mutagenesis was performed using the Q5® Site-Directed Mutagenesis Kit (E0554, NEB). Plasmid DNA was mutated via a PCR reaction using the cycling conditions outlined in the kit protocol. Custom primers (**Appendix Table 2**) were designed using NEBaseChanger™ software (NEB) and purchased from Integrated DNA Technologies (IDT).

To confirm successful amplification, PCR products were separated by agarose gel electrophoresis using 1% agarose gels (1% (w/v) agarose in TAE buffer (40 mM Tris base, 20 mM acetic acid, 1 mM EDTA)). Bands were visualised through the addition of SYBR™ Safe DNA gel stain (S33102, Invitrogen) to gels. 2 µL 6X gel loading dye (B7025S, NEB) was added to 10 µL PCR product and samples run at 100 V for 1 hour in TAE buffer alongside 1 kb Plus DNA Ladder (N3200S, NEB). Agarose gels were imaged using an InGenius gel documentation system (Syngene).

Subsequently, 1 µL of the remaining PCR products were used in KLD treatments as outlined in the kit protocol to degrade template DNA and ligate PCR products. Chemically competent bacteria were then transformed with 5 µL of each KLD mix as described in 2.1.3 and plasmid DNA prepared as before (2.1.4).

Sanger sequencing was performed by GENEWIZ to confirm successful mutagenesis using vector-specific sequencing primers. The resulting chromatograms were analysed using BioEdit 7.2 software.

2.3 Mammalian cell culture

2.3.1 Cell lines and maintenance

The mammalian transformed cell lines used in this thesis are detailed in **Appendix Table 3**. All cells were maintained in either Dulbecco's Modified Eagle Medium (DMEM; D6429, Sigma-Aldrich) supplemented with 10% foetal bovine serum (FBS; 10500064, Gibco) and 50 U/mL penicillin-streptomycin (15070063, Gibco), or Eagle's Minimum Essential Medium (EMEM; M4655, Sigma-Aldrich) supplemented with 20% FBS, 1% non-essential amino acids solution (NEAA; 11140068, Gibco) and 50 U/mL penicillin-streptomycin. These are henceforth referred to as complete media. Cells were grown in T75 flasks (Sarstedt) kept in a humidified incubator at 37°C and 5% CO_2 (Sanyo). All cell culture work was carried out in a Class II biological safety cabinet.

Upon reaching ~80-90% confluency, cells were passaged. Media was aspirated, cells washed once with sterile phosphate-buffered saline (PBS) and detached by applying 1X trypsin-EDTA solution (0.05% trypsin, 0.02% EDTA in sterile PBS). Cells were returned to the incubator until they appeared rounded. Once detached, trypsin was inactivated via the addition of complete media. Cells were then either reseeded at a 1:2-1:10 cell suspension:complete media ratio as appropriate for further culture or counted manually using a haemocytometer and seeded as necessary for future experiments.

2.3.2 Freezing and thawing of cell lines

In order to freeze cells for long term storage, cells were counted manually using a haemocytometer after routine passaging and pelleted by centrifugation at 700 x g for 5 min at 4°C. Cells were resuspended in an appropriate volume of freezing media (10% DMSO, 90% complete media) to give a 1 x 10^6 cells/mL suspension.

This was aliquoted into cryotubes and placed in a Mr Frosty™ Freezing Container (5100-0001, ThermoFisher Scientific) overnight at -80°C before transferring to liquid nitrogen.

To revive frozen cells, cryotubes were removed from liquid nitrogen and placed on ice before transferring to a 37°C water bath until defrosted. The 1 mL cell suspension was placed into a cell culture flask with 9 mL complete media and returned to the incubator overnight. Growth media was replaced with fresh media the following morning. A minimum of two passages were performed before using cells in experiments.

2.3.3 Serum starvation

Where necessary, serum starvation was performed prior to further experimental procedures to lower the basal level of activation of signalling pathways of interest. For this, complete media was removed and cells washed thoroughly with sterile PBS. DMEM supplemented with 50 U/mL penicillin-streptomycin only (i.e. 0% FBS) was added and cells incubated under the described conditions for 24 hours before performing the required experimental procedures.

2.3.4 Transfection of plasmid DNA

The plasmids used in this thesis are detailed in **Appendix Table 1**. For transfection of plasmid DNA, cells were seeded into six-well plates at an appropriate density and incubated overnight as described. The required amount of DNA was added to 200 µL Opti-MEM™ I Reduced Serum Media (11058021, Gibco). In a separate tube, the required volume of Lipofectamine™ 2000 Transfection Reagent (11668019, Invitrogen) to give a 1:2.5 DNA:Lipofectamine ratio was added to 200 µL Opti-MEM. After incubating for 5 min at RT, the diluted Lipofectamine was added to the diluted DNA, mixed gently by pipetting and

incubated for a further 20 min. Culture media was removed from cells and replaced with Opti-MEM after washing once with sterile PBS, before adding the transfection mix dropwise. Cells were incubated overnight before replacing the Opti-MEM with complete media. Cells were returned to the incubator until the experiment endpoint.

2.3.5 Transfection of siRNA

The siRNAs used in this thesis are outlined in **Appendix Table 4**. For transfection of siRNA, cells were seeded into six-well plates at an appropriate density and incubated overnight as described. The required amount of siRNA was added to 200 µL Opti-MEM, whilst in a separate tube, the required volume of Lipofectamine to give a 1:2 siRNA:Lipofectamine ratio was added to 200 µL Opti-MEM. After incubating for 5 min at RT, the diluted Lipofectamine was added to the diluted siRNA, mixed gently by pipetting and incubated for a further 20 min. Culture media was removed from cells and replaced with Opti-MEM after washing once with sterile PBS, before adding the transfection mix dropwise. Cells were incubated overnight before replacing the Opti-MEM with complete media. Cells were returned to the incubator until the experiment endpoint.

2.3.6 Production of 2nd generation lentivirus

To prepare lentiviruses, HEK293TT cells were seeded at a density of 4.5 x 10^5 cells/well into six-well culture plates overnight. At 24 hours post-seeding, cells were co-transfected with 0.8 µg pCRV1-NLGP, 0.4 µg pCMV-VSV-G and 0.8 µg of either pZIP-hEF1α-zsGreen-Puro-shNTC or one of three pZIP-hEF1α-zsGreen-Puro-shSUR1 constructs using the described protocol for transfection of plasmid DNA (2.3.4). Successful transfection was confirmed by immunofluorescent visualisation of ZsGreen expression. At 48 hours post-

transfection, virus-containing supernatant was harvested from cells and passed through a 0.45 µm Minisart™ NML Syringe Filter (10109180, Sartorius) to remove cell debris. Sequence information for the shRNAs is detailed in **Appendix Table 5**.

2.3.7 Lentivirus transduction

For transduction of lentiviruses, cells were seeded at an appropriate density in 60 mm culture dishes and incubated as described for 24 hours. Media was removed and replaced with filtered virus-containing culture media prepared as described (2.3.6). Cells were incubated overnight at 37°C in the presence of viral vectors, before removing viral supernatant and replacing with fresh media after washing cells once in sterile PBS. Cells were then returned to the incubator.

2.3.8 Selection of transduced cells

At 48 hours post-transduction, cells were split as necessary using the described protocol (2.3.1). To select for successfully transduced cells, complete media was supplemented with 1 µg/mL puromycin (ant-pr-1, InvivoGen) and cells cultured for 3-6 days. Selection was considered to be complete once non-transduced cells displayed complete cell death upon visual inspection. Surviving cells were returned to media lacking puromycin and expanded into T75 flasks.

2.3.9 Production of monoclonal cell lines

After transduction and selection as described (2.3.7, 2.3.8) monoclonal cell lines were generated through fluorescence-activated cell sorting (FACS). Upon routine passaging, cells were counted manually using a haemocytometer before pelleting by centrifugation at 300 x g for 5 min at 4°C. The supernatant was discarded, and cells resuspended in an appropriate volume of sorting buffer (sterile PBS containing 25 mM HEPES and 2% (v/v) FBS) to give a 1 x 10^6 cells/mL

suspension. Cells were sorted using a FACS Melody (BD Biosciences) running FACS Chorus software (BD Biosciences) by gating for single cells expressing zsGreen. Non-transduced cells were also prepared as described and used as a negative control. For each starting population, one cell was sorted per well of a 96-well plate containing complete DMEM. Cells were then incubated as described and expanded into monoclonal populations. FACS was performed by Dr Sally Boxall and Dr Ruth Hughes (FBS Bioimaging and Flow Cytometry Facility, University of Leeds).

2.4 Protein biochemistry

2.4.1 Cell lysis

Cell culture media was aspirated and cells washed once in PBS. Cells were then scraped into an appropriate volume of radioimmunoprecipitation assay (RIPA) buffer (50 mM Tris-HCl pH 7.4, 150 mM NaCl, 1% (v/v) Triton X-100, 0.5% (w/v) sodium deoxycholate, 0.1% (w/v) sodium dodecyl sulphate (SDS), 10 mM NaF, 1X cOmplete™ EDTA-free Protease Inhibitor Cocktail (PI; 11873580001, Roche)). Cells were incubated on ice for 20 min or snap-frozen at -80°C overnight to aid lysis. Lysates were then transferred to Eppendorf tubes and centrifuged at 17,000 x g for 10 min at 4°C to pellet cell debris.

2.4.2 Bicinchoninic acid (BCA) assay for protein concentration

The protein concentration of whole cell lysates was determined using a Pierce™ BCA Protein Assay Kit (23225, ThermoFisher Scientific) following the provided protocol for microplates. After a 15 min incubation at room temperature (RT), absorbance at 562 nm was determined using a PowerWave XS2 Microplate Spectrophotometer and Gen5 1.11 software (BioTek Instruments Inc.). Standard

curves were generated in Excel (Microsoft) using the absorbance values in order to determine sample protein concentration.

2.4.3 SDS polyacrylamide gel electrophoresis (SDS-PAGE)

Proteins were resolved by molecular weight using Mini-PROTEAN Tetra cells (Bio-Rad). 8-15% SDS-polyacrylamide gels were prepared according to desired resolution (resolving gel: 8-15% (v/v) acrylamide, 375 mM Tris-HCl pH 8.8, 0.1% (w/v) SDS, 0.1% (w/v) APS, 0.1% (v/v) TEMED; stacking gel: 6% (v/v) acrylamide, 125 mM Tris-HCl pH 6.8, 0.1% (w/v) SDS, 0.1% (w/v) APS, 0.1% (v/v) TEMED). 2X Laemmli sample buffer (125 mM Tris-HCl pH6.8, 4% (w/v) SDS, 20% (v/v) glycerol, 0.004% (w/v) bromophenol blue, 1% (v/v) 2-mercaptoethanol) was added to whole cell lysates containing 20 - 50 µg protein and boiled for 10 min. Samples were loaded alongside BLUeye Pre-Stained Protein Ladder (S6-0024, Geneflow). Electrophoresis was carried out at 80 - 160 V in 1 x SDS running buffer (25 mM Tris base, 192 mM glycine, 0.1% (w/v) SDS) until proteins were resolved.

2.4.4 Western blotting

Separated proteins were transferred to Amersham™ Protran™ NC Nitrocellulose membranes (10600002, GE Healthcare) using a Trans-Blot® Turbo™ Transfer System (Bio-Rad) set to 1 A, 25 V for 30 min. The composition of transfer buffer used was as follows: 25 mM Tris base, 192 mM glycine, 20% (v/v) methanol. Membranes were then blocked by incubating in blocking solution (5% (w/v) skimmed milk powder in TBS-T (25 mM Tris-HCl pH 7.5, 138 mM NaCl, 0.1% (v/v) Tween 20)) for 1 hour at RT. Primary antibodies (**Appendix Table 6**) were diluted in either blocking solution or 5% (w/v) bovine serum albumin (BSA) in TBS-T as necessary and incubations performed overnight at 4°C on a rocker.

After washing four times for 5 min with TBS-T, membranes were incubated with the appropriate horseradish peroxidase-conjugated secondary antibody (**Appendix Table 6**) diluted 1:5000 in blocking solution for 2 hours at RT. Another four washes with TBS-T for 5 min were performed to remove unbound secondary antibody. Blots were visualised by the enhanced chemiluminescence (ECL) method: membranes were briefly incubated in equal volumes of Molly Brew™ solution A (100 mM Tris-HCl pH 8.5, 2.5 mM luminol, 0.4 mM p-coumaric acid) and solution B (100 mM Tris-HCl pH 8.5, 0.02% (w/w) H_2O_2) before being placed in a protective sleeve and exposed to CL-XPosure™ film (34090, ThermoFisher Scientific). Films were developed using an Xograph Compact X4 machine. To allow reprobing, membranes were incubated with ReBlot Plus Strong Antibody Stripping Solution (2504, Sigma-Aldrich) for 10 min at RT.

2.5 Ion channel modulators and small molecule inhibitors

The chemical compounds used in this study are detailed in **Table 2.1**. The concentration used for each drug compound was optimised to ensure minimal off-target effects.

Table 2.1 Ion channel modulators and small molecule inhibitors used in this study. Drugs were used at the concentrations listed here unless stated otherwise. Stock solutions, typically at 1000X concentration, were prepared in all cases.

Drug	Function	Source	Dissolved in	Final concentration
TEA	Broad spectrum K^+ channel inhibitor	Sigma-Aldrich (T2265-25G)	H_2O	25 mM
Quinine		Sigma-Aldrich (145904-10G)	DMSO	100 µM

Drug	Function	Source	Dissolved in	Final concentration
Quinidine		Sigma-Aldrich (Q3625-5G)	DMSO	100 µM
Glibenclamide	K_{ATP} channel inhibitor	Sigma-Aldrich (G0639-5G)	DMSO	10 µM
Tolbutamide		Sigma-Aldrich (T0891-25G)	DMSO	200 µM
Diazoxide	K_{ATP} channel activator	Sigma-Aldrich (D9035)	DMSO	50 µM
Mithramycin A	SP1 inhibitor	Active Motif (14129)	DMSO	50 nM
Thymidine	Inhibits DNA synthesis; causes G1/S arrest	Sigma-Aldrich (T9250-5G)	H_2O	2 mM
RO3306	CDK1 inhibitor; causes G2 arrest	Sigma-Aldrich (217699-5MG)	DMSO	9 µM
Nocodazole	Inhibits microtubule polymerisation; causes mitotic arrest	Stratech (A8487-APE-10mg)	DMSO	100 nM
U0126	MEK1/2 inhibitor	Cell Guidance Systems (SM106-5)	DMSO	20 µM
Staurosporine	Broad spectrum kinase inhibitor; induces apoptosis	Cambridge Bioscience (CAY81590-500 ug)	DMSO	1 µM

2.6 Reverse transcription-quantitative PCR (RT-qPCR)

2.6.1 Cell lysis and RNA extraction

Cells were lysed by aspirating culture media, washing once with PBS and scraping cells into an appropriate volume of TRK lysis buffer (Omega Bio-tek). Cells were incubated on ice for 20 min or snap-frozen at -80°C overnight to aid lysis. Total RNA was extracted from cells using the E.Z.N.A.® Total RNA Kit I (R6834-02, Omega Bio-Tek) following the provided protocol for cultured cells. RNA was eluted in 40 µL nuclease-free water and the concentration determined using a NanoDrop™ One Microvolume UV-Vis Spectrophotometer. RNA was aliquoted and diluted to 50 ng/µL before storing at -80°C until required in downstream analysis.

2.6.2 Quantitative PCR (qPCR)

qPCR was performed using the GoTaq® 1-Step RT-qPCR System (A6020, Promega) following the manufacturer's protocol. Reactions were performed in 96-well plates with each consisting of: 50 ng RNA, 5 µL GoTaq® qPCR Master Mix, 0.2 µL GoScript™ RT Mix, 500 nM each of forward and reverse primers, and nuclease-free water up to a total volume of 10 µL. qPCR reactions were performed using a CFX Connect Real-Time PCR Detection System (Bio-Rad) with the following cycling conditions: reverse transcription for 10 min at 50°C, reverse transcriptase inactivation/polymerase activation for 5 min at 95°C, followed by 40 cycles of denaturation (95°C for 10 sec) and combined annealing, extension and data collection (60°C for 30 sec). This was followed by a melt curve analysis consisting of 5 sec each at 0.5°C increments between 65°C and 95°C. Data was examined using CFX Maestro software (Bio-Rad) before exporting to Excel for analysis via the ΔΔCt method to determine relative expression levels [336].

The primer sequences used in this thesis are detailed in **Appendix Table 7**; with *U6* used as a normalising gene. Where necessary, primers were designed using Primer-BLAST software (NIH) to ensure primers were gene-specific and spanned an exon-exon junction. OligoAnalyzer (IDT) was used to ensure primers displayed minimal complementarity and lacked internal secondary structures. All primers were purchased from IDT.

2.7 Chromatin immunoprecipitation (ChIP)

2.7.1 Preparation of chromatin

Three 100 mm culture dishes of cells at 80-90% confluency were used per experimental condition. Following treatment as required, cells were fixed via addition of formaldehyde solution (8187081000, Sigma-Aldrich) directly to culture media at a final concentration of 1% (v/v) and incubated for 10 min at RT. Fixation was quenched by adding glycine at a final concentration of 125 mM and cells incubated for a further 5 min. Cells were washed twice in ice-cold PBS, before scraping into 15 mL PBS and pelleting by centrifugation at 700 x g for 5 min at 4°C. Cells were lysed with 2 mL lysis buffer 1 (10 mM Tris-HCl pH 8.0, 10 mM NaCl, 0.2% (v/v) NP-40, 50 µg/mL phenylmethylsulphonyl fluoride (PMSF), 1X PI) on ice for 10 min and nuclei pelleted by centrifugation at 700 x g for 5 min at 4°C. The supernatant was removed, and nuclei lysed in 1 mL lysis buffer 2 (50 mM Tris-HCl pH 8.1, 10 mM NaCl, 1% (w/v) SDS, 50 µg/mL PMSF, 1X PI). Chromatin was sheared immediately following lysis by sonication using a Soniprep 150 (MSE). Sonication was performed for 10 bursts of 15 sec at 50% amplitude, with 1 min on ice between bursts. Cell debris was pelleted by centrifugation at 1200 x g for 10 min at 4°C.

2.7.2 Immunoprecipitation (IP)

To perform the IP, 400 µL chromatin was diluted five-fold in dilution buffer (20 mM Tris-HCl pH 8.0, 150 mM NaCl, 2 mM EDTA, 0.01% (w/v) SDS, 0.1% (v/v) Triton X-100, 50 µg/mL PMSF, 1X PI) to give a total volume of 2 mL. Chromatin was precleared to reduce non-specific binding by incubating with 10 µL Pierce™ Protein A/G Magnetic Beads (88802, ThermoFisher Scientific), prewashed in dilution buffer three times, for 30 min at 4°C with gentle rotation. Beads were collected using a 12-tube magnet (36912, Qiagen). A 40 µL aliquot of the supernatant was taken to use as a 2% input sample and stored at -80°C until required. 7.5 µL of cJun antibody (9165, Cell Signalling Technology (CST)), or an equivalent amount of isotype-matched rabbit IgG antibody (ab37415, Abcam), was added to the remaining chromatin and incubated overnight at 4°C with gentle rotation.

The following day, 25 µL Pierce™ Protein A/G Magnetic Beads were added to each IP and samples incubated for 2 hours at 4°C with gentle rotation. Beads were collected as before using a 12-tube magnet. Beads were sequentially washed twice with 750 µL low salt wash buffer (20 mM Tris-HCl pH 8.0, 50 mM NaCl, 2 mM EDTA, 0.1% (w/v) SDS, 1% (v/v) Triton X-100), twice with 750 µL high salt wash buffer (20 mM Tris-HCl pH 8.0, 500 mM NaCl, 2 mM EDTA, 0.01% (w/v) SDS, 1% (v/v) Triton X-100), once with 750 µL LiCl wash buffer (10 mM Tris-HCl pH 8.0, 250 mM LiCl, 1 mM EDTA, 1% (v/v) NP-40, 1% (w/v) sodium deoxycholate), and twice with 750 µL TE buffer (10 mM Tris-HCl pH 8.0, 1 mM EDTA). Beads were collected using a magnetic rack between each wash.

DNA was eluted by adding 100 µL elution buffer (0.1 M $NaHCO_3$, 0.1% (w/v) SDS) and incubating at 37°C for 15 min with vortexing. Beads were collected and the supernatant transferred to a fresh tube. This was repeated and eluates

combined. Beads were washed with 200 µL TE buffer and collected as before, and the supernatant combined with previous eluates to give a total volume of 400 µL. The 2% input sample taken prior to the IP was defrosted and the volume adjusted to 400 µL by adding 200 µL elution buffer and 160 µL TE buffer.

To reverse crosslinking and to degrade RNA, 2 µL RNase A (EN0531, ThermoFisher Scientific) and 24 µL 5 M NaCl were added to each tube, and samples incubated overnight at 65°C with vortexing. The following day, 10 µL proteinase K (K1037, ApexBio Technology) was added and samples incubated at 55°C for 2 hours with vortexing to degrade proteins.

2.7.3 DNA purification

DNA was purified via phenol-chloroform extraction. One volume (~450 µL) of phenol:chloroform:isoamyl alcohol 25:24:1 (P3803, Sigma-Aldrich) was added to each sample and tubes were shaken vigorously for at least 1 min. Tubes were centrifuged at 17,000 x g for 5 min at RT to separate the phases. The upper aqueous phase containing DNA was transferred to a fresh tube. To this, 2 volumes (~900 µL) of ethanol, 1/10 volume (~45 µL) 3M sodium acetate pH 5.2, and 1 µL glycogen (R0551, ThermoFisher Scientific) were added and the samples vortexed to mix. Tubes were incubated at -80°C for ~1 hour and then centrifuged at 17,000 x g for 10 min at 4°C to pellet DNA. The supernatant was removed, and the pellet washed twice in 500 µL 70% (v/v) ethanol before centrifuging at 17,000 x g for 5 min at 4°C. The pellet was air-dried, then resuspended in 30 µL nuclease-free H_2O.

2.7.4 Quantitative PCR (qPCR)

qPCR was performed using the GoTaq® qPCR System (A6001, Promega) following the manufacturer's protocol. Reactions were performed in 96-well plates

with each consisting of: 1 µL purified DNA, 5 µL GoTaq® qPCR Master Mix, 500 nM each of forward and reverse primers, and nuclease-free water up to a total volume of 10 µL. qPCR reactions were performed using a CFX Connect Real-Time PCR Detection System (Bio-Rad) with the following cycling conditions: polymerase activation for 3 min at 95°C, followed by 40 cycles of denaturation (95°C for 15 sec) and combined annealing, extension and data collection (60°C for 1 min). This was followed by a melt curve analysis consisting of 5 sec each at 0.5°C increments between 65°C and 95°C. Data was examined using CFX Maestro software (Bio-Rad) before exporting to Excel for analysis by calculating fold enrichment over IgG. The primer sequences used for qPCR analysis of ChIP DNA are detailed in **Appendix Table 8**.

2.8 Electrophysiology

HeLa cells were seeded on coverslips in 12-well culture plates at 10-20% confluency to prevent cell-cell contact. Following attachment, cells were treated with DMSO, 10 µM glibenclamide, 50 µM diazoxide, or with both channel modulators in combination for 16 hours. Following treatment, patch pipettes (2–4 MΩ) were filled with pipette solution (5 mM HEPES-KOH pH 7.2, 140 mM KCl, 1.2 mM MgCl2, 1 mM CaCl2, 10 mM EGTA, 1 mM MgATP, 0.5 mM NaUDP) and culture media removed from cells and replaced with external solution (5mM HEPES-KOH pH 7.4, 140 mM KCl, 2.6 mM CaCl2, 1.2 mM MgCl2). Whole cell patch clamp recordings were performed using an Axopatch 200B amplifier/Digidata 1200 interface controlled by Clampex 9.0 software (Molecular Devices). A series of depolarising steps, from −100 to +60 mV in 10-mV increments for 100 ms each, was applied to cells and the K^+ current measured. Offline analysis was performed using the data analysis package Clampfit 9.0

(Molecular Devices). Electrophysiology was performed by Dr Holli Carden (University of Leeds).

2.9 Flow cytometry

2.9.1 Cell cycle analysis

Cells were harvested at the appropriate experimental endpoint and fixed overnight in 70% ethanol at -20°C. Ethanol was removed by centrifugation at 500 x g for 5 min and cells washed twice in PBS containing 0.5% (w/v) BSA. Cells were resuspended in 500 µL staining buffer (0.5% (w/v) BSA, 0.25% (v/v) RNase A/T1 mix and 16 µg/mL propidium iodide (PI; P4864, Sigma-Aldrich) in PBS) and samples incubated at RT for 30 min protected from light. Samples were processed using a CytoFLEX S flow cytometer (Beckman Coutler) and data analysed using CytExpert software (Beckman Coulter). An excitation wavelength of 561 nm and a band pass filter of 561_585-42A was used.

2.9.2 Annexin V assay

Annexin V apoptosis assays were performed using the TACS® Annexin V-FITC Kit (4830-01-K, R&D Systems) following the manufacturer's protocol. After treatment as required, cells were harvested by aspirating and retaining culture media (to collect detached apoptotic cells) with the remaining cells detached by trypsinisation. The retained media and trypsin cell suspension was combined and centrifuged at 300 x g for 5 min to pellet cells before washing once in cold PBS and pelleting again. Cells were resuspended in 100 µL Annexin V reagent (10 µL 10X binding buffer, 10 µL PI, 1 µL Annexin V-FITC (pre-diluted 1:25 in 1X binding buffer), 79 µL ddH_2O) and incubated for 15 min at RT protected from light. 400 µL of 1X binding buffer was then added and samples processed immediately using a CytoFLEX S flow cytometer and CytExpert software. Excitation

wavelengths of 488 nm and 561 nm, and band pass filters of 488_525-40A and 561_585-42A were used. Annexin V-FITC positive cells were designated as early apoptotic, whilst dual Annexin V-FITC/PI positive cells were designated as late apoptotic. Cells negative for both Annexin V and PI staining were considered to be healthy. Treatment of cells with the broad-spectrum kinase inhibitor staurosporine (**Table 2.1**) was used to induce apoptosis as a positive control for this assay.

2.9.3 DiBAC$_4$(3) assay to measure membrane potential

At the appropriate experimental endpoint, the membrane potential-sensitive dye Bis-(1,3-Dibutylbarbituric Acid) Trimethine Oxonol (DiBAC$_4$(3); B438, Invitrogen) was added directly to culture media at a final concentration of 200 nM. Cells were incubated in the presence of the dye for 20 min at 37°C in the dark. Culture media was then removed, cells washed once in sterile PBS and harvested by scraping into sterile PBS. Cells were pelleted by centrifugation at 300 x g for 5 min, and the pellet resuspended in 500 µL sterile PBS for flow cytometry analysis. Analysis was performed using a CytoFLEX S machine and CytExpert software. An excitation wavelength of 488 nm and a band pass filter of 488_525-40A was used.

2.10 Luciferase reporter assays

Cells were seeded into 12-well culture plates at an appropriate density. After 24 hours, cells were co-transfected with plasmids expressing firefly luciferase under the control of the relevant promoter and a constitutively expressing *Renilla* luciferase construct (an internal control for transfection efficiency) in a 10:1 firefly:*Renilla* ratio. Transfection of luciferase reporter constructs was performed using the described protocol for transfection of plasmid DNA (2.3.4). The reporter constructs used in this study are detailed in **Appendix Table 1**. At the

experimental endpoint, culture media was aspirated, cells washed once in PBS and lysed in an appropriate volume of passive lysis buffer (Promega) for 15 min at RT with gentle rocking. Samples were then frozen at -80°C to aid lysis. Luciferase activity was measured using the Dual-Luciferase® Reporter Assay System (E1910, Promega). Luciferase Assay Reagent II (LAR II) and Stop & Glo® Reagent were prepared as outlined in the manufacturer's protocol and then diluted 1:4 in ddH_2O prior to use. Assays were performed using opaque, white 96-well plates (655074, Greiner Bio-One) and all reagents were warmed to RT before use. 50 µL LAR II was added to 10 µL lysate and firefly luciferase activity measured, before adding 50 µL Stop & Glo® Reagent and measuring *Renilla* luciferase activity. For each sample, luminescence readings were performed in triplicate and values measured at 0.5 sec intervals for a period of 5 sec, before calculating an average value. Data was collected using a FLUOstar OPTIMA Microplate Reader (BMG Labtech) and associated software, before exporting to Excel for analysis. Relative firefly luciferase activity for each sample was determined by normalising against the corresponding *Renilla* luminescence readings.

2.11 Proliferation assays

2.11.1 Growth curve assay

After treatment as necessary, cells were detached by trypsinisation and reseeded at a density of 2 x 10^4 cells/well (HeLa, HN8) or 5 x 10^4 cells/well (SiHa, UM-SCC-47, UM-SCC-104) in 12-well plates. Cells were subsequently harvested daily by trypsinisation for a period of five days and manually counted using a haemocytometer.

2.11.2 Colony formation assay

After treatment as necessary, cells were detached by trypsinisation and reseeded at 500 cells/well in six-well plates. Cells were examined daily by microscopy until visible colonies were observed (~10-14 days). At this stage, culture media was aspirated and cells washed once in PBS. Colonies were fixed and stained in crystal violet staining solution (1% (w/v) crystal violet (CHE1680, Scientific Laboratory Supplies (SLS)), 25% (v/v) methanol in ddH_2O) for 15 min at RT. Plates were washed thoroughly with water to remove excess crystal violet and colonies counted manually.

Where colonies could not be counted accurately (UM-SCC-47 cells), plates were destained by incubation in 500 µL 10% (v/v) acetic acid solution for 15 min at RT with gentle agitation. 200 µL of the resulting samples were transferred to a 96-well plate and absorbance at 562 nm determined using a PowerWave XS2 Microplate Spectrophotometer and Gen5 1.11 software (BioTek Instruments Inc.). Background absorbance was subtracted from each reading and relative absorbance calculated.

2.11.3 Soft agar assay

For soft agar assays, 60 mm cell culture dishes were coated with a layer of complete media containing 0.5% (w/v) TopVision Low Melting Point Agarose (R0801, ThermoFisher Scientific) and allowed to set at 4°C for 30 min. Simultaneously, cells were detached by trypsinisation after treatment as required and counted manually using a haemocytometer. Cell suspensions of 1000 cells/mL in complete media containing 0.35% (w/v) agarose were added to the bottom layer of agarose and again allowed to set. Plates were then overlaid with complete media and incubated for 14-21 days until visible colonies could be observed. Colonies were counted manually.

2.12 *In vivo* tumourigenicity assay

In vivo experiments were performed using monoclonal HeLa cell lines stably expressing either a non-targeting shRNA (shNTC) or an SUR1-specific shRNA (shSUR1 A), generated as described in 2.3.6-2.3.9. Upon routine passaging, the cell suspension was retained and cells counted manually using a haemocytometer. Approximately 4 x 10^6 cells per cell line were pelleted by centrifugation at 700 x g for 5 min at 4°C. The cells were then washed twice in ice-cold sterile PBS and pelleted as before. Cells were resuspended in a total volume of 500 µL sterile PBS.

Female 6-8 week old SCID mice (Charles River Laboratories) were used for the *in vivo* experiment. Five mice were used per experimental group, with each injected subcutaneously with 50 µL cell suspension (~5 x 10^5 cells). Once palpable tumours had formed, measurements for all groups were taken thrice weekly. After tumours reached 10 mm in either dimension, mice were monitored daily. Mice were sacrificed once tumours reached 15 mm in any dimension. No toxicity, including significant weight loss, was seen in any of the mice. Upon sacrifice, tumours were excised and stored in 4% (w/v) formaldehyde solution in PBS for later analysis. Injection of cells and all subsequent animal work was performed by Ms Debra Evans (University of Leeds). Tumour volume was calculated with the formula $V = 0.5*L*W^2$.

2.13 Immunohistochemistry (IHC)

Fixed tumours from 2.12 were washed three times in PBS for 10 min each to remove the formaldehyde fixative. Tumours were then placed in bijoux tubes containing 70% (v/v) ethanol and sent for paraffin embedding and sectioning (performed by Ms Gemma Hemmings (Faculty of Medicine and Health, University

of Leeds)). Tissue sections were adhered to SuperFrost Plus™ microscope slides (Fisher Scientific).

To perform immunohistochemistry (IHC), slides were first heated to 70°C on a heat block for ~10 min to melt the paraffin wax. Following this, antigen retrieval was performed by placing slides in MenaPath Access Revelation buffer (MP-607-X500, A. Menarini Diagnostics) and heating to 110°C for 15 min in a Decloaking Chamber™ NxGen (DC2012-220V, Biocare Medical) containing 500 mL distilled water. Subsequently, slides were transferred firstly to wash buffer (20X TBS-T with Tween 20 (ab64204, Abcam) diluted in ddH_2O) and then rinsed under gently running tap water for ~2 min. Residual water was removed from slides and sufficient BLOXALL® Endogenous Blocking Solution (SP-6000-100, Vector Laboratories) was added to cover the tissue sections in order to block endogenous peroxidase activity. Following incubation for 15 min at RT, blocking reagent was removed and slides washed in wash buffer. Residual wash buffer was removed and sufficient 2.5% normal horse serum added and slides were again incubated for 15 min. Slides were washed once in wash buffer, before incubating in primary antibodies specific for either SUR1 (PA5-50836, Invitrogen) or Ki-67(M724029-2, Agilent) diluted 1:100 in Antibody Diluent (003218, ThermoFisher Scientific) for 1 hour at RT.

To remove unbound primary antibody, slides were washed thrice in wash buffer for 3 min each. The appropriate secondary antibody was then added (either ImmPRESS® HRP Horse Anti-Mouse IgG Polymer Detection Kit or ImmPRESS® HRP Horse Anti-Rabbit IgG Polymer Detection Kit (MP-7401-50 and MP-7402-50 respectively, Vector Laboratories)) and slides incubated for 30 min at RT. A secondary antibody only control was also performed alongside. Slides were again washed thrice in wash buffer before incubating in 150 µL ImmPACT® DAB

reagent (SK-4105, Vector Laboratories) for 5 min at RT. Residual DAB solution was removed and slides placed in wash buffer and then under gently running tap water. To counterstain, slides were placed in Mayer's haematoxylin solution (51275-500mL, Sigma-Aldrich) for 1 min and then Scott's tap water substitute (S5134-100mL, Sigma-Aldrich) for 2 min, before rinsing under cold tap water.

Prior to mounting, tissue sections were dehydrated by incubating in increasing concentrations of ethanol (75% (v/v) ethanol for 15 sec, 95% (v/v) for 2 min, 100% for 3 min twice) and then xylene (three times for 3 min each). To mount slides, a small amount of BioMount DPX Low (BML-500, BioGnost) was added to a coverslip (COV12450, Solmedia) and the slide placed atop, ensuring all air bubbles were removed by pressing firmly.

Once mounted, slides were scanned at 20X magnification using an AxioScan Z.1 Slide Scanner (Zeiss); this was performed by Dr Ruth Hughes (FBS Bioimaging and Flow Cytometry Facility, University of Leeds). Images were examined using ZEN software (Zeiss) and exported as TIF files. Quantification of staining was performed in an automated manner using ImageJ software and the IHC Profiler plug-in [337, 338]. Histology scores (H-score) were calculated based on the staining intensity and the percentage of positively stained cells [339]. Staining intensities were classified into four categories: 0, no staining; 1, low positive staining; 2, positive staining; 3, strong positive staining. The H-score was calculated using the following formula:

H-score = (3 × % strong positive) + (2 × % positive) + (% low positive)

thus giving a range of 0-300.

2.14 Analyses of publicly available datasets

RNA-sequencing data for head and neck squamous cell carcinomas and normal healthy controls was downloaded from The Cancer Genome Atlas (TCGA) using cBioPortal (https://www.cbioportal.org/) [340]. Expression values were transformed using the $\log_2(x + 1)$ method, where x represents the raw RSEM output for each sample. Gene expression data obtained using microarrays was downloaded from the Gene Expression Omnibus (GEO; accession GSE6791) [341, 342].

2.15 Statistical analysis

Preparation of graphs and all statistical analysis was performed using Prism 9.2.0 software (GraphPad). Data was analysed using a two-tailed Student's t-test unless indicated otherwise. Kaplan-Meier survival data was analysed using the log-rank (Mantel-Cox) test. Differential gene expression between normal, HPV- and HPV+ tumour tissue was analysed using the Wilcoxon rank sum test.

Chapter 3 K_{ATP} channel activity is upregulated by the HPV E7 oncoprotein and is necessary for efficient viral gene expression

3.1 Introduction

High-risk HPVs are the causal factor in over 5% of all human cancers, including >99.7% of cervical cancers, a significant proportion of those at other sites in the anogenital region, as well as a growing number of oropharyngeal cancers [6, 50]. The main drivers of HPV-associated pathologies are the oncoproteins E5, E6 and E7 which together act to prolong the proliferation, and delay differentiation, of the host keratinocyte [50, 143]. Many of the mechanisms by which this is achieved have been widely studied: HR-HPV E7 drives S-phase re-entry via binding to and inducing degradation of pRb and the related pocket proteins p107 and p130 [186-188, 194, 343], whilst E6 concurrently targets p53 for proteasome-mediated degradation, inhibiting pro-apoptotic signalling in response to DNA damage caused by the abnormal S-phase entry [145, 344]. Additionally, E6 modulates a multitude of host signalling pathways, including the Hippo, JNK1/2 and JAK/STAT pathways, to further promote proliferation and delay differentiation [163, 167, 168, 174]. Whilst the role of HPV E5 is not well understood, it has been shown to drive cell proliferation by promoting EGFR-induced signalling [345-347].

Critically, a comprehensive understanding of the host factors modulated by HPV during transformation is still lacking. It is therefore necessary to identify novel HPV-host interactions and to establish whether they may constitute potential new therapeutic targets. This is particularly important as, despite the availability of prophylactic vaccines, there are currently no effective anti-viral drugs for use against HPV. Current therapeutics rely on the widely used yet non-specific DNA-damaging agent cisplatin in combination with radiotherapy [348, 349]. However, resistance to cisplatin, either intrinsic or acquired, is a significant problem [350].

Although this issue can be somewhat alleviated through the use of combination therapy involving cisplatin alongside paclitaxel, there is an urgent need to develop more targeted therapies for the treatment of HPV-associated malignancies [351]. Ion channels represent ideal candidates for novel HPV-specific therapeutics due to the abundance of licensed and clinically-available drugs targeting the complexes which could be repurposed if demonstrated to be effective. Indeed, approximately 20% of all current FDA-approved drugs act upon ion channels [327].

Preliminary findings from the Macdonald group have highlighted a potential importance of potassium ion (K^+) channels for efficient HPV gene expression. In particular, a pharmacological screen performed in primary keratinocytes containing the HPV18 genome indicated that the activity of host K_{ATP} channels may be of particular importance [352]. These channels are hetero-octameric plasma membrane complexes consisting of four inwardly-rectifying pore-forming subunits (Kir6.x) surrounded by four regulatory SURx subunits [236]. No previous link has been established between HPV and K_{ATP} channels, but the channels have been shown to be expressed highly in some cancers, and channel inhibition can result in decreased proliferation [328-332]. The aim of this chapter is to assess the importance of host K_{ATP} channels for efficient HPV gene expression in cervical cancer cells and to determine if, and by what means, HPV enhances expression of K_{ATP} channel subunits.

3.2 Results

3.2.1 Broadly acting inhibitors demonstrate the importance of K^+ channels for HPV

Preliminary findings from the Macdonald group have highlighted a potential importance of K^+ channels for efficient HPV gene expression. To validate this, HPV18+ HeLa cells (derived from a cervical adenocarcinoma) were treated with increasing doses of broadly acting K^+ channel inhibitors, with E7 protein expression used as a readout. Treatment with tetraethylammonium (TEA), a quaternary ammonium compound which binds both internally and externally to almost all K^+ channels to obstruct K^+ flow, resulted in a dose-dependent decrease in expression of the E7 protein (**Fig 3.1A**) [353]. These findings were replicated when cells were treated with increasing, but sub-lethal, doses of a second broad spectrum K^+ channel blocker quinine (**Fig 3.1B**).

To further confirm these results, the K^+ gradient across the plasma membrane of cells was disrupted via the addition of K^+ salts to the culture media. The cytosolic K^+ concentration is typically ~140 mM, whilst the external concentration is distinctly lower (~5 mM) (**Fig 3.1C**). The external K^+ concentration was raised through addition of differing concentrations of potassium chloride (KCl) up to a concentration of 140 mM, equal with the cytosol concentration, thus totally collapsing the K^+ potential. This resulted in a concentration-dependent reduction in HPV18 E7 protein levels (**Fig 3.1D**). To illustrate that this effect was specific to K^+ ions, cells were also treated with increasing concentrations of sodium chloride (NaCl): although a reduced impact on E7 protein levels was observed, there was still a significant loss of expression at the highest concentration (**Fig 3.1D**). Given the dramatic reduction in E7 levels observed between 50 and 100 mM KCl, additional doses at smaller intervals were used. This revealed that when the

external K^+ concentration was steadily raised above 50 mM, reductions in HPV protein expression began to occur, to a much greater extent than with NaCl (**Fig 3.1E**). To exclude the possibility that the addition of Cl^- ions to the media could be affecting oncoprotein expression, HeLa cells were treated with a single dose (70 mM) of a second K^+ salt potassium sulphate (K_2SO_4), alongside KCl and NaCl as before; the stark decrease in E7 protein levels with both KCl and K_2SO_4 confirmed the high sensitivity of HPV oncoprotein expression to disrupted K^+ flux (**Fig 3.1F**). Finally, HeLa cells were treated with the full panel of broadly acting K^+ channel blockers used here, all of which greatly reduced E7 protein levels, whilst NaCl had minimal impact (**Fig 3.1G**).

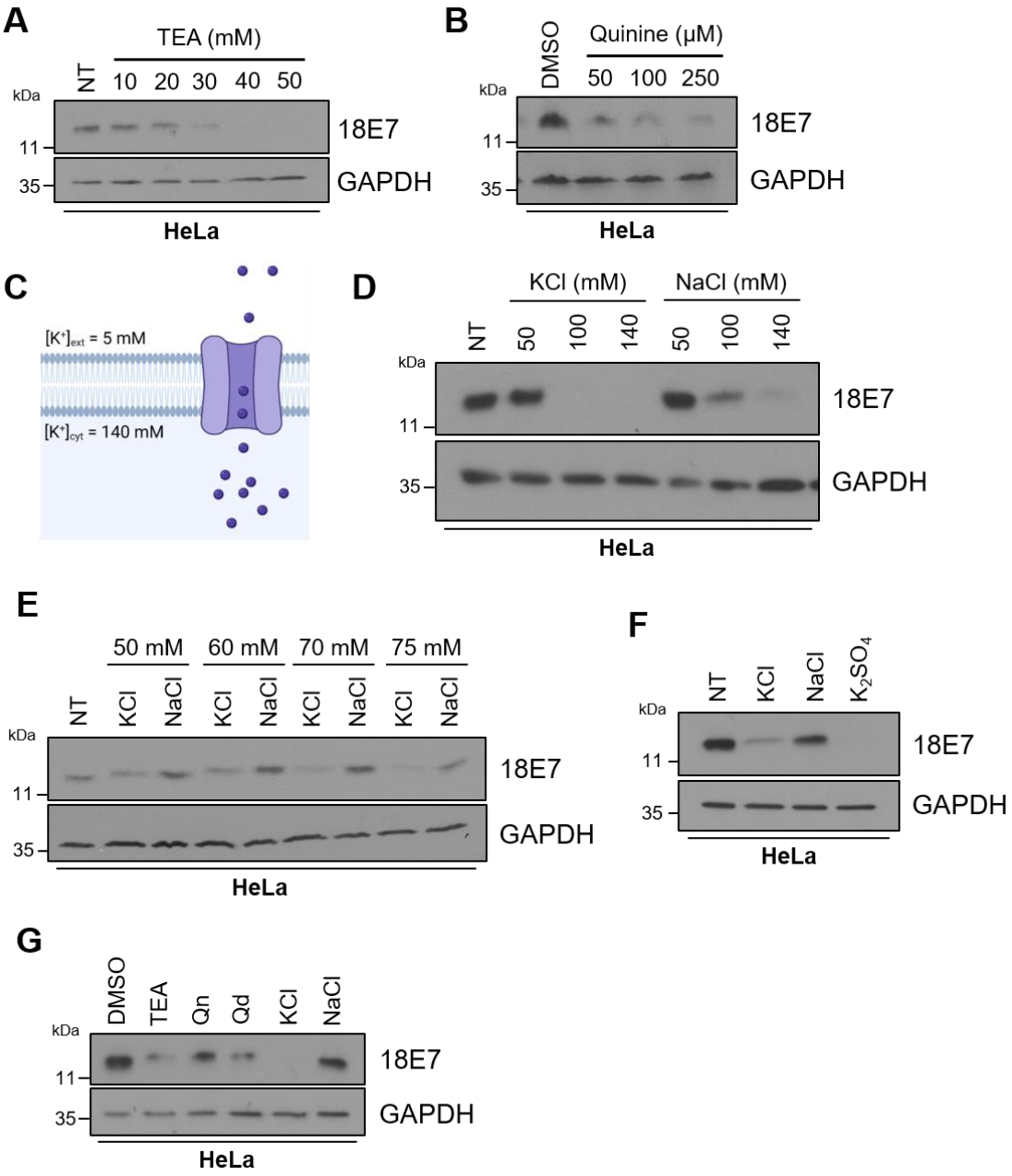

Figure 3.1 Broadly acting inhibitors illustrate the importance of K^+ channels for HPV gene expression. A-B) Representative western blots of E7 expression in HeLa cells treated with increasing doses of (A) TEA or (B) quinine. GAPDH served as a loading control. C) Schematic illustrating the cytosolic and external K^+ ion concentrations. Figure created using BioRENDER.com. D-E) Representative western blots of E7 protein expression in HeLa cells treated with increasing doses of KCl or NaCl. GAPDH served as a loading control. F) Representative western blot of HeLa cells treated with 70 mM KCl, NaCl or K_2SO_4. GAPDH served as a loading control. G) Representative western blot of HeLa cells treated with the full panel of K^+ channel blockers (25 mM TEA, 100 μM quinine (Qn), 100 μM quinidine (Qd), 70 mM KCl) or 70 mM NaCl. GAPDH served as a loading control. A minimum of three biological repeats were performed.

3.2.2 K_{ATP} channel activity is important for HPV oncoprotein expression

An initial pharmacological screen performed in primary human keratinocytes containing the HPV18 genome by the Macdonald group indicated that the effects observed above with broad-spectrum K^+ channel inhibitors may be specifically due to the activity of K_{ATP} channels [352]. To explore whether this was also the case in HPV+ transformed cell lines, HeLa (HPV18+) and SiHa (HPV16+) cells were treated with increasing concentrations of glibenclamide, an inhibitor of K_{ATP} channels. A significant decrease in expression of both HPV oncoproteins was observed at both the mRNA level (**Fig 3.2A**) and the protein level (**Fig 3.2B**) at concentrations as low as 10 μM. In order to ensure that the effect of glibenclamide treatment on viral oncoprotein expression was due to the inhibition of K_{ATP} channel activity rather than off-target effects, we first analysed the membrane potential of cells using the fluorescent dye Bis-(1,3-Dibutylbarbituric Acid) Trimethine Oxonol ($DiBAC_4(3)$) [354, 355]. The ability of this dye to enter cells is proportional to the polarisation of the plasma membrane, with the dye more readily entering cells when the membrane becomes depolarised (**Fig 3.2C**). The dose-dependent increase in fluorescence observed after glibenclamide treatment therefore indicates an increasing level of depolarisation, consistent with a reduction in K_{ATP} channel opening and hence retention of positively-charged K^+ ions within the cell (**Fig 3.2D**). To further exclude the possibility of off-target effects, cells were treated with tolbutamide, a second member of the sulfonylurea class of drugs which inhibit K_{ATP} channels. Significantly, this also resulted in a dose-dependent decrease in oncoprotein expression at the mRNA (**Fig 3.2E**) and protein level (**Fig 3.2F**), with a similar corresponding increase in $DiBAC_4(3)$

fluorescence (**Fig 3.2G**). Together, these data demonstrate that K_{ATP} channels are important for HPV gene expression in cervical cancer cells.

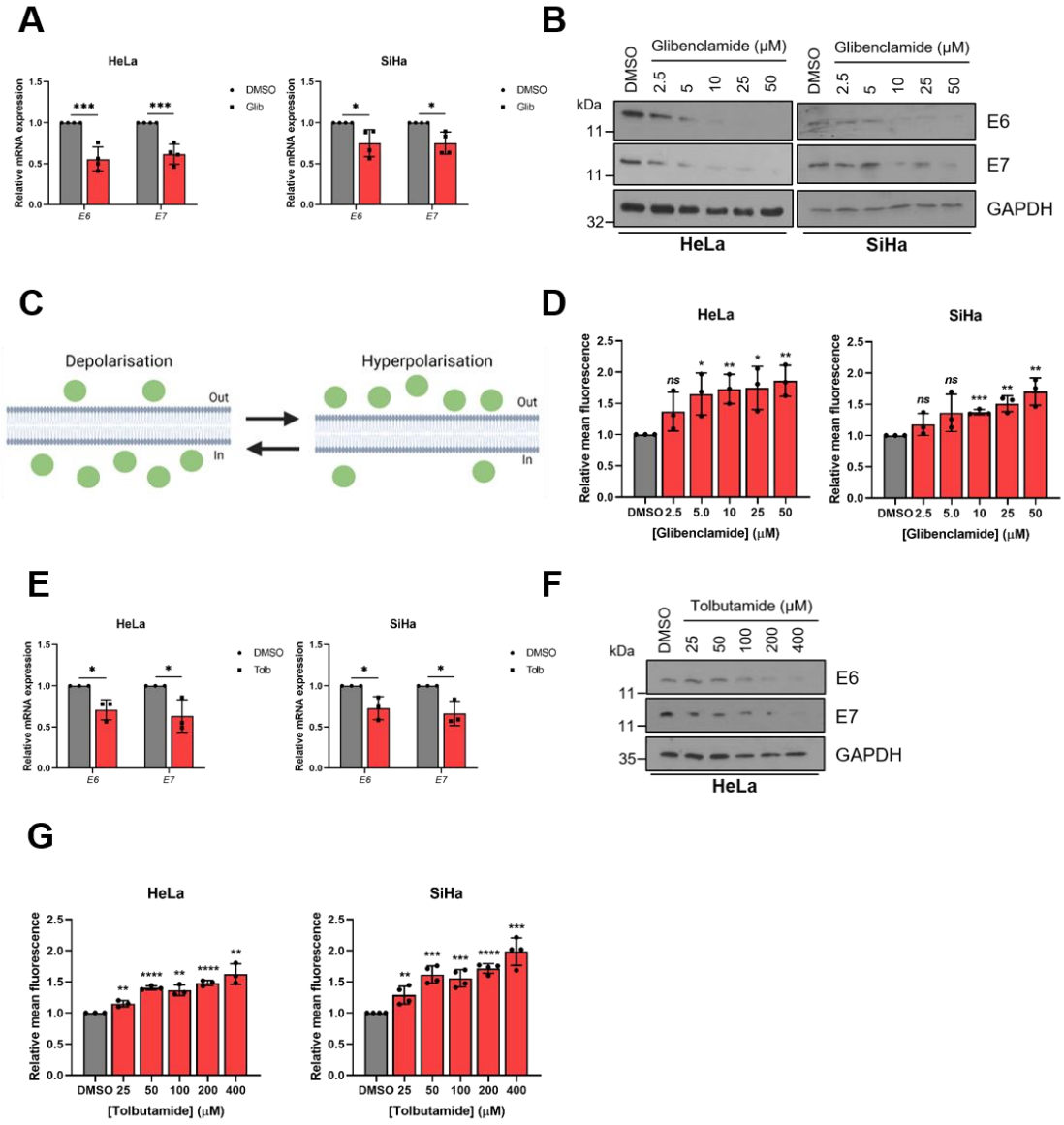

Figure 3.2 K_{ATP} channel activity is important for HPV oncoprotein expression. A) Expression levels of *E6* and *E7* mRNA in HeLa and SiHa cells treated with glibenclamide (10 μM) measured by RT-qPCR. Samples were normalised against *U6* mRNA levels. B) Representative western blots of E6 and E7 expression in HeLa and SiHa cells treated with increasing doses of glibenclamide. GAPDH served as a loading control. C) Schematic illustrating the plasma membrane permeability of $DiBAC_4(3)$. Figure created using BioRENDER.com. D) Mean $DiBAC_4(3)$ fluorescence levels in HeLa and SiHa cells treated with increasing dose of glibenclamide. Samples were normalised to DMSO controls. E) Expression levels of *E6* and *E7* mRNA in HeLa and SiHa cells treated with tolbutamide (200 μM) measured by RT-qPCR. Samples were normalised against *U6* mRNA levels. F) Representative western blots of E6 and E7 expression in HeLa and SiHa cells treated with increasing doses of tolbutamide. GAPDH served as a loading control. G) Mean $DiBAC_4(3)$ fluorescence levels in HeLa and SiHa cells treated with increasing dose of tolbutamide. Samples were normalised to DMSO controls. Bars represent means ± standard deviation (SD) of a minimum of three biological replicates with individual data points

displayed. *Ns* not significant, *P<0.05, **P<0.01, ***P<0.001, ****P<0.0001 (Student's t-test).

3.2.3 Activation of K_{ATP} channels promotes HPV oncoprotein expression

To confirm the effects on oncoprotein expression observed with K_{ATP} channel inhibitors, HPV+ cervical cancer cells were also treated with diazoxide, an activator of K_{ATP} channels that preferentially acts upon SUR1-containing complexes [236]. This resulted in a significant dose-dependent increase in HPV oncoprotein expression at both the mRNA level (**Fig 3.3A**) and the protein level (**Fig 3.3B**). As before, analysis of $DiBAC_4(3)$ fluorescence was performed to assess the impact of diazoxide treatment on the plasma membrane potential. A dose-dependent decrease in fluorescence, particularly apparent after application of 50 µM diazoxide was observed, indicating increasing levels of membrane hyperpolarisation, consistent with increased K_{ATP} channel activity (**Fig 3.3C**). Importantly, treatment of HPV+ cervical cancer cells with either channel blocker (glibenclamide or tolbutamide) abolished the diazoxide-induced increase in HPV oncoprotein expression. (**Fig 3.3D**). Finally, in order to assess the impact of modulating K_{ATP} channel activity in a more direct manner than studying the plasma membrane potential using $DiBAC_4(3)$, electrophysiological analysis was performed in HeLa cells. A clear outward K^+ current was observed in the DMSO-treated cells, which was greatly increased upon application of the activator diazoxide (**Fig 3.3E**). Importantly, addition of the channel inhibitor glibenclamide completely prevented the diazoxide-induced increase in K^+ current, whilst glibenclamide treatment alone significantly reduced basal K^+ currents (**Fig 3.3E**). Taken together, these data confirm that K_{ATP} channels are present and active in cervical cancer cells, and that their activity is important in the regulation of HPV gene expression.

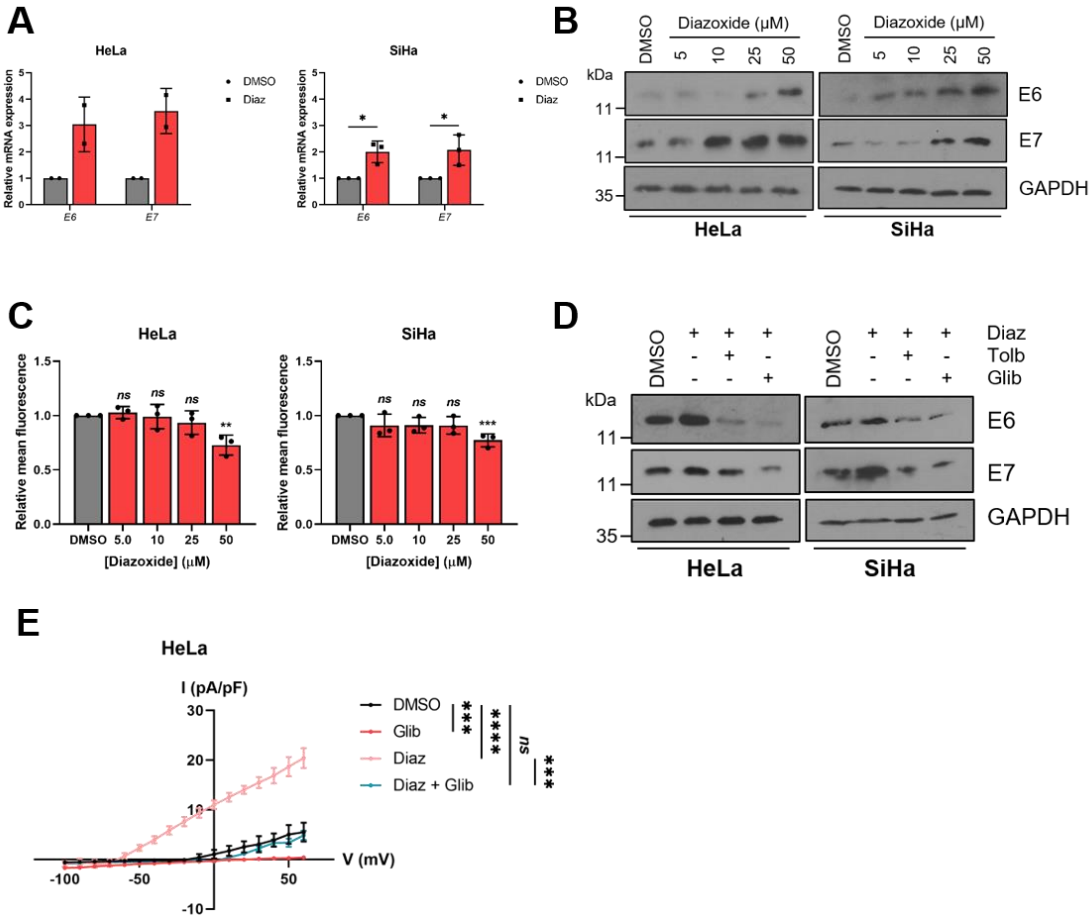

Figure 3.3 Activation of K_{ATP} channels promotes HPV oncoprotein expression. A) Expression of *E6* and *E7* mRNA in HeLa (n = 2) and SiHa cells treated with diazoxide (50 μM) measured by RT-qPCR. Samples were normalised against *U6* mRNA levels. B) Representative western blots of E6 and E7 expression in HeLa and SiHa cells treated with increasing doses of diazoxide. GAPDH served as a loading control. C) Mean $DiBAC_4(3)$ fluorescence levels in HeLa and SiHa cells treated with increasing dose of diazoxide. Samples were normalised to DMSO control. D) Representative western blots of E6 and E7 expression in HeLa and SiHa cells treated with diazoxide (50 μM) alone or in combination with glibenclamide (10 μM) or tolbutamide (200 μM). E) Mean current density-voltage relationships for K^+ currents in HeLa cells treated with DMSO, diazoxide (50 μM), glibenclamide (10 μM), or both diazoxide and glibenclamide for 16 hours, measured by whole cell patch clamping (n = 5 for all treatments). Patch clamping performed by Dr Holli Carden (University of Leeds). Data shown represents means ± standard deviation (SD) of a minimum of three biological replicates (unless stated otherwise) with individual data points displayed where appropriate. *Ns* not significant, *P<0.05, **P<0.01, ***P<0.001, ****P<0.0001 (Student's t-test).

3.2.4 Depletion of the SUR1 subunit of K_{ATP} channels impairs HPV gene expression

Given the importance of K_{ATP} channels for HPV oncoprotein expression illustrated here, it was hypothesised that HPV may regulate expression of channel subunits.

However, multiple isoforms of both K_{ATP} channel subunit types (Kir6.x and SURx) exist. Therefore, in order to understand both which particular subunit isoforms are expressed in cervical tissue, and to reveal whether HPV is capable of upregulating subunit expression, the mRNA levels of all subunits was quantified in a panel of cervical cancer cell lines by RT-qPCR. This revealed that expression of the SUR1 subunit was significantly higher in all four of the HPV+ cancer cell lines examined, compared to HPV- C33A cells and primary keratinocytes [352]. We therefore focussed on the SUR1 subunit for the purposes of this study.

Accordingly, the effects of suppressing SUR1 expression on HPV gene expression were investigated. Knockdown of SUR1 using a pool of specific siRNAs in both HPV16+ (SiHa) and HPV18+ (HeLa) cervical cancer cells was performed and silencing efficiency measured by RT-qPCR (**Fig 3.4A**). $DiBAC_4(3)$ fluorescence was used to ascertain the effect of siRNA depletion of SUR1 on the plasma membrane potential (i.e. to ensure a functional impact on channel activity); we observed a ~2 fold increase in fluorescence after siRNA treatment, indicating a significant membrane depolarisation characteristic of a reduction in K_{ATP} channel activity (**Fig 3.4B**). After confirming a successful knockdown, we then analysed the impact on E6 and E7 expression. This revealed a significant decrease in HPV oncoprotein expression, measured both at the transcript and protein level, following suppression of SUR1 expression (**Fig 3.4C-D**). Finally, to confirm that the effect of SUR1 depletion on HPV gene expression was due to a direct impact on transcription, luciferase reporter constructs containing the HPV16 or HPV18 upstream regulatory regions (URRs) were employed. We observed a significant decrease in relative luciferase activity after SUR1 knockdown with both URR reporter plasmids (**Fig 3.4E**). Together, these data

indicate that K_{ATP} channels are critical for HPV oncoprotein expression and have a direct impact on transcription from the URR.

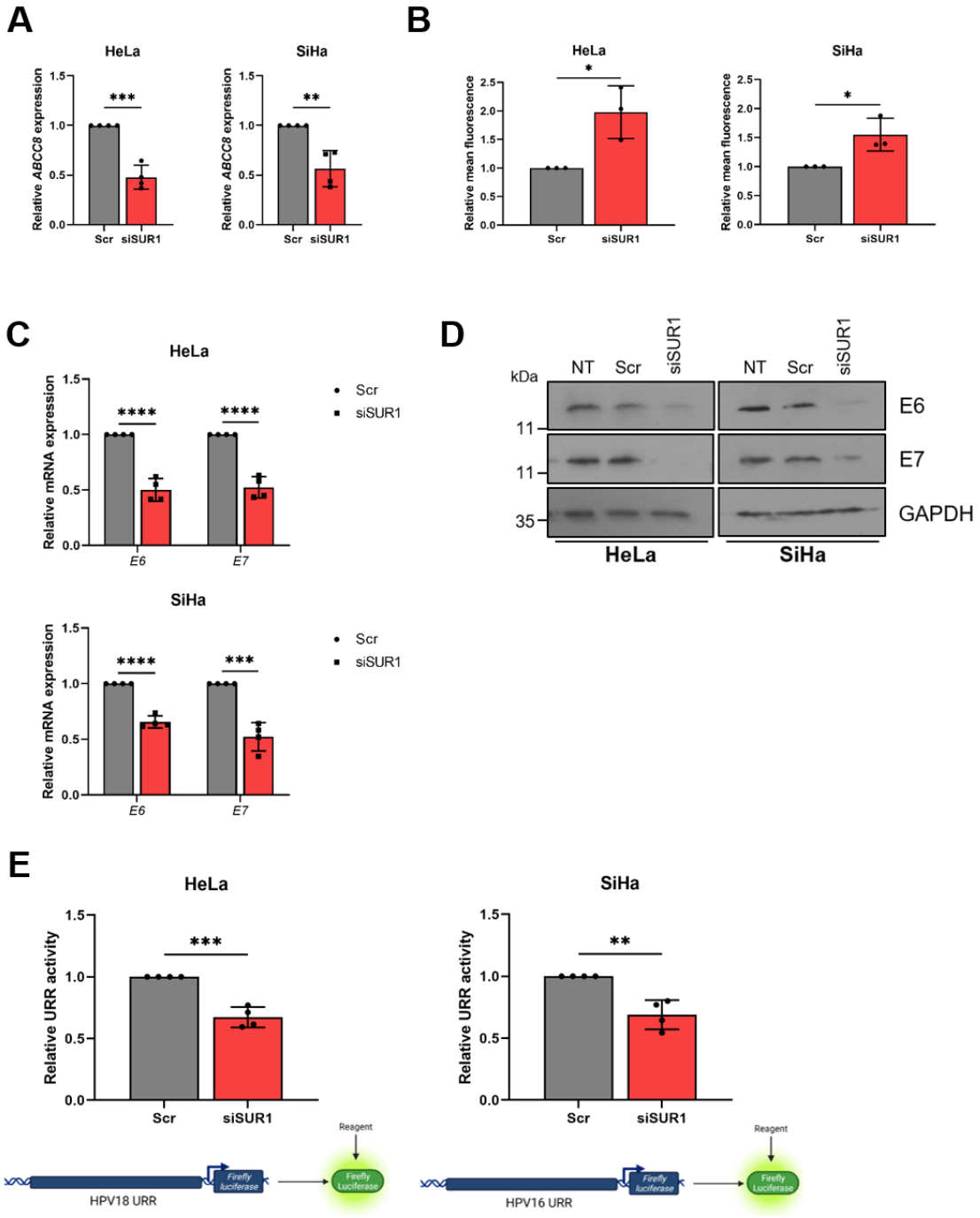

Figure 3.4 Depletion of SUR1 impedes HPV gene expression in cervical cancer cells. A) Relative expression of *ABCC8* mRNA in HeLa and SiHa cells transfected with a pool of SUR1-specific siRNA measured by RT-qPCR. Samples were normalised against *U6* mRNA levels. B) Relative mean $DiBAC_4(3)$ fluorescence levels in HeLa and SiHa cells transfected with SUR1 siRNA. C) Relative expression of *E6* and *E7* mRNA in HeLa and SiHa cells transfected with SUR1 siRNA measured by RT-qPCR. Samples were normalised against *U6* mRNA levels. D) Representative western blots of E6 and E7 expression in HeLa and SiHa cells transfected with SUR1 siRNA. GAPDH served as a loading control. E) Relative firefly luminescence in HeLa and SiHa cells co-transfected with SUR1 siRNA and either a HPV18 or HPV16 URR reporter plasmid as illustrated. Luminescence values were normalised against *Renilla* luciferase activity and data is displayed relative to scramble controls. Figure created using BioRENDER.com. Bar graphs

represent means ± SD of a minimum of three biological replicates with individual data points displayed. *P<0.05, **P<0.01, ***P<0.001, ****P<0.0001 (Student's t-test).

3.2.5 Kir6.2 knockdown similarly reduces HPV gene expression

In order to confirm that the effects on HPV gene expression observed following SUR1 knockdown were K_{ATP} channel-dependent, rather than a channel-independent function of SUR1, the levels of Kir6.2 (the pore-forming subunit of K_{ATP} channels) were also depleted using a pool of specific siRNAs. As before, silencing efficiency was measured by RT-qPCR, revealing a >50% knockdown in both cell lines used (**Fig 3.5A**). Similarly, the impact of Kir6.2 depletion on the plasma membrane potential was also analysed. The ~2 fold and ~1.5 fold increases in $DiBAC_4(3)$ fluorescence detected in HeLa and SiHa cells respectively were broadly in line with the changes observed following SUR1 knockdown (**Fig 3.5B**). The impact of Kir6.2 suppression on HPV oncoprotein expression was then investigated. This revealed a significant reduction in both mRNA and protein levels of E6 and E7 (**Fig 3.5C-D**), thus confirming that the impacts of SUR1 depletion observed previously are indeed K_{ATP} channel-dependent.

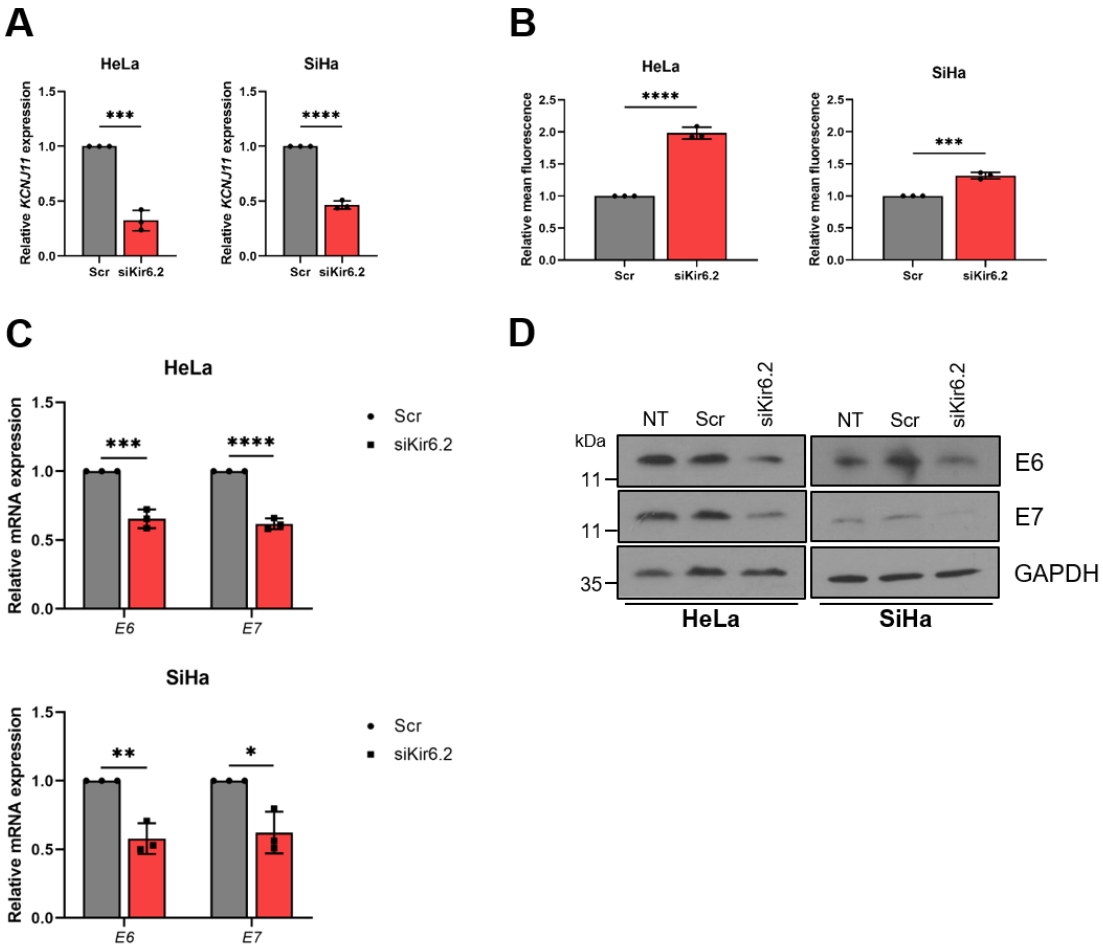

Figure 3.5 Depletion of Kir6.2 also impedes HPV gene expression in cervical cancer cells. A) Relative expression of *KNCJ11* mRNA in HeLa and SiHa cells transfected with a pool of Kir6.2-specific siRNA measured by RT-qPCR. Samples were normalised against *U6* mRNA levels. Performed by Dr Ethan Morgan. B) Relative mean DiBAC$_4$(3) fluorescence levels in HeLa and SiHa cells transfected with Kir6.2 siRNA. C) Relative expression of *E6* and *E7* mRNA in HeLa and SiHa cells transfected with Kir6.2 siRNA measured by RT-qPCR. Samples were normalised against *U6* mRNA levels. Performed by Dr Ethan Morgan. D) Representative western blots of E6 and E7 expression in HeLa and SiHa cells transfected with Kir6.2 siRNA. GAPDH served as a loading control. Bar graphs represent means ± SD of three biological replicates with individual data points displayed. *P<0.05, **P<0.01, ***P<0.001, ****P<0.0001 (Student's t-test).

3.2.6 SUR2 knockdown has no impact on HPV gene expression

When analysing the expression of K_{ATP} channel subunits in a panel of cervical cancer cell lines, it was noted that despite observing a consistent increase in SUR1 expression across the HPV+ cell lines, there was no increase in mRNA levels of the SUR2 subunit in any of these cell lines when compared to primary keratinocytes [352]. Seemingly this indicates that, although present within the

cell, SUR2-containing K_{ATP} channels may not be necessary for HPV gene expression. To test this, SUR2 levels were depleted using a pool of specific siRNAs. The knockdown efficiency was in line with that following transfection of SUR1- or Kir6.2-specific siRNAs (**Fig 3.6A**). When investigating the impact on plasma membrane potential, we observed a small increase in $DiBAC_4(3)$ fluorescence indicative of depolarisation), suggesting that a small minority of K_{ATP} channels in HPV+ cervical cancer cells may be composed of the SUR2 subunit (**Fig 3.6B**). Importantly however, SUR2 knockdown had no impact on HPV oncoprotein expression in either HPV16+ or HPV18+ cervical cancer cells, in line with data demonstrating that HPV does not upregulate expression of the SUR2 subunit of K_{ATP} channels (**Fig 3.6C-D**) [352].

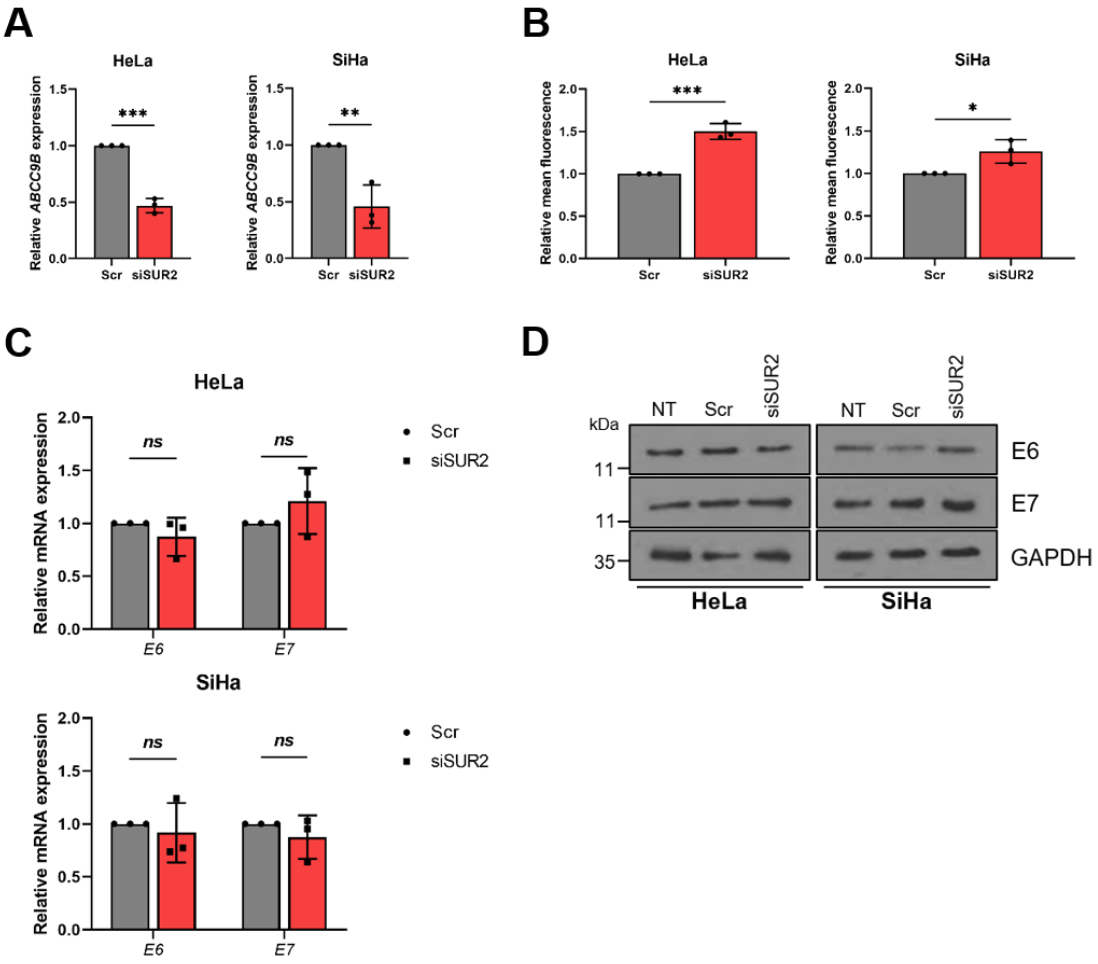

Figure 3.6 Depletion of SUR2 has no impact upon HPV gene expression in cervical cancer cells. A) Relative expression of *ABCC9B* mRNA in HeLa and SiHa cells transfected with a pool of SUR2-specific siRNA measured by RT-qPCR. Samples were normalised against *U6* mRNA levels. Performed by Dr Ethan Morgan. B) Relative mean $DiBAC_4(3)$ fluorescence levels in HeLa and SiHa cells transfected with SUR2 siRNA. C) Relative expression of *E6* and *E7* mRNA in HeLa and SiHa cells transfected with SUR2 siRNA measured by RT-qPCR. Samples were normalised against *U6* mRNA levels. Performed by Dr Ethan Morgan. D) Representative western blots of E6 and E7 expression in HeLa and SiHa cells transfected with SUR2 siRNA. GAPDH served as a loading control. Bar graphs represent means ± SD of three biological replicates with individual data points displayed. *Ns* not significant, *P<0.05, **P<0.01, ***P<0.001 (Student's t-test).

3.2.7 Expression of the SUR1 subunit of K_{ATP} channels is upregulated by HPV E7

Next, the mechanism behind the observed HPV-induced increase in SUR1 expression was explored. It was hypothesised that SUR1 upregulation could be occurring in an oncoprotein-dependent manner, given that HPV E6 and E7 are known to interact with, modulate the activity of, or indeed alter the expression of

a multitude of host factors in order to drive proliferation of the host cell [50]. To test this, expression of both E6 and E7 was repressed using siRNA in HPV+ cervical cancer cell lines. We observed a ~70% decrease in *ABCC8* (SUR1) mRNA levels following knockdown of oncogene expression, indicating that oncoprotein expression is likely necessary to upregulate SUR1 expression (**Fig 3.7A**). In order to gain an understanding of which particular oncoprotein drives the increase in SUR1 expression, the E6 and E7 oncoproteins of HPV18 were overexpressed in turn and in combination in HPV- C33A cells. HPV18 E6 did not induce any significant change in *ABCC8* mRNA levels, but expression of HPV18 E7 led to a ~2.5 fold increase in *ABCC8* expression (**Fig 3.7B**). Although co-expression of E6 alongside E7 also increased *ABCC8* mRNA levels, the degree to which expression was increased was less than with HPV18 E7 alone, indicating that the E7 oncoprotein is the sole driver of SUR1 expression. To confirm this, C33A cell lines stably expressing HA-tagged HPV18 oncoproteins were generated as previously described [174]. In agreement with the transient overexpression data, a significant upregulation of *ABCC8* mRNA levels was only observed in cells expressing HA-E7 (**Fig 3.7C**).

To confirm that the observed changes in SUR1 expression resulted in functional effects on K_{ATP} channel activity, the plasma membrane potential of cells was assayed following silencing of E7 in HPV+ cervical cancer cells. This resulted in a ~2 fold increase in $DiBAC_4(3)$ fluorescence (**Fig 3.7D**), indicative of membrane depolarisation and consistent with a reduction in K_{ATP} channel opening. Additionally, overexpression of HPV18 E7 was performed in HPV- cervical cancer cells. A significant decrease in $DiBAC_4(3)$ fluorescence, indicative of membrane hyperpolarisation, was detected (**Fig 3.7E-F**). This was entirely abolished both by treatment with glibenclamide or siRNA-mediated knockdown of SUR1,

suggesting that the hyperpolarisation was due to an E7-dependent increase in K_{ATP} channel activity.

Finally, we wanted to understand to what extent this upregulation of SUR1 expression and K_{ATP} channel activity contributed to the increase in proliferation induced by the E7 oncoprotein. To test this, the colony forming ability of the C33A cells stably expressing HPV18 E7 described here was examined, revealing a significant increase in the relative number of colonies compared to the vector only control (**Fig 3.7G**). This was as expected given the vast array of host cell factors E7 is known to manipulate in order to promote cell growth [50]. Interestingly, upon SUR1 knockdown in the E7-expressing cells, a significant decrease in colony forming ability was observed, indicating that modulation of K_{ATP} channel activity could perhaps be an important mechanism by which the E7 oncoprotein stimulates proliferation (**Fig 3.7G**). However, this reduction in colony number was not complete (~1.15 fold relative to vector only control), confirming that K_{ATP} channels are not the sole mechanism by which E7 promotes proliferation.

In summary, these data indicate that the E7 oncoprotein, rather than E6, is the major factor regulating HPV-induced increases in SUR1 expression.

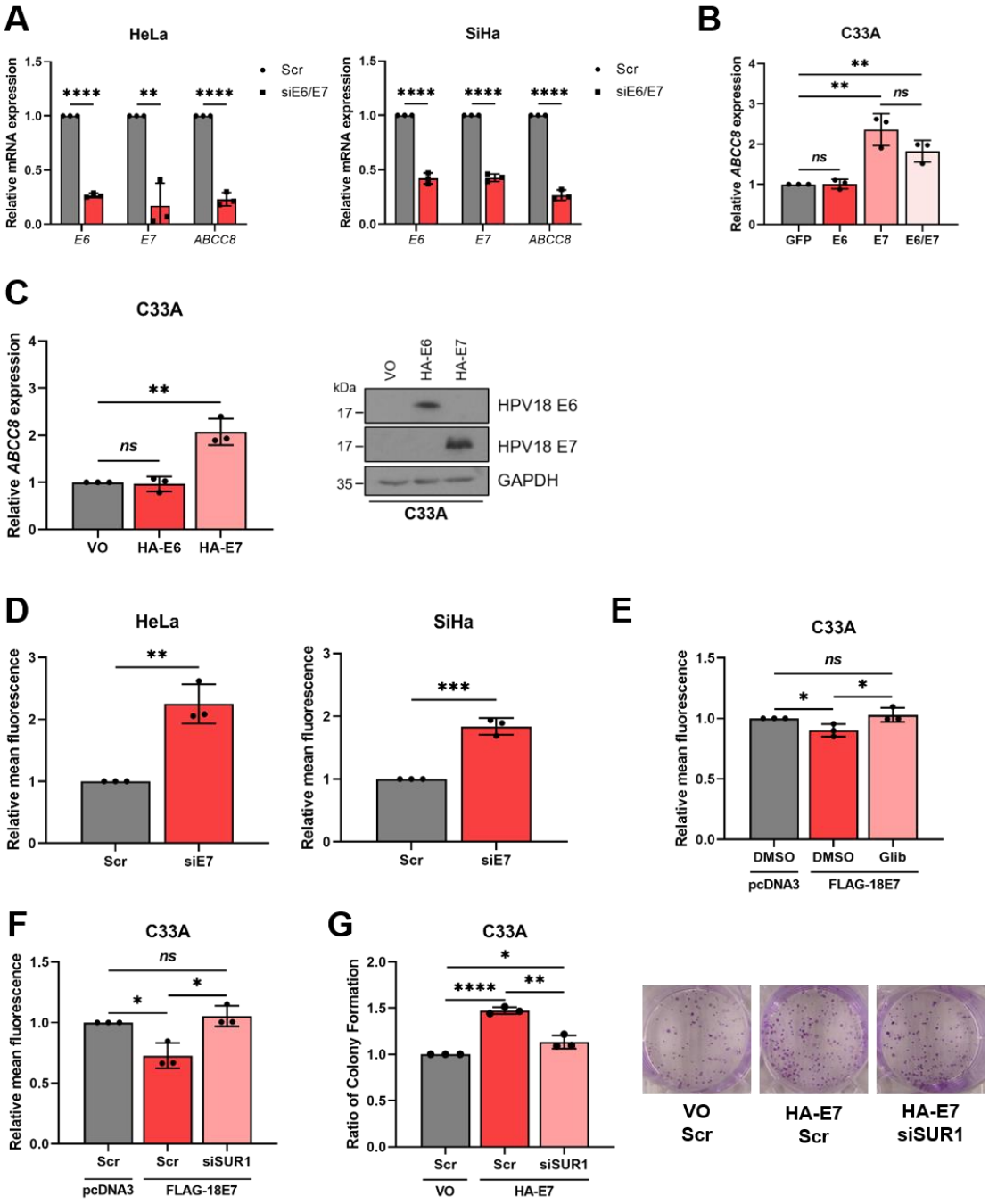

Figure 3.7 Expression of the SUR1 subunit of K_{ATP} channels is upregulated by HPV E7. A) Relative *ABCC8* mRNA expression measured by RT-qPCR in HeLa and SiHa cells co-transfected with E6- and E7-specific siRNA. Samples were normalised against *U6* mRNA levels. Successful knockdown was confirmed by analysing *E6* and *E7* mRNA levels. Performed by Dr Ethan Morgan. B) Expression levels of *ABCC8* mRNA measured by RT-qPCR in C33A cells transfected with GFP-tagged HPV18 oncoproteins. Samples were normalised against *U6* mRNA levels. Successful transfection was confirmed by immunofluorescence and analysis of *GFP* mRNA expression. C) Relative expression of *ABCC8* mRNA in C33A cells stably expressing HA-tagged HPV18 oncoproteins measured by RT-qPCR. Samples were normalised against *U6* mRNA levels. Expression of oncoproteins was confirmed by western blot. D) Mean $DiBAC_4(3)$ fluorescence levels in HeLa and SiHa cells after transfection of HPV E7-specific siRNA. Samples were

normalised to the scramble control. Successful knockdown was confirmed by western blot (not shown). E) Mean $DiBAC_4(3)$ fluorescence levels in C33A cells after transfection of FLAG-tagged HPV18 E7 and treatment with either DMSO or glibenclamide (10 μM). Samples were normalised to the pcDNA3-transfected control. Expression of FLAG-E7 was confirmed by western blot. F) Mean $DiBAC_4(3)$ fluorescence levels in C33A cells after co-transfection of FLAG-tagged HPV18 E7 and SUR1-specific siRNA. Samples were normalised to the pcDNA3/scramble-transfected control. G) Colony formation assay of C33A cells stably expressing HA-tagged HPV18 E7 transfected with either non-targetting or SUR1-specific siRNA. Bars represent means ± SD of three biological replicates with individual data points displayed. *Ns* not significant, *P<0.05, **P<0.01, ***P<0.001, ****P<0.0001 (Student's t-test).

3.2.8 Mutations in HPV18 E7 prevent upregulation of SUR1 expression

Next, we wanted to gain an understanding of how HPV E7 upregulates SUR1 expression. In order to do this, a series of mutants was generated at key residues in a plasmid encoding a codon-optimised and GFP-tagged version of HPV18 E7 (**Fig 3.8A**). Two mutations within the LxCxE motif, critical for pRb binding, were engineered: a deletion of 4 residues (Δ24-27) and a single amino acid substitution (C27S), both of which have been previously shown to abrogate binding to pRb [193]. The Δ24-27 mutant additionally fails to bind the related Rb family member p107 [193]. A double mutant at the casein kinase II (CKII) phospho-acceptor sites was also generated (SS32/34AA), these alanine substitutions completely abolish CKII phosphorylation, which has been shown to significantly enhance binding to Rb family members and the stimulation of cell proliferation [189, 193, 356]. Although the E7 L74R mutation generated here has not been previously characterised, the same mutation at the conserved L67 residues of HPV16 and HPV31 E7 abrogates binding to histone deacetylases (HDACs), and in the case of HPV31, prevents episome maintenance [357, 358]. Further, HPV16 E7 L67R displays reduced ability to stimulate the transcriptional activity of hypoxia inducible factor 1α (HIF-1α), which is known to drive *ABCC8* transcription [257,

359]. Finally, a C-terminal C98S mutant, located within one of the two CxxC zinc-binding sites, was also constructed.

After generating the panel of E7 mutants, their impact on *ABCC8* mRNA expression was assessed following transfection into HPV- C33A cells. Somewhat surprisingly, none of the mutants were able to recapitulate the profound increase in *ABCC8* mRNA levels induced by WT E7 (**Fig 3.8B**). The two pRb binding domain mutants (Δ24-27 and C27S), as well as the CKII phosphorylation site mutant, resulted a small increase in SUR1 expression of ~1.5 fold, but no change in *ABCC8* mRNA levels was detected with HPV18 E7 C98S.

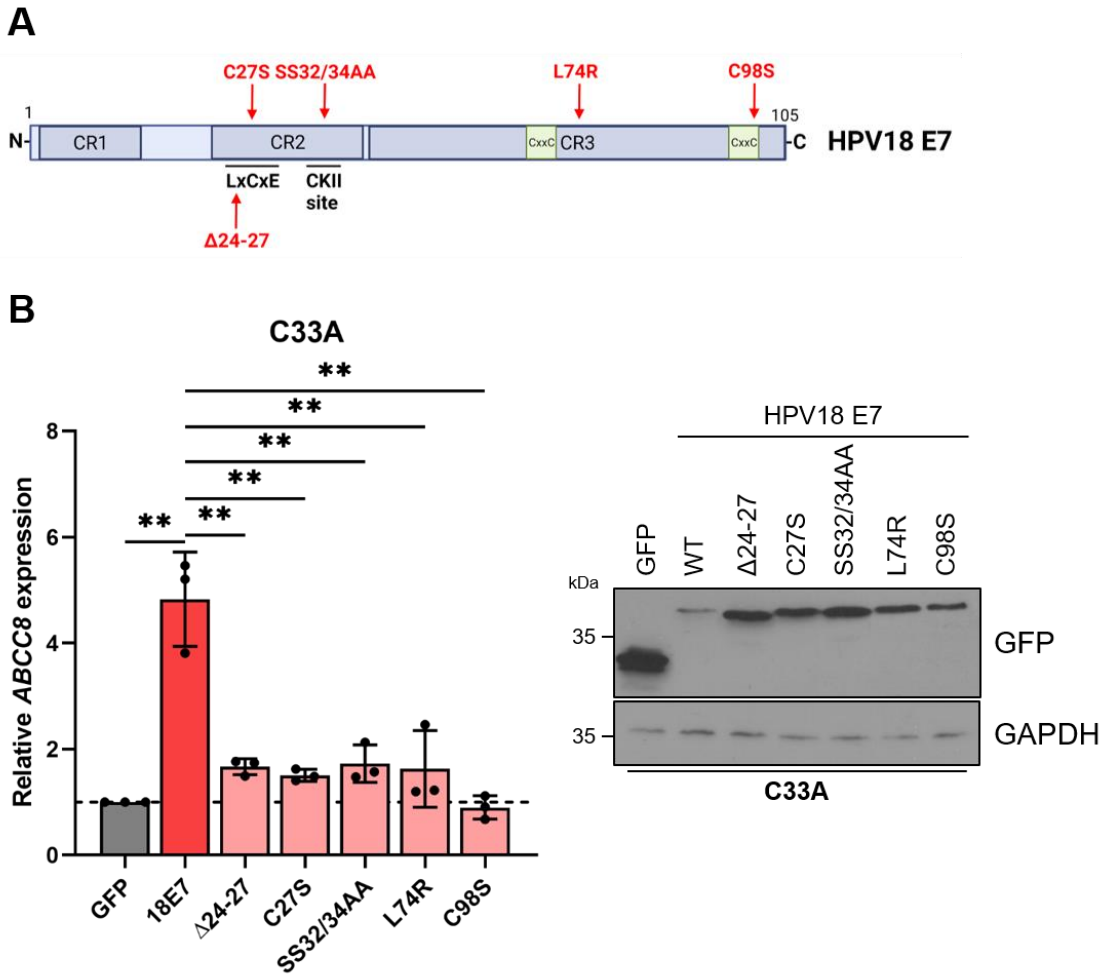

Figure 3.8 Mutations in HPV18 E7 prevent upregulation of SUR1 expression. A) Structure of HPV18 E7 with mutations generated herein highlighted in red. B) Expression level of ABCC8 measured by RT-qPCR in C33A cells transfected with GFP or GFP-tagged HPV18 E7 (wild-type or mutated). Samples were normalised against *U6* mRNA levels. Successful transfection was confirmed by immunofluorescence (not shown) and western blot (right). Bars represent means ± SD of three biological replicates with individual data points displayed. **P<0.01 (Student's t-test).

3.2.9 HPV E7 may upregulate SUR1 expression via the transcription factor SP1

In order to further elucidate the mechanism of E7-induced upregulation of SUR1 expression, the promoter region of *ABCC8* was analysed. The promoter of *ABCC8* is known to harbour binding sites for the host transcription factor SP1; enhancer (E)-box motifs, which permit binding of basic helix-loop-helix (bHLH) transcription factors such as c-Myc; and hypoxic response elements (HREs) to allow HIF1α binding [253, 254, 257]. To confirm this, and to identify other potential

transcriptional regulators, an online transcription factor binding site prediction tool (AliBaba 2.1) was employed using a ~600 bp section of sequence lying immediately upstream of the *ABCC8* transcription start site (TSS) [360]. This revealed a total of 68 potential binding sites, 32 of which were for SP1 (**Fig 3.9A**). SP1 is a ubiquitously expressed, 785 amino acid transcription factor shown to regulate the expression of thousands of genes implicated in a diverse array of cellular functions including proliferation, differentiation and angiogenesis [361]. To narrow down candidate binding sites, the same ~600 bp region of the *ABCC8* promoter was analysed for exact sequence matches to the core SP1 consensus binding sequence 5'-GGGCGG-3' in the forwards orientation [362]. This revealed the presence of four putative binding sites for SP1 (**Fig 3.9B**). Indeed, one of these sites exactly matched the full SP1 consensus sequence of 5'-(G/T)GGGCGG(G/A)(G/A)(C/T)-3', illustrating that it is potentially a high affinity SP1 binding site [362].

In order to experimentally validate the association of SP1 with these candidate binding sites, chromatin immunoprecipitation (ChIP) was performed, followed by qPCR utilising primers flanking the region containing the putative SP1 binding sites. This demonstrated a significant enrichment for SP1 at this region over the IgG isotype control in HeLa cells (**Fig 3.9C**). Further, a luciferase reporter construct containing the *ABCC8* promoter region upstream of firefly luciferase was employed. This confirmed that the *ABCC8* promoter is highly active in both HPV16+ and HPV18+ cervical cancer cell lines (**Fig 3.9D**). To validate the importance of SP1 for the expression of *ABCC8* in HPV+ cervical cancer cells, the four putative SP1 binding sites identified herein were deleted in turn. Relative *ABCC8* promoter activity was significantly reduced upon deletion of any of these

four SP1 binding sites, highlighting the critical role of the transcription factor for *ABCC8* expression in HPV+ cancer cells (**Fig 3.9E**).

To further confirm the importance of SP1 for efficient *ABCC8* expression, a selective small molecule inhibitor of was used. Mithramycin A (MithA) binds to GC-rich DNA sequences, thus displacing SP1 from target gene promoters [363]. Treatment of HeLa cells with MithA resulted in a significant decrease in *ABCC8* (SUR1) mRNA expression of greater than 50% (**Fig 3.9F**). The transcript levels of two other genes whose expression is reported to be SP1 dependent were also analysed [364-367]. mRNA expression of *CCND1* (cyclin D1) and *EGFR* were reduced to an even greater extent than *ABCC8* following MithA treatment, perhaps suggesting other factors may also have a role in regulating *ABCC8* expression. Given the potential off-target effects of small molecule inhibitors, cell lines stably expressing SP1-specific shRNA were generated. Two distinct shRNA sequences were utilised; these resulted in a 55% and 30% reduction in *SP1* mRNA expression respectively (**Fig 3.9G**). The expression of *ABCC8* was then analysed, revealing marked decreases in mRNA levels in comparison to the shNEG control cell line. Together, these data indicate that SP1 is critical for efficient *ABCC8* expression in HPV+ cancer cells.

A

Transcription Factor	Binding sites identified
SP1	32
EGR1/EGR2	5
AP-2α	4
USF1	4
ETF	3
C/EBPα	2
CTCF	2
ERα	2
MyoD	2
TRA-1	2
WT1	2
AP-1	1
CPEB	1
CREB	1
ELF1	1
Oct1	1
PTF1	1
TCF12	1
YY1	1

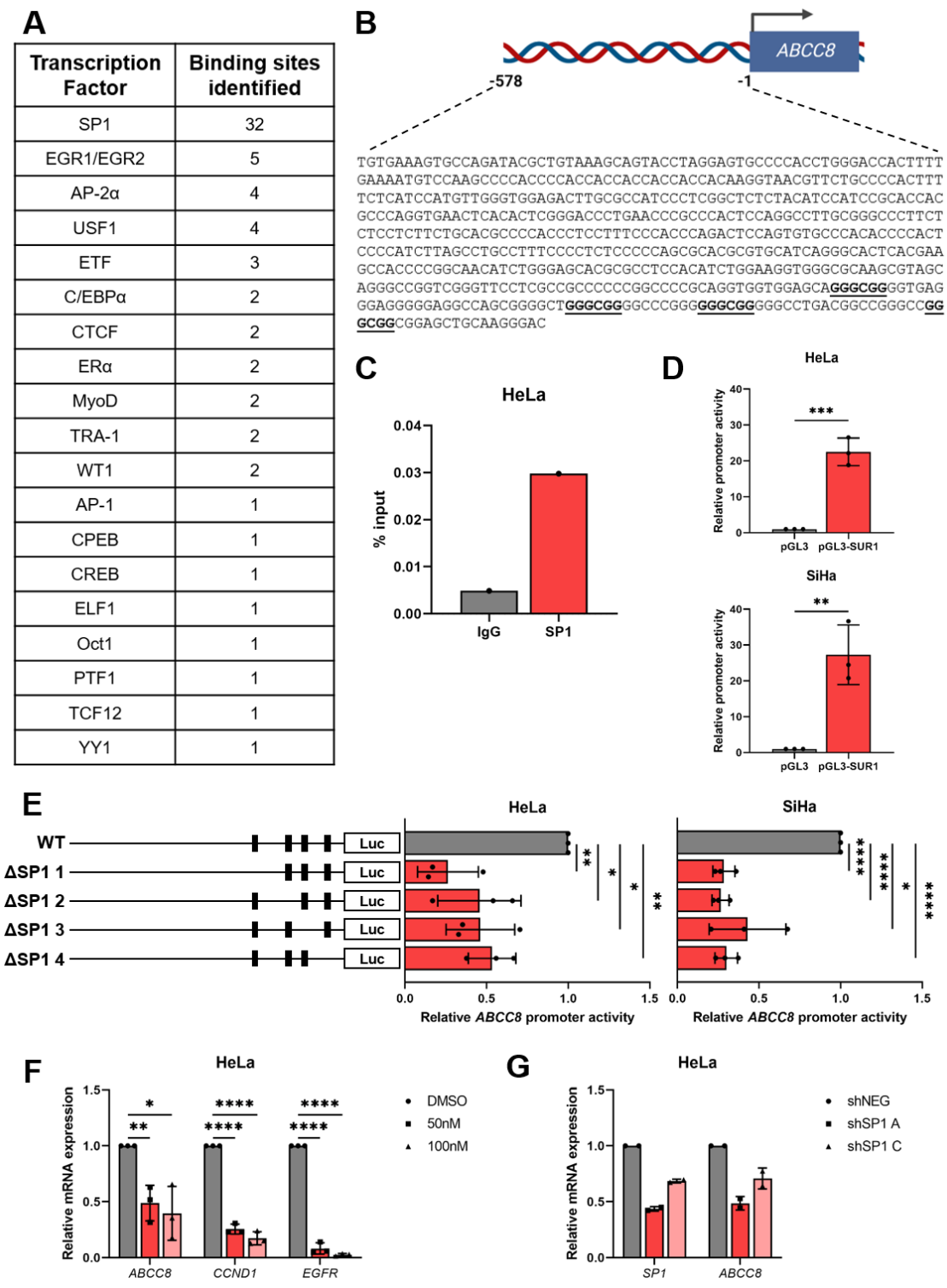

Figure 3.9 The host transcription factor SP1 is critical for *ABCC8* promoter activity in HPV+ cancer cells. A) Identification of transcription factor binding sites within the *ABCC8* promoter using AliBaba 2.1 [360]. B) Schematic displaying the four consensus SP1 binding sites within the *ABCC8* promoter. Figure created using BioRENDER.com. C) ChIP-qPCR analysis of SP1 binding to the *ABCC8* promoter region in HeLa cells. SP1 binding is presented as a percentage of the input sample (n = 1). D) Relative firefly luminescence in HeLa and SiHa cells transfected with a reporter plasmid containing the *ABCC8* promoter. Luminescence values were

normalised against *Renilla* luciferase activity. E) Relative firefly luminescence in HeLa and SiHa cells transfected with an *ABCC8* promoter reporter construct (either wild type (WT) or containing a deletion at one of the four SP1 binding sites (ΔSP1)). Luminescence values were normalised against *Renilla* luciferase activity. F) mRNA expression of *ABCC8, CCND1* and *EGFR* in HeLa cells treated with DMSO or the indicated concentration of mithramycin A (MithA) for 24 hours, measured by RT-qPCR. Samples were normalised against *U6* mRNA levels and data is displayed relative to the DMSO control. G) mRNA expression of *ABCC8* and *SP1* in HeLa cells stably expressing either a non-targetting shRNA (shNEG) or one of two SP1-specific shRNAs (shSP1), measured by RT-qPCR. Samples were normalised against *U6* mRNA levels and data is displayed relative to the shNEG control (n = 2). Bars represent means ± SD of three biological replicates, unless stated otherwise, with individual data points displayed. *P<0.05, **P<0.01, ***P<0.001, ****P<0.0001 (Student's t-test).

Thus far, it has been demonstrated that the E7 oncoprotein drives SUR1 expression, and that SP1 is required for efficient transcription from the *ABCC8* promoter. It was therefore hypothesised that E7 may be regulating SUR1 expression via altering the expression and/or activity of SP1. To initially test this, an siRNA knockdown strategy was taken to silence expression of the HPV oncoproteins and the impact on SP1 levels analysed. This revealed significant decreases in SP1 expression following E6/E7 knockdown at both the mRNA and protein level (**Fig 3.10A-B**), suggesting that the oncoproteins may be regulating SP1 expression. Importantly, this data does not exclude a potential role for E6 in the regulation of SP1. Therefore, SP1 expression was analysed in HPV- C33A cell lines stably expressing HA-tagged versions of either HPV18 E6 or E7. Surprisingly, this demonstrated a small, albeit non-significant, decrease in the mRNA expression of *SP1* in cells in which HPV18 E6 was present, and no change in *SP1* levels in the E7-expressing cells (**Fig 3.10C**). Analysis of the protein levels of SP1 by western blot validated these findings (**Fig 3.10D**). This suggests that, although the oncoproteins are necessary for SP1 expression, they are not sufficient to induce its upregulation.

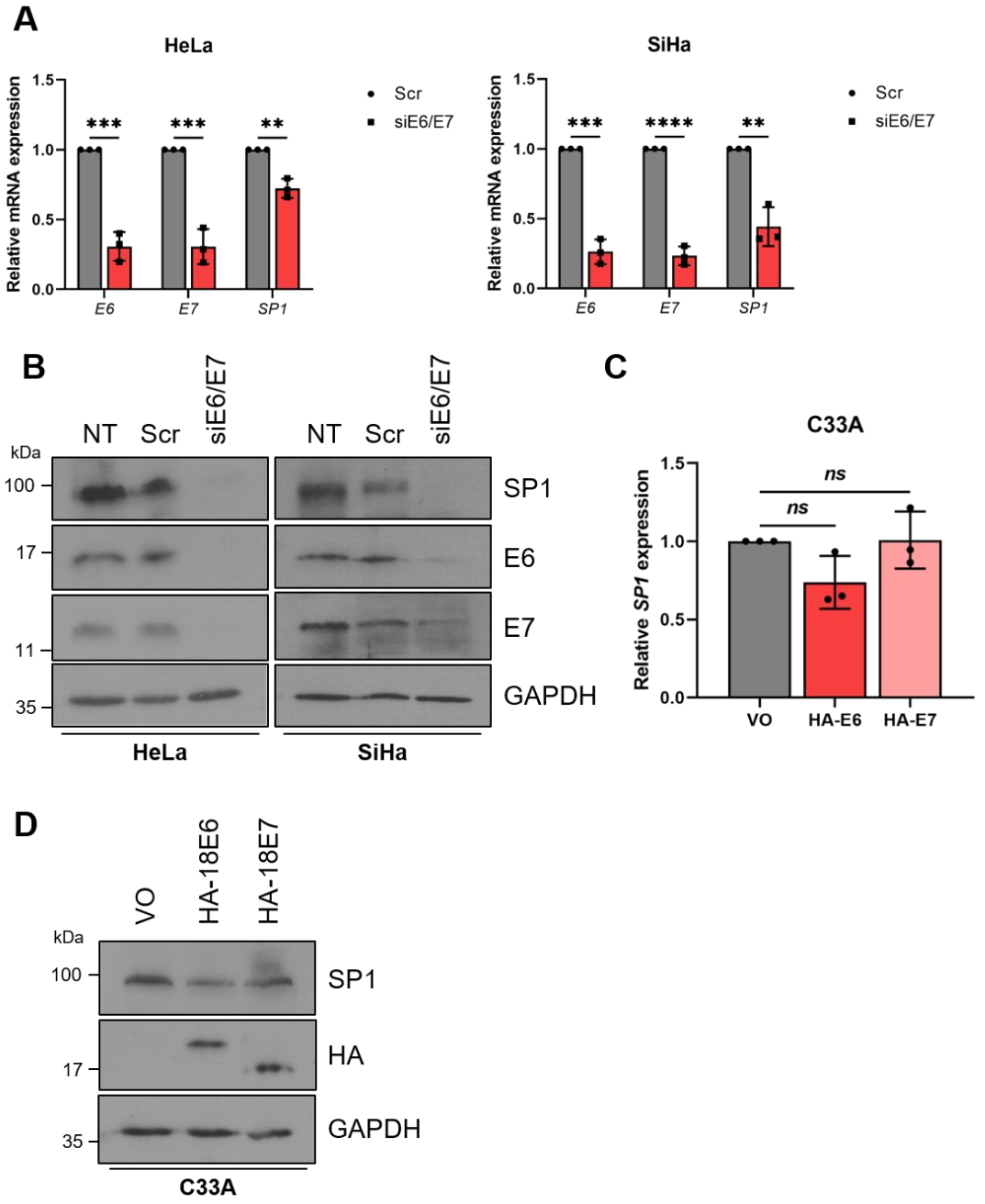

Figure 3.10 HPV E7 is necessary but not sufficient for the expression of the host transcription factor SP1. A) mRNA expression of *E6*, *E7* and *SP1* in HeLa and SiHa cells co-transfected with E6 and E7-specific siRNA, measured by RT-qPCR. Samples were normalised against *U6* mRNA levels and data is displayed relative to the scramble controls. B) Representative western blots of SP1, E6 and E7 expression in HeLa and SiHa cells transfected with E6 and E7 siRNA. GAPDH served as a loading control. C) mRNA expression of *SP1* in C33A cells stably expressing HA-tagged HPV18 oncoproteins measured by RT-qPCR. Samples were normalised against *U6* mRNA levels. D) Representative western blot of SP1 in C33A cells stably expressing HA-tagged HPV18 oncoproteins. GAPDH served as a loading control. Bars represent means ± SD of three biological replicates with individual data points displayed. *Ns* not significant, *P<0.05, **P<0.01, ***P<0.001, ****P<0.0001 (Student's t-test).

3.3 Discussion

It is vital to identify novel virus-host interactions that are critical for HPV-mediated transformation as, despite the availability of prophylactic vaccines, there are currently no effective anti-viral treatments for HPV-associated disease. Here, this study identifies a novel host factor, the ATP-sensitive potassium ion (K_{ATP}) channel, as a crucial regulator of HPV gene expression in cervical cancer cells. Inhibition of K_{ATP} channel activity, via either pharmacological means or through siRNA-mediated knockdown, significantly impedes HPV oncoprotein expression. The use of luciferase reporter constructs illustrates that this is due to a direct effect on transcription from the viral URR. Furthermore, we reveal that HPV upregulates expression of the SUR1 regulatory subunit of K_{ATP} channels in an E7-dependent manner, potentially involving the host transcription factor SP1.

A growing number of viruses have been shown to modulate or require the activity of host ion channels [368]. Indeed, several viruses encode their own ion channels, termed ‘viroporins’, including the HPV E5 protein [123, 125]. Together, this underlines the importance of regulating host ion channel homeostasis during infection. Importantly, this study is the first to our knowledge to explicitly demonstrate modulation of ion channel activity by HPV, and that this is important for HPV gene expression. Previous studies have identified increased expression of a voltage-gated sodium channel ($Na_V1.6$) in cervical cancer biopsy samples, but no attempt was made to attribute this to HPV [369]. Further, although a previous publication has analysed the expression of K_{ATP} channels in cervical cancer cell lines, again no attempt was made to analyse the contribution of HPV to this [332]. More widely, few reports exist of a dependence on host K_{ATP} channel activity for viral replication. One study identified that inhibition of K_{ATP} channels via glibenclamide treatment precludes HIV cell entry but, in contrast, cardiac K_{ATP}

channel activity was found to be detrimental to Flock House virus (FHV) infection of *Drosophila* [370, 371]. Significantly however, no evidence exists to suggest that either of these viruses actively modulate the gating and/or expression of these channels, as has been demonstrated for HPV here.

This study identified the critical importance of K_{ATP} channel activity for efficient HPV gene expression by analysing both the mRNA and protein levels of the viral oncoproteins. Further, this was shown to be mediated via direct impacts on HPV early promoter activity, rather than alterations to mRNA stability for example, through the use of luciferase reporter assays. However, a key remaining issue is the question of *how* K_{ATP} channel activity impacts upon viral transcription. The HPV URR is known to contain binding sites for multiple host factors, including AP-1, Oct1, SP1 and YY1, which serve to regulate HPV transcription [88, 372-376]. This therefore raises the possibility that K_{ATP} channel opening could regulate the activity of some of these host transcriptional regulators. Alternatively, the viral chromatin is known to be under exquisite epigenetic regulation via post-translational modifications to histone proteins and CpG DNA methylation, involving a plethora of host epigenetic regulators [377]; the activity of these host factors could also be modulated by K_{ATP} channels. Beyond this, it would also be of interest to extend these studies to assess the importance of these ion channels in the differentiation-dependent life cycle of the virus.

In order to confirm that the effects on HPV oncoprotein expression observed during this study following SUR1 knockdown or glibenclamide treatment were due to decreased K_{ATP} channel activity, silencing of the pore-forming Kir6.2 subunit was also performed. We felt this pertinent as recent studies concluded that the oncogenic activities of SUR1 in non-small cell lung carcinoma (NSCLC) were independent of K_{ATP} channels [334, 335], and SUR1 is reported to have a

supplementary role in regulating activity of an ATP-sensitive, non-selective ion channel in astrocytes [378, 379]. However, we observed almost identical effects on HPV oncoprotein expression following Kir6.2 knockdown, leading us to conclude that SUR1 does not act in a K_{ATP} channel-independent manner in cervical cancer. This fits with the current assembly hypothesis for K_{ATP} channels, whereby neither subunit can be trafficked beyond the ER unless fully assembled into hetero-octameric channels, suggesting that knockdown of either subunit should be sufficient to disrupt K_{ATP} channel activity [259, 260, 262].

To understand how HPV upregulates SUR1 expression, we decided to initially focus on the roles of the oncoproteins E6 and E7 as they are known to bring about a multitude of changes within the host cell in order to drive proliferation [50, 143]. Our analyses revealed that the E7 oncoprotein, rather than E6, was responsible for promoting K_{ATP} channel activity. This was the case for both HPV16 and HPV18. The extent to which K_{ATP} channels contribute to the ability of E7 to promote proliferation was then analysed. This revealed that although SUR1 knockdown led to a reduction in the E7-mediated increase in colony-forming ability, the reversal was not complete, consistent with the wealth of data highlighting the numerous mechanisms E7 possesses to drive cell growth [50]. Following this, to understand the underlying mechanism behind the E7-induced increase in SUR1 expression, a series of mutants was generated targetting key attributes of E7, such as its ability to degrade pRb. Surprisingly, none of the mutants were able to upregulate SUR1 expression to a similar extent as the wild type protein, perhaps suggesting that these mutations could be disrupting the overall structure of the protein. As an alternative approach, it would be useful for future studies to determine whether the upregulation of SUR1 is a property

exclusive to the high-risk HPV types associated with cancer development, or shared among all HPV types.

In addition to looking at the HPV oncoproteins, the *ABCC8* promoter sequence was also analysed to help unravel the mechanism of HPV-mediated upregulation. Previous reports have identified SP1 binding sites within both the mouse and human *ABCC8* promoters, findings that were confirmed by this study [253, 254]. To validate that SP1 was able to activate *ABCC8* transcription in the context of HPV+ cervical cancer cells, ChIP and luciferase reporter assays were performed. This revealed that SP1 readily associates with the *ABCC8* promoter and that deletion of any of the SP1 binding sites significantly reduces promoter activity. To further confirm these findings a small molecule inhibitor, which displaces SP1 from target gene promoters [363], and SP1 knockdown cell lines were employed. Although both of these approaches led to a loss of *ABCC8* mRNA expression, a significant caveat is the presence of an SP1 binding site within the HPV URR that is critical for promoter activation [88, 373, 374]. Therefore, it will be important for future studies to answer the question of whether this loss of expression is due to a direct loss of SP1 binding to the *ABCC8* promoter, or rather a reduction in transcription directed by the HPV URR, thus preventing E7-mediated upregulation of *ABCC8* transcription via an as-yet-undefined mechanism. To this end, overexpression of E7 could be performed following SP1 knockdown or inhibition, to analyse to what extent the decrease in SUR1 expression can be rescued.

Given the clear role of SP1 in regulating SUR1 expression in HPV+ cancer cells we identified, the impact of the HPV oncoproteins on SP1 expression was then analysed. Surprisingly, given the critical importance of SP1 to the host cell, this aspect of HPV biology is thus far poorly understood. Although SP1 is vital for HPV

oncoprotein expression [88, 373, 374], the inverse relationship (i.e. the impact of HPV on SP1 expression) is not well-characterised. SP1 protein levels have been reported to be increased in cervical cancer, but the underlying mechanism remains unclear, with both stabilisation of the protein and downregulation of an SP1-targetting miRNA having been reported [380, 381]. Importantly, neither study assessed the contribution of HPV to these mechanisms. Herein, we identified that although E6 and E7 are necessary for SP1 expression, they are not sufficient to induce the upregulation of SP1 in a HPV- cell line. Significantly, this study did not analyse the relative expression of SP1 in HPV- and HPV+ cell lines: it may be the case that, given the role of SP1 in regulating proliferation, C33A cells, as a transformed cell line, already possess increased SP1 levels. Alternatively, the oncoproteins could also be impacting upon the activity of SP1. A recent report has suggested that, when exogenously expressed, HPV16 E7 is capable of binding SP1, potentially enhancing its binding to target promoters [382]. Further, the transcription factor can be phosphorylated at residues including T278, T453 and T739, which together act to stabilise and enhance the transactivation potential of SP1 [383-385]. Thus, the potential regulation of SP1 phosphorylation by HPV E7 may warrant further investigation.

In summary, this analysis reveals that host K_{ATP} channels play a crucial role in regulating HPV gene expression in cervical cancer cells. Upregulation of the K_{ATP} channel regulatory subunit SUR1 by HPV E7 contributes towards increased K_{ATP} channel activity, which in turn drives a feed forward loop enhancing HPV oncoprotein expression. The mechanism behind the enhanced SUR1 expression was also investigated, revealing a potentially important role for the host transcription factor SP1. A further characterisation of K_{ATP} channels in HPV-associated disease is now warranted in order to determine their impact on cell

proliferation and key host signalling networks (Chapter 4), and to reveal whether K_{ATP} channels play a similar role in other HPV-associated cancers (Chapter 5).

Chapter 4 K_{ATP} channels activate MAPK and AP-1 signalling to drive proliferation in cervical cancer cells

4.1 Introduction

HPV is the causal factor in almost all cases of cervical cancer [50]. There are currently 15 HPV types considered to be high-risk due to their association with the development of malignancies, although HPV types 16 and 18 are responsible for the majority of these, with 55% and 15% of cervical cancers cases positive for HPV16 and HPV18 respectively [6, 25]. Highlighting its importance, cancer of the cervix is the fourth most common malignancy in women worldwide and the fourth leading cause of cancer-related deaths in women: in 2018, around 570,000 people were diagnosed with cervical cancer and over 300,000 deaths worldwide could be attributed to the disease [386].

The main drivers of HPV-associated pathologies are the oncoproteins E5, E6 and E7 [50, 143]. Together, they act to delay differentiation, inhibit apoptosis and drive proliferation of the host keratinocyte. Many of the mechanisms by which these oncoproteins contribute to carcinogenesis are well characterised, including disruption of the G1/S cell cycle checkpoint by E7 via inhibition and degradation of pRb [186-188, 194, 343], and blockade of pro-apoptotic signalling mediated by p53 in response to replication stress by the E6 oncoprotein [145, 344]. Importantly however, a comprehensive understanding of the signalling pathways manipulated by HPV is lacking, and novel mechanisms by which the virus stimulated cell proliferation continue to be identified.

The importance of ion channels in the regulation of the cell cycle and cell proliferation has become increasingly recognised [323-326, 387]. Cells undergo a rapid hyperpolarisation during progression through the G1-S phase checkpoint, which is then reversed during G2 [325]. It is thought that K^+ channels are

particularly important for this initial hyperpolarisation, with a number of K^+ efflux channels having been observed to be increased in expression and activity during G1 [324, 325]. Of these, K_{ATP} channels have been shown to be expressed highly in some cancers, and channel inhibition can result in decreased proliferation [328-332].

A small number of studies have investigated the impact of host K_{ATP} channels on key mitogenic signalling pathways. The MAPK cascades are key networks that regulate a wide variety of processes, including cell proliferation and survival, and culminate in the phosphorylation of extracellular signal-regulated kinase 1/2 (ERK1/2), c-Jun N-terminal kinase 1/2 (JNK1/2), and p38 MAP kinase [388]. Investigations into the role of K_{ATP} channels in glioma cell proliferation identified a reduction in ERK1/2 signalling following K_{ATP} channel blockade or siRNA knockdown of the Kir6.2 subunit, whilst increased ERK1/2 phosphorylation was observed with diazoxide treatment [333, 389]. Furthermore, treatment of THP-1 monocyte cells with either of two K_{ATP} channel activators (diazoxide and pinacidil) enhanced ERK1/2 activation in a MEK1/2-dependent manner [390]. In contrast, K_{ATP} channel inhibition via glibenclamide treatment was found to enhance JNK1/2 activation in a gastric cancer cell line model [328].

The data in the previous chapter highlight a critical role for host K_{ATP} channels in regulating HPV gene expression in cervical cancer cells. The aim of this chapter is to extend this by examining the effect of inhibiting K_{ATP} channels on key cellular phenotypes including proliferation, cell cycle progression and apoptosis. Further, the mechanism by which HPV gene expression is regulated by K_{ATP} channels is unknown; this will be investigated in this chapter.

4.2 Results

4.2.1 Stable knockdown of SUR1 negatively affects cervical cancer cell proliferation

In order to understand whether K_{ATP} channels have a role in driving the proliferation of HPV+ cervical cancer cells, stable knockdown cell lines were generated using shRNAs specific for SUR1. HeLa cells were transduced with lentiviruses harbouring a vector which upon integration into the cellular genome, express either a non-targetting shRNA or a SUR1-specific shRNA, as well as a fluorescent marker (ZsGreen) and a puromycin resistance gene. To select for cells that had been successfully transduced, puromycin treatment was used, followed by fluorescence-associated cell sorting (FACS) to isolate individual cells (**Fig 4.1A**). These cells were then expanded to generate monoclonal cell lines, which were subsequently screened for *ABCC8* (SUR1) mRNA expression by RT-qPCR to confirm successful knockdowns. This revealed a ~50% reduction in *ABCC8* mRNA expression compared to a non-targetting shRNA control (shNTC), consistent across two monoclonal knockdown lines with differing shRNA sequences (**Fig 4.1B**). This is concordant with the level of knockdown observed following transfection of SUR1-specific siRNA in the preceding chapter (**Fig 3.4A**). To confirm that stable suppression of SUR1 expression had the same impact on HPV gene expression as both glibenclamide treatment and transient SUR1 knockdown, the mRNA and protein levels of E6 and E7 were analysed. This revealed a ~50% decrease in *E6* and *E7* mRNA expression, consistent across both knockdown lines, findings that were validated at the protein level by western blot (**Fig 4.1C-D**).

Following establishment of the knockdown cell lines, their proliferative capacity was analysed. A profound decrease in the growth rate of shSUR1-expressing

cells was recorded (**Fig 4.1E**). Consistent with this, the anchorage-dependent and anchorage-independent colony forming ability of these cells was also greatly reduced, to approximately 40% and 25% of the ability of the shNTC control respectively (**Fig 4.1F-G**). Together, these data indicate that K_{ATP} channels promote proliferation in HPV+ cervical cancer cell lines.

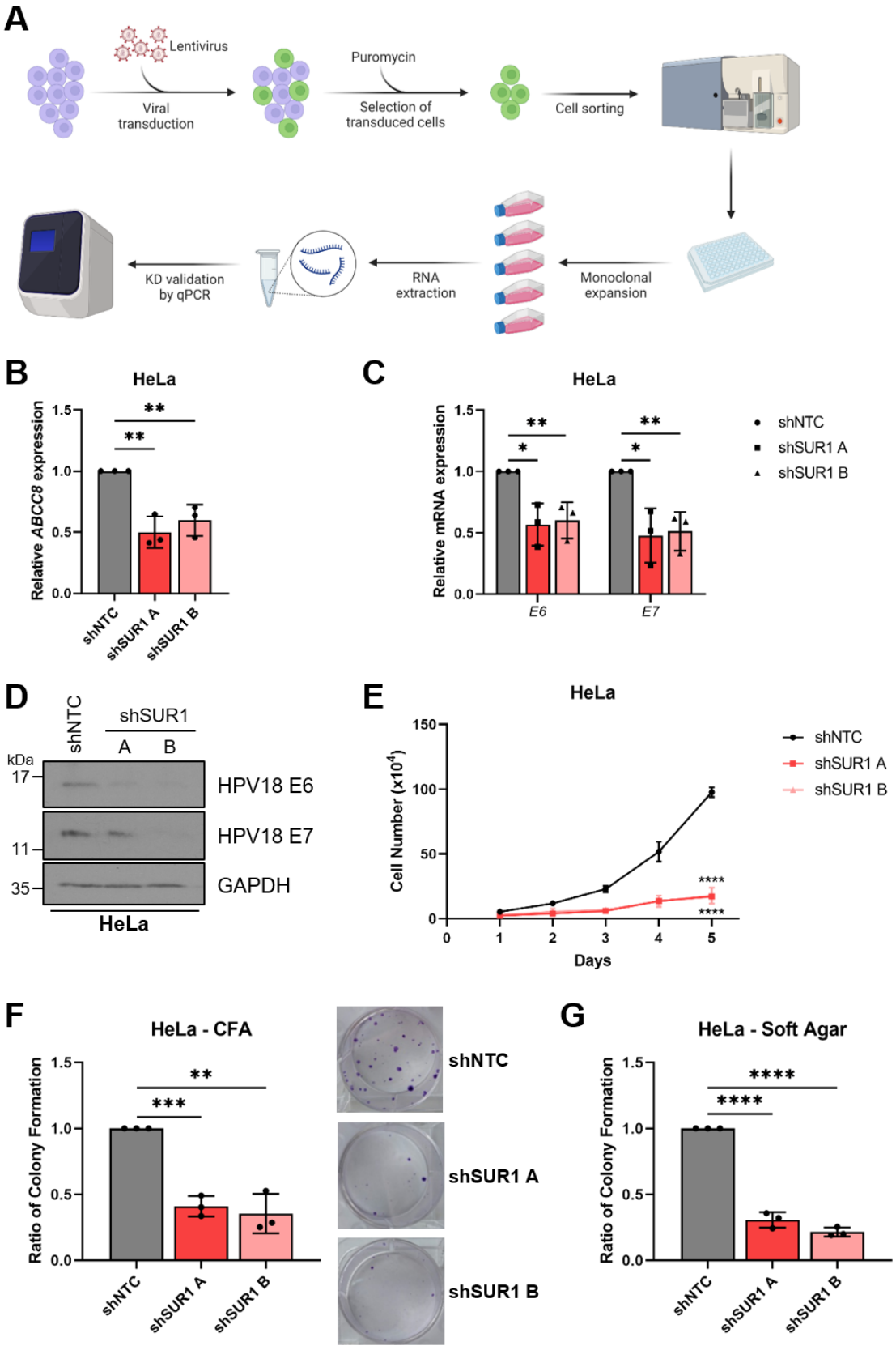

Figure 4.1 Stable knockdown of SUR1 negatively affects cervical cancer cell proliferation. A) Schematic illustrating the process of generating stable SUR1 knockdown cell lines. Figure created using BioRENDER.com. B-C) Relative expression of *ABCC8* (B) and *E6* and *E7* (C) mRNA in monoclonal HeLa cell lines stably expressing either non-targetting (shNTC) or SUR1-specific shRNA measured by RT-qPCR. Samples were normalised against

***U6* mRNA levels. D) Representative western blots of E6 and E7 expression in HeLa SUR1 knockdown cell lines. GAPDH served as a loading control. E-G) Growth curve analysis (E), colony formation assay (to measure anchorage-dependent growth) (F) and soft agar assay (to measure anchorage-independent growth) (G) of HeLa SUR1 knockdown cell lines. Data shown is means ± SD of a minimum of three biological replicates with individual data points displayed where appropriate. *P<0.05, **P<0.01, ***P<0.001, ****P<0.0001 (Student's t-test).**

4.2.2 Kir6.2 knockdown similarly inhibits proliferation of cervical cancer cells

In order to strengthen the findings above that indicate K_{ATP} channels have a role in driving proliferation, and to eliminate the possibility of K_{ATP} channel-independent SUR1 functions, the growth rate of cervical cancer cells was monitored following transient knockdown of Kir6.2, the pore-forming subunit of K_{ATP} channels. In both HPV16+ and HPV18+ cells, a significant decrease in proliferation was observed in cells with reduced Kir6.2 expression (**Fig 4.2A**). Further, a significant reduction in anchorage-dependent (~30% in HeLa and ~60% in SiHa) and anchorage-independent (~40% across both cell lines) colony forming ability was also recorded following Kir6.2 knockdown (**Fig 4.2B-C**). This therefore confirms that knockdown of either K_{ATP} channel subunit is sufficient to inhibit the proliferation of HPV+ cervical cancer cells.

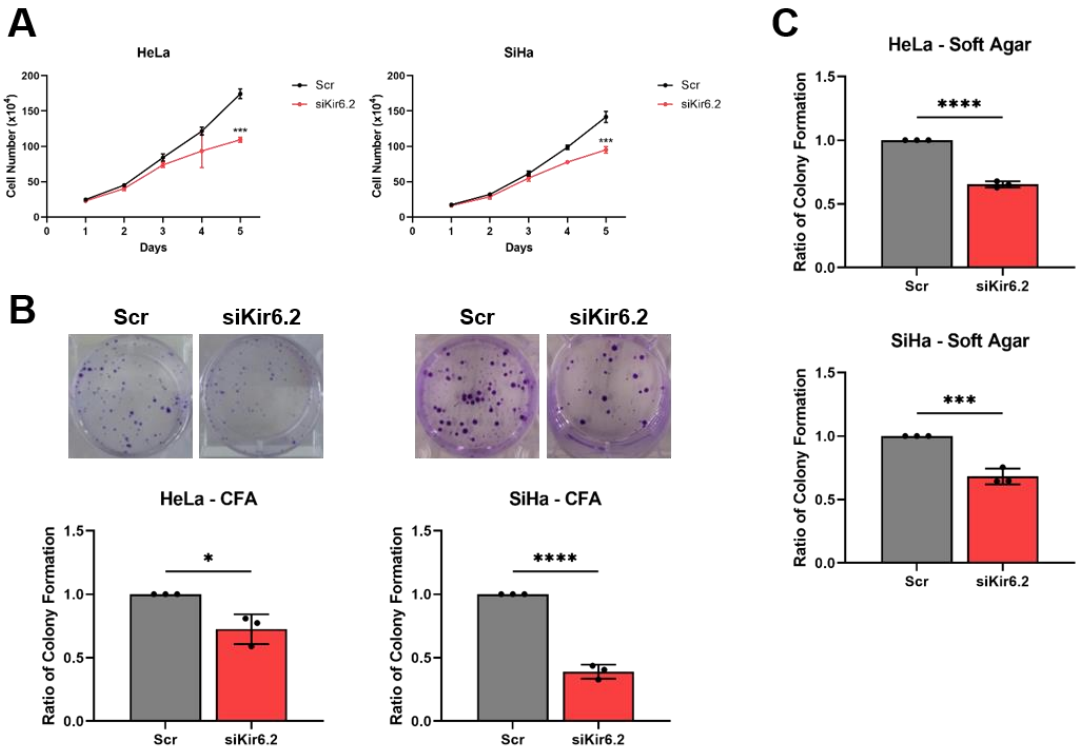

Figure 4.2 Kir6.2 knockdown similarly inhibits proliferation of cervical cancer cells. Growth curve analysis (A), colony formation assay (B) and soft agar assay (C) of HeLa and SiHa cells after transfection of Kir6.2-specific siRNA. Data represent means ± SD of three biological replicates with individual data points displayed where appropriate. *P<0.05, **P<0.01, ***P<0.001, ****P<0.0001 (Student's t-test). Parts (A) and (C) performed by Dr Ethan Morgan.

4.2.3 SUR2 knockdown has no impact on cervical cancer cell proliferation

In the preceding chapter it was identified that unlike SUR1, expression of the alternative regulatory subunit SUR2B was not increased in any of the HPV+ cervical cancer cell lines, and SUR2B knockdown did not have an impact on HPV gene expression. It was therefore hypothesised that SUR2B knockdown would similarly have no effect on the proliferation of HPV+ cervical cancer cells. In line with this, we observed no significant reduction in the proliferation of either HeLa or SiHa cells following transfection of SUR2-specific siRNA (**Fig 4.3A**). Furthermore, no effect on either the anchorage-dependent or anchorage-independent colony forming ability of SUR2 knockdown cells was recorded in comparison to the scramble siRNA control (**Fig 4.3B-C**). This therefore suggests

that SUR1-containing, rather than SUR2-comprised, K_{ATP} channels are required for the proliferation of HPV+ cervical cancer cells.

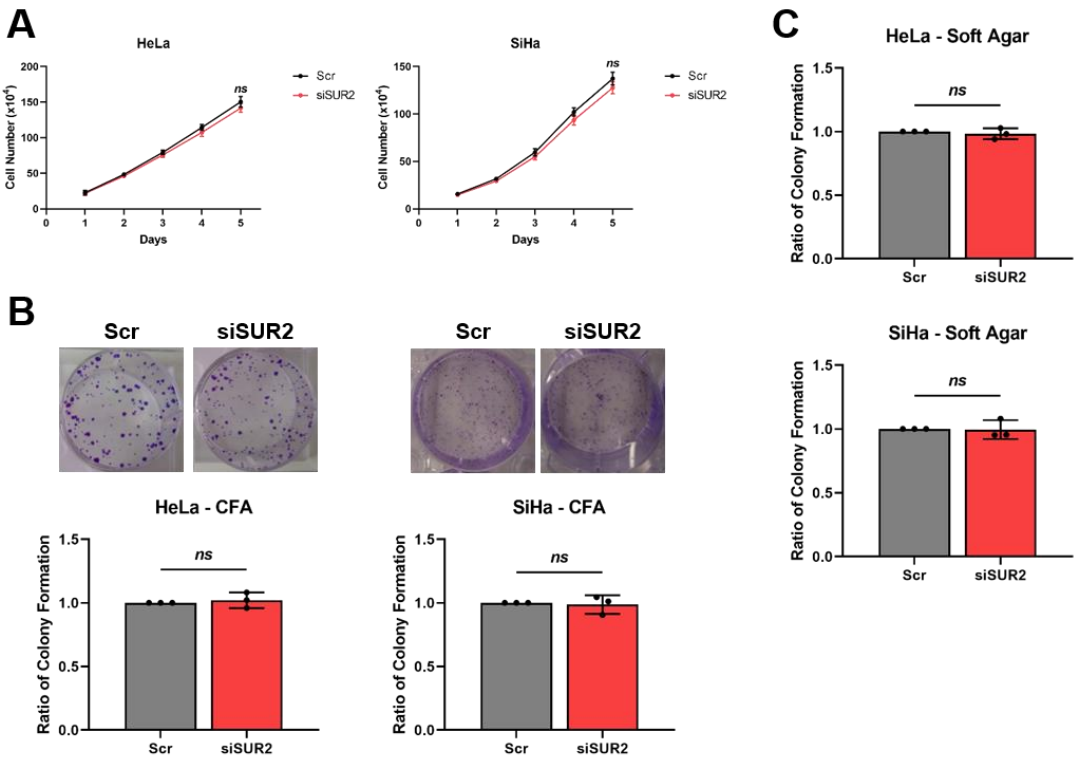

Figure 4.3 SUR2 knockdown has no impact on cervical cancer cell proliferation. Growth curve analysis (A), colony formation assay (B) and soft agar assay (C) of HeLa and SiHa cells after transfection of SUR2-specific siRNA. Data represent means ± SD of three biological replicates with individual data points displayed where appropriate. *Ns* not significant (Student's t-test). Parts (A) and (C) performed by Dr Ethan Morgan.

4.2.4 K_{ATP} channel inhibition arrests cells in G1 phase of the cell cycle

To gain an understanding of how the proliferation defect following K_{ATP} channel knockdown is manifested, the cell cycle distribution of HPV+ cervical cancer cells was assessed using DNA staining and flow cytometry. We felt this to be particularly pertinent as K_{ATP} channel inhibition has been shown to result in a G1 cell cycle phase arrest in glioma and breast cancer cell lines [329, 330]. Initially, in order to optimise the flow cytometry assay, HeLa cells were treated with a panel of inhibitors known to induce arrests at various stages of the cell cycle. Thymidine treatment interrupts the deoxynucleotide metabolism pathway, thus

preventing DNA synthesis and arresting cells at the G1/S phase transition. Addition of RO3306, a specific CDK1 inhibitor, or nocodazole, a microtubule depolymerising agent, results in a G2 or M phase arrest respectively (**Fig 4.4A**) [391, 392]. These expected effects were observed in this assay: thymidine treatment increased the proportion of cells in the G1 phase, with a corresponding decrease in the proportion of cells in G2/M (**Fig 4.4B**). Conversely, both RO3306 and nocodazole caused a significant increase in the number of cells in G2 or M phase, with a large reduction in the proportions in G1 (**Fig 4.4B**). As this assay determines the cell cycle phase only via measuring the DNA content of cells, cells in the G2 and M phases are indistinguishable due to both having a 4N chromosome number.

Following optimisation of the assay, it was used to analyse the cell cycle distribution of bulk, asynchronously dividing populations of cells following either K_{ATP} channel inhibition or siRNA-mediated knockdown of SUR1. This revealed a significant increase in the proportion of cells in G1 phase after both treatments, consistent across both HPV16+ and HPV18+ cervical cancer cells (**Fig 4.4C-D**). Interestingly, a corresponding decrease in the percentage of cells in S phase was noted following siRNA knockdown of SUR1, but this was not seen after glibenclamide treatment.

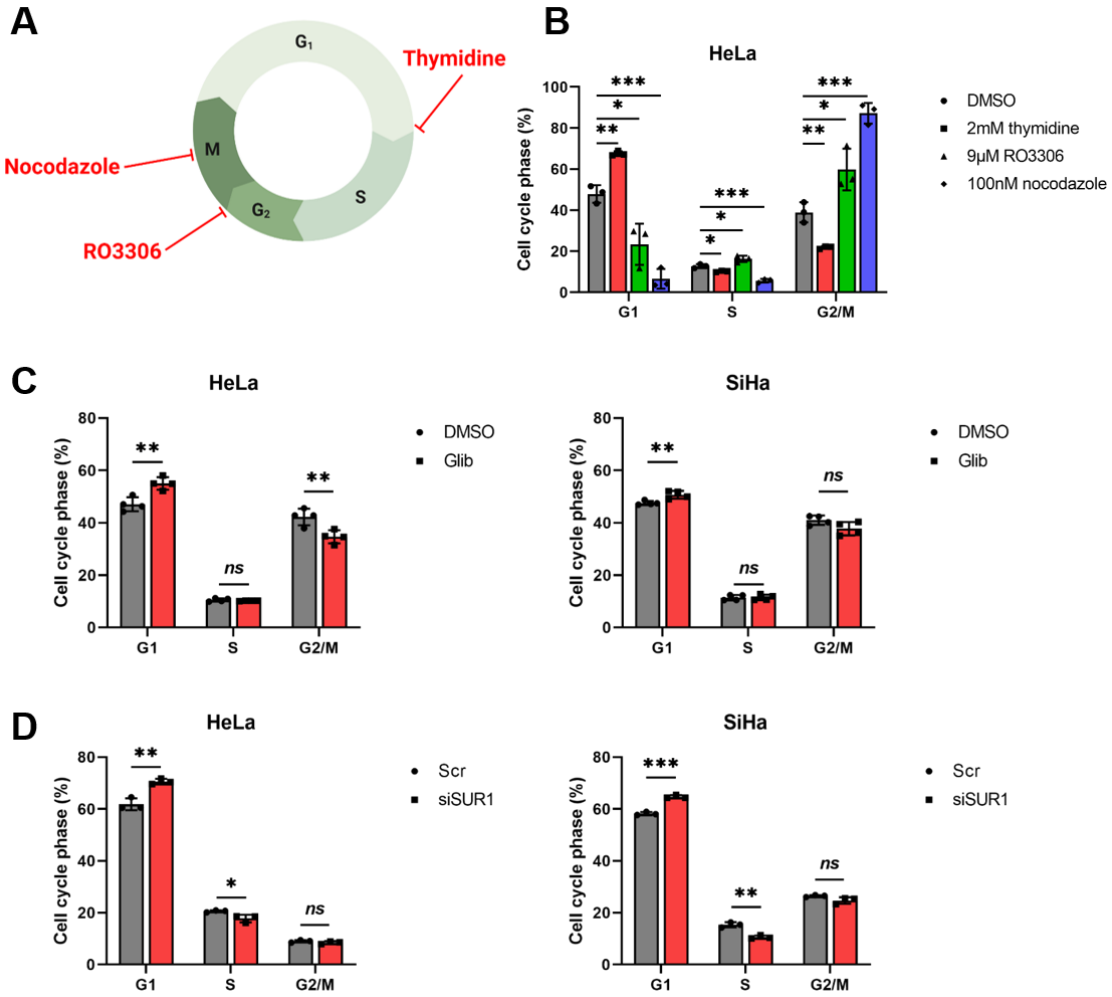

Figure 4.4 K_{ATP} channel inhibition arrests cervical cancer cells in G1 phase of the cell cycle. A) Schematic depicting stages of the cell cycle and the stage at which thymidine, RO3306 and nocodazole arrest cells in. Figure created using BioRENDER.com. B) Flow cytometry analysis of cell cycle phase distribution of HeLa cells treated with DMSO, 2 mM thymidine, 9 μM RO3306 or 100 nM nocodazole for 16 hours. C-D) Cell cycle analysis of HeLa and SiHa cells following (C) treatment with either DMSO or glibenclamide (25 μM) for 48 hours or (D) transfection of SUR1-specific siRNA. Bars represent means ± SD of three biological replicates with individual data points displayed. *Ns* not significant, *P<0.05, **P<0.01, ***P<0.001 (Student's t-test).

4.2.5 K_{ATP} channel inhibition results in a reduction in expression of cyclins D1 and E1

As cyclins are key regulators of cell cycle progression via their control of cyclin dependent kinase (CDK) activity, the expression of a panel of key cyclins was measured after glibenclamide treatment or suppression of SUR1 levels. A significant decrease in expression of cyclin D1 (*CCND1*) and cyclin E1 (*CCNE1*)

of approximately 30-50% was observed at the mRNA level (**Fig 4.5A-B**). Both of these cyclins regulate progression through G1 and into S phase via binding to and activating CDK4/6 and CDK2 respectively [393]. These effects were consistent across both HeLa and SiHa cell lines and across both treatments. Furthermore, western blot analysis of the protein expression of cyclins D1 and E1 validated these findings (**Fig 4.5C-D**). In contrast, only minimal changes in cyclin A2 (*CCNA2*) levels and no significant effect on cyclin B1 (*CCNB1*) expression was observed at the mRNA level (**Fig 4.5A-B**), with similar observations for protein expression recorded by western blot (**Fig 4.5C-D**). Taken together with the cell cycle distribution experiments, these data suggest that K_{ATP} channels drive proliferation via promoting commitment to the cell cycle and stimulating progression into S phase.

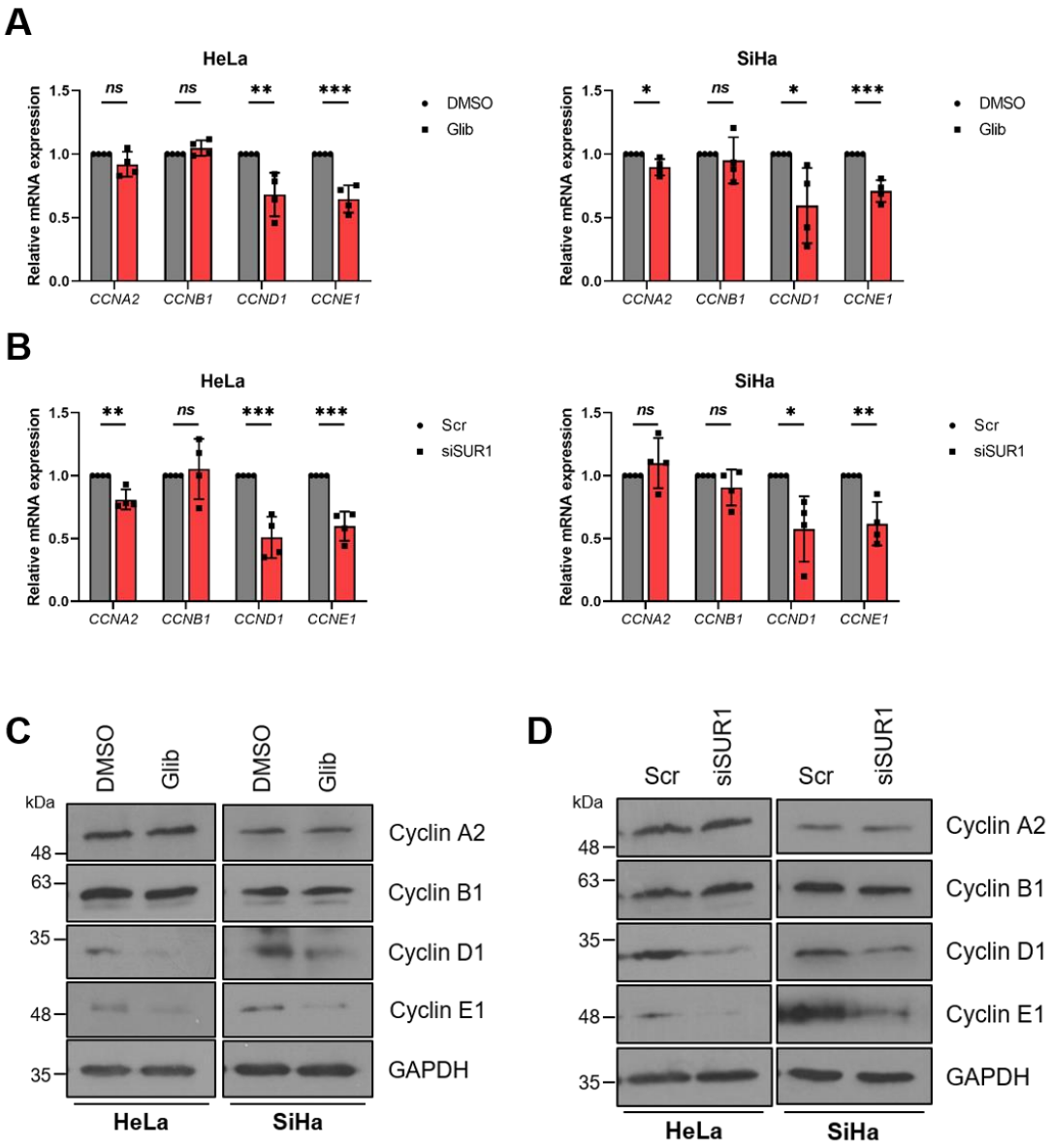

Figure 4.5 K_{ATP} channel inhibition results in a reduction in expression of cyclins D1 and E1. A-B) mRNA expression of *CCNA2*, *CCNB1*, *CCND1* and *CCNE1* in HeLa and SiHa cells following (A) treatment with either DMSO or glibenclamide (10 µM) for 24 hours or (B) transfection of SUR1-specific siRNA measured by RT-qPCR. Samples were normalised against *U6* mRNA levels and data is displayed relative to DMSO or scramble controls. C-D) Representative western blots for the expression of cyclins A2, B1, D1 and E1 in HeLa and SiHa cells following (C) treatment with either DMSO or glibenclamide (10 µM) for 24 hours or (D) transfection of SUR1-specific siRNA. GAPSH served as a loading control. Bars represent means ± SD of three biological replicates with individual data points displayed. *Ns* not significant, *P<0.05, **P<0.01, ***P<0.001 (Student's t-test).

4.2.6 K_{ATP} channels are not required for the survival of HPV+ cervical cancer cells

After characterising the effect of K_{ATP} channel activity on cell cycle progression, we also wanted to investigate the impact of channel inhibition on the survival of HPV+ cervical cancer cells, in order to see whether this also contributed to the proliferation defect observed. Interestingly, increased levels of apoptosis, a form of programmed cell death, has been reported in some cancer types after K_{ATP} channel blockade [328, 330, 331]. To determine whether K_{ATP} channels are required for the survival of HPV+ cervical cancer cells, the activation of caspase-3, an executioner caspase that is activated in response to cell death stimuli and is critical in mediating apoptotic signalling, was investigated following glibenclamide treatment [394]. Caspase-3 is activated via proteolytic processing by caspase-9 [394]. Interestingly however, no cleavage of caspase-3 was detected following K_{ATP} channel inhibition for the duration of time used routinely throughout this study (24 hours) (**Fig 4.6A**). To determine whether prolonged inhibition of K_{ATP} channels would result in the induction of apoptosis, HeLa and SiHa cells were also treated with glibenclamide for 48 and 72 hours. Even following these longer treatment durations, no caspase-3 cleavage was observed (**Fig 4.6A**). To validate these findings, the proteolytic cleavage of poly(ADP) ribose polymerase (PARP), a downstream target of caspase-3 was investigated [395]. Concordant with the absence of caspase-3 cleavage, no PARP cleavage could be detected at any time point (**Fig 4.6A**). To confirm that apoptosis could be successfully induced in these cell lines and that the cleaved forms of caspase-3 and PARP could be detected by western blot, treatment with staurosporine (STS) was used. STS is a non-selective protein kinase inhibitor that readily

induces apoptosis in a wide variety of cell lines. Treatment of both HeLa and SiHa cells with STS for 6 hours was sufficient to induce the caspase cleavage cascade.

To confirm these findings using an orthogonal approach, Annexin V assays were performed. An early event during apoptosis is the exposure of phosphatidylserine (PS) residues on the outer surface of the plasma membrane [396]. This can be detected by Annexin V, a phospholipid binding protein with a high affinity for PS [396]. Flow cytometry assays were carried out in which cells were co-stained with fluorescein isothiocyanate (FITC)-labelled Annexin V and PI following glibenclamide treatment. K_{ATP} channel blockade did not result in an increase in the percentage of cells in either early apoptosis (FITC+, PI-) or late apoptosis (FITC+, PI+) at any of the time points investigated (**Fig 4.6B**). Taken together, these data confirm that K_{ATP} channel inhibition does not impact upon the survival of HPV+ cervical cancer cells.

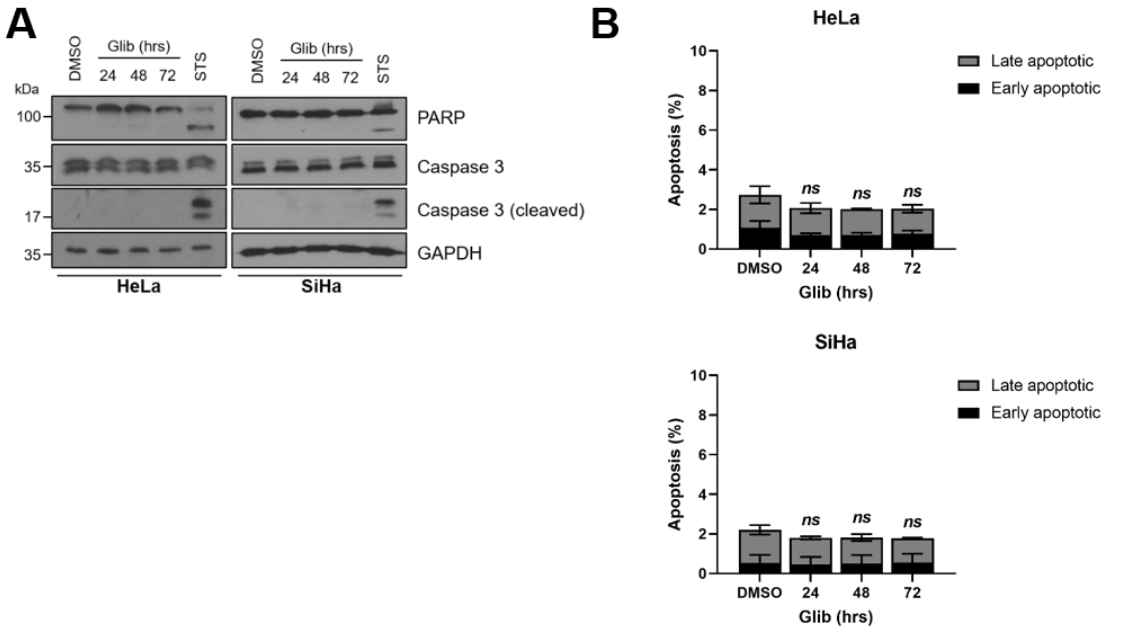

Figure 4.6 K_{ATP} channels are not required for the survival of HPV+ cervical cancer cells. A) Representative western blots of PARP and caspase 3 cleavage in HeLa and SiHa cells treated with DMSO or glibenclamide (10 μM) for the indicated durations. Staurosporine treatment (STS, 1 μM for 6 hours) served as a positive control for apoptosis induction. GAPDH served as a loading control. B) Flow cytometry analysis of Annexin V assay using HeLa and SiHa cells treated with DMSO or glibenclamide (10 μM) for the indicated durations. Bars represent means ± SD of three biological replicates. *Ns* not significant (Student's t-test).

4.2.7 K_{ATP} channel activity does not regulate epithelial to mesenchymal transition (EMT)

Epithelial to mesenchymal transition (EMT) is a collective term for the acquisition of a mesenchymal cell phenotype by epithelial cells. EMT is a common occurrence during tumour progression and allows solid tumours to increase their invasiveness and metastatic potential [397]. EMT has been shown to play an important role in cervical cancer progression and metastasis via increasing tumour cell invasion and motility [398]. The key mediators of EMT are the so-called EMT-activating transcription factors (EMT-TFs), which include Snail, Slug, TWIST1 and ZEB1 [397]. To initially investigate whether K_{ATP} channels may be promoting EMT in HPV+ cervical cancer, the expression of these key EMT-TFs was analysed by RT-qPCR following stable SUR1 knockdown. Surprisingly, no

decrease in the mRNA expression of *SNAI1* (Snail), *TWIST1* or *ZEB1* was observed in either of the knockdown cell lines in comparison to the shNTC control (**Fig 4.7A**). In fact, an increase in relative expression of *SNAI2* (Slug) of over two fold was seen, suggesting that K_{ATP} channels may not be critical for the regulation of EMT in HPV+ cervical cancer cells. However, this analysis does not discount any potential changes in the activity of these EMT-TFs, or indeed alterations to the target gene promoters to which they are binding. To attempt to resolve this issue, the mRNA expression of an additional panel of genes was examined. Key biomarkers for EMT were analysed, including the mesenchymal markers vimentin, N-cadherin and fibronectin, the expression of which has been shown to increase in response to EMT-TF activity [397]. However, no change in *VIM* (vimentin) or *FN1* (fibronectin) mRNA expression was detected, whilst a small ~1.5 fold increase in *CDH2* (N-cadherin) expression was observed, following loss of K_{ATP} channel activity (**Fig 4.7B**). Furthermore, upon analysis of the expression of two matrix metalloproteases (MMPs), which act to degrade components of the extracellular matrix (ECM) thus facilitating migration and invasion, no change in *MMP2* and an increase in *MMP9* mRNA expression was found in the SUR1 knockdown cell lines (**Fig 4.7B**). Finally, expression of *tight junction protein 1* (*TJP1*), a marker of an epithelial cell phenotype which is typically downregulated during EMT was analysed. Although a small but significant increase in *TJP1* mRNA was identified in one of the SUR1 knockdown cell lines, this was not replicated in the second (**Fig 4.7B**).

To validate these findings at the protein level, western blot analysis of a selection of the EMT markers described here was performed. This revealed no change in the protein levels of Snail or vimentin and an increase in Slug expression, concordant with prior analysis of the mRNA expression of these biomarkers (**Fig**

4.7C). In summary, these data suggest that, although linked to the proliferative capacity of HPV+ cervical cancer cells, K_{ATP} channel activity is not involved in regulating the migratory potential of these cells via promotion of EMT.

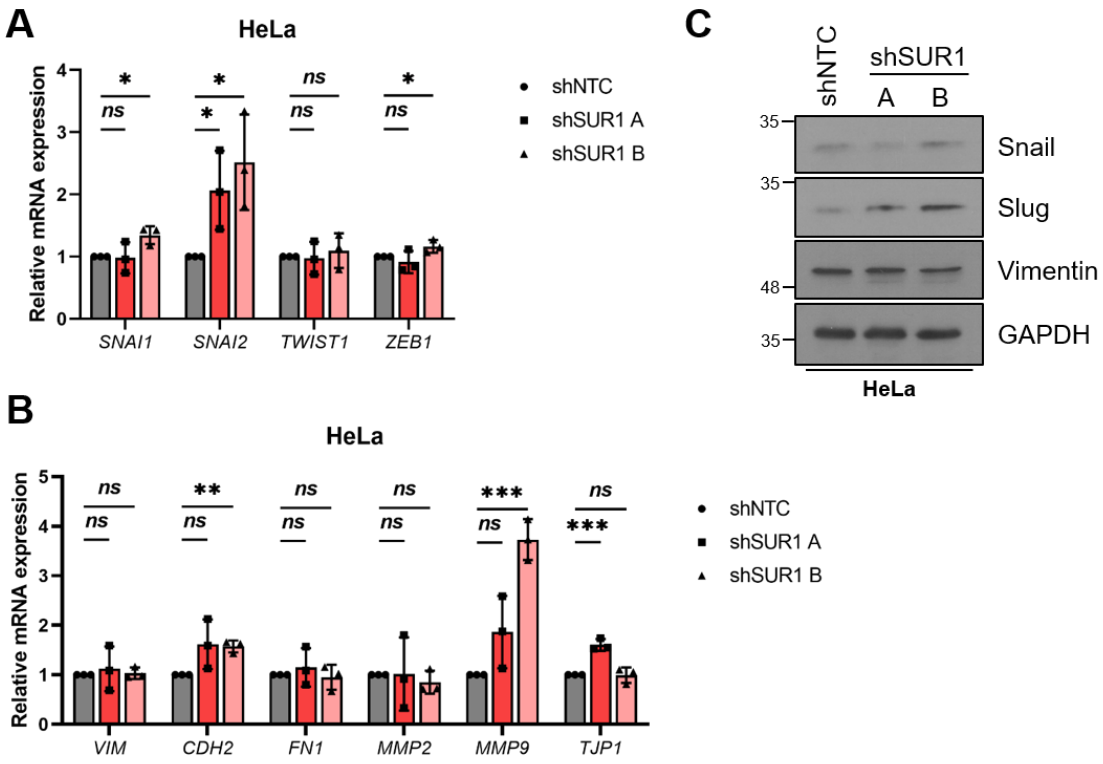

Figure 4.7 K_{ATP} channel activity does not regulate epithelial to mesenchymal transition (EMT). A) mRNA expression of EMT-activating transcription factors (EMT-TFs) – *SNAI1, SNAI2, TWIST1, ZEB1* – in HeLa cells stably expressing one of two SUR1-specific shRNAs measured by RT-qPCR. Samples were normalised against *U6* mRNA levels and data is displayed relative to the shNTC control. B) mRNA expression of EMT markers (*VIM*, *CDH2*, *FN1*, *MMP2*, *MMP9*, *TJP1*) in HeLa cells stably expressing one of two SUR1-specific shRNAs measured by RT-qPCR. Samples were normalised against *U6* mRNA levels and data is displayed relative to the shNTC control. C) Representative western blots of Snail, Slug and vimentin expression in HeLa cells stably expressing one of two SUR1-specific shRNAs. GAPDH served as a loading control. Bars represent means ± SD of three biological replicates with individual data points displayed. *Ns* not significant, *P<0.05, **P<0.01, ***P<0.001 (Student's t-test).

4.2.8 K_{ATP} channels drive proliferation and oncoprotein expression by activating a MAPK/AP-1 signalling axis

We next wanted to gain an understanding into the underlying signalling mechanisms by which K_{ATP} channels promote proliferation in HPV+ cervical

cancer cells. K_{ATP} channel opening can lead to the activation of ERK1/2 signalling [333, 389] and MAPK signalling is known to be a crucial driver of cell proliferation [399], so we therefore analysed the phosphorylation levels of the MAP kinase ERK1/2 after stimulation of cells with diazoxide. This revealed a significant increase in ERK1/2 phosphorylation post-stimulation which was reversed following the addition of the specific MEK1/2 inhibitor U0126 (**Fig 4.8A**) [400]. Additionally, an increase in HPV18 E7 protein levels was observed, consistent with experiments in the previous chapter; this was also reduced with U0126 treatment. Interestingly, an increase in both the phosphorylation and total protein expression of the AP-1 family member cJun was also observed (**Fig 4.8A**). AP-1 transcription factors are composed of dimers of proteins belonging to the Jun, Fos, Maf and ATF sub-families, and can regulate a wide variety of cellular processes, including proliferation, survival and differentiation [401]. This indicates that cJun/AP-1 could be a downstream target of ERK1/2 following K_{ATP} channel stimulation.

To confirm these observations, overexpression of both K_{ATP} channel subunits in combination was performed. This similarly resulted in increased ERK1/2 phosphorylation, increases in both cJun phosphorylation and total protein levels, as well as enhanced E7 expression (**Fig 4.8B**). As before, these increases were reversed, in part, by the addition of U0126. In order to confirm that the changes in expression and phosphorylation of cJun observed corresponded to alterations in AP-1 activity, we employed a luciferase reporter construct containing three tandem AP-1 binding sites [163, 402]. K_{ATP} channel overexpression led to a ~4 fold increase in relative AP-1 activity, which was significantly reduced in the presence of U0126 (**Fig 4.8C**), suggesting that K_{ATP} channels can promote the activation of AP-1.

Following this, we performed assays to answer the question of whether the activation of this MAPK/AP-1 signalling axis is necessary for the pro-proliferative effects of K_{ATP} channels. To examine this, the proliferation rate and colony-forming ability of HeLa cells was analysed following K_{ATP} channel subunit overexpression, in the presence and absence of U0126. As expected, an increase in both proliferation and colony-forming ability was observed following overexpression of K_{ATP} channel subunits, but this was entirely reversed via MEK1/2 inhibition (**Fig 4.8D-E**). Together, these data illustrate that K_{ATP} channels activate ERK1/2 and AP-1 signalling, and that this is required for the pro-proliferative effects of K_{ATP} channels.

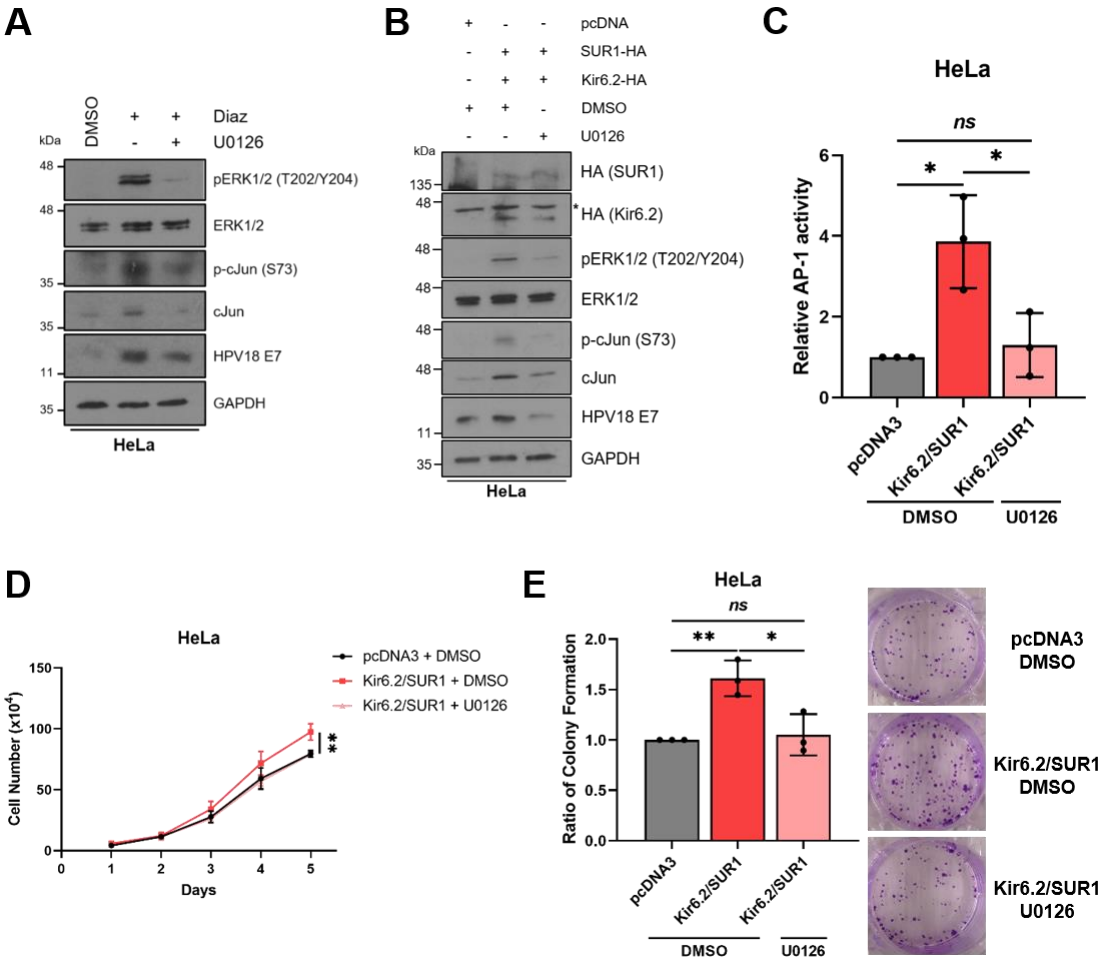

Figure 4.8 K_{ATP} channels drive proliferation by activating a MAPK/AP-1 signalling axis. A-B) Representative western blots of phospho-ERK1/2, ERK1/2, phospho-cJun, cJun and E7 in HeLa cells either A) serum starved for 24 hours prior to treatment with diazoxide (50 µM), with and without the MEK1/2 inhibitor U0126 (20 µM), for 24 hours or B) transfected with plasmids expressing HA-tagged Kir6.2 and SUR1, with and without U0126 treatment (20 µM). * denotes the presence of a non-specific band. GAPDH served as a loading control. C) Relative firefly luminescence in HeLa cells co-transfected with plasmids expressing HA-tagged Kir6.2 and SUR1 and an AP-1-driven reporter construct. Cells were also treated with DMSO or the MEK1/2 inhibitor U0126 (20 µM) for 24 hours. Luminescence values were normalised against *Renilla* luciferase activity. Performed by Ms Molly Patterson. D-E) Growth curve analysis (D) and colony formation assay (E) of HeLa cells after co-transfection with plasmids expressing HA-tagged Kir6.2 and SUR1 and treatment with DMSO or U0126 (20 µM) for 24 hours. Bars represent means ± SD of a minimum of three biological replicates with individual data points displayed when appropriate. *Ns* not significant, *P<0.05, **P<0.01, ***P<0.001 (Student's t-test).

To validate the above findings using an orthogonal approach, the impact of K_{ATP} channel blockade on AP-1 activity was next analysed. Using the same AP-1 luciferase reporter construct as before, a ~30% reduction in AP-1 activity was

observed in both HeLa and SiHa cells following glibenclamide treatment (**Fig 4.9A**). Consistent with this, a highly similar reduction in the mRNA expression of *JUN* was also detected by RT-qPCR in both cell lines after treatment with the K_{ATP} channel inhibitor (**Fig 4.9B**). Further, transfection of SUR1-specific siRNA in HeLa cells also decreased AP-1 activity, measured by luciferase reporter, by ~40% (**Fig 4.9C**). Finally, to investigate whether this loss of AP-1 transactivational potential following modulation of K_{ATP} channel activity was due to the recruitment of cJun/AP-1 to target binding sites being affected, ChIP-qPCR assays were performed. For illustrative purposes, the binding of cJun to two consensus AP-1 sites located within the HPV18 URR, one in the enhancer and one in the promoter-proximal region, was analysed [163]. Many HPV types possess AP-1 binding sites within their respective URRs, and the integrity of both HPV18 AP-1 sites has been shown to be critical for efficient early gene expression [376, 403-405]. This revealed that SUR1 knockdown using siRNA profoundly reduced cJun recruitment to both binding sites within the viral URR, relative to the scramble control (**Fig 4.9D**). Together, these data highlight the critical role K_{ATP} channels may have in regulating AP-1 activity and oncoprotein expression.

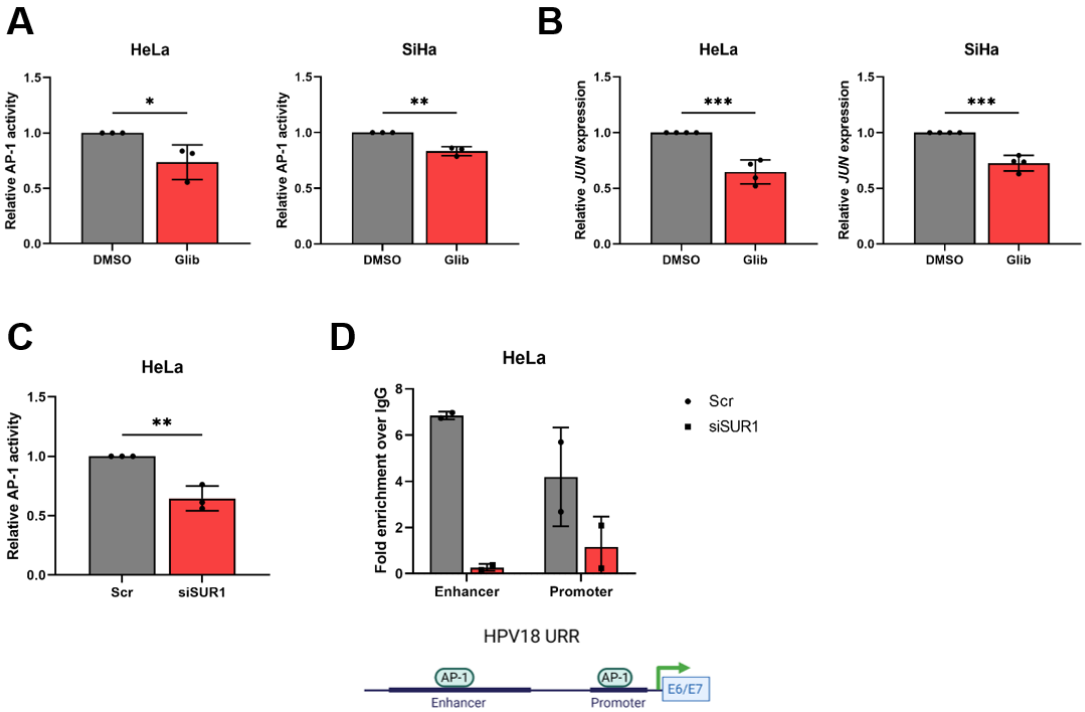

Figure 4.9 Inhibition of K_{ATP} channels reduces AP-1 expression, activity and recruitment to target gene promoters. A) Relative firefly luminescence in HeLa and SiHa cells transfected with an AP-1-driven reporter plasmid and treated with glibenclamide (10 µM) for 24 hours. Luminescence values were normalised against *Renilla* luciferase activity. B) mRNA expression of *JUN* in HeLa and SiHa cells treated with glibenclamide (10 µM) for 24 hours, measured by RT-qPCR. Samples were normalised against *U6* mRNA levels. C) Relative firefly luminescence in HeLa cells co-transfected with an AP-1-driven reporter plasmid and SUR1-specific siRNA. Luminescence values were normalised against *Renilla* luciferase activity. D) ChIP-qPCR analysis of cJun binding to two AP-1 sites within the HPV18 URR in HeLa cells transfected with SUR1-specific siRNA. cJun binding is presented as a fold increase over IgG binding (n = 2). Figure created using BioRENDER.com. Bars represent means ± SD of a minimum of three biological replicates with individual data points displayed, unless stated otherwise. *Ns* not significant, *P<0.05, **P<0.01, ***P<0.001 (Student's t-test).

To further confirm our observations highlighting the importance of AP-1 in K_{ATP} channel-induced proliferation and oncoprotein expression, the impact of inhibiting AP-1 activity following K_{ATP} stimulation was analysed. To this end, we employed a dominant-negative JunD construct (ΔJunD): this encodes a truncated form of JunD which is able to dimerise with other AP-1 family members yet lacks a transcriptional activation domain [406]. Previous studies in our lab have validated that ΔJunD expression almost completely abolishes AP-1 activity [163].

Transfection of this construct resulted in a reversal of the diazoxide-induced HPV oncoprotein expression (**Fig 4.10**).

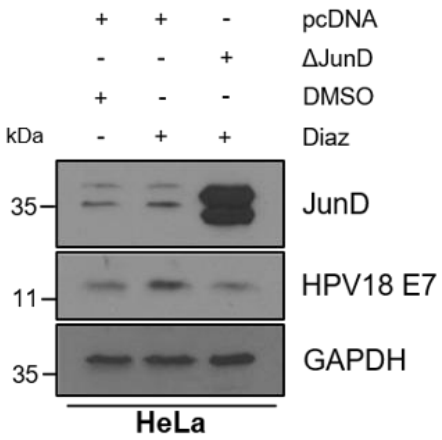

Figure 4.10 Blockade of AP1 activity prevents K_{ATP} channel-induced HPV gene expression. Representative western blots for JunD, E6 and E7 expression in HeLa cells treated with diazoxide (50 μM), with and without transfection of a plasmid expressing ΔJunD. Cells were serum-starved for 24 hours prior to treatment. GAPDH served as a loading control.

4.2.9 Reintroduction of cJun restores proliferation and oncoprotein expression in SUR1 KD cells

Next, to further confirm the importance of AP-1 for K_{ATP} channel-induced proliferation, we wanted to investigate whether restoration of cJun/AP-1 signalling to HeLa cells following SUR1 knockdown would be able to rescue their proliferative defect. To this end, an expression vector for a constitutively active mutant of cJun was employed [407-410]. This mutant, S63/73D, consists of two serine to aspartic acid mutations at the key S63 and S73 residues, whose phosphorylation by the MAPKs ERK1/2 and JNK1/2 is required for cJun activation [411-414]. S63/S73 phosphorylation is thought to facilitate the interaction of cJun with the coactivator CPB/p300, thus permitting transcriptional upregulation of target genes [415, 416]. As noted previously, transfection of SUR1-specific siRNA resulted in a significant reduction in the proliferation and colony-forming ability of HeLa cells (**Fig 4.11A-B**). However, when active cJun was reintroduced, a small but significant restoration of proliferation was observed (**Fig 4.11A-B**).

This suggests that cJun phosphorylation on S63 and S73 is required to promote HPV+ cervical cancer cell proliferation.

Next, we tested whether a similar rescue to the expression of the HPV oncoproteins was also observed. Western blot analysis demonstrated a reduction in E7 protein levels following SUR1 knockdown, as expected, which was fully restored via active cJun overexpression (**Fig 4.11C**). Together, these data suggest that cJun is important for driving proliferation downstream of K_{ATP} channels.

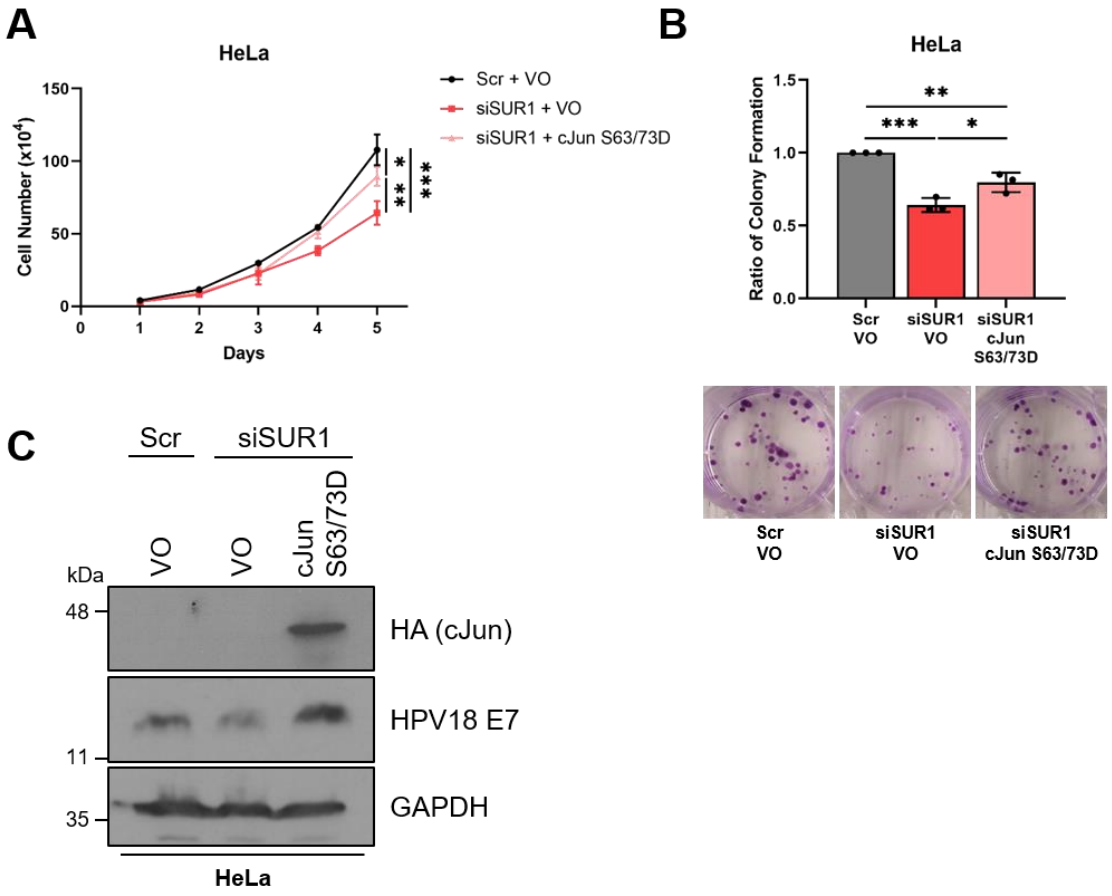

Figure 4.11 Reintroduction of cJun following SUR1 knockdown restores proliferation and HPV oncoprotein expression. A-B) Growth curve analysis (A) and colony formation assay (B) of HeLa cells co-transfected with SUR1-specific siRNA and a plasmid expressing a constitutively-active form of cJun (S63/73D). C) Representative western blots for HA and E7 expression in HeLa cells treated as above (n = 2). GAPDH served as a loading control. Data shown represents means ± SD of three biological replicates (unless stated otherwise) with individual data points displayed where appropriate. *Ns* not significant, *P<0.05, **P<0.01, ***P<0.001 (Student's t-test).

4.2.10 K_{ATP} channels contribute to the activation of AP-1 signalling and HPV transcription by E7

Data in the preceding chapter identified that the HPV E7 oncoprotein was responsible for upregulating expression of SUR1, thus enhancing K_{ATP} channel activity. Therefore, the impact of expressing E7 in a HPV- cell line on AP-1 activity was analysed, in the presence and absence of a K_{ATP} channel modulator. It has previously been reported that HPV16 E7 is capable of interacting with AP-1 transcription factors, enhancing their transactivational potential [417]. Unsurprisingly therefore, expression of HPV18 E7 resulted in a ~1.5 fold increase in AP-1 activity, as measured by luciferase reporter assay (**Fig 4.12A**). Significantly, this increase in activity was reversed, in part, via glibenclamide treatment, suggesting that E7-mediated activation of K_{ATP} channels may be one of multiple mechanisms by which the oncoprotein promotes AP-1 activity. To ensure that this was not an artefact due to off-target effects of glibenclamide, the experiment was repeated using SUR1-specific siRNA. Knockdown of SUR1 expression led to a highly similar partial reversal of the E7-induced upregulation of AP-1 activity (**Fig 4.12B**). To further confirm this, the impact on AP-1 transactivity was also investigated in C33A cells stably expressing HPV18 E7. As expected, a ~1.7 fold increase in AP-1 driven luciferase activity was detected in the E7-expressing cells, which was reduced by half following K_{ATP} channel inhibition (**Fig 4.12C**). Together, these data suggest that K_{ATP} channels may be an important mechanism by which E7 promotes AP-1 activity.

The experiments described above analyse the activity of AP-1 following E7 expression. However, they do not address the question of whether E7 is capable of modulating the expression of AP-1 subunits via activation of K_{ATP} channels. To resolve this, the protein levels of the prototypical AP-1 family members cFos and

cJun were analysed in C33A cells transiently expressing GFP-tagged HPV18 E7, in the presence and absence of glibenclamide. Interestingly, we observed an increase in protein levels of cJun in the presence of HPV18 E7 which was reversed by glibenclamide treatment, but no alterations to cFos expression (**Fig 4.12D**). This suggests that E7 activation of K_{ATP} channels may be specifically upregulating the expression of particular AP-1 subunits. Further, this is in agreement with data earlier in the chapter highlighting changes in the expression of cJun following K_{ATP} channel modulation in HeLa cells.

Next, the extent to which K_{ATP} channels contribute towards E7-mediated upregulation of HPV early gene expression was analysed. AP-1 activity is critical for HPV gene expression [163, 376, 403-405], so it was hypothesised that overexpression of E7 would promote HPV URR activity via its activation of AP-1. In line with this, a ~2.5 fold increase in transcription driven by the HPV18 URR was detected, via luciferase reporter assay, following expression of E7 in HPV-C33A cells (**Fig 4.12E**). This was reduced, partially albeit significantly, with K_{ATP} channel inhibition, suggesting the presence of a feedback loop in which E7 drives its own transcription through activation of K_{ATP} channels. To confirm this, an siRNA knockdown strategy was employed. As before, a greater than 2 fold increase in URR activity was observed in the presence of E7, which was partially reduced with SUR1 knockdown (**Fig 4.12F**). Together, these data suggest that HPV E7 expression is sufficient to promote AP-1 URR promoter activity via its upregulation of K_{ATP} channels.

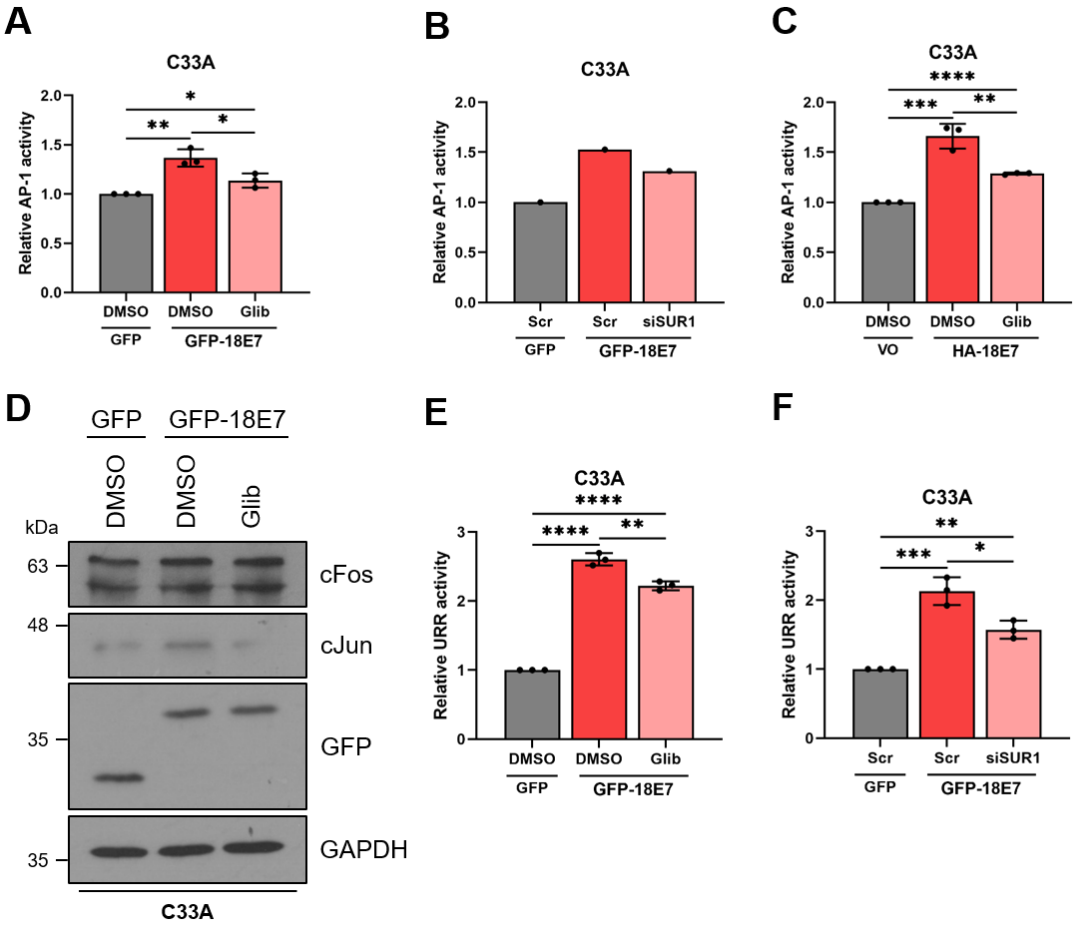

Figure 4.12 Activation of AP-1 signalling and HPV transcription by E7 occurs via K_{ATP} channels. A-C) Relative firefly luminescence in C33A cells transfected with an AP-1-driven reporter plasmid and A) co-transfected with a GFP or GFP-18E7 expression vector and treated with DMSO or glibenclamide (10 μM) for 24 hours, B) co-transfected with a GFP or GFP-18E7 expression vector and scramble or SUR1-specific siRNA (n = 1), or C) stably expressing HA-tagged HPV18 E7 and treated with DMSO or glibenclamide (10 μM) for 24 hours. Luminescence values were normalised against *Renilla* luciferase activity. D) Representative western blot of cFos and cJun expression in C33A cells transfected with a GFP or GFP-18E7 expression vector and treated with DMSO or glibenclamide (10 μM) for 24 hours (n = 1). GAPDH served as a loading control. E-F) Relative firefly luminescence in C33A cells transfected with an HPV18 URR-driven reporter plasmid and treated as in (A-B). Luminescence values were normalised against *Renilla* luciferase activity. Bars represent means ± SD of three biological replicates with individual data points displayed, unless stated otherwise. *Ns* not significant, *P<0.05, **P<0.01, ***P<0.001, ****P<0.0001 (Student's t-test).

4.2.11 K_{ATP} channels drive proliferation in an *in vivo* mouse model

Finally, in order confirm the earlier *in vitro* observations which indicate that K_{ATP} channels are critical in driving proliferation in HPV+ cervical cancer cells, *in vivo*

tumourigenicity experiments using SCID mice were performed. Animals were subcutaneously injected with HPV18+ HeLa cells stably expressing either a non-targetting shRNA (shNTC) or a SUR1-specific shRNA (cell lines described in 4.2.1), and tumour growth was monitored over a period of ~6 weeks. All mice developed tumours and no toxicity, including significant weight loss, was seen in any of the animals. Critically, a significant delay in the growth of tumours in all mice injected with SUR1 knockdown cells was observed in comparison to the shNTC controls (**Fig 4.13A**). To quantify this delay in growth, the period of time between injection of tumours and growth to a set volume (250 mm^3) was calculated. This revealed that the SUR1-depleted tumours took an additional 11 days on average to reach an equivalent volume (**Fig 4.13B**). Further, animals bearing SUR1-depleted tumours displayed prolonged survival, with one mouse remaining alive at the conclusion of the study (**Fig 4.13C**). Together, these data demonstrate that K_{ATP} channels drive the growth of HPV+ cervical cancer cell xenografts.

Following sacrifice of the animals, tumour tissue was collected, fixed and sectioned to allow for probing for the expression of proliferation markers by IHC. Staining was performed on sections from the same five mice from each experimental group that were included in the tumour growth analyses. Staining was undertaken for Ki67, an antigen present during all active phases of the cell cycle but absent in quiescent and senescent cells. Surprisingly, this revealed highly similar protein levels of Ki67 in tumours taken from both shNTC-injected mice and shSUR1-injected mice, suggesting similar levels of proliferation at the time of sacrifice (**Fig 4.13D**). To confirm that the knockdown of SUR1 was maintained throughout the *in vivo* experiment, IHC staining for SUR1 protein levels was also carried out. Unexpectedly, there was no reduction in staining

intensity in tumours taken from the shSUR1 A group of mice, indicating that the knockdown had been lost at some point between injection of the cells and animal sacrifice (**Fig 4.13D**).

To confirm these observations, staining was quantified using ImageJ and the IHC Profiler plugin, allowing the calculation of H-scores based on the percentage of positively stained tumour cells and the staining intensity [337-339]. This confirmed that there was no difference in the staining for either SUR1 or Ki67 between the two experimental groups (**Fig 4.13E**). Importantly, no staining was detected with either of the secondary antibody only controls, indicating that the staining was specific to the protein of interest in both cases.

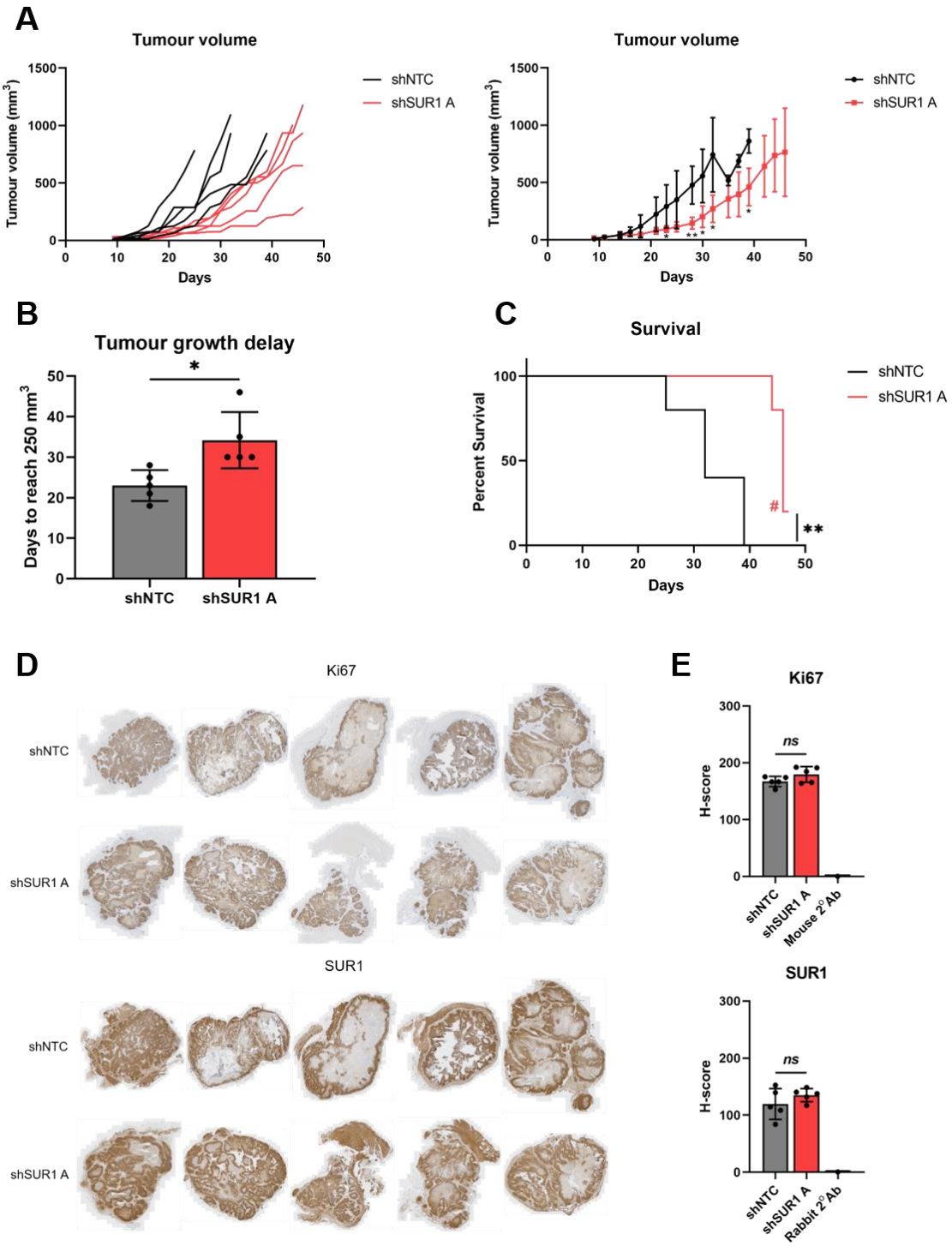

Figure 4.13 K_{ATP} channels drive proliferation in an *in vivo* mouse model. A) Tumour growth curves for mice implanted with HeLa cells stably expressing either a non-targetting (shNTC) or an SUR1-specific shRNA (shSUR1 A). Tumour volume was calculated using the formula $V=0.5*L*W^2$. Individual curves for each replicate (left) and curves representing mean values ± SD of five mice per group (right) are displayed. B) Tumour growth delay, calculated as the days taken to reach a volume of 250 mm^3, for mice implanted with HeLa cells stably expressing either a non-targetting (shNTC) or an SUR1-specific shRNA (shSUR1 A). Bars represent means ± SD of five biological replicates with individual data points displayed. *P<0.05 (Student's t-test). C) Kaplan-Meier survival curve of mice bearing shNTC

and shSUR1 A tumours. # indicates that one mice remained alive at the conclusion of the study. **P<0.01 (log-rank (Mantel-Cox) test). D) Immunohistochemistry (IHC) staining of Ki67 (top) and SUR1 (bottom) protein expression in tumour sections taken from mice implanted with HeLa cells stably expressing either a non-targetting (shNTC) or an SUR1-specific shRNA. E) Quantification of IHC staining in D). Bars represent mean H-scores ± SD of five biological replicates with individual data points displayed. *Ns* not significant (Student's t-test).

4.3 Discussion

The preceding chapter presented evidence that a novel host factor, the K_{ATP} channel, is a crucial regulator of HPV gene expression in cervical cancer cells. The data presented in this study advances upon the previous findings by identifying the critical role of K_{ATP} channels in regulating the proliferation of these cells. Loss of K_{ATP} channel activity, either via stable suppression of SUR1 expression or transient knockdown of Kir6.2, resulted in a profound reduction in proliferation and colony-forming ability, likely due to disruption to the progression of cells through G1 phase of the cell cycle. Surprisingly however, we found that K_{ATP} channels have no impact upon either the survival or the migratory potential (through regulation of EMT) of cervical cancer cells. The mechanism by which the pro-proliferative effects of K_{ATP} channels is mediated was also investigated, revealing that the channels promote activation of the MAP kinase ERK1/2 and subsequently the host transcription factor AP-1. Finally, we provide *in vivo* confirmation of the importance of K_{ATP} channels: SUR1 deficient tumours displayed significantly reduced growth and the mice bearing them experienced prolonged survival. Taken together, these data emphasise the highly important role K_{ATP} channels have in driving the continued proliferation of HPV+ cervical cancer cells.

Using a combination of shRNA-mediated knockdown of SUR1 and transient suppression of Kir6.2 expression, this study identifies a clear role for K_{ATP} channels in regulating the proliferation of HPV+ cervical cancer cells. A significant reduction was noted across all assays used to assess the proliferative potential of cells, namely growth curves, colony formation assays and soft agar assays. Additional investigations in our lab have confirmed that a highly similar loss of proliferation occurs following transfection of SUR1-specific siRNA [352]. Further,

treatment with glibenclamide has also been shown to inhibit cell growth of HPV+ cervical cancer cell lines, but critically not HPV- C33A cells [352]. A previous study similarly reported the growth inhibitory effects of glibenclamide on cervical cancer cells via MTT assay [332]. However, this report used greatly increased drug concentrations than those employed here, enhancing the risk of off-target effects, and interestingly only observed decreased proliferation in HeLa cells, C33A cells and primary keratinocytes, yet not in either of the HPV16+ cell lines examined [332]. Importantly, we demonstrate that silencing of the alternative regulatory subunit SUR2 had no impact upon the proliferation of either HPV16+ or HPV18+ cell lines, in agreement with data from the preceding chapter in which no effect on HPV oncoprotein expression was observed following SUR2 knockdown.

We observed that inhibition of K_{ATP} channels, through either pharmacological means or SUR1 knockdown, resulted in an increase in the proportion of cells in G1 phase and, consistently, a decrease in cyclin D1 and E1 expression. This is in line with prior reports in glioma and breast cancer cell lines [329, 330, 333]. Further, this fits with an increasing recognition of the importance of ion channels in the regulation of the cell cycle and cell proliferation [323-325]. It is thought that cells undergo a rapid hyperpolarisation during progression through the G1-S phase checkpoint, for which K^+ efflux channels are particularly important [324, 325]. Our data indicates that, at least in cervical cancer, K_{ATP} channels may contribute towards this hyperpolarisation event.

To our surprise, given the negative impact of K_{ATP} channel knockdown on HPV+ cervical cancer cell proliferation, no effect on the expression of EMT-related genes was observed in shSUR1 cell lines. This is in contrast to data from NSCLC models, in which glibenclamide treatment has been shown to promote expression

of the epithelial marker E-cadherin and downregulate expression of the mesenchymal marker N-cadherin, with a corresponding decrease in cell migration [334]. However, it is worth noting that this study concluded the pro-proliferative effects of SUR1 in NSCLC are mediated via a K_{ATP} channel-independent mechanism. In contrast, treatment of breast cancer cell lines with minoxidil, a K_{ATP} channel activator, reduced invasiveness, suggesting that K_{ATP} channels may act to inhibit the migratory potential of these cells [418]. However, this would directly contrast with earlier work in breast cancer cell lines, in which glibenclamide was shown to inhibit cell proliferation via a G1 arrest, whilst minoxidil had the inverse effect [329]. Clearly, further work is required to fully uncover the impact of K_{ATP} channel activity on cell migration and EMT. To begin, the findings in this study with stable SUR1 knockdown cell lines should be validated by repeating with K_{ATP} channel modulators, and migration, invasion, and would healing assays performed.

Ion channels represent ideal candidates for novel cancer therapeutics given the abundance of licensed and clinically-available drugs targeting the complexes which could be repurposed if demonstrated to be effective [327]. We therefore investigated whether K_{ATP} channel inhibition had a cytotoxic effect on cervical cancer cells. Somewhat surprisingly, given the impact on HPV oncoprotein expression, we did not observe any evidence for increased cell death following glibenclamide treatment. This is in contrast to previous experiments in gastric cancer, glioma and hepatocellular carcinoma cell lines [328, 330, 331], yet in agreement with observations in breast cancer cells [329]. These differences may potentially reflect the cell type-specific roles of K_{ATP} channels, or perhaps be a result of differing subunit compositions in the cell types analysed. Despite this, the clear reduction in proliferation observed following K_{ATP} channel knockdown

highlights their potential for targetting in novel therapies. It would be of interest for further studies to analyse whether K_{ATP} channel inhibition sensitised cervical cancer cells to established chemotherapeutic agents. Current therapies rely on the widely used yet non-specific DNA-damaging agent cisplatin in combination with radiotherapy [348, 349], but resistance to cisplatin, either intrinsic or acquired, is a significant problem [350]. In support of this idea, ion channel modulators have previously been shown to increase cisplatin efficacy in colorectal cancer, and glibenclamide can act in a synergistic manner with the chemotherapeutic agent doxorubicin in the killing of lung, liver and breast cancer cells [329, 419, 420]. Further, it would be of significant interest to discover, through the use of washout experiments, the duration of glibenclamide treatment that is required to induce a stable G1 cell cycle arrest. For example, treatment with the CDK4/6 inhibitor palbociclib, licenced for breast cancer therapy, for short periods of time followed by washout is insufficient to induce a permanent G1 arrest, yet upon removal of the drug after prolonged inhibition, cells fail to re-enter the cell cycle [421]. Whether a similar scenario occurs with glibenclamide warrants investigation.

Following our initial analyses of HPV+ transformed cell lines *in vitro*, we performed *in vivo* tumourigenicity assays using cells stably expressing SUR1-specific shRNAs. We observed significant delays to tumour growth with cells displaying reduced SUR1 expression resulting in prolonged survival, thus providing validation for our earlier *in vitro* work. Somewhat surprisingly however, upon analysis of tumour tissue at the experimental endpoint, we failed to observe any difference in the protein expression of either SUR1 or Ki67, a proliferation marker, between the two groups. The absence of staining with the secondary antibody only controls highlights the specificity of the primary antibodies;

nevertheless RNA could be extracted from tissue sections and mRNA expression levels of *ABCC8* and *MKI67* analysed to validate these findings. Perhaps the most likely explanation is that knockdown efficiency was lost during the course of the experiment, perhaps due to methylation-mediated silencing of the human elongation factor-1 alpha (EF-1α) promoter that was used to drive transcription of the shRNA, as well as the ZsGreen and puromycin resistance genes. If this is indeed the case, it could be argued that silencing of the shRNA highlights how critical K_{ATP} channel expression may be for the proliferation of HPV+ cervical cancer cells. As alternative strategy, and in an attempt to circumvent a potential silencing issue, a CRISPR knockout strategy could be employed to completely ablate SUR1 expression. Regardless, the clear impact suppression of K_{ATP} channel activity has on the growth of HPV+ cervical cancer cells indicates that further work is now warranted to confirm whether the licenced K_{ATP} channel inhibitors could be repurposed and used alongside current therapies.

We revealed that the pro-proliferative effects of K_{ATP} channels are mediated via activation of ERK1/2 and subsequently the AP-1 family member cJun. Previous reports have examined the importance of these signalling pathways in HPV infection and cervical cancer [128, 163, 376, 422-424]. Indeed, a recent study elegantly showed a strong correlation between ERK1/2 activity and cervical disease progression, and highlighted the importance of ERK1/2 and AP-1 signalling for oncoprotein expression in both a life cycle model of HPV infection and using an oropharyngeal squamous cell carcinoma cell line [424]. Interestingly, this study additionally identified the AP-1 family members cFos and JunB as contributors towards oncogene transcription, whilst previous analysis in this laboratory has revealed that both cJun and JunD are upregulated in HPV18+ keratinocytes and cervical cancer cell lines [163, 424]. As AP-1 can be comprised

of Jun family homodimers or heterodimers with Fos, ATF or MAF family proteins, further studies may be warranted to determine the most frequent makeup of AP-1 dimers in HPV+ cells [401].

Significantly, the extent to which the proliferation and colony-forming ability of SUR1-depleted HeLa cells was rescued by the reintroduction of a constitutively active form of cJun (S63/73D) was only partial. This may be because phosphorylation at additional residues is required for complete cJun activation. Indeed, phosphorylation at T91 and T93 is linked to enhanced cJun activity and, in some cases, phosphorylation at all four residues (S63, S73, T91 and T93) is necessary for releasing cJun target genes from transcriptional repression [425-427]. Therefore, further cJun mutants possessing additional phosphomimetic mutations could be employed. However, it is thought that while both ERK1/2 and JNK1/2 are able to catalyse the phosphorylation of S63/S73, only JNK1/2 can phosphorylate the T91/T93 residues [428]. Thus it is questionable whether additional phosphomimetic mutations would enhance the restoration of proliferation observed here. Alternatively, our data could indicate that other targets downstream of ERK1/2 signalling, in addition to cJun/AP-1, may also be critical in mediating the pro-proliferative effects of K_{ATP} channels. Indeed, ERK1/2 is known to activate a wide variety of host transcriptional regulators in addition to AP-1 members, both directly (e.g. ETS family transcription factors, c-MYC) and indirectly via phosphorylation of MSK1/2 (e.g. CREB) [429-431]. Of particular interest is the transcription factor SP1: phosphorylation by ERK1/2 enhances its transactivation potential and the protein is known to be critical for HPV URR promoter activity [88, 373, 374, 384, 385]. The degree to which these transcriptional regulators contribute to proliferation and HPV oncoprotein

expression induced by K_{ATP} channels in cervical cancer cells warrants investigation.

In summary, this chapter reveals the vital role of host K_{ATP} channels in regulating proliferation of HPV+ cervical cancer cells. This is likely mediated via promoting progression through G1 phase of the cell cycle and regulation of cyclin D1 and cyclin E1 expression. Further, stimulation of cell growth is achieved by activation of ERK1/2 and AP-1 signalling and we provide *in vivo* confirmation of the importance of K_{ATP} channels for cervical cancer cell proliferation. Future studies to understand whether these host ion channels have a similar importance in other HPV-associated diseases, such as oropharyngeal cancers is now warranted (Chapter 5).

Chapter 5 K_{ATP} channels are not required for the proliferation of head and neck squamous cell carcinoma (HNSCC) cells

5.1 Introduction

Head and neck squamous cell carcinomas (HNSCCs) are a group of malignancies that develop in the mucosal epithelium at sites within the oral cavity, nasopharynx, oropharynx, hypopharynx and larynx [432]. Collectively, HNSCC is the seventh most common cancer worldwide, accounting for almost 900,000 cases and in excess of 400,000 deaths worldwide in 2020 [32, 433]. The major risk factors for HNSCC include tobacco and alcohol consumption and infection with HPV [432, 434, 435]. Interestingly, HPV infection is most commonly associated with tumours arising in the oropharynx, and indeed the majority of oropharyngeal cancers are HPV+, whilst HNSCCs of the oral cavity and larynx are still primarily linked to smoking and alcohol use [92, 432, 436]. As such the disease is often broadly divided into HPV+ and HPV- HNSCC.

Importantly, the mutational profiles and changes in gene expression differ significantly between HPV+ and HPV- HNSCC. As would be expected, mutations in the *TP53* tumour suppressor are found almost exclusively in HPV- HNSCCs due to the ability of HPV E6 to target p53 for proteasomal degradation [92, 145, 344]. Indeed, a similar pattern is seen for somatic mutations in the *CDKN2A* gene [92]. Conversely, HPV+ oropharyngeal tumours commonly display focal amplification of the *E2F1* locus [92]. Together, this highlights the need to consider HPV+ and HPV- HNSCCs as separate diseases, including when considering potential therapeutic approaches.

As the pathogenesis of HPV+ HNSCC is clearly distinct from that of HPV- HNSCCs, this raises the possibility of developing novel cancer therapeutics based upon targetting the particular vulnerabilities of each group. Host ion

channels represent ideal candidates for novel therapeutics due to the abundance of licensed and clinically available drugs targeting the complexes which could be repurposed if demonstrated to be effective. Indeed, approximately 20% of all current FDA-approved drugs act upon ion channels [327].

The role of ion channels in driving the proliferation of HNSCC is poorly characterised [437]. Some K^+ channels have been studied, and the voltage-gated K^+ channels $K_v3.4$, $K_v10.1$ and $K_v11.4$ have all been shown to be upregulated in HNSCC tissue samples and cell lines [438-440]. However, none of these studies accounted for the HPV status of the tissue samples studied, and focussed their analyses solely on HPV- cell lines. More widely, the calcium-activated chloride channel ANO1/TMEM16A is highly expressed in a large proportion of HNSCC tumours, but this is predominantly in HPV- rather than HPV+ HNSCCs [441-443]. Thus, the impact of HPV on expression and/or activity of K^+ channels, and more widely the entire host channelome, in HNSCC is not well understood.

The data in the preceding chapters identifies a key role for host K_{ATP} channels in regulating HPV gene expression and proliferation in cervical cancer cells, and demonstrates that this is achieved via the activation of host MAPK and AP-1 signalling. This chapter will attempt to extend these findings in order to ascertain whether this newly-identified role for K_{ATP} channels is specific to HPV+ cervical cancers, or could also be a feature in HPV+ HNSCCs.

5.2 Results

5.2.1 K_{ATP} channel expression may be upregulated in HPV+ HNSCC cells

To initially gain an understanding of whether K_{ATP} channels may have a role in HPV+ oropharyngeal cancers, we investigated the expression of K_{ATP} channel subunits in a panel of HNSCC cell lines. We felt this to be pertinent as no previous study, to our knowledge, has attempted to ascertain whether K_{ATP} channels are expressed in head and neck tissue and if so, what channel subunits are present. Importantly, the expression of K_{ATP} channel subunits displays significant tissue-specific variability [236]. The panel used included three HPV- cell lines (HN8, HN30, SCC-61) and three HPV16+ cell lines (UM-SCC-47, UM-SCC-104, UPCI:SCC-152). We were able to detect, by RT-qPCR, expression of the Kir6.1 (*KCNJ8*), Kir6.2 (*KCNJ11*) and SUR1 (*ABCC8*) subunits in all cell lines examined, yet could not detect expression of either splice isoform of the *ABCC9* (SUR2) transcript (**Fig 5.1A**). Interestingly, the mRNA expression of *ABCC8* was significantly increased by ~3-5 fold in all of the HPV16+ cell lines, in comparison to the HN8 control, yet no increase was seen in either of the other HPV- cell lines tested. The same pattern was observed when *KCNJ11* mRNA levels were analysed, with the HPV16+ cell lines displaying ~4 fold higher expression levels. However, this was not replicated in our *KCNJ8* findings, where there was no significant change in expression in any of the cell lines.

To confirm these findings, we mined available online datasets. Firstly, data from The Cancer Genome Atlas (TCGA) was analysed for the mRNA expression levels of *ABCC8* and *KCNJ11*. This revealed that *KCNJ11* mRNA expression was significantly higher in the HPV+ tumours (n = 80) compared to HPV- samples (n = 434), confirming our findings in cell line models (**Fig 5.1B**). However, comparing

both of these subsets to a collection of normal controls provided surprising findings. There was no significant difference in *KCNJ11* expression between healthy tissue control (n = 44) and HPV+ HNSCC samples, and the apparent difference between HPV+ and HPV- HNSCCs was instead due to a downregulation of *KNCJ11* mRNA levels in the HPV- group (**Fig 5.1B**).

Next, the expression of *ABCC8* was analysed in this collection of TCGA samples. To our surprise, a significant number of samples in all categories displayed no detectable expression of *ABCC8*. Despite this, median mRNA expression in HPV- HNSCC tumours was significantly lower than in normal tissue, but less of a reduction was observed with HPV+ HNSCC tumours (**Fig 5.1B**).

A second publically available dataset, consisting of microarray expression analysis of a panel of HPV- and HPV+ HNSCC tumours, as well as healthy controls, was also mined for the mRNA expression of *ABCC8* and *KCNJ11 [342]*. Surprisingly, no significant difference in the mRNA levels of either *ABCC8* or *KCNJ11* could be observed between any of the three groups (**Fig 5.1C**). Taken together, these data suggest that the K_{ATP} channel subunits Kir6.1, Kir6.2 and SUR1 are expressed in head and neck tissue, but the impact of HPV16 on the expression of Kir6.2 and SUR1 remains unclear.

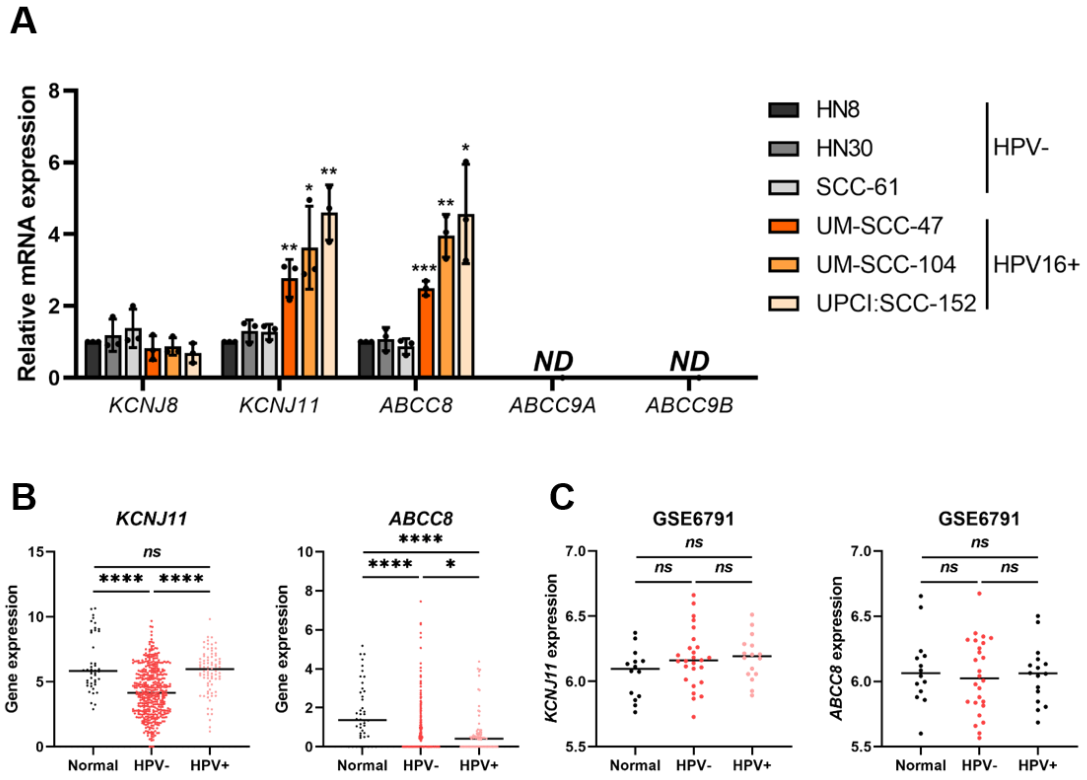

Figure 5.1 K_{ATP} channel expression in HNSCC cells. A) mRNA expression levels of K_{ATP} channel subunits in a panel of three HPV- HNSCC cell lines (HN8, HN30, SCC-61) and three HPV16+ HNSCC cell lines (UM-SCC-47, UM-SCC-104, UPCI:SCC-152) detected by RT-qPCR. Samples were normalised against *U6* mRNA levels. Data is displayed relative to the HN8 control and represents means ± standard deviation (SD) of three biological replicates. *ND*, no expression detectable. *P<0.05, **P<0.01, ***P<0.001 (Student's t-test). B) Expression analysis of *KCNJ11* and *ABCC8* from TCGA HNSCCs, displayed as expression in normal tissue (n = 44) versus HPV- (n = 434) versus HPV+ (n = 80) tumours. Expression calculated from RNA-seq data using RSEM and transformed using the $log_2(x+1)$ method. C) Microarray expression analysis of *KCNJ11* and *ABCC8* using data acquired from the GSE6791 database, displayed as expression in normal tissue (n = 14) versus HPV- (n = 26) versus HPV+ (n = 16) tumours. Statistical significance in (B) and (C) was assessed using the Wilcoxon rank-sum test (*ns* not significant, *P<0.05, **P<0.01, ***P<0.001, ****P<0.0001).

5.2.2 K_{ATP} channels are active in HPV+ HNSCC cell lines

After identifying that the K_{ATP} channel subunits Kir6.1, Kir6.2 and SUR1 are expressed in HNSCC cell lines, and that Kir6.2 and SUR1 may be upregulated in HPV+ cell lines, we wanted to confirm the presence of active K_{ATP} channels. To test this, we analysed the membrane potential of cells using the fluorescent dye $DiBAC_4(3)$ [354, 355]. The ability of this dye to enter cells is proportional to the degree to which the plasma membrane is depolarised. This revealed that

treatment of HPV16+ UM-SCC-47 or UM-SCC-104 cells with glibenclamide resulted in an increase in $DiBAC_4(3)$ fluorescence, indicating membrane depolarisation and consistent with a reduction in K_{ATP} channel opening (**Fig 5.2A**). The scale of this increase (~1.3-1.4 fold with 10 µM glibenclamide) is highly similar to that seen in HPV+ cervical cancer cells following K_{ATP} channel blockade (Chapter 3). Furthermore, increased $DiBAC_4(3)$ fluorescence was also observed with tolbutamide treatment, a member of the same class of sulfonylurea drugs as glibenclamide (**Fig 5.2B**), together suggesting that these HPV16+ HNSCC cell lines possess active K_{ATP} channels.

In an attempt to confirm these observations, HPV16+ cells were stimulated with diazoxide, a K_{ATP} channel opener that acts preferentially on SUR1-containing complexes [236]. To our surprise, we did not detect any significant alteration in the plasma membrane potential of cells at the time point analysed following K_{ATP} channel stimulation (**Fig 5.2C**). This contrasts with the inhibitor data in these cell lines and thus casts doubt upon whether HPV+ HNSCC cell lines possess functional K_{ATP} channels.

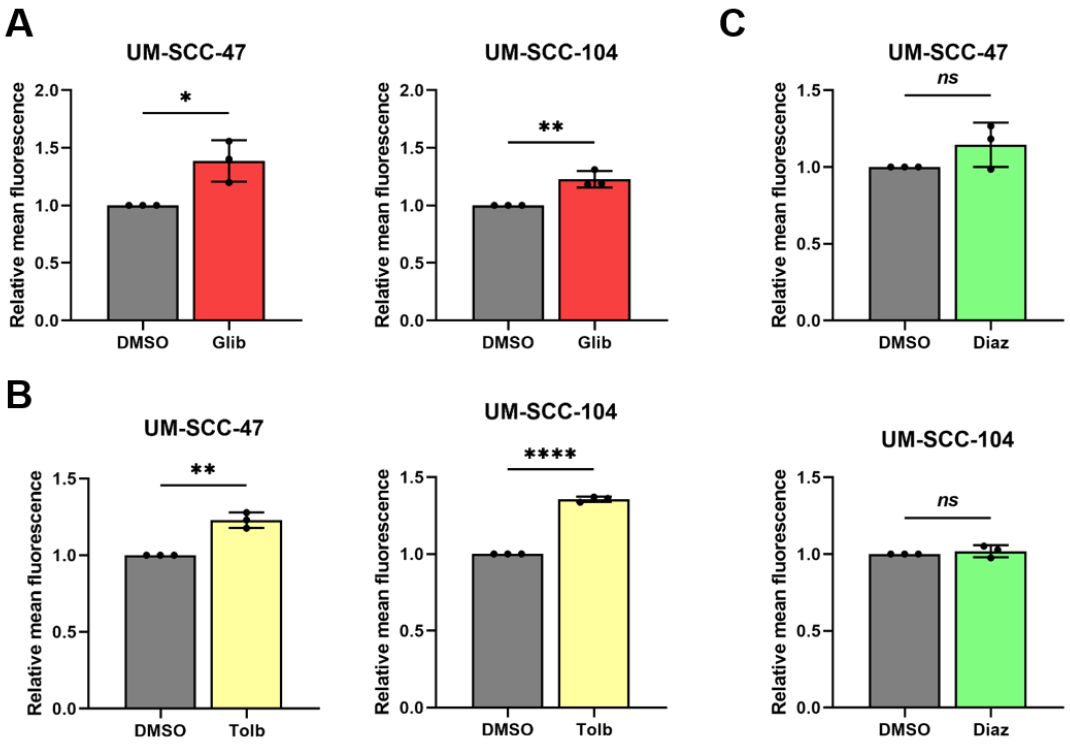

Figure 5.2 The impact of K_{ATP} channel modulators on the plasma membrane potential of HNSCC cells. Mean $DiBAC_4(3)$ fluorescence levels in UM-SCC-47 and UM-SCC-104 cells treated with A) 10 µM glibenclamide, B) 200 µM tolbutamide or C) 50 µM diazoxide. Samples were normalised to the appropriate DMSO control. Bars represent means ± standard deviation (SD) of three biological replicates with individual data points displayed. *Ns* not significant, *P<0.05, **P<0.01, ***P<0.001, ****P<0.0001 (Student's t-test).

5.2.3 The role of E6 and E7 in driving K_{ATP} channel expression is unclear

Next, we wanted to gain an understanding of whether HPV has a role in upregulating the expression of SUR1 and Kir6.2 in HNSCC cell lines. It was hypothesised that it may be an oncoprotein driven event since E6 and E7 are known to modulate the expression and activity of a multitude of cellular factors [50]. Further, observations in a preceding chapter illustrated that SUR1 upregulation in HPV+ cervical cancer cells is achieved in an E7-dependent manner. To test this, an siRNA knockdown approach was employed and the expression of both E6 and E7 was silenced in two HPV16+ HNSCC cell lines (**Fig 5.3A-B**). In both cell lines, a knockdown efficiency of ~50% or greater was confirmed for both oncogenes by RT-qPCR. Confirmation that siRNA transfection

also had the desired impact on the protein expression of E6 and E7 was carried out via western blot analysis (**Fig 5.3A-B**). Interestingly, in UM-SCC-47 cells, suppression of E6/E7 expression resulted in a profound decrease in mRNA levels of both *ABCC8* and *KCNJ11* when compared to scramble controls (**Fig 5.3A**). However, to our surprise, these findings could not be replicated in the second HPV16+ cell line, UM-SCC-104, where no effect on either *ABCC8* or *KCNJ11* expression was observed following E6/E7 knockdown (**Fig 5.3B**).

Following this, to confirm that the reduction in Kir6.2 and SUR1 expression in UM-SCC-47 cells after E6/E7 knockdown corresponded to changes in K_{ATP} channel activity, analysis of the membrane potential of cells was performed using the fluorescent dye $DiBAC_4(3)$ [354, 355]. Upon silencing of E6/E7, a ~1.3 fold increase in fluorescence was detected, indicative of membrane depolarisation and consistent with a loss of K_{ATP} channel activity (**Fig 5.3C**). Further, this is in line with the degree of change observed in these cells following either glibenclamide or tolbutamide treatment. This therefore suggests that, at least in the context of UM-SCC-47 cells, HPV oncoprotein expression is required for K_{ATP} channel subunit expression.

In an attempt to resolve the apparent differences between the two HPV16+ cell lines analysed, the impact of overexpressing the HPV oncoproteins in HPV- HNSCC cell lines was investigated. To this end, HN8 and HN30 cells stably expressing HA-tagged HPV16 E6 or HPV16 E7 were generated (**Fig 5.3D**). Upon analysis of K_{ATP} channel subunit expression in these cell lines by RT-qPCR, it was found that neither E6 nor E7 were capable of upregulating mRNA expression of either *KCNJ11* or *ABCC8* (**Fig 5.3E**). This was consistent across both HPV- cell lines examined. Together, this suggests that expression of the HPV

oncoproteins is not sufficient to upregulate K_{ATP} channel subunit expression in HNSCC cells.

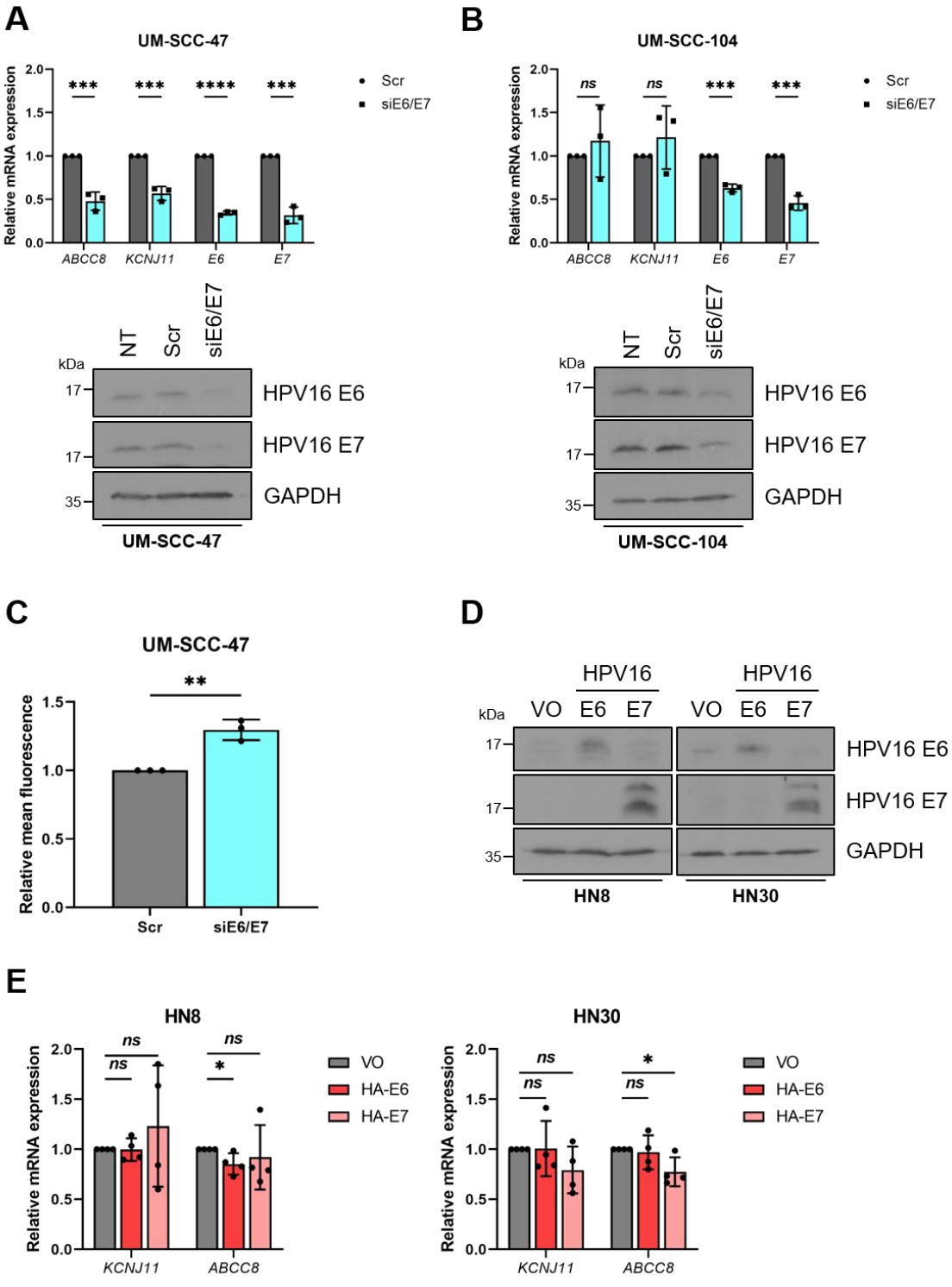

Figure 5.3 The role of HPV oncoproteins in regulating K_{ATP} channel subunit expression in HNSCC cell lines. A-B) mRNA expression of *ABCC8* and *KCNJ11* in UM-SCC-47 (A) and UM-SCC-104 (B) cells after transfection of E6- and E7-specific siRNAs, measured by RT-qPCR. Successful transfection was confirmed by analysing mRNA and protein expression of the HPV oncoproteins. Samples were normalised against *U6* mRNA levels and GAPDH served as a loading control for western blots. C) Mean $DiBAC_4(3)$ fluorescence in UM-SCC-47 cells co-transfected with E6- and E7-specific siRNAs. Samples were normalised to the scramble control. D) Representative western blots of E6 and E7 expression in HN8 and HN30

cells stably expressing the HPV16 oncoproteins. GAPDH served as a loading control. E) mRNA expression of *ABCC8* and *KCNJ11* in HN8 and HN30 cells stably expressing either HPV16 E6 or HPV16 E7. Samples were normalised against *U6* mRNA levels. Bars represent means ± standard deviation (SD) of three biological replicates with individual data points displayed. *Ns* not significant, *P<0.05, **P<0.01, ***P<0.001, ****P<0.0001 (Student's t-test).

5.2.4 K_{ATP} channel inhibition reduces HPV oncoprotein expression

Next, the impact of inhibiting K_{ATP} channel conductance on the expression of HPV oncoproteins was investigated. Data in a preceding chapter revealed that, in HPV+ cervical cancer cells, K_{ATP} channel activity is required for efficient expression of E6 and E7 via regulation of transcription directed by the HPV URR. It was therefore hypothesised that in HPV+ HNSCC cell lines, a similar effect might be observed.

Initially, UM-SCC-47 and UM-SCC-104 cells were treated with the K_{ATP} channel blocker glibenclamide and E6 and E7 expression assayed. In both cell lines, a decrease of 30-40% in the mRNA levels of *E6* and *E7* was observed (**Fig 5.4A**). To confirm, cells were similarly treated with a second K_{ATP} channel inhibitor tolbutamide; this also resulted in a ~40% reduction in mRNA expression of the oncogenes (**Fig 5.4B**). To validate these findings, analysis of the protein expression of E6 and E7 was performed via western blot. A profound decrease in both HPV16 oncoproteins was observed in UM-SCC-104 cells following glibenclamide treatment (**Fig 5.4C**). This suggests that K_{ATP} activity may be required for efficient oncoprotein expression.

Prior analysis of HPV+ cervical cancer cell lines revealed that the impact of K_{ATP} channel activity on oncoprotein expression was due to alterations in transcriptional activity directed by the URR. Therefore, to investigate whether this was also the case in HPV+ HNSCC, a luciferase reporter vector was employed in which the HPV16 URR had been cloned upstream of the firefly luciferase gene

[444]. Treatment of either UM-SCC-47 or UM-SCC-104 cells with glibenclamide to inhibit K_{ATP} channel ion flux resulted in a significant reduction in relative HPV URR activity (**Fig 5.4D**). Importantly, the same effect was seen when these cells were treated with the alternative K_{ATP} channel inhibitor tolbutamide (**Fig 5.4E**). Together therefore, these data illustrate that K_{ATP} channel inhibitors have a detrimental effect upon HPV gene expression in HNSCC cell lines.

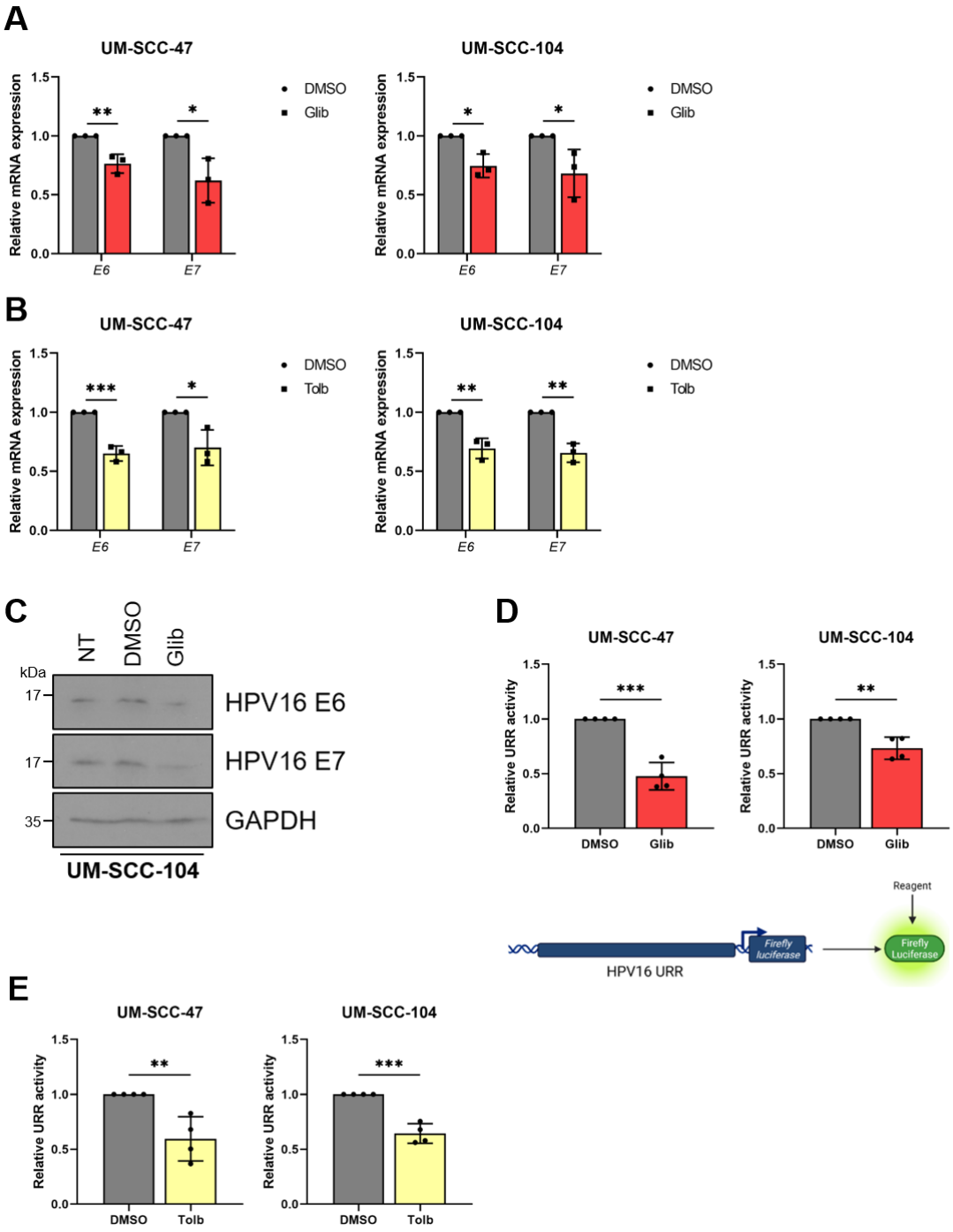

Figure 5.4 K_{ATP} channel inhibition impedes HPV oncoprotein expression in HNSCC cells. A-B) mRNA expression of *E6* and *E7* in UM-SCC-47 and UM-SCC-104 treated with 10 µM glibenclamide (A) or 200 µM tolbutamide (B), measured by RT-qPCR. Samples were normalised against *U6* mRNA levels and data is displayed relative to the appropriate DMSO control. C) Representative western blots of E6 and E7 protein levels in UM-SCC-104 cells treated with 10 µM glibenclamide (n = 2). GAPDH served as a loading control. D-E) Relative firefly luminescence in UM-SCC-47 and UM-SCC-104 cells transfected with an HPV16 URR-driven reporter plasmid and treated with either 10 µM glibenclamide (E) or 200 µM tolbutamide (F). Luminescence values were normalised against *Renilla* luciferase activity. Figure created using BioRENDER.com. Bars represent means ± standard deviation (SD) of a minimum of three biological replicates, unless stated

otherwise, with individual data points displayed. *P<0.05, **P<0.01, ***P<0.001 (Student's t-test).

5.2.5 Depletion of SUR1 or Kir6.2 has minimal impact upon HPV gene expression

To confirm the findings in the previous section highlighting a potential role for K_{ATP} channels in regulating HPV oncoprotein expression, we employed a knockdown strategy. This was to eliminate any potential off-target effects of the small molecule inhibitors previously used. Specifically, cells stably expressing either non-targetting (shNTC) or SUR1-specific shRNAs were generated using the UM-SCC-47 cell line. Knockdown efficiency was assayed via RT-qPCR, revealing a ~50% reduction in *ABCC8* mRNA levels (**Fig 5.5A**). Subsequently, the expression of the HPV oncoproteins E6 and E7 was examined. Surprisingly, given the prior small molecule inhibitor data, no consistent effect on mRNA expression of the HPV oncogenes was observed (**Fig 5.5B**). Despite recording a small but significant decrease in *E7* mRNA levels in one of the SUR1 knockdown lines, this was not replicated in the second knockdown. Furthermore, analysis of the protein levels of E6 and E7 confirmed that K_{ATP} channel loss did not impact upon expression of HPV proteins (**Fig 5.5C**).

To validate these findings, the impact of suppressing K_{ATP} channel subunit expression in a second HPV+ HNSCC cell line was assessed. To this end, UM-SCC-104 cells were transfected with siRNA specific for SUR1 and Kir6.2, alone in combination. This permitted an assessment of the impact of supressing both K_{ATP} channel subunits. Again, knockdown efficiency was assessed via RT-qPCR, demonstrating a ~30-40% reduction in *ABCC8* and *KCNJ11* mRNA levels (**Fig 5.5D**). However, neither knockdown of SUR1, nor suppression of Kir6.2 expression, had a significant impact on the mRNA expression of *E6* and *E7* in

this cell line (**Fig 5.5D**). Indeed, the same observations were recorded upon simultaneous knockdown of SUR1 and Kir6.2. To confirm, protein expression of HPV E6 and E7 was analysed via western blot. In contrast to the RT-qPCR data, a slight reduction in E7 protein expression was observed following SUR1 knockdown, but this was not replicated in the E6 expression data (**Fig 5.5E**). Further, no changes in E6 or E7 protein levels were detected with Kir6.2 suppression, or indeed dual knockdown (**Fig 5.5E**). In summary, these data indicate that K_{ATP} channel subunit expression is not required for efficient HPV gene expression.

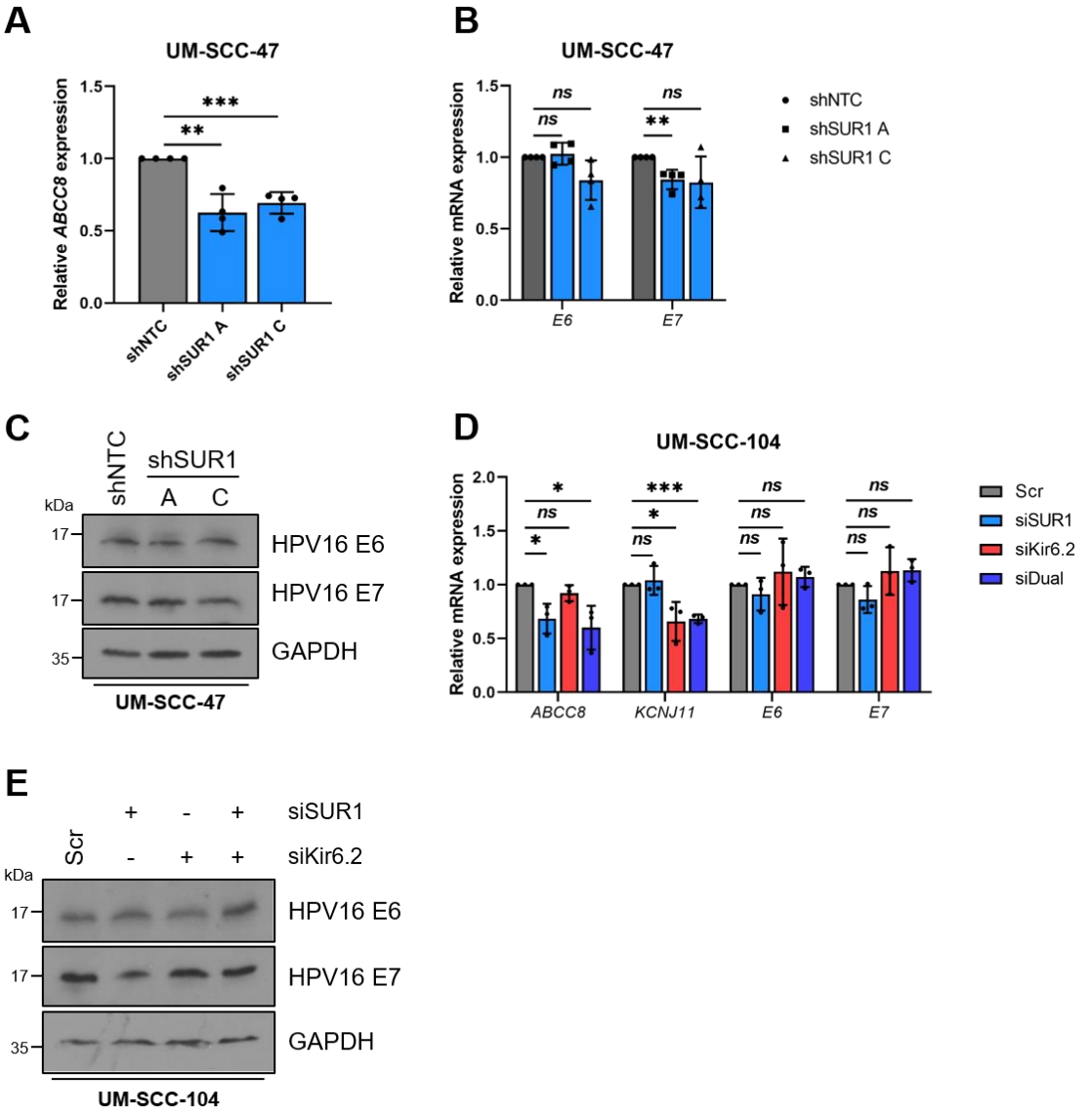

Figure 5.5 Depletion of SUR1 and/or Kir6.2 has a minimal impact on HPV gene expression in HNSCC cell lines. A-B) mRNA expression of *ABCC8* (A) and *E6* and *E7* (B) in UM-SCC-47 cells stably expressing either non-targetting (shNTC) or SUR1-specific shRNAs, measured by RT-qPCR. Samples were normalised against *U6* mRNA levels. C) Representative western blots of E6 and E7 protein levels in UM-SCC-47 cells stably expressing non-targetting (shNTC) or SUR1-specific shRNAs. GAPDH served as a loading control. D) mRNA expression of *E6* and *E7* in UM-SCC-104 cells transfected with siRNAs specific for SUR1 and Kir6.2, alone or in combination, measured by RT-qPCR. Samples were normalised against *U6* mRNA levels and successful transfection was confirmed by analysing *ABCC8* and *KCNJ11* mRNA expression. E) Representative western blots of E6 and E7 protein levels in UM-SCC-104 cells transfected with siRNAs specific for SUR1 and Kir6.2, alone or in combination. GAPDH served as a loading control. Bars represent means ± standard deviation (SD) of a minimum of three biological replicates with individual data points displayed. *Ns* not significant, *P<0.05, **P<0.01, ***P<0.001 (Student's t-test).

5.2.6 K_{ATP} channel knockdown has no impact on the proliferation of a HPV- HNSCC cell line

Next, the impact K_{ATP} channels have on the proliferative capacity of HNSCC cells was assessed. To begin, a HPV- cell line (HN8) was analysed. As these cells have low, yet detectable, expression of the K_{ATP} channel subunits Kir6.2 and SUR1, it was hypothesised that loss of channel activity would have minimal impact on cell proliferation. To test this, an shRNA knockdown strategy was employed using shRNAs targetting the *ABCC8* coding sequence. Cell lines stably expressing either a non-targetting (shNTC) or one of two SUR1-specific shRNAs (shSUR1) were generated and knockdown efficiency evaluated by RT-qPCR. This revealed a ~50% reduction in *ABCC8* mRNA expression (**Fig 5.6A**). The proliferation of these cells was then monitored over a period of five days. As expected, minimal impact on cell growth was observed (**Fig 5.6B**). To confirm, colony formation assays, a measure of the anchorage-dependent growth of cells, were performed. The colony forming ability was unchanged following suppression of SUR1 expression (**Fig 5.6C**). Soft agar assays to ascertain the anchorage-independent proliferative capacity, and hence metastatic potential, of these cells were also attempted. However, an inability of these cells to form colonies in soft agar, regardless of SUR1 expression levels, was noted, in line with an absence of reports in the literature [445]. Together, these data suggest that K_{ATP} channels are not required for the proliferation of HPV- HNSCC cells.

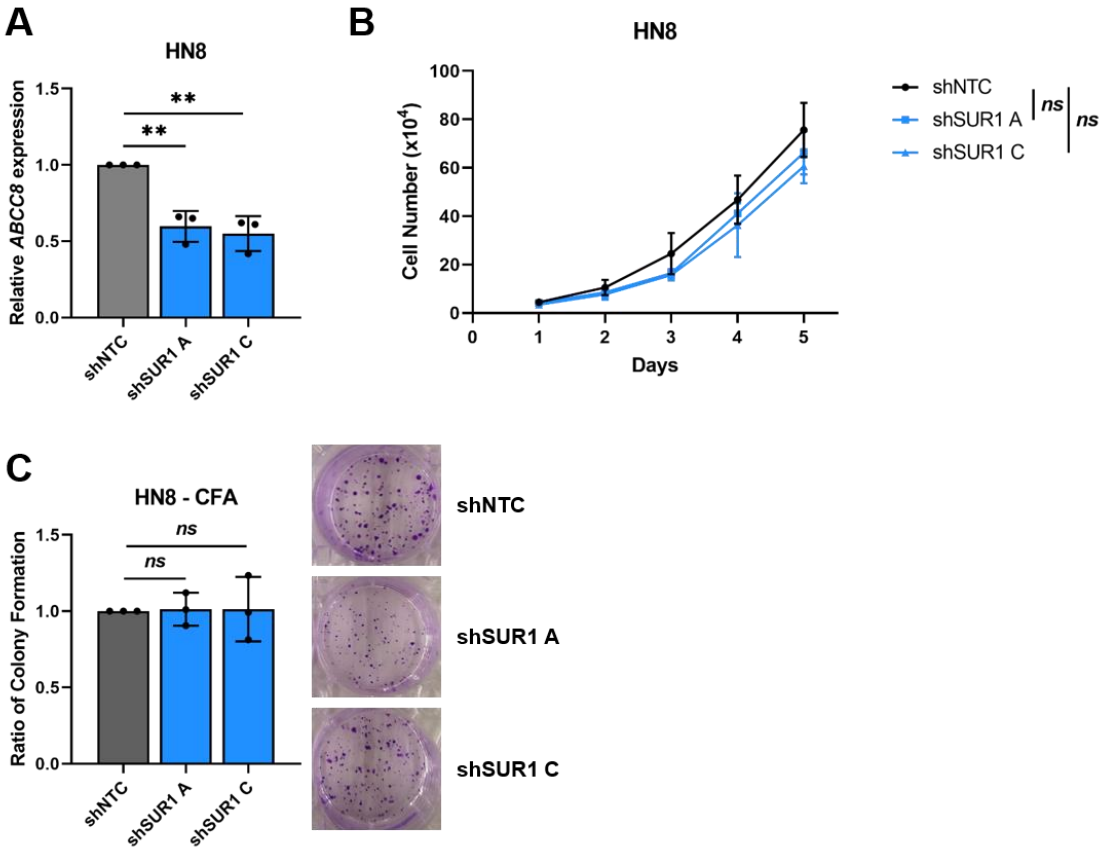

Figure 5.6 SUR1 knockdown has no impact on the proliferation of a HPV- HNSCC cell line. A) mRNA expression of *ABCC8* in HN8 cells stably expressing either a non-targetting (shNTC) or one of two SUR1-specific shRNAs (shSUR1) measured by RT-qPCR. Samples were normalised against *U6* mRNA levels. B-C) Growth curve analysis (B) and colony formation assay (C) of HN8 SUR1 knockdown cell lines. Data shown is means ± SD of three biological replicates with individual data points displayed where appropriate. *Ns* not significant, *P<0.05, **P<0.01 (Student's t-test).

5.2.7 K_{ATP} channels are also not necessary for the proliferation of HPV+ HNSCC cells

After confirming that K_{ATP} channels were not required for the proliferation of a HPV- HNSCC cell line, the impact of the channels on HPV16+ HNSCC cells was next assessed. Given that our findings illustrate these cells display increased expression of the K_{ATP} channel subunits Kir6.2 and SUR1, and our small molecule inhibitor data highlights a potential impact upon HPV gene expression following channel inhibition, it was postulated that disruption of K_{ATP} channel function may negatively impact the proliferation of HPV+ HNSCC cells. To examine this, the

proliferation rate of UM-SCC-47 cells stably expressing SUR1-specific shRNAs was analysed. To our surprise, no reduction in the proliferation of these cells was observed with reduced SUR1 expression (**Fig 5.7A**). To confirm this, the anchorage-dependent colony-forming ability of these cell lines was also assayed. Due to the tendency of this cell line to form larger, merged colonies which were highly variable in size, colony-forming ability was quantified by destaining plates and measuring the relative absorbance, rather than counting colonies manually. In agreement with the proliferation data, stable SUR1 knockdown failed to result in a reduction to the relative colony-forming ability of these cells (**Fig 5.7B**). In fact, a small, yet insignificant, increase in relative absorbance was detected in one of the two knockdown cell lines. The anchorage-independent colony-forming ability was unable to be assessed due to the inability of this cell line to grow in soft agar that was found, in line with an absence of prior reports [445].

To validate these observations, the dependence of a second HPV+ HNSCC cell line, UM-SCC-104, on K_{ATP} channel expression for its proliferation was next analysed. An siRNA knockdown strategy was employed, enabling an assessment of the impact of suppression of either SUR1, Kir6.2 or both subunits in combination on cell proliferation. In line with our UM-SCC-47 data, no reduction in the proliferation rate was found with either SUR1 knockdown or Kir6.2 knockdown (**Fig 5.7C**). Further, no loss of colony formation was observed following transfection of SUR1- and Kir6.2-specific siRNAs, either alone or in combination (**Fig 5.7D**). This cell line did display an ability to grow in soft agar and thus anchorage-independent colony formation could be assessed. However, no reduction in relative colony number with Kir6.2 knockdown, and surprisingly a small increase with SUR1 suppression, was identified (**Fig 5.7E**). Taken together,

these findings illustrate that K_{ATP} channels are not essential for the proliferation of HNSCC cell lines, regardless of HPV status.

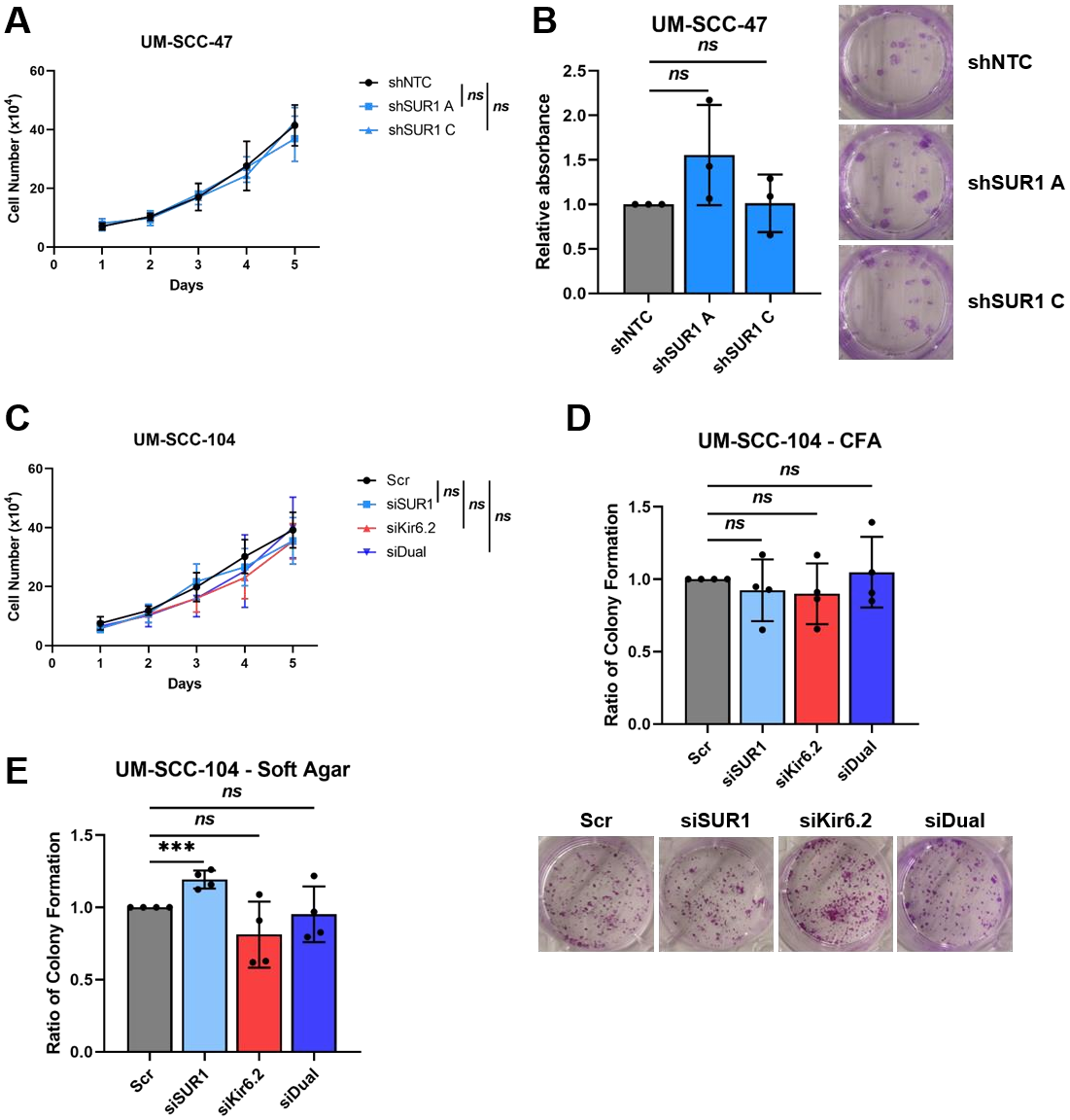

Figure 5.7 K_{ATP} channels are not necessary for the proliferation of HPV+ HNSCC cell lines. A-B) Growth curve analysis (A) and colony formation assay (B) of UM-SCC-47 cells stably expressing either non-targetting or SUR1-specific shRNA. C-E) Growth curve analysis (C), colony formation assay (D) and soft agar assay (E) of UM-SCC-104 cells after transfection of SUR1-specific and Kir6.2-specific siRNAs, alone or in combination. Data shown is means ± SD of a minimum of three biological replicates with individual data points displayed where appropriate. *Ns* not significant, *P<0.05, **P<0.01, ***P<0.001 (Student's t-test).

5.3 Discussion

The previous chapters identified and characterised the crucial role of host K_{ATP} channels in regulating proliferation and HPV oncoprotein expression in HPV+ cervical cancer cells. The results presented in this chapter are an attempt to extend these findings by investigating the importance of K_{ATP} channels in HNSCC cells. It was discovered that expression of the K_{ATP} channel subunits Kir6.2 and SUR1 are consistently upregulated at the mRNA level in *in vitro* models of HPV+ HNSCC and that these cells likely possess active K_{ATP} channels at the plasma membrane. Further, channel inhibitors reduced HPV oncoprotein expression. However, knockdown of K_{ATP} channel subunits had little impact on the proliferation of HNSCC cells, regardless of HPV status, thus casting doubt upon the significance of K_{ATP} channel activity in the regulation of HNSCC cell growth.

This report was the first, to our knowledge, to investigate the expression and role of K_{ATP} channels in HNSCC. It was discovered, through analysing the mRNA expression of K_{ATP} channel subunits across a panel of HNSCC cell lines, that Kir6.1, Kir6.2 and SUR1 are consistently expressed. In contrast, we were unable to detect expression of either splice isoform of *ABCC9*. Of significant interest to us was the variability in K_{ATP} channel subunit expression between HPV- and HPV+ HNSCC cell lines. We found that both Kir6.2 and SUR1 were consistently and significantly upregulated in HPV+ HNSCC cell lines in comparison to HPV- control cells, highlighting a potential role for the virus in upregulating channel expression. However, this analysis did not take into account the basal expression level of K_{ATP} channel subunits in normal (i.e. non-malignant) head and neck tissues. Thus, we analysed publically available online datasets to compare K_{ATP} channel expression in HNSCCs to normal tissue [92, 340, 342]. Surprisingly, although TCGA data confirmed that mRNA expression of *KCNJ11* and *ABCC8*

was significantly increased in HPV+ HNSCCs relative to HPV- tumour samples, there was no increase in HPV+ cancers relative to normal tissue. Therefore, to confirm, additional experiments could be performed to compare expression of K_{ATP} channels between the HNSCC cell lines used herein and human oral keratinocytes (HOKs).

Despite the lack of prior studies on K_{ATP} channels in the context of HNSCC, a selection of other K^+ channels have been analysed [437]. Among these, voltage-gated potassium channels dominate, with $K_v3.4$, $K_v10.1$ and $K_v11.4$ all having been shown to be upregulated in HNSCC tissue samples and cell lines [438-440]. More widely, ANO1/TMEM16A, a calcium-activated chloride channel [442], is highly expressed in a large proportion of HNSCC tumours due to the amplification of a region on chromosome 11 [443, 446]. It has been shown to stimulate proliferation via activation of the RAS-RAF-MEK-ERK pathway, perhaps through an interaction with EGFR at the plasma membrane which acts to enhance its stability, thus increasing downstream MAPK signalling [443, 447, 448]. Importantly, ANO1 inhibition enhanced sensitivity of cells to EGFR-targeted therapy [449]. Given the impact of K_{ATP} channel activity on MAPK signalling in HPV+ cervical cancer identified in the preceding chapter, stimulation of this pathway in HNSCC cells may warrant investigation.

To ensure that the upregulation of SUR1 and Kir6.2 we observed in the HPV+ HNSCC cell lines corresponded to the presence of active K_{ATP} channels at the plasma membrane, we analysed the membrane potential of cells using the fluorescent dye $DiBAC_4(3)$. As we detected alterations in fluorescence following inhibition of K_{ATP} channels, it was concluded that HPV+ HNSCC cells, much like HPV+ cervical cancer cells, do possess active channels. Confusingly however, upon K_{ATP} channel stimulation, no change in the $DiBAC_4(3)$ fluorescence was

observed. This is in contrast to earlier observations in HPV+ cervical cancer cells, in which a decrease in fluorescence of ~25% was observed following diazoxide treatment (Chapter 3), indicative of membrane hyperpolarisation and consistent with increased channel opening. To resolve this apparent conflict, different time points post diazoxide stimulation could be analysed: it may be the case that K_{ATP} channel dynamics differ between HNSCC and cervical cancer cell lines and a shorter (or longer) stimulation period is required in order to observe a decrease in $DiBAC_4(3)$ fluorescence. Alternatively, patch clamping electrophysiology could be performed to more directly assess the impact of K_{ATP} channel modulation on cellular K^+ currents. Beyond this, an additional experiment that may be of interest would be to perform $DiBAC_4(3)$ assays using HPV- HNSCC cell lines following application of K_{ATP} channel modulators. One might hypothesise that, given the lower endogenous K_{ATP} channel expression these cell lines were found to have during this investigation, that although some changes in the membrane potential may be identified, these may be to a lesser extent than observed in HPV16+ cells.

After identifying that the HPV+ HNSCC cell lines examined here possessed significantly higher K_{ATP} channel expression than HPV- cells, we attempted to ascertain the mechanism behind this. Simultaneous knockdown of E6 and E7, the key drivers of transformation in HPV+ cells, led to a reduction in K_{ATP} channel expression and a corresponding depolarisation of the plasma membrane potential in one of the cell lines studied (UM-SCC-47). However, these findings could not be replicated in UM-SCC-104 cells. These cell line-specific results could perhaps be related to slight differences in tumour site: UM-SCC-47 cells were derived from a lateral tongue tumour whilst the UM-SCC-104 cell line was established from a recurrent floor of mouth tumour [450, 451]. Nevertheless, in an attempt to reconcile these seemingly conflicting results, overexpression of the

HPV16 oncoproteins was performed. In both of the cell lines in which this was carried out, neither E6 nor E7 upregulated K_{ATP} channel subunit expression, suggesting that oncoprotein expression alone is insufficient to induce K_{ATP} channel upregulation. This may indicate that the increased Kir6.2 and SUR1 expression we observed in all HPV+ HNSCC cell lines examined, relative to HPV- controls, is a result of an E6/E7-independent mechanism. For example, recurrent amplifications in the 11p15.1 chromosomal region harbouring the *ABCC8* and *KCNJ11* genes would result in the same phenotype observed herein. Thus, the frequency of copy number alterations at this locus in HNSCCs should be determined using available online data such as that from TCGA [92].

It was observed that K_{ATP} channel blockade, using two structurally distinct small molecule inhibitors, resulted in a decrease in *E6* and *E7* mRNA expression. Analysis of the protein levels of the HPV oncoproteins following glibenclamide treatment in UM-SCC-104 cells validated these findings. Further, use of a luciferase reporter construct containing the HPV16 URR confirmed that this impact on HPV gene expression is likely due to direct effects on transcription driven by the HPV early promoter. However, when we attempted to validate these data using an orthogonal approach (siRNA/shRNA-mediated knockdown of channel subunits), we could not replicate the findings. One explanation for the seemingly conflictory data would be that glibenclamide and tolbutamide are acting upon an alternative cellular target, distinct to the SUR1 subunit of K_{ATP} channels. Both inhibitors influence K_{ATP} channel gating via binding to the SUR1 subunit [236, 245], but these compounds do have well characterised off-target effects. For example, both glibenclamide and tolbutamide inhibit whole-cell Cl^- currents mediated by the cystic fibrosis transmembrane conductance regulator (CFTR), [452, 453]. To test this hypothesis, the impact of the CFTR-specific

inhibitor $CFTR_{inh}$-172 on HPV gene expression in HPV+ HNSCCs could be investigated [454, 455]. However, CFTR expression has been found to be significantly downregulated in HNSCC tissue compared to normal controls due to promoter hypermethylation, perhaps making it an unlikely target of sulfonylureas in this context [456, 457].

To our surprise, given the differing expression levels of K_{ATP} channel subunits between HPV+ and HPV- HNSCC cell lines that were observed, it was found that neither subtype of head and neck cancer requires the expression of K_{ATP} channels for efficient cell growth. Through the use of either stable suppression of SUR1, or transient knockdown of SUR1 or Kir6.2, alone and in combination, we demonstrated that none of the cell lines examined (HN8, UM-SCC-47, UM-SCC-104) were dependent upon K_{ATP} channel expression for their proliferation or colony-forming ability. However, given that neither of these approaches were found to have an impact on HPV oncoprotein expression in our assays, it is perhaps less surprising that no effect on proliferation was observed. To confirm our findings, proliferation assays could be repeated following sulfonylurea treatment, as these drugs were found to have an impact on HPV gene expression in the HPV+ HNSCC cell lines examined.

Interestingly, recent reports have identified a novel K_{ATP} inhibitor, SpTx-1, which acts primarily by targeting the Kir6.2 subunit rather than SUR1, thus displaying a distinct mechanism of action to sulfonylureas [458, 459]. Analysing the impact of SpTx-1 on HPV oncoprotein expression and the proliferation of HPV+ HNSCC cell lines is therefore a critical next step, as this will aid in understanding whether the effects observed herein with glibenclamide and tolbutamide are due to inhibition of K_{ATP} channels or rather off-target effects.

In summary, this study is the first to undertake a comprehensive analysis of the expression and importance of K_{ATP} channels in HNSCC. We reveal that the K_{ATP} channel subunits Kir6.1, Kir6.2 and SUR1 are expressed in *in vitro* models of HNSCC and may be upregulated by HPV, possibly in an oncoprotein-independent manner. Blocking channel activity via small molecule inhibitors negatively impacted HPV gene expression, but these findings could not be replicated with knockdown of K_{ATP} channel subunits. Further, SUR1 and/or Kir6.2 knockdown failed to impact the proliferation of either HPV- or HPV+ HNSCC cell lines, suggesting that K_{ATP} channels may not promote tumour progression in HNSCC. If so, this represents a clear distinction between the molecular drivers of tumourigenesis between HPV+ cervical cancer and HPV+ HNSCC, thus having clear implications when considering novel therapeutic options.

Chapter 6 Final Discussion and Summary

The work presented in this thesis represents the most detailed characterisation of the role of a host ion channel in HPV-associated cancers. Building upon preliminary findings from the Macdonald group, this study identifies the K_{ATP} channel as a critical regulator of HPV gene expression (Chapter 3) and cell proliferation (Chapter 4) in cervical cancer cells (**Fig 6.1**). However, analysis of HNSCC cells gave conflicting results, with loss of channel expression not found to impact upon cell proliferation (Chapter 5).

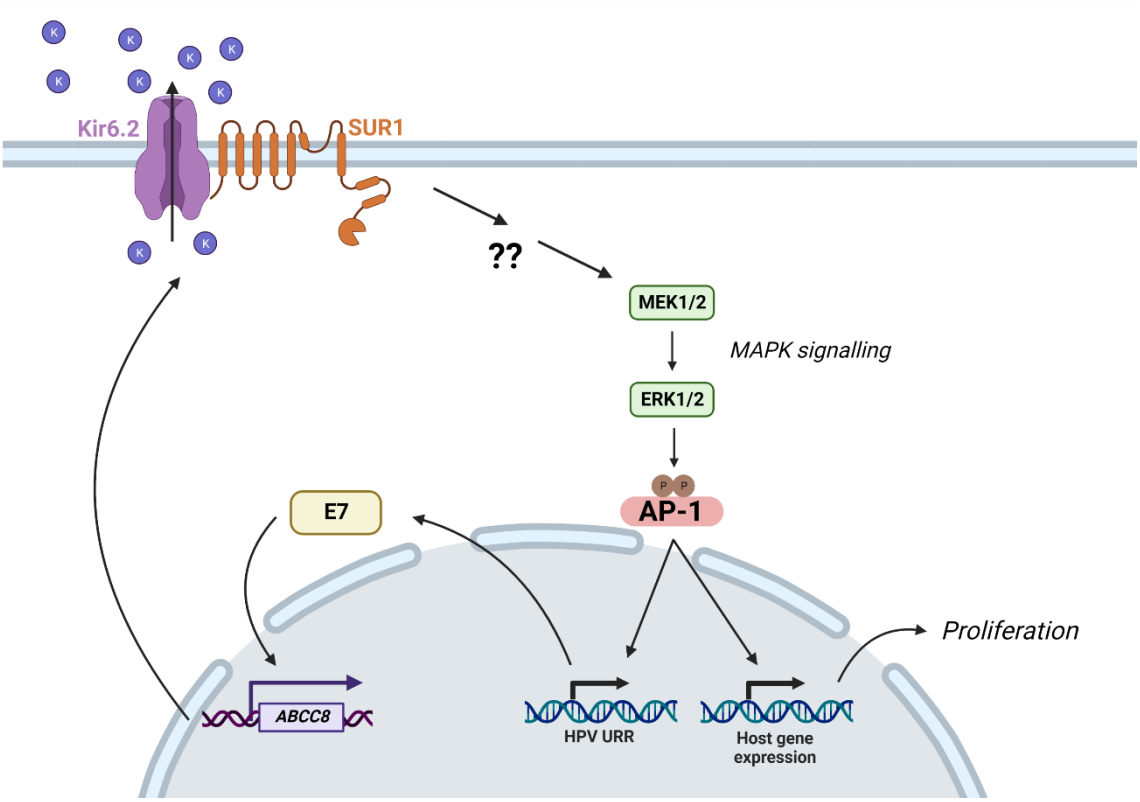

Figure 6.1 Schematic demonstrating E7-mediated upregulation of K_{ATP} channel expression and activity in HPV+ cervical cancer. HPV E7 upregulates expression of *ABCC8*, the gene encoding SUR1 which constitutes the regulatory subunit of K_{ATP} channels. Increased K_{ATP} channel activity contributes towards the activation of MAPK and AP-1 signalling. This, in turn, drives transcription from the viral URR and host gene expression changes which together stimulate proliferation. Figure created using BioRENDER.com.

An increasing number of viruses have been shown to modulate either the activity or expression of host ion channels, highlighting the importance of regulating ion channel homeostasis during infection [368]. Significantly, this was the first study

to demonstrate modulation of a host ion channel by HPV and that this is required for HPV-mediated transformation. A prior analysis identified increased expression of the sodium channel $Na_v1.6$ in cervical cancer, and K_{ATP} channel expression in cervical cell lines has previously been reported, but no attempt was made to attribute these observations to HPV [332, 369].

The underlying mechanism of K_{ATP} channel upregulation by HPV was also investigated during the course of this study, revealing that the E7 oncoprotein, rather than E6, is responsible for promoting the expression of *ABCC8*, encoding the regulatory SUR1 subunit of K_{ATP} channels. However, the exact mechanism used by E7 remains elusive: analysis of a panel of HPV18 E7 mutants herein failed to conclusively demonstrate which domains of the oncoprotein are required for this function. Despite this, analysis of the promoter region of *ABCC8* confirmed the presence of TSS-proximal SP1 binding sites [253, 254], which were found to be critical for SUR1 expression in HPV+ cervical cancer cells. Thus the potential impact of HPV E7 on the transcription factor SP1 was also investigated. SP1 protein levels have been reported to be increased in cervical cancer, but the underlying mechanism remains unclear, with both stabilisation of the protein and downregulation of an SP1-targetting miRNA having been reported [380, 381]. It was identified that although the HPV oncoproteins were essential for SP1 expression, E7 expression alone was not sufficient to induce SP1 upregulation. A further characterisation of the role of the HPV oncoproteins in regulating SP1 expression and activity is therefore warranted.

Additionally, a key outstanding question is the issue of why upregulation of SUR1, and not in combination with Kir6.2, is sufficient in HPV+ cervical cancer cells. Indeed, the *ABCC8* and *KNCJ11* genes encoding SUR1 and Kir6.2, as well as the *ABCC9* and *KCNJ8* genes encoding SUR2 and Kir6.1 are adjacent to one

another, respectively, in the human genome, suggesting the possibility of a degree of transcriptional co-regulation [236]. One possible explanation for this is that the host cells already express Kir6.2 to a sufficient degree, ensuring that the virus only need induce upregulation of the SUR1 component of the channel. This would align with the current assembly hypothesis, in which Kir6.2 subunits cannot be trafficked beyond the ER unless fully assembled into functional octamers in complex with SUR1, due to the presence of arginine-based ER retention motifs [259-261]. Thus SUR1 protein levels could be considered to be the limiting factor in K_{ATP} channel plasma membrane expression. To test this, the subcellular localisation of Kir6.2 molecules could be investigated upon overexpression of SUR1 in HPV- cell lines: one might expect to observe a relocalisation of Kir6.2 towards the plasma membrane.

Beyond transcriptional upregulation, several cellular signalling pathways have been demonstrated to regulate K_{ATP} channel gating. For example, in smooth muscle cells of the vasculature, PKA directly phosphorylates residues within Kir6.1 and SUR2B, significantly enhancing channel opening in the presence of vasodilators [285, 286]. Notably, PKA phosphorylation sites have also been identified in Kir6.2 and SUR1, suggesting a general method of K_{ATP} channel regulation [287, 288]. Given this, the relative importance of PKA activity in regulating K_{ATP} channel gating in the context of cervical cancer cells may warrant further study. Tantalisingly, modulation of the cyclic adenosine monophosphate (cAMP)-PKA pathway by HPV is, to our knowledge, yet to have been demonstrated.

This study revealed, via both pharmacological means and through siRNA-mediated knockdown, that loss of K_{ATP} channel activity significantly impedes HPV gene expression in cervical cancer cells. Further, luciferase reporter constructs

revealed that this was due to a direct impact on transcription driven by the viral URR. Subsequently, we demonstrated that these effects are mediated via induction of a MAPK/AP-1 signalling pathway which, in turn, contributes to the continued proliferation of HPV+ cervical cancer cells. Previous reports have highlighted the critical role of ERK1/2 and AP-1 signalling in regulating both HPV gene expression and cervical cancer cell proliferation [128, 163, 376, 422-424]. Importantly, however, few reports of K_{ATP} channel-mediated activation of ERK1/2 exist, and no evidence exists, to our knowledge, for increased AP-1 signalling in response to K_{ATP} channel stimulation.

A question that remains outstanding is the issue of *how* K_{ATP} channel activation leads to the induction of MAPK and AP-1 signalling. Although stimulation of ERK1/2 following activation of K_{ATP} channels has been previously reported in *in vitro* models of glioma, these studies did not investigate the effects of K_{ATP} channels on the upstream canonical EGFR-RAS-RAF signalling cascade [333, 389]. Rather, heightened ERK1/2 phosphorylation was attributed to K_{ATP} channel-induced reactive oxygen species (ROS) production [389]. Whilst excessive concentrations of ROS cause a stress response and ultimately growth arrest and cell death, H_2O_2, the major ROS, is a critical signalling molecule at physiological concentrations [460]. Furthermore, elevated ROS levels have been detected in the majority of cancers and can promote cell survival and proliferation [461-463]. ROS-mediated activation of ERK1/2 has been widely reported and indeed multiple mechanisms of how ROS can activate ERK1/2 are known [461]. For example, RAS GTPase can be directly activated via ROS, promoting its guanine nucleotide exchange and downstream signalling, whilst levels of dual specificity protein phosphatase 6 (DUSP6), a negative regulator of ERK1/2, were found to be decreased in response to ROS production in ovarian cancer cells [464, 465].

Thus, the impact of K_{ATP} channel activity on ROS generation in HPV+ cells, and whether this induces ERK1/2 and AP-1 signalling, warrants further investigation.

In order to extend the findings of this study, and to investigate whether the critical role of K_{ATP} channels in cell growth regulation in cervical cancer was common to other HPV-associated malignancies, the impact of K_{ATP} channel modulation on a panel of HNSCC cell lines was analysed. Surprisingly, although mRNA expression of *KCNJ11* and *ABCC8* was increased in HPV16+ HNSCC cell lines compared to HPV- cancer cells, hinting at possible HPV-mediated upregulation, the proliferation of all cell lines examined was not found to be dependent on K_{ATP} channel expression. This suggests that, among HPV-associated diseases, K_{ATP} channels may be playing a cervical cancer-specific role. The reasons for this remain unclear but could perhaps be linked to the inherent differences between the tissue sites of origin. If this is indeed the case, further research into the differences between the molecular drivers of carcinogenesis in HPV+ cervical cancer and HPV+ HNSCC is warranted, as this will have clear implications in the development of novel therapeutic options.

To confirm our findings in HPV+ cervical cancer and HNSCC cells, *in vitro* models of additional HPV-driven malignancies should be examined. Anal squamous cell carcinoma (ASCC), historically neglected due to the lack of tractable model systems, would constitute an excellent next step due to the recent derivation of five ASCC cell lines (four HPV+, one HPV-) via tumour explants [466]. Cell culture models of penile cancer, of which 50% are HPV-attributable, and vulvar cancer (25% HPV+) have also been developed in the recent decades but critically, all of these bar one vulvar SCC cell line are HPV-, constituting a major gap in the necessary tools to aid our understanding of these diseases [27, 467-470].

In conclusion, upregulation of host K_{ATP} channel expression and activity by HPV E7 is essential for efficient HPV gene expression in cervical cancer cell lines. Similarly, K_{ATP} channel activity was found to be critical for the proliferation of HPV+ cervical cancer cells due to activation of a MAPK/AP-1 signalling axis. However, the role of K_{ATP} channels in HNSCC cells is less clear as channel knockdown did not result in a decrease in cell proliferation. Further research to undertake a complete characterisation of the role of K_{ATP} channels in all HPV-associated diseases is now warranted in order to determine whether the clinically approved inhibitors of these channels could represent an effective therapeutic option.

References

1. Van Doorslaer K, Li Z, Xirasagar S, Maes P, Kaminsky D, Liou D, Sun Q, Kaur R, Huyen Y, McBride AA. The Papillomavirus Episteme: a major update to the papillomavirus sequence database. Nucleic Acids Res. 2017;45(D1):D499-D506. doi: 10.1093/nar/gkw879.
2. Jabbar SF, Park S, Schweizer J, Berard-Bergery M, Pitot HC, Lee D, Lambert PF. Cervical cancers require the continuous expression of the human papillomavirus type 16 E7 oncoprotein even in the presence of the viral E6 oncoprotein. Cancer Res. 2012;72(16):4008-16. doi: 10.1158/0008-5472.CAN-11-3085.
3. Bernard HU, Burk RD, Chen Z, van Doorslaer K, zur Hausen H, de Villiers EM. Classification of papillomaviruses (PVs) based on 189 PV types and proposal of taxonomic amendments. Virology. 2010;401(1):70-9. doi: 10.1016/j.virol.2010.02.002.
4. de Villiers EM, Fauquet C, Broker TR, Bernard HU, zur Hausen H. Classification of papillomaviruses. Virology. 2004;324(1):17-27. doi: 10.1016/j.virol.2004.03.033.
5. Muhr LSA, Eklund C, Dillner J. Towards quality and order in human papillomavirus research. Virology. 2018;519:74-6. doi: 10.1016/j.virol.2018.04.003.
6. Graham SV. The human papillomavirus replication cycle, and its links to cancer progression: a comprehensive review. Clin Sci (Lond). 2017;131(17):2201-21. doi: 10.1042/cs20160786.
7. Stanley M. Pathology and epidemiology of HPV infection in females. Gynecol Oncol. 2010;117(2 Suppl):S5-10. doi: 10.1016/j.ygyno.2010.01.024.
8. Tommasino M. The biology of beta human papillomaviruses. Virus Res. 2017;231:128-38. doi: 10.1016/j.virusres.2016.11.013.
9. de Sanjose S, Diaz M, Castellsague X, Clifford G, Bruni L, Munoz N, Bosch FX. Worldwide prevalence and genotype distribution of cervical human papillomavirus DNA in women with normal cytology: a meta-analysis. Lancet Infect Dis. 2007;7(7):453-9. doi: 10.1016/S1473-3099(07)70158-5.
10. Winer RL, Hughes JP, Feng Q, O'Reilly S, Kiviat NB, Holmes KK, Koutsky LA. Condom use and the risk of genital human papillomavirus infection in young women. N Engl J Med. 2006;354(25):2645-54. doi: 10.1056/NEJMoa053284.
11. Cubie HA. Diseases associated with human papillomavirus infection. Virology. 2013;445(1-2):21-34. doi: 10.1016/j.virol.2013.06.007.
12. Sabeena S, Bhat P, Kamath V, Arunkumar G. Possible non-sexual modes of transmission of human papilloma virus. J Obstet Gynaecol Res. 2017;43(3):429-35. doi: 10.1111/jog.13248.
13. Doorbar J, Egawa N, Griffin H, Kranjec C, Murakami I. Human papillomavirus molecular biology and disease association. Rev Med Virol. 2015;25:2-23. doi: 10.1002/rmv.1822.
14. Witchey DJ, Witchey NB, Roth-Kauffman MM, Kauffman MK. Plantar Warts: Epidemiology, Pathophysiology, and Clinical Management. J Am Osteopath Assoc. 2018;118(2):92-105. doi: 10.7556/jaoa.2018.024.
15. Sterling JC, Handfield-Jones S, Hudson PM, British Association of D. Guidelines for the management of cutaneous warts. Br J Dermatol. 2001;144(1):4-11. doi: 10.1046/j.1365-2133.2001.04066.x.
16. Kalinska-Bienias A, Kowalewski C, Majewski S. The EVER genes - the genetic etiology of carcinogenesis in epidermodysplasia verruciformis and a

possible role in non-epidermodysplasia verruciformis patients. Postepy Dermatol Alergol. 2016;33(2):75-80. doi: 10.5114/ada.2016.59145.
17. Ramoz N, Rueda LA, Bouadjar B, Montoya LS, Orth G, Favre M. Mutations in two adjacent novel genes are associated with epidermodysplasia verruciformis. Nat Genet. 2002;32(4):579-81. doi: 10.1038/ng1044.
18. Chahoud J, Semaan A, Chen Y, Cao M, Rieber AG, Rady P, Tyring SK. Association Between beta-Genus Human Papillomavirus and Cutaneous Squamous Cell Carcinoma in Immunocompetent Individuals-A Meta-analysis. JAMA Dermatol. 2016;152(12):1354-64. doi: 10.1001/jamadermatol.2015.4530.
19. Weissenborn SJ, Nindl I, Purdie K, Harwood C, Proby C, Breuer J, Majewski S, Pfister H, Wieland U. Human papillomavirus-DNA loads in actinic keratoses exceed those in non-melanoma skin cancers. J Invest Dermatol. 2005;125(1):93-7. doi: 10.1111/j.0022-202X.2005.23733.x.
20. Hawkins MG, Winder DM, Ball SL, Vaughan K, Sonnex C, Stanley MA, Sterling JC, Goon PK. Detection of specific HPV subtypes responsible for the pathogenesis of condylomata acuminata. Virol J. 2013;10:137. doi: 10.1186/1743-422X-10-137.
21. Yanofsky VR, Patel RV, Goldenberg G. Genital warts: a comprehensive review. J Clin Aesthet Dermatol. 2012;5(6):25-36. doi.
22. Derkay CS, Wiatrak B. Recurrent respiratory papillomatosis: a review. Laryngoscope. 2008;118(7):1236-47. doi: 10.1097/MLG.0b013e31816a7135.
23. Gerein V, Rastorguev E, Gerein J, Draf W, Schirren J. Incidence, age at onset, and potential reasons of malignant transformation in recurrent respiratory papillomatosis patients: 20 years experience. Otolaryngol Head Neck Surg. 2005;132(3):392-4. doi: 10.1016/j.otohns.2004.09.035.
24. Bennett LK, Hinshaw M. Heck's disease: diagnosis and susceptibility. Pediatr Dermatol. 2009;26(1):87-9. doi: 10.1111/j.1525-1470.2008.00830.x.
25. Munoz N, Bosch FX, de Sanjose S, Herrero R, Castellsague X, Shah KV, Snijders PJ, Meijer CJ, International Agency for Research on Cancer Multicenter Cervical Cancer Study G. Epidemiologic classification of human papillomavirus types associated with cervical cancer. N Engl J Med. 2003;348(6):518-27. doi: 10.1056/NEJMoa021641.
26. Durst M, Gissmann L, Ikenberg H, zur Hausen H. A papillomavirus DNA from a cervical carcinoma and its prevalence in cancer biopsy samples from different geographic regions. Proc Natl Acad Sci U S A. 1983;80(12):3812-5. doi: 10.1073/pnas.80.12.3812.
27. de Martel C, Plummer M, Vignat J, Franceschi S. Worldwide burden of cancer attributable to HPV by site, country and HPV type. Int J Cancer. 2017;141(4):664-70. doi: 10.1002/ijc.30716.
28. Doorbar J, Quint W, Banks L, Bravo IG, Stoler M, Broker TR, Stanley MA. The biology and life-cycle of human papillomaviruses. Vaccine. 2012;30 Suppl 5:F55-70. doi: 10.1016/j.vaccine.2012.06.083.
29. Mehanna H, Beech T, Nicholson T, El-Hariry I, McConkey C, Paleri V, Roberts S. Prevalence of human papillomavirus in oropharyngeal and nonoropharyngeal head and neck cancer--systematic review and meta-analysis of trends by time and region. Head Neck. 2013;35(5):747-55. doi: 10.1002/hed.22015.
30. Forman D, de Martel C, Lacey CJ, Soerjomataram I, Lortet-Tieulent J, Bruni L, Vignat J, Ferlay J, Bray F, Plummer M, Franceschi S. Global burden of human papillomavirus and related diseases. Vaccine. 2012;30 Suppl 5:F12-23. doi: 10.1016/j.vaccine.2012.07.055.

31. Chesson HW, Dunne EF, Hariri S, Markowitz LE. The estimated lifetime probability of acquiring human papillomavirus in the United States. Sex Transm Dis. 2014;41(11):660-4. doi: 10.1097/OLQ.0000000000000193.
32. Sung H, Ferlay J, Siegel RL, Laversanne M, Soerjomataram I, Jemal A, Bray F. Global Cancer Statistics 2020: GLOBOCAN Estimates of Incidence and Mortality Worldwide for 36 Cancers in 185 Countries. CA Cancer J Clin. 2021;71(3):209-49. doi: 10.3322/caac.21660.
33. Cohen PA, Jhingran A, Oaknin A, Denny L. Cervical cancer. Lancet. 2019;393(10167):169-82. doi: 10.1016/S0140-6736(18)32470-X.
34. Ferlay J EM, Lam F, Colombet M, Mery L, Piñeros M, Znaor A, Soerjomataram I, Bray F. Global Cancer Observatory: Cancer Today. Lyon, France: International Agency for Research on Cancer. 2018 [Available from: https://gco.iarc.fr/today.
35. Gillison ML, Alemany L, Snijders PJ, Chaturvedi A, Steinberg BM, Schwartz S, Castellsague X. Human papillomavirus and diseases of the upper airway: head and neck cancer and respiratory papillomatosis. Vaccine. 2012;30 Suppl 5:F34-54. doi: 10.1016/j.vaccine.2012.05.070.
36. Crosbie EJ, Einstein MH, Franceschi S, Kitchener HC. Human papillomavirus and cervical cancer. Lancet. 2013;382(9895):889-99. doi: 10.1016/S0140-6736(13)60022-7.
37. Garland SM, Hernandez-Avila M, Wheeler CM, Perez G, Harper DM, Leodolter S, Tang GW, Ferris DG, Steben M, Bryan J, Taddeo FJ, Railkar R, Esser MT, Sings HL, Nelson M, Boslego J, Sattler C, Barr E, Koutsky LA, Females United to Unilaterally Reduce Endo/Ectocervical Disease II. Quadrivalent vaccine against human papillomavirus to prevent anogenital diseases. N Engl J Med. 2007;356(19):1928-43. doi: 10.1056/NEJMoa061760.
38. Huh WK, Joura EA, Giuliano AR, Iversen OE, de Andrade RP, Ault KA, Bartholomew D, Cestero RM, Fedrizzi EN, Hirschberg AL, Mayrand MH, Ruiz-Sternberg AM, Stapleton JT, Wiley DJ, Ferenczy A, Kurman R, Ronnett BM, Stoler MH, Cuzick J, Garland SM, Kjaer SK, Bautista OM, Haupt R, Moeller E, Ritter M, Roberts CC, Shields C, Luxembourg A. Final efficacy, immunogenicity, and safety analyses of a nine-valent human papillomavirus vaccine in women aged 16-26 years: a randomised, double-blind trial. Lancet. 2017;390(10108):2143-59. doi: 10.1016/S0140-6736(17)31821-4.
39. Drolet M, Benard E, Perez N, Brisson M, Group HPVVIS. Population-level impact and herd effects following the introduction of human papillomavirus vaccination programmes: updated systematic review and meta-analysis. Lancet. 2019;394(10197):497-509. doi: 10.1016/S0140-6736(19)30298-3.
40. Wigle J, Coast E, Watson-Jones D. Human papillomavirus (HPV) vaccine implementation in low and middle-income countries (LMICs): health system experiences and prospects. Vaccine. 2013;31(37):3811-7. doi: 10.1016/j.vaccine.2013.06.016.
41. Andrus JK, Sherris J, Fitzsimmons JW, Kane MA, Aguado MT. Introduction of human papillomavirus vaccines into developing countries - international strategies for funding and procurement. Vaccine. 2008;26 Suppl 10:K87-92. doi: 10.1016/j.vaccine.2008.05.003.
42. LaMontagne DS, Bloem PJN, Brotherton JML, Gallagher KE, Badiane O, Ndiaye C. Progress in HPV vaccination in low- and lower-middle-income countries. Int J Gynaecol Obstet. 2017;138 Suppl 1:7-14. doi: 10.1002/ijgo.12186.
43. Castanon A, Landy R, Pesola F, Windridge P, Sasieni P. Prediction of cervical cancer incidence in England, UK, up to 2040, under four scenarios: a

modelling study. Lancet Public Health. 2018;3(1):e34-e43. doi: 10.1016/S2468-2667(17)30222-0.
44. Landy R, Pesola F, Castanon A, Sasieni P. Impact of cervical screening on cervical cancer mortality: estimation using stage-specific results from a nested case-control study. Br J Cancer. 2016;115(9):1140-6. doi: 10.1038/bjc.2016.290.
45. Ronco G, Dillner J, Elfstrom KM, Tunesi S, Snijders PJ, Arbyn M, Kitchener H, Segnan N, Gilham C, Giorgi-Rossi P, Berkhof J, Peto J, Meijer CJ, International HPVswg. Efficacy of HPV-based screening for prevention of invasive cervical cancer: follow-up of four European randomised controlled trials. Lancet. 2014;383(9916):524-32. doi: 10.1016/S0140-6736(13)62218-7.
46. Force USPST, Curry SJ, Krist AH, Owens DK, Barry MJ, Caughey AB, Davidson KW, Doubeni CA, Epling JW, Jr., Kemper AR, Kubik M, Landefeld CS, Mangione CM, Phipps MG, Silverstein M, Simon MA, Tseng CW, Wong JB. Screening for Cervical Cancer: US Preventive Services Task Force Recommendation Statement. JAMA. 2018;320(7):674-86. doi: 10.1001/jama.2018.10897.
47. Rebolj M, Rimmer J, Denton K, Tidy J, Mathews C, Ellis K, Smith J, Evans C, Giles T, Frew V, Tyler X, Sargent A, Parker J, Holbrook M, Hunt K, Tidbury P, Levine T, Smith D, Patnick J, Stubbs R, Moss S, Kitchener H. Primary cervical screening with high risk human papillomavirus testing: observational study. BMJ. 2019;364:l240. doi: 10.1136/bmj.l240.
48. Schiffman M, de Sanjose S. False positive cervical HPV screening test results. Papillomavirus Res. 2019;7:184-7. doi: 10.1016/j.pvr.2019.04.012.
49. Peralta-Zaragoza O, Bermudez-Morales VH, Perez-Plasencia C, Salazar-Leon J, Gomez-Ceron C, Madrid-Marina V. Targeted treatments for cervical cancer: a review. Onco Targets Ther. 2012;5:315-28. doi: 10.2147/OTT.S25123.
50. Scarth JA, Patterson MR, Morgan EL, Macdonald A. The human papillomavirus oncoproteins: a review of the host pathways targeted on the road to transformation. J Gen Virol. 2021;102(3). doi: 10.1099/jgv.0.001540.
51. Hebner CM, Laimins LA. Human papillomaviruses: basic mechanisms of pathogenesis and oncogenicity. Rev Med Virol. 2006;16(2):83-97. doi: 10.1002/rmv.488.
52. Lace MJ, Anson JR, Thomas GS, Turek LP, Haugen TH. The E8^E2 gene product of human papillomavirus type 16 represses early transcription and replication but is dispensable for viral plasmid persistence in keratinocytes. J Virol. 2008;82(21):10841-53. doi: 10.1128/jvi.01481-08.
53. Wang XH, Meyers C, Wang HK, Chow LT, Zheng ZM. Construction of a Full Transcription Map of Human Papillomavirus Type 18 during Productive Viral Infection. J Virol. 2011;85(16):8080-92. doi: 10.1128/jvi.00670-11.
54. Herfs M, Yamamoto Y, Laury A, Wang X, Nucci MR, McLaughlin-Drubin ME, Munger K, Feldman S, McKeon FD, Xian W, Crum CP. A discrete population of squamocolumnar junction cells implicated in the pathogenesis of cervical cancer. Proc Natl Acad Sci U S A. 2012;109(26):10516-21. doi: 10.1073/pnas.1202684109.
55. Raff AB, Woodham AW, Raff LM, Skeate JG, Yan L, Da Silva DM, Schelhaas M, Kast WM. The evolving field of human papillomavirus receptor research: a review of binding and entry. J Virol. 2013;87(11):6062-72. doi: 10.1128/jvi.00330-13.
56. Schelhaas M, Shah B, Holzer M, Blattmann P, Kuhling L, Day PM, Schiller JT, Helenius A. Entry of human papillomavirus type 16 by actin-dependent, clathrin- and lipid raft-independent endocytosis. PLoS Pathog. 2012;8(4):e1002657. doi: 10.1371/journal.ppat.1002657.

57. DiGiuseppe S, Bienkowska-Haba M, Guion LGM, Keiffer TR, Sapp M. Human papillomavirus major capsid protein L1 remains associated with the incoming viral genome throughout the entry process. J Virol. 2017. doi: 10.1128/jvi.00537-17.
58. Uhlorn BL, Jackson R, Li S, Bratton SM, Van Doorslaer K, Campos SK. Vesicular trafficking permits evasion of cGAS/STING surveillance during initial human papillomavirus infection. PLoS Pathog. 2020;16(11):e1009028. doi: 10.1371/journal.ppat.1009028.
59. Pyeon D, Pearce SM, Lank SM, Ahlquist P, Lambert PF. Establishment of human papillomavirus infection requires cell cycle progression. PLoS Pathog. 2009;5(2):e1000318. doi: 10.1371/journal.ppat.1000318.
60. Ribeiro AL, Caodaglio AS, Sichero L. Regulation of HPV transcription. Clinics (Sao Paulo). 2018;73(suppl 1):e486s. doi: 10.6061/clinics/2018/e486s.
61. Day PM, Roden RB, Lowy DR, Schiller JT. The papillomavirus minor capsid protein, L2, induces localization of the major capsid protein, L1, and the viral transcription/replication protein, E2, to PML oncogenic domains. J Virol. 1998;72(1):142-50. doi.
62. Holmgren SC, Patterson NA, Ozbun MA, Lambert PF. The minor capsid protein L2 contributes to two steps in the human papillomavirus type 31 life cycle. J Virol. 2005;79(7):3938-48. doi: 10.1128/JVI.79.7.3938-3948.2005.
63. Buck CB, Thompson CD, Pang YY, Lowy DR, Schiller JT. Maturation of papillomavirus capsids. J Virol. 2005;79(5):2839-46. doi: 10.1128/JVI.79.5.2839-2846.2005.
64. Bergvall M, Melendy T, Archambault J. The E1 proteins. Virology. 2013;445(1-2):35-56. doi: 10.1016/j.virol.2013.07.020.
65. Amin AA, Titolo S, Pelletier A, Fink D, Cordingley MG, Archambault J. Identification of domains of the HPV11 E1 protein required for DNA replication in vitro. Virology. 2000;272(1):137-50. doi: 10.1006/viro.2000.0328.
66. Chen G, Stenlund A. The E1 initiator recognizes multiple overlapping sites in the papillomavirus origin of DNA replication. J Virol. 2001;75(1):292-302. doi: 10.1128/JVI.75.1.292-302.2001.
67. Schuck S, Stenlund A. Assembly of a double hexameric helicase. Mol Cell. 2005;20(3):377-89. doi: 10.1016/j.molcel.2005.09.020.
68. Whelan F, Stead JA, Shkumatov AV, Svergun DI, Sanders CM, Antson AA. A flexible brace maintains the assembly of a hexameric replicative helicase during DNA unwinding. Nucleic Acids Res. 2012;40(5):2271-83. doi: 10.1093/nar/gkr906.
69. Egawa N, Nakahara T, Ohno S, Narisawa-Saito M, Yugawa T, Fujita M, Yamato K, Natori Y, Kiyono T. The E1 protein of human papillomavirus type 16 is dispensable for maintenance replication of the viral genome. J Virol. 2012;86(6):3276-83. doi: 10.1128/JVI.06450-11.
70. Moody CA, Fradet-Turcotte A, Archambault J, Laimins LA. Human papillomaviruses activate caspases upon epithelial differentiation to induce viral genome amplification. Proc Natl Acad Sci U S A. 2007;104(49):19541-6. doi: 10.1073/pnas.0707947104.
71. Yu JH, Lin BY, Deng W, Broker TR, Chow LT. Mitogen-activated protein kinases activate the nuclear localization sequence of human papillomavirus type 11 E1 DNA helicase to promote efficient nuclear import. J Virol. 2007;81(10):5066-78. doi: 10.1128/JVI.02480-06.
72. Fradet-Turcotte A, Moody C, Laimins LA, Archambault J. Nuclear export of human papillomavirus type 31 E1 is regulated by Cdk2 phosphorylation and

required for viral genome maintenance. J Virol. 2010;84(22):11747-60. doi: 10.1128/JVI.01445-10.
73. McBride AA. The papillomavirus E2 proteins. Virology. 2013;445(1-2):57-79. doi: 10.1016/j.virol.2013.06.006.
74. Zou N, Lin BY, Duan F, Lee KY, Jin G, Guan R, Yao G, Lefkowitz EJ, Broker TR, Chow LT. The hinge of the human papillomavirus type 11 E2 protein contains major determinants for nuclear localization and nuclear matrix association. J Virol. 2000;74(8):3761-70. doi: 10.1128/jvi.74.8.3761-3770.2000.
75. Sekhar V, McBride AA. Phosphorylation regulates binding of the human papillomavirus type 8 E2 protein to host chromosomes. J Virol. 2012;86(18):10047-58. doi: 10.1128/JVI.01140-12.
76. Androphy EJ, Lowy DR, Schiller JT. Bovine papillomavirus E2 trans-activating gene product binds to specific sites in papillomavirus DNA. Nature. 1987;325(6099):70-3. doi: 10.1038/325070a0.
77. Sanders CM, Stenlund A. Recruitment and loading of the E1 initiator protein: an ATP-dependent process catalysed by a transcription factor. EMBO J. 1998;17(23):7044-55. doi: 10.1093/emboj/17.23.7044.
78. Schuck S, Stenlund A. Mechanistic analysis of local ori melting and helicase assembly by the papillomavirus E1 protein. Mol Cell. 2011;43(5):776-87. doi: 10.1016/j.molcel.2011.06.026.
79. Loo YM, Melendy T. Recruitment of replication protein A by the papillomavirus E1 protein and modulation by single-stranded DNA. J Virol. 2004;78(4):1605-15. doi: 10.1128/jvi.78.4.1605-1615.2004.
80. Clower RV, Fisk JC, Melendy T. Papillomavirus E1 protein binds to and stimulates human topoisomerase I. J Virol. 2006;80(3):1584-7. doi: 10.1128/JVI.80.3.1584-1587.2006.
81. Ilves I, Kivi S, Ustav M. Long-term episomal maintenance of bovine papillomavirus type 1 plasmids is determined by attachment to host chromosomes, which Is mediated by the viral E2 protein and its binding sites. J Virol. 1999;73(5):4404-12. doi.
82. Skiadopoulos MH, McBride AA. Bovine papillomavirus type 1 genomes and the E2 transactivator protein are closely associated with mitotic chromatin. J Virol. 1998;72(3):2079-88. doi.
83. You J, Croyle JL, Nishimura A, Ozato K, Howley PM. Interaction of the bovine papillomavirus E2 protein with Brd4 tethers the viral DNA to host mitotic chromosomes. Cell. 2004;117(3):349-60. doi: 10.1016/s0092-8674(04)00402-7.
84. McPhillips MG, Oliveira JG, Spindler JE, Mitra R, McBride AA. Brd4 is required for E2-mediated transcriptional activation but not genome partitioning of all papillomaviruses. J Virol. 2006;80(19):9530-43. doi: 10.1128/JVI.01105-06.
85. McBride AA, Oliveira JG, McPhillips MG. Partitioning viral genomes in mitosis: same idea, different targets. Cell Cycle. 2006;5(14):1499-502. doi: 10.4161/cc.5.14.3094.
86. Donaldson MM, Boner W, Morgan IM. TopBP1 regulates human papillomavirus type 16 E2 interaction with chromatin. J Virol. 2007;81(8):4338-42. doi: 10.1128/JVI.02353-06.
87. Prabhakar AT, James CD, Das D, Fontan CT, Otoa R, Wang X, Bristol ML, Morgan IM. Interaction with TopBP1 mediates human papillomavirus 16 E2 plasmid segregation/retention function and stability during the viral life cycle. bioRxiv. 2022:2022.01.28.478274. doi: 10.1101/2022.01.28.478274 %J bioRxiv.
88. Tan SH, Gloss B, Bernard HU. During negative regulation of the human papillomavirus-16 E6 promoter, the viral E2 protein can displace Sp1 from a

proximal promoter element. Nucleic Acids Res. 1992;20(2):251-6. doi: 10.1093/nar/20.2.251.
89. Yan J, Li Q, Lievens S, Tavernier J, You J. Abrogation of the Brd4-positive transcription elongation factor B complex by papillomavirus E2 protein contributes to viral oncogene repression. J Virol. 2010;84(1):76-87. doi: 10.1128/JVI.01647-09.
90. Wu SY, Lee AY, Hou SY, Kemper JK, Erdjument-Bromage H, Tempst P, Chiang CM. Brd4 links chromatin targeting to HPV transcriptional silencing. Genes Dev. 2006;20(17):2383-96. doi: 10.1101/gad.1448206.
91. Steger G, Corbach S. Dose-dependent regulation of the early promoter of human papillomavirus type 18 by the viral E2 protein. J Virol. 1997;71(1):50-8. doi.
92. The Cancer Genome Atlas Network. Comprehensive genomic characterization of head and neck squamous cell carcinomas. Nature. 2015;517(7536):576-82. doi: 10.1038/nature14129.
93. Jeon S, Allen-Hoffmann BL, Lambert PF. Integration of human papillomavirus type 16 into the human genome correlates with a selective growth advantage of cells. J Virol. 1995;69(5):2989-97. doi.
94. Buck CB, Cheng N, Thompson CD, Lowy DR, Steven AC, Schiller JT, Trus BL. Arrangement of L2 within the papillomavirus capsid. J Virol. 2008;82(11):5190-7. doi: 10.1128/JVI.02726-07.
95. Dasgupta J, Bienkowska-Haba M, Ortega ME, Patel HD, Bodevin S, Spillmann D, Bishop B, Sapp M, Chen XS. Structural basis of oligosaccharide receptor recognition by human papillomavirus. J Biol Chem. 2011;286(4):2617-24. doi: 10.1074/jbc.M110.160184.
96. Johnson KM, Kines RC, Roberts JN, Lowy DR, Schiller JT, Day PM. Role of heparan sulfate in attachment to and infection of the murine female genital tract by human papillomavirus. J Virol. 2009;83(5):2067-74. doi: 10.1128/jvi.02190-08.
97. Cerqueira C, Samperio Ventayol P, Vogeley C, Schelhaas M. Kallikrein-8 Proteolytically Processes Human Papillomaviruses in the Extracellular Space To Facilitate Entry into Host Cells. J Virol. 2015;89(14):7038-52. doi: 10.1128/JVI.00234-15.
98. Bienkowska-Haba M, Patel HD, Sapp M. Target cell cyclophilins facilitate human papillomavirus type 16 infection. PLoS Pathog. 2009;5(7):e1000524. doi: 10.1371/journal.ppat.1000524.
99. Richards RM, Lowy DR, Schiller JT, Day PM. Cleavage of the papillomavirus minor capsid protein, L2, at a furin consensus site is necessary for infection. Proc Natl Acad Sci U S A. 2006;103(5):1522-7. doi: 10.1073/pnas.0508815103.
100. Aksoy P, Gottschalk EY, Meneses PI. HPV entry into cells. Mutat Res Rev Mutat Res. 2017;772:13-22. doi: 10.1016/j.mrrev.2016.09.004.
101. Day PM, Thompson CD, Schowalter RM, Lowy DR, Schiller JT. Identification of a role for the trans-Golgi network in human papillomavirus 16 pseudovirus infection. J Virol. 2013;87(7):3862-70. doi: 10.1128/JVI.03222-12.
102. Zhang P, Monteiro da Silva G, Deatherage C, Burd C, DiMaio D. Cell-Penetrating Peptide Mediates Intracellular Membrane Passage of Human Papillomavirus L2 Protein to Trigger Retrograde Trafficking. Cell. 2018;174(6):1465-76 e13. doi: 10.1016/j.cell.2018.07.031.
103. Bronnimann MP, Chapman JA, Park CK, Campos SK. A transmembrane domain and GxxxG motifs within L2 are essential for papillomavirus infection. J Virol. 2013;87(1):464-73. doi: 10.1128/JVI.01539-12.

104. Siddiqa A, Broniarczyk J, Banks L. Papillomaviruses and Endocytic Trafficking. Int J Mol Sci. 2018;19(9). doi: 10.3390/ijms19092619.
105. Popa A, Zhang W, Harrison MS, Goodner K, Kazakov T, Goodwin EC, Lipovsky A, Burd CG, DiMaio D. Direct binding of retromer to human papillomavirus type 16 minor capsid protein L2 mediates endosome exit during viral infection. PLoS Pathog. 2015;11(2):e1004699. doi: 10.1371/journal.ppat.1004699.
106. DiGiuseppe S, Luszczek W, Keiffer TR, Bienkowska-Haba M, Guion LG, Sapp MJ. Incoming human papillomavirus type 16 genome resides in a vesicular compartment throughout mitosis. Proc Natl Acad Sci U S A. 2016;113(22):6289-94. doi: 10.1073/pnas.1600638113.
107. Aydin I, Villalonga-Planells R, Greune L, Bronnimann MP, Calton CM, Becker M, Lai KY, Campos SK, Schmidt MA, Schelhaas M. A central region in the minor capsid protein of papillomaviruses facilitates viral genome tethering and membrane penetration for mitotic nuclear entry. PLoS Pathog. 2017;13(5):e1006308. doi: 10.1371/journal.ppat.1006308.
108. Nelson LM, Rose RC, Moroianu J. Nuclear import strategies of high risk HPV16 L1 major capsid protein. J Biol Chem. 2002;277(26):23958-64. doi: 10.1074/jbc.M200724200.
109. Bird G, O'Donnell M, Moroianu J, Garcea RL. Possible role for cellular karyopherins in regulating polyomavirus and papillomavirus capsid assembly. J Virol. 2008;82(20):9848-57. doi: 10.1128/JVI.01221-08.
110. Florin L, Becker KA, Sapp C, Lambert C, Sirma H, Muller M, Streeck RE, Sapp M. Nuclear translocation of papillomavirus minor capsid protein L2 requires Hsc70. J Virol. 2004;78(11):5546-53. doi: 10.1128/JVI.78.11.5546-5553.2004.
111. Day PM, Thompson CD, Pang YY, Lowy DR, Schiller JT. Involvement of Nucleophosmin (NPM1/B23) in Assembly of Infectious HPV16 Capsids. Papillomavirus Res. 2015;1:74-89. doi: 10.1016/j.pvr.2015.06.005.
112. Marusic MB, Mencin N, Licen M, Banks L, Grm HS. Modification of human papillomavirus minor capsid protein L2 by sumoylation. J Virol. 2010;84(21):11585-9. doi: 10.1128/JVI.01269-10.
113. Doorbar J. The E4 protein; structure, function and patterns of expression. Virology. 2013;445(1-2):80-98. doi: 10.1016/j.virol.2013.07.008.
114. Doorbar J, Foo C, Coleman N, Medcalf L, Hartley O, Prospero T, Napthine S, Sterling J, Winter G, Griffin H. Characterization of events during the late stages of HPV16 infection in vivo using high-affinity synthetic Fabs to E4. Virology. 1997;238(1):40-52. doi: 10.1006/viro.1997.8768.
115. Wilson R, Ryan GB, Knight GL, Laimins LA, Roberts S. The full-length E1E4 protein of human papillomavirus type 18 modulates differentiation-dependent viral DNA amplification and late gene expression. Virology. 2007;362(2):453-60. doi: 10.1016/j.virol.2007.01.005.
116. Egawa N, Wang Q, Griffin HM, Murakami I, Jackson D, Mahmood R, Doorbar J. HPV16 and 18 genome amplification show different E4-dependence, with 16E4 enhancing E1 nuclear accumulation and replicative efficiency via its cell cycle arrest and kinase activation functions. PLoS Pathog. 2017;13(3):e1006282. doi: 10.1371/journal.ppat.1006282.
117. Davy CE, Jackson DJ, Raj K, Peh WL, Southern SA, Das P, Sorathia R, Laskey P, Middleton K, Nakahara T, Wang Q, Masterson PJ, Lambert PF, Cuthill S, Millar JB, Doorbar J. Human papillomavirus type 16 E1 E4-induced G2 arrest is associated with cytoplasmic retention of active Cdk1/cyclin B1 complexes. J Virol. 2005;79(7):3998-4011. doi: 10.1128/JVI.79.7.3998-4011.2005.

118. Wang Q, Kennedy A, Das P, McIntosh PB, Howell SA, Isaacson ER, Hinz SA, Davy C, Doorbar J. Phosphorylation of the human papillomavirus type 16 E1--E4 protein at T57 by ERK triggers a structural change that enhances keratin binding and protein stability. J Virol. 2009;83(8):3668-83. doi: 10.1128/JVI.02063-08.
119. Khan J, Davy CE, McIntosh PB, Jackson DJ, Hinz S, Wang Q, Doorbar J. Role of calpain in the formation of human papillomavirus type 16 E1^E4 amyloid fibers and reorganization of the keratin network. J Virol. 2011;85(19):9984-97. doi: 10.1128/JVI.02158-10.
120. DiMaio D, Petti LM. The E5 proteins. Virology. 2013;445(1-2):99-114. doi: 10.1016/j.virol.2013.05.006.
121. Müller M, Prescott EL, Wasson CW, Macdonald A. Human papillomavirus E5 oncoprotein: function and potential target for antiviral therapeutics. Future Virol. 2015;10(1):27–39. doi: 10.2217/fvl.14.99.
122. Maufort JP, Shai A, Pitot HC, Lambert PF. A role for HPV16 E5 in cervical carcinogenesis. Cancer Res. 2010;70(7):2924-31. doi: 10.1158/0008-5472.CAN-09-3436.
123. Wetherill LF, Holmes KK, Verow M, Muller M, Howell G, Harris M, Fishwick C, Stonehouse N, Foster R, Blair GE, Griffin S, Macdonald A. High-risk human papillomavirus E5 oncoprotein displays channel-forming activity sensitive to small-molecule inhibitors. J Virol. 2012;86(9):5341-51. doi: 10.1128/jvi.06243-11.
124. Scott C, Griffin S. Viroporins: structure, function and potential as antiviral targets. J Gen Virol. 2015;96(8):2000-27. doi: 10.1099/vir.0.000201.
125. Wetherill LF, Wasson CW, Swinscoe G, Kealy D, Foster R, Griffin S, Macdonald A. Alkyl-imino sugars inhibit the pro-oncogenic ion channel function of human papillomavirus (HPV) E5. Antiviral Res. 2018;158:113-21. doi: 10.1016/j.antiviral.2018.08.005.
126. Genther SM, Sterling S, Duensing S, Munger K, Sattler C, Lambert PF. Quantitative role of the human papillomavirus type 16 E5 gene during the productive stage of the viral life cycle. J Virol. 2003;77(5):2832-42. doi: 10.1128/jvi.77.5.2832-2842.2003.
127. Fehrmann F, Klumpp DJ, Laimins LA. Human papillomavirus type 31 E5 protein supports cell cycle progression and activates late viral functions upon epithelial differentiation. J Virol. 2003;77(5):2819-31. doi: 10.1128/jvi.77.5.2819-2831.2003.
128. Wasson CW, Morgan EL, Muller M, Ross RL, Hartley M, Roberts S, Macdonald A. Human papillomavirus type 18 E5 oncogene supports cell cycle progression and impairs epithelial differentiation by modulating growth factor receptor signalling during the virus life cycle. Oncotarget. 2017;8(61):103581-600. doi: 10.18632/oncotarget.21658.
129. Genther Williams SM, Disbrow GL, Schlegel R, Lee D, Threadgill DW, Lambert PF. Requirement of epidermal growth factor receptor for hyperplasia induced by E5, a high-risk human papillomavirus oncogene. Cancer Res. 2005;65(15):6534-42. doi: 10.1158/0008-5472.CAN-05-0083.
130. Suprynowicz FA, Krawczyk E, Hebert JD, Sudarshan SR, Simic V, Kamonjoh CM, Schlegel R. The human papillomavirus type 16 E5 oncoprotein inhibits epidermal growth factor trafficking independently of endosome acidification. J Virol. 2010;84(20):10619-29. doi: 10.1128/jvi.00831-10.
131. Purpura V, Belleudi F, Caputo S, Torrisi MR. HPV16 E5 and KGFR/FGFR2b interplay in differentiating epithelial cells. Oncotarget. 2013;4(2):192-205. doi: 10.18632/oncotarget.803.

132. Ashrafi GH, Haghshenas MR, Marchetti B, O'Brien PM, Campo MS. E5 protein of human papillomavirus type 16 selectively downregulates surface HLA class I. Int J Cancer. 2005;113(2):276-83. doi: 10.1002/ijc.20558.
133. Cromme FV, Meijer CJ, Snijders PJ, Uyterlinde A, Kenemans P, Helmerhorst T, Stern PL, van den Brule AJ, Walboomers JM. Analysis of MHC class I and II expression in relation to presence of HPV genotypes in premalignant and malignant cervical lesions. Br J Cancer. 1993;67(6):1372-80. doi: 10.1038/bjc.1993.254.
134. Ritz U, Momburg F, Pilch H, Huber C, Maeurer MJ, Seliger B. Deficient expression of components of the MHC class I antigen processing machinery in human cervical carcinoma. Int J Oncol. 2001;19(6):1211-20. doi: 10.3892/ijo.19.6.1211.
135. Ashrafi GH, Haghshenas M, Marchetti B, Campo MS. E5 protein of human papillomavirus 16 downregulates HLA class I and interacts with the heavy chain via its first hydrophobic domain. Int J Cancer. 2006;119(9):2105-12. doi: 10.1002/ijc.22089.
136. Halavaty K, Regan J, Mehta K, Laimins L. Human papillomavirus E5 oncoproteins bind the A4 endoplasmic reticulum protein to regulate proliferative ability upon differentiation. Virology. 2014;452-453:223-30. doi: 10.1016/j.virol.2014.01.013.
137. Regan JA, Laimins LA. Bap31 is a novel target of the human papillomavirus E5 protein. J Virol. 2008;82(20):10042-51. doi: 10.1128/JVI.01240-08.
138. Zhang B, Li P, Wang E, Brahmi Z, Dunn KW, Blum JS, Roman A. The E5 protein of human papillomavirus type 16 perturbs MHC class II antigen maturation in human foreskin keratinocytes treated with interferon-gamma. Virology. 2003;310(1):100-8. doi: 10.1016/s0042-6822(03)00103-x.
139. Campo MS, Graham SV, Cortese MS, Ashrafi GH, Araibi EH, Dornan ES, Miners K, Nunes C, Man S. HPV-16 E5 down-regulates expression of surface HLA class I and reduces recognition by CD8 T cells. Virology. 2010;407(1):137-42. doi: 10.1016/j.virol.2010.07.044.
140. Howie HL, Katzenellenbogen RA, Galloway DA. Papillomavirus E6 proteins. Virology. 2009;384(2):324-34. doi: 10.1016/j.virol.2008.11.017.
141. Vande Pol SB, Klingelhutz AJ. Papillomavirus E6 oncoproteins. Virology. 2013;445(1-2):115-37. doi: 10.1016/j.virol.2013.04.026.
142. Munger K, Phelps WC, Bubb V, Howley PM, Schlegel R. The E6 and E7 genes of the human papillomavirus type 16 together are necessary and sufficient for transformation of primary human keratinocytes. J Virol. 1989;63(10):4417-21. doi.
143. Moody CA, Laimins LA. Human papillomavirus oncoproteins: pathways to transformation. Nat Rev Cancer. 2010;10(8):550-60. doi: 10.1038/nrc2886.
144. Huibregtse JM, Scheffner M, Howley PM. Localization of the E6-AP regions that direct human papillomavirus E6 binding, association with p53, and ubiquitination of associated proteins. Mol Cell Biol. 1993;13(8):4918-27. doi.
145. Scheffner M, Huibregtse JM, Vierstra RD, Howley PM. The HPV-16 E6 and E6-AP complex functions as a ubiquitin-protein ligase in the ubiquitination of p53. Cell. 1993;75(3):495-505. doi: 10.1016/0092-8674(93)90384-3.
146. Lechner MS, Laimins LA. Inhibition of p53 DNA binding by human papillomavirus E6 proteins. J Virol. 1994;68(7):4262-73. doi.
147. Thomas MC, Chiang CM. E6 oncoprotein represses p53-dependent gene activation via inhibition of protein acetylation independently of inducing p53 degradation. Mol Cell. 2005;17(2):251-64. doi: 10.1016/j.molcel.2004.12.016.

148. Patel D, Huang SM, Baglia LA, McCance DJ. The E6 protein of human papillomavirus type 16 binds to and inhibits co-activation by CBP and p300. EMBO J. 1999;18(18):5061-72. doi: 10.1093/emboj/18.18.5061.
149. Kumar A, Zhao Y, Meng G, Zeng M, Srinivasan S, Delmolino LM, Gao Q, Dimri G, Weber GF, Wazer DE, Band H, Band V. Human papillomavirus oncoprotein E6 inactivates the transcriptional coactivator human ADA3. Mol Cell Biol. 2002;22(16):5801-12. doi: 10.1128/mcb.22.16.5801-5812.2002.
150. Thomas M, Banks L. Inhibition of Bak-induced apoptosis by HPV-18 E6. Oncogene. 1998;17(23):2943-54. doi: 10.1038/sj.onc.1202223.
151. Thomas M, Banks L. Human papillomavirus (HPV) E6 interactions with Bak are conserved amongst E6 proteins from high and low risk HPV types. J Gen Virol. 1999;80 (Pt 6):1513-7. doi: 10.1099/0022-1317-80-6-1513.
152. Filippova M, Song H, Connolly JL, Dermody TS, Duerksen-Hughes PJ. The human papillomavirus 16 E6 protein binds to tumor necrosis factor (TNF) R1 and protects cells from TNF-induced apoptosis. J Biol Chem. 2002;277(24):21730-9. doi: 10.1074/jbc.M200113200.
153. Filippova M, Parkhurst L, Duerksen-Hughes PJ. The human papillomavirus 16 E6 protein binds to Fas-associated death domain and protects cells from Fas-triggered apoptosis. J Biol Chem. 2004;279(24):25729-44. doi: 10.1074/jbc.M401172200.
154. Garnett TO, Filippova M, Duerksen-Hughes PJ. Accelerated degradation of FADD and procaspase 8 in cells expressing human papilloma virus 16 E6 impairs TRAIL-mediated apoptosis. Cell Death Differ. 2006;13(11):1915-26. doi: 10.1038/sj.cdd.4401886.
155. Ganti K, Broniarczyk J, Manoubi W, Massimi P, Mittal S, Pim D, Szalmas A, Thatte J, Thomas M, Tomaic V, Banks L. The Human Papillomavirus E6 PDZ Binding Motif: From Life Cycle to Malignancy. Viruses. 2015;7(7):3530-51. doi: 10.3390/v7072785.
156. Liu Y, Chen JJ, Gao Q, Dalal S, Hong Y, Mansur CP, Band V, Androphy EJ. Multiple functions of human papillomavirus type 16 E6 contribute to the immortalization of mammary epithelial cells. J Virol. 1999;73(9):7297-307. doi.
157. Nguyen ML, Nguyen MM, Lee D, Griep AE, Lambert PF. The PDZ ligand domain of the human papillomavirus type 16 E6 protein is required for E6's induction of epithelial hyperplasia in vivo. J Virol. 2003;77(12):6957-64. doi: 10.1128/jvi.77.12.6957-6964.2003.
158. Gardiol D, Kuhne C, Glaunsinger B, Lee SS, Javier R, Banks L. Oncogenic human papillomavirus E6 proteins target the discs large tumour suppressor for proteasome-mediated degradation. Oncogene. 1999;18(40):5487-96. doi: 10.1038/sj.onc.1202920.
159. Nakagawa S, Huibregtse JM. Human scribble (Vartul) is targeted for ubiquitin-mediated degradation by the high-risk papillomavirus E6 proteins and the E6AP ubiquitin-protein ligase. Mol Cell Biol. 2000;20(21):8244-53. doi: 10.1128/mcb.20.21.8244-8253.2000.
160. Glaunsinger BA, Lee SS, Thomas M, Banks L, Javier R. Interactions of the PDZ-protein MAGI-1 with adenovirus E4-ORF1 and high-risk papillomavirus E6 oncoproteins. Oncogene. 2000;19(46):5270-80. doi: 10.1038/sj.onc.1203906.
161. Thomas M, Laura R, Hepner K, Guccione E, Sawyers C, Lasky L, Banks L. Oncogenic human papillomavirus E6 proteins target the MAGI-2 and MAGI-3 proteins for degradation. Oncogene. 2002;21(33):5088-96. doi: 10.1038/sj.onc.1205668.
162. Ganti K, Massimi P, Manzo-Merino J, Tomaic V, Pim D, Playford MP, Lizano M, Roberts S, Kranjec C, Doorbar J, Banks L. Interaction of the Human

Papillomavirus E6 Oncoprotein with Sorting Nexin 27 Modulates Endocytic Cargo Transport Pathways. PLoS Pathog. 2016;12(9):e1005854. doi: 10.1371/journal.ppat.1005854.
163. Morgan EL, Scarth JA, Patterson MR, Wasson CW, Hemingway GC, Barba-Moreno D, Macdonald A. E6-mediated activation of JNK drives EGFR signalling to promote proliferation and viral oncoprotein expression in cervical cancer. Cell Death Differ. 2021;28(5):1669-87. doi: 10.1038/s41418-020-00693-9.
164. Banks L, Pim D, Thomas M. Human tumour viruses and the deregulation of cell polarity in cancer. Nat Rev Cancer. 2012;12(12):877-86. doi: 10.1038/nrc3400.
165. Thomas M, Myers MP, Massimi P, Guarnaccia C, Banks L. Analysis of Multiple HPV E6 PDZ Interactions Defines Type-Specific PDZ Fingerprints That Predict Oncogenic Potential. PLoS Pathog. 2016;12(8):e1005766. doi: 10.1371/journal.ppat.1005766.
166. Boon SS, Banks L. High-risk human papillomavirus E6 oncoproteins interact with 14-3-3zeta in a PDZ binding motif-dependent manner. J Virol. 2013;87(3):1586-95. doi: 10.1128/JVI.02074-12.
167. Morgan EL, Wasson CW, Hanson L, Kealy D, Pentland I, McGuire V, Scarpini C, Coleman N, Arthur JSC, Parish JL, Roberts S, Macdonald A. STAT3 activation by E6 is essential for the differentiation-dependent HPV18 life cycle. PLoS Pathog. 2018;14(4):e1006975. doi: 10.1371/journal.ppat.1006975.
168. Morgan EL, Macdonald A. Autocrine STAT3 activation in HPV positive cervical cancer through a virus-driven Rac1-NFkappaB-IL-6 signalling axis. PLoS Pathog. 2019;15(6):e1007835. doi: 10.1371/journal.ppat.1007835.
169. Morgan EL, Macdonald A. JAK2 Inhibition Impairs Proliferation and Sensitises Cervical Cancer Cells to Cisplatin-Induced Cell Death. Cancers (Basel). 2019;11(12). doi: 10.3390/cancers11121934.
170. Spangle JM, Munger K. The HPV16 E6 oncoprotein causes prolonged receptor protein tyrosine kinase signaling and enhances internalization of phosphorylated receptor species. PLoS Pathog. 2013;9(3):e1003237. doi: 10.1371/journal.ppat.1003237.
171. Rampias T, Boutati E, Pectasides E, Sasaki C, Kountourakis P, Weinberger P, Psyrri A. Activation of Wnt signaling pathway by human papillomavirus E6 and E7 oncogenes in HPV16-positive oropharyngeal squamous carcinoma cells. Mol Cancer Res. 2010;8(3):433-43. doi: 10.1158/1541-7786.mcr-09-0345.
172. Chen PM, Cheng YW, Wang YC, Wu TC, Chen CY, Lee H. Up-regulation of FOXM1 by E6 oncoprotein through the MZF1/NKX2-1 axis is required for human papillomavirus-associated tumorigenesis. Neoplasia. 2014;16(11):961-71. doi: 10.1016/j.neo.2014.09.010.
173. He C, Mao D, Hua G, Lv X, Chen X, Angeletti PC, Dong J, Remmenga SW, Rodabaugh KJ, Zhou J, Lambert PF, Yang P, Davis JS, Wang C. The Hippo/YAP pathway interacts with EGFR signaling and HPV oncoproteins to regulate cervical cancer progression. EMBO Mol Med. 2015;7(11):1426-49. doi: 10.15252/emmm.201404976.
174. Morgan EL, Patterson MR, Ryder EL, Lee SY, Wasson CW, Harper KL, Li Y, Griffin S, Blair GE, Whitehouse A, Macdonald A. MicroRNA-18a targeting of the STK4/MST1 tumour suppressor is necessary for transformation in HPV positive cervical cancer. PLoS Pathog. 2020;16(6):e1008624. doi: 10.1371/journal.ppat.1008624.

175. Klingelhutz AJ, Foster SA, McDougall JK. Telomerase activation by the E6 gene product of human papillomavirus type 16. Nature. 1996;380(6569):79-82. doi: 10.1038/380079a0.
176. Oh ST, Kyo S, Laimins LA. Telomerase activation by human papillomavirus type 16 E6 protein: induction of human telomerase reverse transcriptase expression through Myc and GC-rich Sp1 binding sites. J Virol. 2001;75(12):5559-66. doi: 10.1128/JVI.75.12.5559-5566.2001.
177. Liu X, Yuan H, Fu B, Disbrow GL, Apolinario T, Tomaic V, Kelley ML, Baker CC, Huibregtse J, Schlegel R. The E6AP ubiquitin ligase is required for transactivation of the hTERT promoter by the human papillomavirus E6 oncoprotein. J Biol Chem. 2005;280(11):10807-16. doi: 10.1074/jbc.M410343200.
178. Gewin L, Myers H, Kiyono T, Galloway DA. Identification of a novel telomerase repressor that interacts with the human papillomavirus type-16 E6/E6-AP complex. Genes Dev. 2004;18(18):2269-82. doi: 10.1101/gad.1214704.
179. McMurray HR, McCance DJ. Human papillomavirus type 16 E6 activates TERT gene transcription through induction of c-Myc and release of USF-mediated repression. J Virol. 2003;77(18):9852-61. doi: 10.1128/jvi.77.18.9852-9861.2003.
180. Ronco LV, Karpova AY, Vidal M, Howley PM. Human papillomavirus 16 E6 oncoprotein binds to interferon regulatory factor-3 and inhibits its transcriptional activity. Genes Dev. 1998;12(13):2061-72. doi: 10.1101/gad.12.13.2061.
181. Chiang C, Pauli EK, Biryukov J, Feister KF, Meng M, White EA, Munger K, Howley PM, Meyers C, Gack MU. The Human Papillomavirus E6 Oncoprotein Targets USP15 and TRIM25 To Suppress RIG-I-Mediated Innate Immune Signaling. J Virol. 2018;92(6). doi: 10.1128/JVI.01737-17.
182. Reiser J, Hurst J, Voges M, Krauss P, Munch P, Iftner T, Stubenrauch F. High-risk human papillomaviruses repress constitutive kappa interferon transcription via E6 to prevent pathogen recognition receptor and antiviral-gene expression. J Virol. 2011;85(21):11372-80. doi: 10.1128/JVI.05279-11.
183. Mirabello L, Yeager M, Yu K, Clifford GM, Xiao Y, Zhu B, Cullen M, Boland JF, Wentzensen N, Nelson CW, Raine-Bennett T, Chen Z, Bass S, Song L, Yang Q, Steinberg M, Burdett L, Dean M, Roberson D, Mitchell J, Lorey T, Franceschi S, Castle PE, Walker J, Zuna R, Kreimer AR, Beachler DC, Hildesheim A, Gonzalez P, Porras C, Burk RD, Schiffman M. HPV16 E7 Genetic Conservation Is Critical to Carcinogenesis. Cell. 2017;170(6):1164-74 e6. doi: 10.1016/j.cell.2017.08.001.
184. McLaughlin-Drubin ME, Munger K. The human papillomavirus E7 oncoprotein. Virology. 2009;384(2):335-44. doi: 10.1016/j.virol.2008.10.006.
185. Knapp AA, McManus PM, Bockstall K, Moroianu J. Identification of the nuclear localization and export signals of high risk HPV16 E7 oncoprotein. Virology. 2009;383(1):60-8. doi: 10.1016/j.virol.2008.09.037

10.1016/j.virol.2008.09.037. Epub 2008 Nov 8.
186. Dyson N, Howley PM, Munger K, Harlow E. The human papilloma virus-16 E7 oncoprotein is able to bind to the retinoblastoma gene product. Science. 1989;243(4893):934-7. doi: 10.1126/science.2537532.
187. Munger K, Werness BA, Dyson N, Phelps WC, Harlow E, Howley PM. Complex formation of human papillomavirus E7 proteins with the retinoblastoma tumor suppressor gene product. EMBO J. 1989;8(13):4099-105. doi.

188. Dyson N, Guida P, Munger K, Harlow E. Homologous sequences in adenovirus E1A and human papillomavirus E7 proteins mediate interaction with the same set of cellular proteins. J Virol. 1992;66(12):6893-902. doi.
189. Genovese NJ, Banerjee NS, Broker TR, Chow LT. Casein kinase II motif-dependent phosphorylation of human papillomavirus E7 protein promotes p130 degradation and S-Phase induction in differentiated human keratinocytes. J Virol. 2008;82(10):4862-73. doi: 10.1128/jvi.01202-07.
190. Todorovic B, Hung K, Massimi P, Avvakumov N, Dick FA, Shaw GS, Banks L, Mymryk JS. Conserved region 3 of human papillomavirus 16 E7 contributes to deregulation of the retinoblastoma tumor suppressor. J Virol. 2012;86(24):13313-23. doi: 10.1128/JVI.01637-12.
191. Nor Rashid N, Yusof R, Watson RJ. Disruption of repressive p130-DREAM complexes by human papillomavirus 16 E6/E7 oncoproteins is required for cell-cycle progression in cervical cancer cells. J Gen Virol. 2011;92(Pt 11):2620-7. doi: 10.1099/vir.0.035352-0.
192. James CD, Saini S, Sesay F, Ko K, Felthousen-Rusbasan J, Iness AN, Nulton T, Windle B, Dozmorov MG, Morgan IM, Litovchick L. Restoring the DREAM Complex Inhibits the Proliferation of High-Risk HPV Positive Human Cells. Cancers (Basel). 2021;13(3). doi: 10.3390/cancers13030489.
193. Chien WM, Parker JN, Schmidt-Grimminger DC, Broker TR, Chow LT. Casein kinase II phosphorylation of the human papillomavirus-18 E7 protein is critical for promoting S-phase entry. Cell Growth Differ. 2000;11(8):425-35. doi.
194. Boyer SN, Wazer DE, Band V. E7 protein of human papilloma virus-16 induces degradation of retinoblastoma protein through the ubiquitin-proteasome pathway. Cancer Res. 1996;56(20):4620-4. doi.
195. Huh K, Zhou X, Hayakawa H, Cho JY, Libermann TA, Jin J, Harper JW, Munger K. Human papillomavirus type 16 E7 oncoprotein associates with the cullin 2 ubiquitin ligase complex, which contributes to degradation of the retinoblastoma tumor suppressor. J Virol. 2007;81(18):9737-47. doi: 10.1128/jvi.00881-07.
196. White EA, Sowa ME, Tan MJ, Jeudy S, Hayes SD, Santha S, Munger K, Harper JW, Howley PM. Systematic identification of interactions between host cell proteins and E7 oncoproteins from diverse human papillomaviruses. Proc Natl Acad Sci U S A. 2012;109(5):E260-7. doi: 10.1073/pnas.1116776109.
197. Darnell GA, Schroder WA, Antalis TM, Lambley E, Major L, Gardner J, Birrell G, Cid-Arregui A, Suhrbier A. Human papillomavirus E7 requires the protease calpain to degrade the retinoblastoma protein. J Biol Chem. 2007;282(52):37492-500. doi: 10.1074/jbc.M706860200.
198. Tomita T, Huibregtse JM, Matouschek A. A masked initiation region in retinoblastoma protein regulates its proteasomal degradation. Nat Commun. 2020;11(1):2019. doi: 10.1038/s41467-020-16003-3.
199. Zhang B, Chen W, Roman A. The E7 proteins of low- and high-risk human papillomaviruses share the ability to target the pRB family member p130 for degradation. Proc Natl Acad Sci U S A. 2006;103(2):437-42. doi: 10.1073/pnas.0510012103.
200. Hwang SG, Lee D, Kim J, Seo T, Choe J. Human papillomavirus type 16 E7 binds to E2F1 and activates E2F1-driven transcription in a retinoblastoma protein-independent manner. J Biol Chem. 2002;277(4):2923-30. doi: 10.1074/jbc.M109113200.
201. McLaughlin-Drubin ME, Huh KW, Munger K. Human papillomavirus type 16 E7 oncoprotein associates with E2F6. J Virol. 2008;82(17):8695-705. doi: 10.1128/JVI.00579-08.

202. Nguyen CL, Munger K. Direct association of the HPV16 E7 oncoprotein with cyclin A/CDK2 and cyclin E/CDK2 complexes. Virology. 2008;380(1):21-5. doi: 10.1016/j.virol.2008.07.017.
203. Zerfass-Thome K, Zwerschke W, Mannhardt B, Tindle R, Botz JW, Jansen-Durr P. Inactivation of the cdk inhibitor p27KIP1 by the human papillomavirus type 16 E7 oncoprotein. Oncogene. 1996;13(11):2323-30. doi.
204. Funk JO, Waga S, Harry JB, Espling E, Stillman B, Galloway DA. Inhibition of CDK activity and PCNA-dependent DNA replication by p21 is blocked by interaction with the HPV-16 E7 oncoprotein. Genes Dev. 1997;11(16):2090-100. doi: 10.1101/gad.11.16.2090.
205. Jones DL, Alani RM, Munger K. The human papillomavirus E7 oncoprotein can uncouple cellular differentiation and proliferation in human keratinocytes by abrogating p21Cip1-mediated inhibition of cdk2. Genes Dev. 1997;11(16):2101-11. doi: 10.1101/gad.11.16.2101.
206. White EA, Munger K, Howley PM. High-Risk Human Papillomavirus E7 Proteins Target PTPN14 for Degradation. mBio. 2016;7(5). doi: 10.1128/mBio.01530-16.
207. Szalmas A, Tomaic V, Basukala O, Massimi P, Mittal S, Konya J, Banks L. The PTPN14 Tumor Suppressor Is a Degradation Target of Human Papillomavirus E7. J Virol. 2017;91(7). doi: 10.1128/JVI.00057-17.
208. Hatterschide J, Bohidar AE, Grace M, Nulton TJ, Kim HW, Windle B, Morgan IM, Munger K, White EA. PTPN14 degradation by high-risk human papillomavirus E7 limits keratinocyte differentiation and contributes to HPV-mediated oncogenesis. Proc Natl Acad Sci U S A. 2019;116(14):7033-42. doi: 10.1073/pnas.1819534116.
209. Yun HY, Kim MW, Lee HS, Kim W, Shin JH, Kim H, Shin HC, Park H, Oh BH, Kim WK, Bae KH, Lee SC, Lee EW, Ku B, Kim SJ. Structural basis for recognition of the tumor suppressor protein PTPN14 by the oncoprotein E7 of human papillomavirus. PLoS Biol. 2019;17(7):e3000367. doi: 10.1371/journal.pbio.3000367.
210. Melar-New M, Laimins LA. Human papillomaviruses modulate expression of microRNA 203 upon epithelial differentiation to control levels of p63 proteins. J Virol. 2010;84(10):5212-21. doi: 10.1128/JVI.00078-10.
211. James CD, Fontan CT, Otoa R, Das D, Prabhakar AT, Wang X, Bristol ML, Morgan IM. Human Papillomavirus 16 E6 and E7 Synergistically Repress Innate Immune Gene Transcription. mSphere. 2020;5(1). doi: 10.1128/mSphere.00828-19.
212. Lau L, Gray EE, Brunette RL, Stetson DB. DNA tumor virus oncogenes antagonize the cGAS-STING DNA-sensing pathway. Science. 2015;350(6260):568-71. doi: 10.1126/science.aab3291.
213. Lo Cigno I, Calati F, Borgogna C, Zevini A, Albertini S, Martuscelli L, De Andrea M, Hiscott J, Landolfo S, Gariglio M. Human Papillomavirus E7 Oncoprotein Subverts Host Innate Immunity via SUV39H1-Mediated Epigenetic Silencing of Immune Sensor Genes. J Virol. 2020;94(4). doi: 10.1128/JVI.01812-19.
214. Wu L, Cao J, Cai WL, Lang SM, Horton JR, Jansen DJ, Liu ZZ, Chen JF, Zhang M, Mott BT, Pohida K, Rai G, Kales SC, Henderson MJ, Hu X, Jadhav A, Maloney DJ, Simeonov A, Zhu S, Iwasaki A, Hall MD, Cheng X, Shadel GS, Yan Q. KDM5 histone demethylases repress immune response via suppression of STING. PLoS Biol. 2018;16(8):e2006134. doi: 10.1371/journal.pbio.2006134.
215. Hasan UA, Zannetti C, Parroche P, Goutagny N, Malfroy M, Roblot G, Carreira C, Hussain I, Muller M, Taylor-Papadimitriou J, Picard D, Sylla BS,

Trinchieri G, Medzhitov R, Tommasino M. The human papillomavirus type 16 E7 oncoprotein induces a transcriptional repressor complex on the Toll-like receptor 9 promoter. J Exp Med. 2013;210(7):1369-87. doi: 10.1084/jem.20122394.
216. Barnard P, McMillan NA. The human papillomavirus E7 oncoprotein abrogates signaling mediated by interferon-alpha. Virology. 1999;259(2):305-13. doi: 10.1006/viro.1999.9771.
217. Bergot AS, Ford N, Leggatt GR, Wells JW, Frazer IH, Grimbaldeston MA. HPV16-E7 expression in squamous epithelium creates a local immune suppressive environment via CCL2- and CCL5- mediated recruitment of mast cells. PLoS Pathog. 2014;10(10):e1004466. doi: 10.1371/journal.ppat.1004466.
218. Cicchini L, Westrich JA, Xu T, Vermeer DW, Berger JN, Clambey ET, Lee D, Song JI, Lambert PF, Greer RO, Lee JH, Pyeon D. Suppression of Antitumor Immune Responses by Human Papillomavirus through Epigenetic Downregulation of CXCL14. mBio. 2016;7(3). doi: 10.1128/mBio.00270-16.
219. Bottley G, Watherston OG, Hiew YL, Norrild B, Cook GP, Blair GE. High-risk human papillomavirus E7 expression reduces cell-surface MHC class I molecules and increases susceptibility to natural killer cells. Oncogene. 2008;27(12):1794-9. doi: 10.1038/sj.onc.1210798.
220. Wang HK, Duffy AA, Broker TR, Chow LT. Robust production and passaging of infectious HPV in squamous epithelium of primary human keratinocytes. Genes Dev. 2009;23(2):181-94. doi: 10.1101/gad.1735109.
221. Banerjee NS, Wang HK, Broker TR, Chow LT. Human papillomavirus (HPV) E7 induces prolonged G2 following S phase reentry in differentiated human keratinocytes. J Biol Chem. 2011;286(17):15473-82. doi: 10.1074/jbc.M110.197574.
222. Moody CA, Laimins LA. Human papillomaviruses activate the ATM DNA damage pathway for viral genome amplification upon differentiation. PLoS Pathog. 2009;5(10):e1000605. doi: 10.1371/journal.ppat.1000605.
223. Hong S, Cheng S, Iovane A, Laimins LA. STAT-5 Regulates Transcription of the Topoisomerase IIbeta-Binding Protein 1 (TopBP1) Gene To Activate the ATR Pathway and Promote Human Papillomavirus Replication. MBio. 2015;6(6):e02006-15. doi: 10.1128/mBio.02006-15.
224. Bester AC, Roniger M, Oren YS, Im MM, Sarni D, Chaoat M, Bensimon A, Zamir G, Shewach DS, Kerem B. Nucleotide deficiency promotes genomic instability in early stages of cancer development. Cell. 2011;145(3):435-46. doi: 10.1016/j.cell.2011.03.044.
225. Moody CA. Impact of Replication Stress in Human Papillomavirus Pathogenesis. J Virol. 2019;93(2). doi: 10.1128/JVI.01012-17.
226. Hong S, Laimins LA. The JAK-STAT transcriptional regulator, STAT-5, activates the ATM DNA damage pathway to induce HPV 31 genome amplification upon epithelial differentiation. PLoS Pathog. 2013;9(4):e1003295. doi: 10.1371/journal.ppat.1003295.
227. Hong S, Dutta A, Laimins LA. The acetyltransferase Tip60 is a critical regulator of the differentiation-dependent amplification of human papillomaviruses. J Virol. 2015;89(8):4668-75. doi: 10.1128/JVI.03455-14.
228. Anacker DC, Aloor HL, Shepard CN, Lenzi GM, Johnson BA, Kim B, Moody CA. HPV31 utilizes the ATR-Chk1 pathway to maintain elevated RRM2 levels and a replication-competent environment in differentiating Keratinocytes. Virology. 2016;499:383-96. doi: 10.1016/j.virol.2016.09.028.
229. Mehta K, Laimins L. Human Papillomaviruses Preferentially Recruit DNA Repair Factors to Viral Genomes for Rapid Repair and Amplification. mBio. 2018;9(1). doi: 10.1128/mBio.00064-18.

230. Gillespie KA, Mehta KP, Laimins LA, Moody CA. Human papillomaviruses recruit cellular DNA repair and homologous recombination factors to viral replication centers. J Virol. 2012;86(17):9520-6. doi: 10.1128/JVI.00247-12.
231. Gonzalez C, Baez-Nieto D, Valencia I, Oyarzun I, Rojas P, Naranjo D, Latorre R. K(+) channels: function-structural overview. Compr Physiol. 2012;2(3):2087-149. doi: 10.1002/cphy.c110047.
232. Wei AD, Gutman GA, Aldrich R, Chandy KG, Grissmer S, Wulff H. International Union of Pharmacology. LII. Nomenclature and molecular relationships of calcium-activated potassium channels. Pharmacol Rev. 2005;57(4):463-72. doi: 10.1124/pr.57.4.9.
233. Heginbotham L, Lu Z, Abramson T, MacKinnon R. Mutations in the K+ channel signature sequence. Biophys J. 1994;66(4):1061-7. doi: 10.1016/s0006-3495(94)80887-2.
234. Clement IV JP, Kunjilwar K, Gonzalez G, Schwanstecher M, Panten U, Aguilar-Bryan L, Bryan J. Association and stoichiometry of K(ATP) channel subunits. Neuron. 1997;18(5):827-38. doi: 10.1016/s0896-6273(00)80321-9.
235. Shyng S, Nichols CG. Octameric stoichiometry of the KATP channel complex. J Gen Physiol. 1997;110(6):655-64. doi: 10.1085/jgp.110.6.655.
236. Tinker A, Aziz Q, Li Y, Specterman M. ATP-Sensitive Potassium Channels and Their Physiological and Pathophysiological Roles. Compr Physiol. 2018;8(4):1463-511. doi: 10.1002/cphy.c170048

10.1002/cphy.c170048.
237. Isomoto S, Kondo C, Yamada M, Matsumoto S, Higashiguchi O, Horio Y, Matsuzawa Y, Kurachi Y. A novel sulfonylurea receptor forms with BIR (Kir6.2) a smooth muscle type ATP-sensitive K+ channel. J Biol Chem. 1996;271(40):24321-4. doi: 10.1074/jbc.271.40.24321.
238. Paggio A, Checchetto V, Campo A, Menabo R, Di Marco G, Di Lisa F, Szabo I, Rizzuto R, De Stefani D. Identification of an ATP-sensitive potassium channel in mitochondria. Nature. 2019;572(7771):609-13. doi: 10.1038/s41586-019-1498-3.
239. Inagaki N, Tsuura Y, Namba N, Masuda K, Gonoi T, Horie M, Seino Y, Mizuta M, Seino S. Cloning and functional characterization of a novel ATP-sensitive potassium channel ubiquitously expressed in rat tissues, including pancreatic islets, pituitary, skeletal muscle, and heart. J Biol Chem. 1995;270(11):5691-4. doi: 10.1074/jbc.270.11.5691.
240. Inagaki N, Gonoi T, Clement JPt, Namba N, Inazawa J, Gonzalez G, Aguilar-Bryan L, Seino S, Bryan J. Reconstitution of IKATP: an inward rectifier subunit plus the sulfonylurea receptor. Science. 1995;270(5239):1166-70. doi.
241. Tusnady GE, Bakos E, Varadi A, Sarkadi B. Membrane topology distinguishes a subfamily of the ATP-binding cassette (ABC) transporters. FEBS Lett. 1997;402(1):1-3. doi: 10.1016/s0014-5793(96)01478-0.
242. Sakura H, Ammala C, Smith PA, Gribble FM, Ashcroft FM. Cloning and functional expression of the cDNA encoding a novel ATP-sensitive potassium channel subunit expressed in pancreatic beta-cells, brain, heart and skeletal muscle. FEBS Lett. 1995;377(3):338-44. doi: 10.1016/0014-5793(95)01369-5.
243. Martin GM, Yoshioka C, Rex EA, Fay JF, Xie Q, Whorton MR, Chen JZ, Shyng SL. Cryo-EM structure of the ATP-sensitive potassium channel illuminates mechanisms of assembly and gating. Elife. 2017;6. doi: 10.7554/eLife.24149.
244. Li N, Wu JX, Ding D, Cheng J, Gao N, Chen L. Structure of a Pancreatic ATP-Sensitive Potassium Channel. Cell. 2017;168(1-2):101-10 e10. doi: 10.1016/j.cell.2016.12.028.

245. Martin GM, Kandasamy B, DiMaio F, Yoshioka C, Shyng SL. Anti-diabetic drug binding site in a mammalian KATP channel revealed by Cryo-EM. Elife. 2017;6. doi: 10.7554/eLife.31054.
246. Lee KPK, Chen J, MacKinnon R. Molecular structure of human KATP in complex with ATP and ADP. Elife. 2017;6. doi: 10.7554/eLife.32481.
247. Wu JX, Ding D, Wang M, Kang Y, Zeng X, Chen L. Ligand binding and conformational changes of SUR1 subunit in pancreatic ATP-sensitive potassium channels. Protein Cell. 2018;9(6):553-67. doi: 10.1007/s13238-018-0530-y.
248. Ding D, Wang M, Wu JX, Kang Y, Chen L. The Structural Basis for the Binding of Repaglinide to the Pancreatic KATP Channel. Cell Rep. 2019;27(6):1848-57 e4. doi: 10.1016/j.celrep.2019.04.050.
249. Martin GM, Sung MW, Yang Z, Innes LM, Kandasamy B, David LL, Yoshioka C, Shyng SL. Mechanism of pharmacochaperoning in a mammalian KATP channel revealed by cryo-EM. Elife. 2019;8. doi: 10.7554/eLife.46417.
250. Zhao C, MacKinnon R. Molecular structure of an open human KATP channel. Proc Natl Acad Sci U S A. 2021;118(48). doi: 10.1073/pnas.2112267118.
251. Wang M, Wu JX, Ding D, Chen L. Structural insights into the mechanism of pancreatic KATP channel regulation by nucleotides. Nat Commun. 2022;13(1):2770. doi: 10.1038/s41467-022-30430-4.
252. Zhao G, Kaplan A, Greiser M, Lederer WJ. The surprising complexity of KATP channel biology and of genetic diseases. J Clin Invest. 2020;130(3):1112-5. doi: 10.1172/JCI135759.
253. Ashfield R, Ashcroft SJ. Cloning of the promoters for the beta-cell ATP-sensitive K-channel subunits Kir6.2 and SUR1. Diabetes. 1998;47(8):1274-80. doi: 10.2337/diab.47.8.1274

10.2337/diab.47.8.1274.
254. Hernandez-Sanchez C, Ito Y, Ferrer J, Reitman M, LeRoith D. Characterization of the mouse sulfonylurea receptor 1 promoter and its regulation. J Biol Chem. 1999;274(26):18261-70. doi: 10.1074/jbc.274.26.18261.
255. Kim JW, Seghers V, Cho JH, Kang Y, Kim S, Ryu Y, Baek K, Aguilar-Bryan L, Lee YD, Bryan J, Suh-Kim H. Transactivation of the mouse sulfonylurea receptor I gene by BETA2/NeuroD. Mol Endocrinol. 2002;16(5):1097-107. doi: 10.1210/mend.16.5.0934.
256. Wang H, Gauthier BR, Hagenfeldt-Johansson KA, Iezzi M, Wollheim CB. Foxa2 (HNF3beta) controls multiple genes implicated in metabolism-secretion coupling of glucose-induced insulin release. J Biol Chem. 2002;277(20):17564-70. doi: 10.1074/jbc.M111037200.
257. Woo SK, Kwon MS, Geng Z, Chen Z, Ivanov A, Bhatta S, Gerzanich V, Simard JM. Sequential activation of hypoxia-inducible factor 1 and specificity protein 1 is required for hypoxia-induced transcriptional stimulation of Abcc8. J Cereb Blood Flow Metab. 2012;32(3):525-36. doi: 10.1038/jcbfm.2011.159.
258. Philip-Couderc P, Tavares NI, Roatti A, Lerch R, Montessuit C, Baertschi AJ. Forkhead transcription factors coordinate expression of myocardial KATP channel subunits and energy metabolism. Circ Res. 2008;102(2):e20-35. doi: 10.1161/CIRCRESAHA.107.166744.
259. Zerangue N, Schwappach B, Jan YN, Jan LY. A new ER trafficking signal regulates the subunit stoichiometry of plasma membrane K(ATP) channels. Neuron. 1999;22(3):537-48. doi.

260. Yuan H, Michelsen K, Schwappach B. 14-3-3 dimers probe the assembly status of multimeric membrane proteins. Curr Biol. 2003;13(8):638-46. doi: 10.1016/s0960-9822(03)00208-2.
261. Tucker SJ, Gribble FM, Zhao C, Trapp S, Ashcroft FM. Truncation of Kir6.2 produces ATP-sensitive K+ channels in the absence of the sulphonylurea receptor. Nature. 1997;387(6629):179-83. doi: 10.1038/387179a0.
262. Heusser K, Yuan H, Neagoe I, Tarasov AI, Ashcroft FM, Schwappach B. Scavenging of 14-3-3 proteins reveals their involvement in the cell-surface transport of ATP-sensitive K+ channels. J Cell Sci. 2006;119(Pt 20):4353-63. doi: 10.1242/jcs.03196.
263. Smith AJ, Daut J, Schwappach B. Membrane proteins as 14-3-3 clients in functional regulation and intracellular transport. Physiology (Bethesda). 2011;26(3):181-91. doi: 10.1152/physiol.00042.2010.
264. Arakel EC, Brandenburg S, Uchida K, Zhang H, Lin YW, Kohl T, Schrul B, Sulkin MS, Efimov IR, Nichols CG, Lehnart SE, Schwappach B. Tuning the electrical properties of the heart by differential trafficking of KATP ion channel complexes. J Cell Sci. 2014;127(Pt 9):2106-19. doi: 10.1242/jcs.141440.
265. Yan FF, Pratt EB, Chen PC, Wang F, Skach WR, David LL, Shyng SL. Role of Hsp90 in biogenesis of the beta-cell ATP-sensitive potassium channel complex. Mol Biol Cell. 2010;21(12):1945-54. doi: 10.1091/mbc.E10-02-0116.
266. Wang F, Olson EM, Shyng SL. Role of Derlin-1 protein in proteostasis regulation of ATP-sensitive potassium channels. J Biol Chem. 2012;287(13):10482-93. doi: 10.1074/jbc.M111.312223.
267. Trapp S, Haider S, Jones P, Sansom MS, Ashcroft FM. Identification of residues contributing to the ATP binding site of Kir6.2. Embo j. 2003;22(12):2903-12. doi: 10.1093/emboj/cdg282

10.1093/emboj/cdg282.
268. Gribble FM, Tucker SJ, Haug T, Ashcroft FM. MgATP activates the beta cell KATP channel by interaction with its SUR1 subunit. Proc Natl Acad Sci U S A. 1998;95(12):7185-90. doi: 10.1073/pnas.95.12.7185.
269. Markworth E, Schwanstecher C, Schwanstecher M. ATP4- mediates closure of pancreatic beta-cell ATP-sensitive potassium channels by interaction with 1 of 4 identical sites. Diabetes. 2000;49(9):1413-8. doi: 10.2337/diabetes.49.9.1413

10.2337/diabetes.49.9.1413.
270. Usher SG, Ashcroft FM, Puljung MC. Nucleotide inhibition of the pancreatic ATP-sensitive K+ channel explored with patch-clamp fluorometry. Elife. 2020;9. doi: 10.7554/eLife.52775.
271. Nichols CG, Shyng SL, Nestorowicz A, Glaser B, Clement JPt, Gonzalez G, Aguilar-Bryan L, Permutt MA, Bryan J. Adenosine diphosphate as an intracellular regulator of insulin secretion. Science. 1996;272(5269):1785-7. doi: 10.1126/science.272.5269.1785.
272. Dunne MJ, Petersen OH. Intracellular ADP activates K+ channels that are inhibited by ATP in an insulin-secreting cell line. FEBS Lett. 1986;208(1):59-62. doi: 10.1016/0014-5793(86)81532-0.
273. Ashcroft FM, Kakei M. ATP-sensitive K+ channels in rat pancreatic beta-cells: modulation by ATP and Mg2+ ions. J Physiol. 1989;416:349-67. doi: 10.1113/jphysiol.1989.sp017765.
274. Gribble FM, Tucker SJ, Ashcroft FM. The essential role of the Walker A motifs of SUR1 in K-ATP channel activation by Mg-ADP and diazoxide. Embo j. 1997;16(6):1145-52. doi: 10.1093/emboj/16.6.1145

10.1093/emboj/16.6.1145.
275. Shyng S, Ferrigni T, Nichols CG. Regulation of KATP channel activity by diazoxide and MgADP. Distinct functions of the two nucleotide binding folds of the sulfonylurea receptor. J Gen Physiol. 1997;110(6):643-54. doi: 10.1085/jgp.110.6.643.
276. Proks P, de Wet H, Ashcroft FM. Activation of the K(ATP) channel by Mg-nucleotide interaction with SUR1. J Gen Physiol. 2010;136(4):389-405. doi: 10.1085/jgp.201010475.
277. Vedovato N, Ashcroft FM, Puljung MC. The Nucleotide-Binding Sites of SUR1: A Mechanistic Model. Biophys J. 2015;109(12):2452-60. doi: 10.1016/j.bpj.2015.10.026.
278. Puljung M, Vedovato N, Usher S, Ashcroft F. Activation mechanism of ATP-sensitive K(+) channels explored with real-time nucleotide binding. Elife. 2019;8. doi: 10.7554/eLife.41103.
279. Baukrowitz T, Schulte U, Oliver D, Herlitze S, Krauter T, Tucker SJ, Ruppersberg JP, Fakler B. PIP2 and PIP as determinants for ATP inhibition of KATP channels. Science. 1998;282(5391):1141-4. doi: 10.1126/science.282.5391.1141

10.1126/science.282.5391.1141.
280. Shyng SL, Cukras CA, Harwood J, Nichols CG. Structural determinants of PIP(2) regulation of inward rectifier K(ATP) channels. J Gen Physiol. 2000;116(5):599-608. doi: 10.1085/jgp.116.5.599

10.1085/jgp.116.5.599.
281. Hille B, Dickson EJ, Kruse M, Vivas O, Suh BC. Phosphoinositides regulate ion channels. Biochim Biophys Acta. 2015;1851(6):844-56. doi: 10.1016/j.bbalip.2014.09.010

10.1016/j.bbalip.2014.09.010. Epub 2014 Sep 18.
282. Yang HQ, Martinez-Ortiz W, Hwang J, Fan X, Cardozo TJ, Coetzee WA. Palmitoylation of the KATP channel Kir6.2 subunit promotes channel opening by regulating PIP2 sensitivity. Proc Natl Acad Sci U S A. 2020;117(19):10593-602. doi: 10.1073/pnas.1918088117.
283. Quayle JM, Bonev AD, Brayden JE, Nelson MT. Calcitonin gene-related peptide activated ATP-sensitive K+ currents in rabbit arterial smooth muscle via protein kinase A. J Physiol. 1994;475(1):9-13. doi: 10.1113/jphysiol.1994.sp020045.
284. Wellman GC, Quayle JM, Standen NB. ATP-sensitive K+ channel activation by calcitonin gene-related peptide and protein kinase A in pig coronary arterial smooth muscle. J Physiol. 1998;507 (Pt 1):117-29. doi: 10.1111/j.1469-7793.1998.117bu.x.
285. Quinn KV, Giblin JP, Tinker A. Multisite phosphorylation mechanism for protein kinase A activation of the smooth muscle ATP-sensitive K+ channel. Circ Res. 2004;94(10):1359-66. doi: 10.1161/01.RES.0000128513.34817.c4.
286. Shi Y, Wu Z, Cui N, Shi W, Yang Y, Zhang X, Rojas A, Ha BT, Jiang C. PKA phosphorylation of SUR2B subunit underscores vascular KATP channel activation by beta-adrenergic receptors. Am J Physiol Regul Integr Comp Physiol. 2007;293(3):R1205-14. doi: 10.1152/ajpregu.00337.2007.
287. Beguin P, Nagashima K, Nishimura M, Gonoi T, Seino S. PKA-mediated phosphorylation of the human K(ATP) channel: separate roles of Kir6.2 and SUR1 subunit phosphorylation. EMBO J. 1999;18(17):4722-32. doi: 10.1093/emboj/18.17.4722.

288. Lin YF, Jan YN, Jan LY. Regulation of ATP-sensitive potassium channel function by protein kinase A-mediated phosphorylation in transfected HEK293 cells. EMBO J. 2000;19(5):942-55. doi: 10.1093/emboj/19.5.942.
289. Bonev AD, Nelson MT. Vasoconstrictors inhibit ATP-sensitive K+ channels in arterial smooth muscle through protein kinase C. J Gen Physiol. 1996;108(4):315-23. doi: 10.1085/jgp.108.4.315.
290. Shi Y, Cui N, Shi W, Jiang C. A short motif in Kir6.1 consisting of four phosphorylation repeats underlies the vascular KATP channel inhibition by protein kinase C. J Biol Chem. 2008;283(5):2488-94. doi: 10.1074/jbc.M708769200.
291. Jiao J, Garg V, Yang B, Elton TS, Hu K. Protein kinase C-epsilon induces caveolin-dependent internalization of vascular adenosine 5'-triphosphate-sensitive K+ channels. Hypertension. 2008;52(3):499-506. doi: 10.1161/HYPERTENSIONAHA.108.110817.
292. Hu K, Duan D, Li GR, Nattel S. Protein kinase C activates ATP-sensitive K+ current in human and rabbit ventricular myocytes. Circ Res. 1996;78(3):492-8. doi: 10.1161/01.res.78.3.492.
293. Light PE, Bladen C, Winkfein RJ, Walsh MP, French RJ. Molecular basis of protein kinase C-induced activation of ATP-sensitive potassium channels. Proc Natl Acad Sci U S A. 2000;97(16):9058-63. doi: 10.1073/pnas.160068997.
294. Hu K, Huang CS, Jan YN, Jan LY. ATP-sensitive potassium channel traffic regulation by adenosine and protein kinase C. Neuron. 2003;38(3):417-32. doi: 10.1016/s0896-6273(03)00256-3.
295. Sola D, Rossi L, Schianca GP, Maffioli P, Bigliocca M, Mella R, Corliano F, Fra GP, Bartoli E, Derosa G. Sulfonylureas and their use in clinical practice. Arch Med Sci. 2015;11(4):840-8. doi: 10.5114/aoms.2015.53304.
296. Sturgess NC, Ashford ML, Cook DL, Hales CN. The sulphonylurea receptor may be an ATP-sensitive potassium channel. Lancet. 1985;2(8453):474-5. doi: 10.1016/s0140-6736(85)90403-9.
297. Puljung MC. Cryo-electron microscopy structures and progress toward a dynamic understanding of KATP channels. J Gen Physiol. 2018;150(5):653-69. doi: 10.1085/jgp.201711978.
298. Ashcroft SJ, Ashcroft FM. Properties and functions of ATP-sensitive K-channels. Cell Signal. 1990;2(3):197-214. doi: 10.1016/0898-6568(90)90048-f.
299. Babenko AP, Gonzalez G, Bryan J. Pharmaco-topology of sulfonylurea receptors. Separate domains of the regulatory subunits of K(ATP) channel isoforms are required for selective interaction with K(+) channel openers. J Biol Chem. 2000;275(2):717-20. doi: 10.1074/jbc.275.2.717.
300. Merrins MJ, Corkey BE, Kibbey RG, Prentki M. Metabolic cycles and signals for insulin secretion. Cell Metab. 2022. doi: 10.1016/j.cmet.2022.06.003.
301. Lewandowski SL, Cardone RL, Foster HR, Ho T, Potapenko E, Poudel C, VanDeusen HR, Sdao SM, Alves TC, Zhao X, Capozzi ME, de Souza AH, Jahan I, Thomas CJ, Nunemaker CS, Davis DB, Campbell JE, Kibbey RG, Merrins MJ. Pyruvate Kinase Controls Signal Strength in the Insulin Secretory Pathway. Cell Metab. 2020;32(5):736-50 e5. doi: 10.1016/j.cmet.2020.10.007.
302. Rorsman P, Ramracheya R, Rorsman NJ, Zhang Q. ATP-regulated potassium channels and voltage-gated calcium channels in pancreatic alpha and beta cells: similar functions but reciprocal effects on secretion. Diabetologia. 2014;57(9):1749-61. doi: 10.1007/s00125-014-3279-8.
303. Flagg TP, Kurata HT, Masia R, Caputa G, Magnuson MA, Lefer DJ, Coetzee WA, Nichols CG. Differential structure of atrial and ventricular KATP:

atrial KATP channels require SUR1. Circ Res. 2008;103(12):1458-65. doi: 10.1161/CIRCRESAHA.108.178186.
304. Zingman LV, Hodgson DM, Bast PH, Kane GC, Perez-Terzic C, Gumina RJ, Pucar D, Bienengraeber M, Dzeja PP, Miki T, Seino S, Alekseev AE, Terzic A. Kir6.2 is required for adaptation to stress. Proc Natl Acad Sci U S A. 2002;99(20):13278-83. doi: 10.1073/pnas.212315199.
305. Du Q, Jovanovic S, Clelland A, Sukhodub A, Budas G, Phelan K, Murray-Tait V, Malone L, Jovanovic A. Overexpression of SUR2A generates a cardiac phenotype resistant to ischemia. FASEB J. 2006;20(8):1131-41. doi: 10.1096/fj.05-5483com.
306. Miki T, Suzuki M, Shibasaki T, Uemura H, Sato T, Yamaguchi K, Koseki H, Iwanaga T, Nakaya H, Seino S. Mouse model of Prinzmetal angina by disruption of the inward rectifier Kir6.1. Nat Med. 2002;8(5):466-72. doi: 10.1038/nm0502-466.
307. Chutkow WA, Pu J, Wheeler MT, Wada T, Makielski JC, Burant CF, McNally EM. Episodic coronary artery vasospasm and hypertension develop in the absence of Sur2 K(ATP) channels. J Clin Invest. 2002;110(2):203-8. doi: 10.1172/JCI15672.
308. Pipatpolkai T, Usher S, Stansfeld PJ, Ashcroft FM. New insights into KATP channel gene mutations and neonatal diabetes mellitus. Nat Rev Endocrinol. 2020;16(7):378-93. doi: 10.1038/s41574-020-0351-y.
309. Arnoux JB, Verkarre V, Saint-Martin C, Montravers F, Brassier A, Valayannopoulos V, Brunelle F, Fournet JC, Robert JJ, Aigrain Y, Bellanne-Chantelot C, de Lonlay P. Congenital hyperinsulinism: current trends in diagnosis and therapy. Orphanet J Rare Dis. 2011;6:63. doi: 10.1186/1750-1172-6-63.
310. Shyng SL, Ferrigni T, Shepard JB, Nestorowicz A, Glaser B, Permutt MA, Nichols CG. Functional analyses of novel mutations in the sulfonylurea receptor 1 associated with persistent hyperinsulinemic hypoglycemia of infancy. Diabetes. 1998;47(7):1145-51. doi: 10.2337/diabetes.47.7.1145.
311. Martin GM, Sung MW, Shyng SL. Pharmacological chaperones of ATP-sensitive potassium channels: Mechanistic insight from cryoEM structures. Mol Cell Endocrinol. 2020;502:110667. doi: 10.1016/j.mce.2019.110667.
312. Gloyn AL, Pearson ER, Antcliff JF, Proks P, Bruining GJ, Slingerland AS, Howard N, Srinivasan S, Silva JM, Molnes J, Edghill EL, Frayling TM, Temple IK, Mackay D, Shield JP, Sumnik Z, van Rhijn A, Wales JK, Clark P, Gorman S, Aisenberg J, Ellard S, Njolstad PR, Ashcroft FM, Hattersley AT. Activating mutations in the gene encoding the ATP-sensitive potassium-channel subunit Kir6.2 and permanent neonatal diabetes. N Engl J Med. 2004;350(18):1838-49. doi: 10.1056/NEJMoa032922

10.1056/NEJMoa032922.
313. Babenko AP, Polak M, Cave H, Busiah K, Czernichow P, Scharfmann R, Bryan J, Aguilar-Bryan L, Vaxillaire M, Froguel P. Activating mutations in the ABCC8 gene in neonatal diabetes mellitus. N Engl J Med. 2006;355(5):456-66. doi: 10.1056/NEJMoa055068

10.1056/NEJMoa055068.
314. Ashcroft FM, Puljung MC, Vedovato N. Neonatal Diabetes and the KATP Channel: From Mutation to Therapy. Trends Endocrinol Metab. 2017;28(5):377-87. doi: 10.1016/j.tem.2017.02.003.
315. Gloyn AL, Weedon MN, Owen KR, Turner MJ, Knight BA, Hitman G, Walker M, Levy JC, Sampson M, Halford S, McCarthy MI, Hattersley AT, Frayling TM. Large-scale association studies of variants in genes encoding the pancreatic

beta-cell KATP channel subunits Kir6.2 (KCNJ11) and SUR1 (ABCC8) confirm that the KCNJ11 E23K variant is associated with type 2 diabetes. Diabetes. 2003;52(2):568-72. doi: 10.2337/diabetes.52.2.568.
316. Cantu JM, Garcia-Cruz D, Sanchez-Corona J, Hernandez A, Nazara Z. A distinct osteochondrodysplasia with hypertrichosis- Individualization of a probable autosomal recessive entity. Hum Genet. 1982;60(1):36-41. doi: 10.1007/BF00281261.
317. Harakalova M, van Harssel JJ, Terhal PA, van Lieshout S, Duran K, Renkens I, Amor DJ, Wilson LC, Kirk EP, Turner CL, Shears D, Garcia-Minaur S, Lees MM, Ross A, Venselaar H, Vriend G, Takanari H, Rook MB, van der Heyden MA, Asselbergs FW, Breur HM, Swinkels ME, Scurr IJ, Smithson SF, Knoers NV, van der Smagt JJ, Nijman IJ, Kloosterman WP, van Haelst MM, van Haaften G, Cuppen E. Dominant missense mutations in ABCC9 cause Cantu syndrome. Nat Genet. 2012;44(7):793-6. doi: 10.1038/ng.2324.
318. van Bon BW, Gilissen C, Grange DK, Hennekam RC, Kayserili H, Engels H, Reutter H, Ostergaard JR, Morava E, Tsiakas K, Isidor B, Le Merrer M, Eser M, Wieskamp N, de Vries P, Steehouwer M, Veltman JA, Robertson SP, Brunner HG, de Vries BB, Hoischen A. Cantu syndrome is caused by mutations in ABCC9. Am J Hum Genet. 2012;90(6):1094-101. doi: 10.1016/j.ajhg.2012.04.014.
319. Brownstein CA, Towne MC, Luquette LJ, Harris DJ, Marinakis NS, Meinecke P, Kutsche K, Campeau PM, Yu TW, Margulies DM, Agrawal PB, Beggs AH. Mutation of KCNJ8 in a patient with Cantu syndrome with unique vascular abnormalities - support for the role of K(ATP) channels in this condition. Eur J Med Genet. 2013;56(12):678-82. doi: 10.1016/j.ejmg.2013.09.009.
320. Cooper PE, Reutter H, Woelfle J, Engels H, Grange DK, van Haaften G, van Bon BW, Hoischen A, Nichols CG. Cantu syndrome resulting from activating mutation in the KCNJ8 gene. Hum Mutat. 2014;35(7):809-13. doi: 10.1002/humu.22555.
321. Grange DK, Roessler HI, McClenaghan C, Duran K, Shields K, Remedi MS, Knoers N, Lee JM, Kirk EP, Scurr I, Smithson SF, Singh GK, van Haelst MM, Nichols CG, van Haaften G. Cantu syndrome: Findings from 74 patients in the International Cantu Syndrome Registry. Am J Med Genet C Semin Med Genet. 2019;181(4):658-81. doi: 10.1002/ajmg.c.31753.
322. McClenaghan C, Huang Y, Yan Z, Harter TM, Halabi CM, Chalk R, Kovacs A, van Haaften G, Remedi MS, Nichols CG. Glibenclamide reverses cardiovascular abnormalities of Cantu syndrome driven by KATP channel overactivity. J Clin Invest. 2020;130(3):1116-21. doi: 10.1172/JCI130571.
323. Lang F, Foller M, Lang KS, Lang PA, Ritter M, Gulbins E, Vereninov A, Huber SM. Ion channels in cell proliferation and apoptotic cell death. J Membr Biol. 2005;205(3):147-57. doi: 10.1007/s00232-005-0780-5.
324. Blackiston DJ, McLaughlin KA, Levin M. Bioelectric controls of cell proliferation: ion channels, membrane voltage and the cell cycle. Cell Cycle. 2009;8(21):3527-36. doi: 10.4161/cc.8.21.9888.
325. Urrego D, Tomczak AP, Zahed F, Stuhmer W, Pardo LA. Potassium channels in cell cycle and cell proliferation. Philos Trans R Soc Lond B Biol Sci. 2014;369(1638):20130094. doi: 10.1098/rstb.2013.0094.
326. Prevarskaya N, Skryma R, Shuba Y. Ion Channels in Cancer: Are Cancer Hallmarks Oncochannelopathies? Physiol Rev. 2018;98(2):559-621. doi: 10.1152/physrev.00044.2016.
327. Santos R, Ursu O, Gaulton A, Bento AP, Donadi RS, Bologa CG, Karlsson A, Al-Lazikani B, Hersey A, Oprea TI, Overington JP. A comprehensive map of

molecular drug targets. Nat Rev Drug Discov. 2017;16(1):19-34. doi: 10.1038/nrd.2016.230.
328. Qian X, Li J, Ding J, Wang Z, Duan L, Hu G. Glibenclamide exerts an antitumor activity through reactive oxygen species-c-jun NH2-terminal kinase pathway in human gastric cancer cell line MGC-803. Biochem Pharmacol. 2008;76(12):1705-15. doi: 10.1016/j.bcp.2008.09.009.
329. Nunez M, Medina V, Cricco G, Croci M, Cocca C, Rivera E, Bergoc R, Martin G. Glibenclamide inhibits cell growth by inducing G0/G1 arrest in the human breast cancer cell line MDA-MB-231. BMC Pharmacol Toxicol. 2013;14:6. doi: 10.1186/2050-6511-14-6.
330. Ru Q, Tian X, Wu YX, Wu RH, Pi MS, Li CY. Voltage-gated and ATP-sensitive K+ channels are associated with cell proliferation and tumorigenesis of human glioma. Oncol Rep. 2014;31(2):842-8. doi: 10.3892/or.2013.2875.
331. Yan B, Peng Z, Xing X, Du C. Glibenclamide induces apoptosis by activating reactive oxygen species dependent JNK pathway in hepatocellular carcinoma cells. Biosci Rep. 2017;37(5). doi: 10.1042/bsr20170685.
332. Vazquez-Sanchez AY, Hinojosa LM, Parraguirre-Martinez S, Gonzalez A, Morales F, Montalvo G, Vera E, Hernandez-Gallegos E, Camacho J. Expression of KATP channels in human cervical cancer: Potential tools for diagnosis and therapy. Oncol Lett. 2018;15(5):6302-8. doi: 10.3892/ol.2018.8165.
333. Huang L, Li B, Li W, Guo H, Zou F. ATP-sensitive potassium channels control glioma cells proliferation by regulating ERK activity. Carcinogenesis. 2009;30(5):737-44. doi: 10.1093/carcin/bgp034.
334. Xu K, Sun G, Li M, Chen H, Zhang Z, Qian X, Li P, Xu L, Huang W, Wang X. Glibenclamide Targets Sulfonylurea Receptor 1 to Inhibit p70S6K Activity and Upregulate KLF4 Expression to Suppress Non-Small Cell Lung Carcinoma. Mol Cancer Ther. 2019;18(11):2085-96. doi: 10.1158/1535-7163.MCT-18-1181.
335. Chen H, Zhao L, Meng Y, Qian X, Fan Y, Zhang Q, Wang C, Lin F, Chen B, Xu L, Huang W, Chen J, Wang X. Sulfonylurea receptor 1-expressing cancer cells induce cancer-associated fibroblasts to promote non-small cell lung cancer progression. Cancer Lett. 2022;536:215611. doi: 10.1016/j.canlet.2022.215611.
336. Livak KJ, Schmittgen TD. Analysis of relative gene expression data using real-time quantitative PCR and the 2(-Delta Delta C(T)) Method. Methods. 2001;25(4):402-8. doi: 10.1006/meth.2001.1262.
337. Schneider CA, Rasband WS, Eliceiri KW. NIH Image to ImageJ: 25 years of image analysis. Nat Methods. 2012;9(7):671-5. doi: 10.1038/nmeth.2089.
338. Varghese F, Bukhari AB, Malhotra R, De A. IHC Profiler: an open source plugin for the quantitative evaluation and automated scoring of immunohistochemistry images of human tissue samples. PLoS One. 2014;9(5):e96801. doi: 10.1371/journal.pone.0096801.
339. Detre S, Saclani Jotti G, Dowsett M. A "quickscore" method for immunohistochemical semiquantitation: validation for oestrogen receptor in breast carcinomas. J Clin Pathol. 1995;48(9):876-8. doi: 10.1136/jcp.48.9.876.
340. Hoadley KA, Yau C, Hinoue T, Wolf DM, Lazar AJ, Drill E, Shen R, Taylor AM, Cherniack AD, Thorsson V, Akbani R, Bowlby R, Wong CK, Wiznerowicz M, Sanchez-Vega F, Robertson AG, Schneider BG, Lawrence MS, Noushmehr H, Malta TM, Cancer Genome Atlas N, Stuart JM, Benz CC, Laird PW. Cell-of-Origin Patterns Dominate the Molecular Classification of 10,000 Tumors from 33 Types of Cancer. Cell. 2018;173(2):291-304 e6. doi: 10.1016/j.cell.2018.03.022.
341. Barrett T, Wilhite SE, Ledoux P, Evangelista C, Kim IF, Tomashevsky M, Marshall KA, Phillippy KH, Sherman PM, Holko M, Yefanov A, Lee H, Zhang N, Robertson CL, Serova N, Davis S, Soboleva A. NCBI GEO: archive for functional

genomics data sets--update. Nucleic Acids Res. 2013;41(Database issue):D991-5. doi: 10.1093/nar/gks1193.
342. Pyeon D, Newton MA, Lambert PF, den Boon JA, Sengupta S, Marsit CJ, Woodworth CD, Connor JP, Haugen TH, Smith EM, Kelsey KT, Turek LP, Ahlquist P. Fundamental differences in cell cycle deregulation in human papillomavirus-positive and human papillomavirus-negative head/neck and cervical cancers. Cancer Res. 2007;67(10):4605-19. doi: 10.1158/0008-5472.CAN-06-3619.
343. Gonzalez SL, Stremlau M, He X, Basile JR, Munger K. Degradation of the retinoblastoma tumor suppressor by the human papillomavirus type 16 E7 oncoprotein is important for functional inactivation and is separable from proteasomal degradation of E7. J Virol. 2001;75(16):7583-91. doi: 10.1128/JVI.75.16.7583-7591.2001.
344. Huibregtse JM, Scheffner M, Howley PM. A cellular protein mediates association of p53 with the E6 oncoprotein of human papillomavirus types 16 or 18. EMBO J. 1991;10(13):4129-35. doi.
345. Leechanachai P, Banks L, Moreau F, Matlashewski G. The E5 gene from human papillomavirus type 16 is an oncogene which enhances growth factor-mediated signal transduction to the nucleus. Oncogene. 1992;7(1):19-25. doi.
346. Pim D, Collins M, Banks L. Human papillomavirus type 16 E5 gene stimulates the transforming activity of the epidermal growth factor receptor. Oncogene. 1992;7(1):27-32. doi.
347. Straight SW, Hinkle PM, Jewers RJ, McCance DJ. The E5 oncoprotein of human papillomavirus type 16 transforms fibroblasts and effects the downregulation of the epidermal growth factor receptor in keratinocytes. J Virol. 1993;67(8):4521-32. doi.
348. Rose PG, Bundy BN, Watkins EB, Thigpen JT, Deppe G, Maiman MA, Clarke-Pearson DL, Insalaco S. Concurrent cisplatin-based radiotherapy and chemotherapy for locally advanced cervical cancer. N Engl J Med. 1999;340(15):1144-53. doi: 10.1056/NEJM199904153401502.
349. Ryu SY, Lee WM, Kim K, Park SI, Kim BJ, Kim MH, Choi SC, Cho CK, Nam BH, Lee ED. Randomized clinical trial of weekly vs. triweekly cisplatin-based chemotherapy concurrent with radiotherapy in the treatment of locally advanced cervical cancer. Int J Radiat Oncol Biol Phys. 2011;81(4):e577-81. doi: 10.1016/j.ijrobp.2011.05.002.
350. Zhu H, Luo H, Zhang W, Shen Z, Hu X, Zhu X. Molecular mechanisms of cisplatin resistance in cervical cancer. Drug Des Devel Ther. 2016;10:1885-95. doi: 10.2147/DDDT.S106412.
351. Moore DH, Blessing JA, McQuellon RP, Thaler HT, Cella D, Benda J, Miller DS, Olt G, King S, Boggess JF, Rocereto TF. Phase III study of cisplatin with or without paclitaxel in stage IVB, recurrent, or persistent squamous cell carcinoma of the cervix: a gynecologic oncology group study. J Clin Oncol. 2004;22(15):3113-9. doi: 10.1200/JCO.2004.04.170.
352. Scarth JA, Wasson CW, Patterson MR, Evans D, Barba-Moreno D, Carden H, Whitehouse A, Mankouri J, Samson A, Morgan EL, Macdonald A. Exploitation of ATP-sensitive potassium ion (KATP) channels by HPV promotes cervical cancer cell proliferation by contributing to MAPK/AP-1 signalling. 2022:2022.09.22.508991. doi: 10.1101/2022.09.22.508991 %J bioRxiv.
353. Lenaeus MJ, Vamvouka M, Focia PJ, Gross A. Structural basis of TEA blockade in a model potassium channel. Nat Struct Mol Biol. 2005;12(5):454-9. doi: 10.1038/nsmb929.

354. Brauner T, Hulser DF, Strasser RJ. Comparative measurements of membrane potentials with microelectrodes and voltage-sensitive dyes. Biochim Biophys Acta. 1984;771(2):208-16. doi: 10.1016/0005-2736(84)90535-2.
355. Epps DE, Wolfe ML, Groppi V. Characterization of the steady-state and dynamic fluorescence properties of the potential-sensitive dye bis-(1,3-dibutylbarbituric acid)trimethine oxonol (Dibac4(3)) in model systems and cells. Chem Phys Lipids. 1994;69(2):137-50. doi.
356. Basukala O, Mittal S, Massimi P, Bestagno M, Banks L. The HPV-18 E7 CKII phospho acceptor site is required for maintaining the transformed phenotype of cervical tumour-derived cells. PLoS Pathog. 2019;15(5):e1007769. doi: 10.1371/journal.ppat.1007769

10.1371/journal.ppat.1007769. eCollection 2019 May.
357. Brehm A, Nielsen SJ, Miska EA, McCance DJ, Reid JL, Bannister AJ, Kouzarides T. The E7 oncoprotein associates with Mi2 and histone deacetylase activity to promote cell growth. EMBO J. 1999;18(9):2449-58. doi: 10.1093/emboj/18.9.2449.
358. Longworth MS, Laimins LA. The binding of histone deacetylases and the integrity of zinc finger-like motifs of the E7 protein are essential for the life cycle of human papillomavirus type 31. J Virol. 2004;78(7):3533-41. doi: 10.1128/jvi.78.7.3533-3541.2004.
359. Bodily JM, Mehta KP, Laimins LA. Human papillomavirus E7 enhances hypoxia-inducible factor 1-mediated transcription by inhibiting binding of histone deacetylases. Cancer Res. 2011;71(3):1187-95. doi: 10.1158/0008-5472.CAN-10-2626.
360. Grabe N. AliBaba2: context specific identification of transcription factor binding sites. In Silico Biol. 2002;2(1):S1-15. doi.
361. Beishline K, Azizkhan-Clifford J. Sp1 and the 'hallmarks of cancer'. FEBS J. 2015;282(2):224-58. doi: 10.1111/febs.13148.
362. Kadonaga JT, Jones KA, Tjian R. Promoter-specific activation of RNA polymerase II transcription by Sp1. Trends Biochem Sci. 1986;11(1):20-3. doi: doi.org/10.1016/0968-0004(86)90226-4.
363. Blume SW, Snyder RC, Ray R, Thomas S, Koller CA, Miller DM. Mithramycin inhibits SP1 binding and selectively inhibits transcriptional activity of the dihydrofolate reductase gene in vitro and in vivo. J Clin Invest. 1991;88(5):1613-21. doi: 10.1172/JCI115474.
364. Ishii S, Xu YH, Stratton RH, Roe BA, Merlino GT, Pastan I. Characterization and sequence of the promoter region of the human epidermal growth factor receptor gene. Proc Natl Acad Sci U S A. 1985;82(15):4920-4. doi: 10.1073/pnas.82.15.4920.
365. Kageyama R, Merlino GT, Pastan I. Epidermal growth factor (EGF) receptor gene transcription. Requirement for Sp1 and an EGF receptor-specific factor. J Biol Chem. 1988;263(13):6329-36. doi.
366. Nagata D, Suzuki E, Nishimatsu H, Satonaka H, Goto A, Omata M, Hirata Y. Transcriptional activation of the cyclin D1 gene is mediated by multiple cis-elements, including SP1 sites and a cAMP-responsive element in vascular endothelial cells. J Biol Chem. 2001;276(1):662-9. doi: 10.1074/jbc.M005522200.
367. Grinstein E, Jundt F, Weinert I, Wernet P, Royer HD. Sp1 as G1 cell cycle phase specific transcription factor in epithelial cells. Oncogene. 2002;21(10):1485-92. doi: 10.1038/sj.onc.1205211.

368. Hover S, Foster B, Barr JN, Mankouri J. Viral dependence on cellular ion channels - an emerging anti-viral target? J Gen Virol. 2017;98(3):345-51. doi: 10.1099/jgv.0.000712.
369. Lopez-Charcas O, Espinosa AM, Alfaro A, Herrera-Carrillo Z, Ramirez-Cordero BE, Cortes-Reynosa P, Perez Salazar E, Berumen J, Gomora JC. The invasiveness of human cervical cancer associated to the function of NaV1.6 channels is mediated by MMP-2 activity. Sci Rep. 2018;8(1):12995. doi: 10.1038/s41598-018-31364-y.
370. Dubey RC, Mishra N, Gaur R. G protein-coupled and ATP-sensitive inwardly rectifying potassium ion channels are essential for HIV entry. Sci Rep. 2019;9(1):4113. doi: 10.1038/s41598-019-40968-x.
371. Eleftherianos I, Won S, Chtarbanova S, Squiban B, Ocorr K, Bodmer R, Beutler B, Hoffmann JA, Imler JL. ATP-sensitive potassium channel (K(ATP))-dependent regulation of cardiotropic viral infections. Proc Natl Acad Sci U S A. 2011;108(29):12024-9. doi: 10.1073/pnas.1108926108.
372. Bauknecht T, Angel P, Royer HD, zur Hausen H. Identification of a negative regulatory domain in the human papillomavirus type 18 promoter: interaction with the transcriptional repressor YY1. EMBO J. 1992;11(12):4607-17. doi: 10.1002/j.1460-2075.1992.tb05563.x.
373. Gloss B, Bernard HU. The E6/E7 promoter of human papillomavirus type 16 is activated in the absence of E2 proteins by a sequence-aberrant Sp1 distal element. J Virol. 1990;64(11):5577-84. doi: 10.1128/JVI.64.11.5577-5584.1990.
374. Hoppe-Seyler F, Butz K. Activation of human papillomavirus type 18 E6-E7 oncogene expression by transcription factor Sp1. Nucleic Acids Res. 1992;20(24):6701-6. doi: 10.1093/nar/20.24.6701.
375. Hoppe-Seyler F, Butz K, zur Hausen H. Repression of the human papillomavirus type 18 enhancer by the cellular transcription factor Oct-1. J Virol. 1991;65(10):5613-8. doi: 10.1128/JVI.65.10.5613-5618.1991.
376. Butz K, Hoppe-Seyler F. Transcriptional control of human papillomavirus (HPV) oncogene expression: composition of the HPV type 18 upstream regulatory region. J Virol. 1993;67(11):6476-86. doi.
377. Burley M, Roberts S, Parish JL. Epigenetic regulation of human papillomavirus transcription in the productive virus life cycle. Semin Immunopathol. 2020;42(2):159-71. doi: 10.1007/s00281-019-00773-0.
378. Chen M, Dong Y, Simard JM. Functional coupling between sulfonylurea receptor type 1 and a nonselective cation channel in reactive astrocytes from adult rat brain. J Neurosci. 2003;23(24):8568-77. doi.
379. Simard JM, Chen M, Tarasov KV, Bhatta S, Ivanova S, Melnitchenko L, Tsymbalyuk N, West GA, Gerzanich V. Newly expressed SUR1-regulated NC(Ca-ATP) channel mediates cerebral edema after ischemic stroke. Nat Med. 2006;12(4):433-40. doi: 10.1038/nm1390.
380. Dong W, Li B, Wang J, Song Y, Zhang Z, Fu C. MicroRNA-337 inhibits cell proliferation and invasion of cervical cancer through directly targeting specificity protein 1. Tumour Biol. 2017;39(6):1010428317711323. doi: 10.1177/1010428317711323.
381. Wang YT, Chuang JY, Shen MR, Yang WB, Chang WC, Hung JJ. Sumoylation of specificity protein 1 augments its degradation by changing the localization and increasing the specificity protein 1 proteolytic process. J Mol Biol. 2008;380(5):869-85. doi: 10.1016/j.jmb.2008.05.043.
382. Wang T, Zhang W, Huang W, Hua Z, Li S. LncRNA MALAT1 was regulated by HPV16 E7 independently of pRB in cervical cancer cells. J Cancer. 2021;12(21):6344-55. doi: 10.7150/jca.61194.

383. Chuang JY, Wang YT, Yeh SH, Liu YW, Chang WC, Hung JJ. Phosphorylation by c-Jun NH2-terminal kinase 1 regulates the stability of transcription factor Sp1 during mitosis. Mol Biol Cell. 2008;19(3):1139-51. doi: 10.1091/mbc.E07-09-0881.
384. Milanini-Mongiat J, Pouyssegur J, Pages G. Identification of two Sp1 phosphorylation sites for p42/p44 mitogen-activated protein kinases: their implication in vascular endothelial growth factor gene transcription. J Biol Chem. 2002;277(23):20631-9. doi: 10.1074/jbc.M201753200.
385. Hsu MC, Chang HC, Hung WC. HER-2/neu represses the metastasis suppressor RECK via ERK and Sp transcription factors to promote cell invasion. J Biol Chem. 2006;281(8):4718-25. doi: 10.1074/jbc.M510937200.
386. Bray F, Ferlay J, Soerjomataram I, Siegel RL, Torre LA, Jemal A. Global cancer statistics 2018: GLOBOCAN estimates of incidence and mortality worldwide for 36 cancers in 185 countries. CA Cancer J Clin. 2018;68(6):394-424. doi: 10.3322/caac.21492.
387. Rosendo-Pineda MJ, Moreno CM, Vaca L. Role of ion channels during cell division. Cell Calcium. 2020;91:102258. doi: 10.1016/j.ceca.2020.102258.
388. Morrison DK. MAP kinase pathways. Cold Spring Harb Perspect Biol. 2012;4(11). doi: 10.1101/cshperspect.a011254.
389. Huang L, Li B, Tang S, Guo H, Li W, Huang X, Yan W, Zou F. Mitochondrial KATP Channels Control Glioma Radioresistance by Regulating ROS-Induced ERK Activation. Mol Neurobiol. 2015;52(1):626-37. doi: 10.1007/s12035-014-8888-1.
390. Samavati L, Monick MM, Sanlioglu S, Buettner GR, Oberley LW, Hunninghake GW. Mitochondrial K(ATP) channel openers activate the ERK kinase by an oxidant-dependent mechanism. Am J Physiol Cell Physiol. 2002;283(1):C273-81. doi: 10.1152/ajpcell.00514.2001.
391. Zieve GW, Turnbull D, Mullins JM, McIntosh JR. Production of large numbers of mitotic mammalian cells by use of the reversible microtubule inhibitor nocodazole. Nocodazole accumulated mitotic cells. Exp Cell Res. 1980;126(2):397-405. doi.
392. Vassilev LT, Tovar C, Chen S, Knezevic D, Zhao X, Sun H, Heimbrook DC, Chen L. Selective small-molecule inhibitor reveals critical mitotic functions of human CDK1. Proc Natl Acad Sci U S A. 2006;103(28):10660-5. doi: 10.1073/pnas.0600447103.
393. Pennycook BR, Barr AR. Restriction point regulation at the crossroads between quiescence and cell proliferation. FEBS Lett. 2020. doi: 10.1002/1873-3468.13867.
394. Pop C, Salvesen GS. Human caspases: activation, specificity, and regulation. J Biol Chem. 2009;284(33):21777-81. doi: 10.1074/jbc.R800084200.
395. Lazebnik YA, Kaufmann SH, Desnoyers S, Poirier GG, Earnshaw WC. Cleavage of poly(ADP-ribose) polymerase by a proteinase with properties like ICE. Nature. 1994;371(6495):346-7. doi: 10.1038/371346a0.
396. van Engeland M, Nieland LJ, Ramaekers FC, Schutte B, Reutelingsperger CP. Annexin V-affinity assay: a review on an apoptosis detection system based on phosphatidylserine exposure. Cytometry. 1998;31(1):1-9. doi: 10.1002/(sici)1097-0320(19980101)31:1<1::aid-cyto1>3.0.co;2-r.
397. Ribatti D, Tamma R, Annese T. Epithelial-Mesenchymal Transition in Cancer: A Historical Overview. Transl Oncol. 2020;13(6):100773. doi: 10.1016/j.tranon.2020.100773.

398. Qureshi R, Arora H, Rizvi MA. EMT in cervical cancer: its role in tumour progression and response to therapy. Cancer Lett. 2015;356(2 Pt B):321-31. doi: 10.1016/j.canlet.2014.09.021.
399. Zhang W, Liu HT. MAPK signal pathways in the regulation of cell proliferation in mammalian cells. Cell Res. 2002;12(1):9-18. doi: 10.1038/sj.cr.7290105.
400. Favata MF, Horiuchi KY, Manos EJ, Daulerio AJ, Stradley DA, Feeser WS, Van Dyk DE, Pitts WJ, Earl RA, Hobbs F, Copeland RA, Magolda RL, Scherle PA, Trzaskos JM. Identification of a novel inhibitor of mitogen-activated protein kinase kinase. J Biol Chem. 1998;273(29):18623-32. doi: 10.1074/jbc.273.29.18623.
401. Shaulian E, Karin M. AP-1 as a regulator of cell life and death. Nat Cell Biol. 2002;4(5):E131-6. doi: 10.1038/ncb0502-e131.
402. Macdonald A, Mazaleyrat S, McCormick C, Street A, Burgoyne NJ, Jackson RM, Cazeaux V, Shelton H, Saksela K, Harris M. Further studies on hepatitis C virus NS5A-SH3 domain interactions: identification of residues critical for binding and implications for viral RNA replication and modulation of cell signalling. J Gen Virol. 2005;86(Pt 4):1035-44. doi: 10.1099/vir.0.80734-0.
403. Chong T, Apt D, Gloss B, Isa M, Bernard HU. The enhancer of human papillomavirus type 16: binding sites for the ubiquitous transcription factors oct-1, NFA, TEF-2, NF1, and AP-1 participate in epithelial cell-specific transcription. J Virol. 1991;65(11):5933-43. doi: 10.1128/JVI.65.11.5933-5943.1991.
404. Chong T, Chan WK, Bernard HU. Transcriptional activation of human papillomavirus 16 by nuclear factor I, AP1, steroid receptors and a possibly novel transcription factor, PVF: a model for the composition of genital papillomavirus enhancers. Nucleic Acids Res. 1990;18(3):465-70. doi: 10.1093/nar/18.3.465.
405. Thierry F, Spyrou G, Yaniv M, Howley P. Two AP1 sites binding JunB are essential for human papillomavirus type 18 transcription in keratinocytes. J Virol. 1992;66(6):3740-8. doi.
406. Liu X, Li H, Rajurkar M, Li Q, Cotton JL, Ou J, Zhu LJ, Goel HL, Mercurio AM, Park JS, Davis RJ, Mao J. Tead and AP1 Coordinate Transcription and Motility. Cell Rep. 2016;14(5):1169-80. doi: 10.1016/j.celrep.2015.12.104.
407. Papavassiliou AG, Treier M, Bohmann D. Intramolecular signal transduction in c-Jun. EMBO J. 1995;14(9):2014-9. doi: 10.1002/j.1460-2075.1995.tb07193.x.
408. Treier M, Bohmann D, Mlodzik M. JUN cooperates with the ETS domain protein pointed to induce photoreceptor R7 fate in the Drosophila eye. Cell. 1995;83(5):753-60. doi: 10.1016/0092-8674(95)90188-4.
409. Musti AM, Treier M, Bohmann D. Reduced ubiquitin-dependent degradation of c-Jun after phosphorylation by MAP kinases. Science. 1997;275(5298):400-2. doi: 10.1126/science.275.5298.400.
410. Sundqvist A, Voytyuk O, Hamdi M, Popeijus HE, van der Burgt CB, Janssen J, Martens JWM, Moustakas A, Heldin CH, Ten Dijke P, van Dam H. JNK-Dependent cJun Phosphorylation Mitigates TGFbeta- and EGF-Induced Pre-Malignant Breast Cancer Cell Invasion by Suppressing AP-1-Mediated Transcriptional Responses. Cells. 2019;8(12). doi: 10.3390/cells8121481.
411. Binetruy B, Smeal T, Karin M. Ha-Ras augments c-Jun activity and stimulates phosphorylation of its activation domain. Nature. 1991;351(6322):122-7. doi: 10.1038/351122a0.
412. Smeal T, Binetruy B, Mercola DA, Birrer M, Karin M. Oncogenic and transcriptional cooperation with Ha-Ras requires phosphorylation of c-Jun on serines 63 and 73. Nature. 1991;354(6353):494-6. doi: 10.1038/354494a0.

413. Pulverer BJ, Kyriakis JM, Avruch J, Nikolakaki E, Woodgett JR. Phosphorylation of c-jun mediated by MAP kinases. Nature. 1991;353(6345):670-4. doi: 10.1038/353670a0.
414. Pulverer BJ, Hughes K, Franklin CC, Kraft AS, Leevers SJ, Woodgett JR. Co-purification of mitogen-activated protein kinases with phorbol ester-induced c-Jun kinase activity in U937 leukaemic cells. Oncogene. 1993;8(2):407-15. doi.
415. Bannister AJ, Oehler T, Wilhelm D, Angel P, Kouzarides T. Stimulation of c-Jun activity by CBP: c-Jun residues Ser63/73 are required for CBP induced stimulation in vivo and CBP binding in vitro. Oncogene. 1995;11(12):2509-14. doi.
416. Tsai LN, Ku TK, Salib NK, Crowe DL. Extracellular signals regulate rapid coactivator recruitment at AP-1 sites by altered phosphorylation of both CREB binding protein and c-jun. Mol Cell Biol. 2008;28(13):4240-50. doi: 10.1128/MCB.01489-07.
417. Antinore MJ, Birrer MJ, Patel D, Nader L, McCance DJ. The human papillomavirus type 16 E7 gene product interacts with and trans-activates the AP1 family of transcription factors. EMBO J. 1996;15(8):1950-60. doi.
418. Qiu S, Fraser SP, Pires W, Djamgoz MBA. Anti-invasive effects of minoxidil on human breast cancer cells: combination with ranolazine. Clin Exp Metastasis. 2022;39(4):679-89. doi: 10.1007/s10585-022-10166-7.
419. Pillozzi S, D'Amico M, Bartoli G, Gasparoli L, Petroni G, Crociani O, Marzo T, Guerriero A, Messori L, Severi M, Udisti R, Wulff H, Chandy KG, Becchetti A, Arcangeli A. The combined activation of KCa3.1 and inhibition of Kv11.1/hERG1 currents contribute to overcome Cisplatin resistance in colorectal cancer cells. Br J Cancer. 2018;118(2):200-12. doi: 10.1038/bjc.2017.392.
420. Subramaniyam N, Arumugam S, Ezthupurakkal PB, Ariraman S, Biswas I, Muthuvel SK, Balakrishnan A, Alshammari GM, Chinnasamy T. Unveiling anticancer potential of glibenclamide: Its synergistic cytotoxicity with doxorubicin on cancer cells. J Pharm Biomed Anal. 2018;154:294-301. doi: 10.1016/j.jpba.2018.03.025.
421. Crozier L, Foy R, Mouery BL, Whitaker RH, Corno A, Spanos C, Ly T, Gowen Cook J, Saurin AT. CDK4/6 inhibitors induce replication stress to cause long-term cell cycle withdrawal. EMBO J. 2022;41(6):e108599. doi: 10.15252/embj.2021108599.
422. Cripe TP, Alderborn A, Anderson RD, Parkkinen S, Bergman P, Haugen TH, Pettersson U, Turek LP. Transcriptional activation of the human papillomavirus-16 P97 promoter by an 88-nucleotide enhancer containing distinct cell-dependent and AP-1-responsive modules. New Biol. 1990;2(5):450-63. doi.
423. Kyo S, Klumpp DJ, Inoue M, Kanaya T, Laimins LA. Expression of AP1 during cellular differentiation determines human papillomavirus E6/E7 expression in stratified epithelial cells. J Gen Virol. 1997;78 (Pt 2):401-11. doi: 10.1099/0022-1317-78-2-401

10.1099/0022-1317-78-2-401.
424. Luna AJ, Sterk RT, Griego-Fisher AM, Chung JY, Berggren KL, Bondu V, Barraza-Flores P, Cowan AT, Gan GN, Yilmaz E, Cho H, Kim JH, Hewitt SM, Bauman JE, Ozbun MA. MEK/ERK signaling is a critical regulator of high-risk human papillomavirus oncogene expression revealing therapeutic targets for HPV-induced tumors. PLoS Pathog. 2021;17(1):e1009216. doi: 10.1371/journal.ppat.1009216.

425. Weiss C, Schneider S, Wagner EF, Zhang X, Seto E, Bohmann D. JNK phosphorylation relieves HDAC3-dependent suppression of the transcriptional activity of c-Jun. EMBO J. 2003;22(14):3686-95. doi: 10.1093/emboj/cdg364.
426. Aguilera C, Nakagawa K, Sancho R, Chakraborty A, Hendrich B, Behrens A. c-Jun N-terminal phosphorylation antagonises recruitment of the Mbd3/NuRD repressor complex. Nature. 2011;469(7329):231-5. doi: 10.1038/nature09607.
427. Ogawa S, Lozach J, Jepsen K, Sawka-Verhelle D, Perissi V, Sasik R, Rose DW, Johnson RS, Rosenfeld MG, Glass CK. A nuclear receptor corepressor transcriptional checkpoint controlling activator protein 1-dependent gene networks required for macrophage activation. Proc Natl Acad Sci U S A. 2004;101(40):14461-6. doi: 10.1073/pnas.0405786101.
428. Morton S, Davis RJ, McLaren A, Cohen P. A reinvestigation of the multisite phosphorylation of the transcription factor c-Jun. EMBO J. 2003;22(15):3876-86. doi: 10.1093/emboj/cdg388.
429. Arthur JS. MSK activation and physiological roles. Front Biosci. 2008;13:5866-79. doi: 10.2741/3122.
430. Liu F, Yang X, Geng M, Huang M. Targeting ERK, an Achilles' Heel of the MAPK pathway, in cancer therapy. Acta Pharm Sin B. 2018;8(4):552-62. doi: 10.1016/j.apsb.2018.01.008.
431. Yoon S, Seger R. The extracellular signal-regulated kinase: multiple substrates regulate diverse cellular functions. Growth Factors. 2006;24(1):21-44. doi: 10.1080/02699050500284218.
432. Johnson DE, Burtness B, Leemans CR, Lui VWY, Bauman JE, Grandis JR. Head and neck squamous cell carcinoma. Nat Rev Dis Primers. 2020;6(1):92. doi: 10.1038/s41572-020-00224-3.
433. Ferlay J, Ervik M, Lam F, Colombet M, Mery L, Piñeros M, Znaor A, Soerjomataram I, Bray F. Global Cancer Observatory: Cancer Today. Lyon, France: International Agency for Research on Cancer. 2020 [Available from: https://gco.iarc.fr/today.
434. Blot WJ, McLaughlin JK, Winn DM, Austin DF, Greenberg RS, Preston-Martin S, Bernstein L, Schoenberg JB, Stemhagen A, Fraumeni JF, Jr. Smoking and drinking in relation to oral and pharyngeal cancer. Cancer Res. 1988;48(11):3282-7. doi.
435. Hennessey PT, Westra WH, Califano JA. Human papillomavirus and head and neck squamous cell carcinoma: recent evidence and clinical implications. J Dent Res. 2009;88(4):300-6. doi: 10.1177/0022034509333371.
436. Stein AP, Saha S, Kraninger JL, Swick AD, Yu M, Lambert PF, Kimple RJ. Prevalence of Human Papillomavirus in Oropharyngeal Cancer: A Systematic Review. Cancer J. 2015;21(3):138-46. doi: 10.1097/PPO.0000000000000115.
437. Del-Rio-Ibisate N, Granda-Diaz R, Rodrigo JP, Menendez ST, Garcia-Pedrero JM. Ion Channel Dysregulation in Head and Neck Cancers: Perspectives for Clinical Application. Rev Physiol Biochem Pharmacol. 2021;181:375-427. doi: 10.1007/112_2020_38.
438. Menendez ST, Rodrigo JP, Allonca E, Garcia-Carracedo D, Alvarez-Alija G, Casado-Zapico S, Fresno MF, Rodriguez C, Suarez C, Garcia-Pedrero JM. Expression and clinical significance of the Kv3.4 potassium channel subunit in the development and progression of head and neck squamous cell carcinomas. J Pathol. 2010;221(4):402-10. doi: 10.1002/path.2722.
439. Menendez ST, Villaronga MA, Rodrigo JP, Alvarez-Teijeiro S, Garcia-Carracedo D, Urdinguio RG, Fraga MF, Pardo LA, Viloria CG, Suarez C, Garcia-Pedrero JM. Frequent aberrant expression of the human ether a go-go (hEAG1) potassium channel in head and neck cancer: pathobiological mechanisms and

clinical implications. J Mol Med (Berl). 2012;90(10):1173-84. doi: 10.1007/s00109-012-0893-0.
440. Fernandez-Valle A, Rodrigo JP, Rodriguez-Santamarta T, Villaronga MA, Alvarez-Teijeiro S, Garcia-Pedrero JM, Suarez-Fernandez L, Lequerica-Fernandez P, de Vicente JC. HERG1 potassium channel expression in potentially malignant disorders of the oral mucosa and prognostic relevance in oral squamous cell carcinoma. Head Neck. 2016;38(11):1672-8. doi: 10.1002/hed.24493.
441. Dixit R, Kemp C, Kulich S, Seethala R, Chiosea S, Ling S, Ha PK, Duvvuri U. TMEM16A/ANO1 is differentially expressed in HPV-negative versus HPV-positive head and neck squamous cell carcinoma through promoter methylation. Sci Rep. 2015;5:16657. doi: 10.1038/srep16657.
442. Caputo A, Caci E, Ferrera L, Pedemonte N, Barsanti C, Sondo E, Pfeffer U, Ravazzolo R, Zegarra-Moran O, Galietta LJ. TMEM16A, a membrane protein associated with calcium-dependent chloride channel activity. Science. 2008;322(5901):590-4. doi: 10.1126/science.1163518.
443. Duvvuri U, Shiwarski DJ, Xiao D, Bertrand C, Huang X, Edinger RS, Rock JR, Harfe BD, Henson BJ, Kunzelmann K, Schreiber R, Seethala RS, Egloff AM, Chen X, Lui VW, Grandis JR, Gollin SM. TMEM16A induces MAPK and contributes directly to tumorigenesis and cancer progression. Cancer Res. 2012;72(13):3270-81. doi: 10.1158/0008-5472.CAN-12-0475-T.
444. Bristol ML, James CD, Wang X, Fontan CT, Morgan IM. Estrogen Attenuates the Growth of Human Papillomavirus-Positive Epithelial Cells. mSphere. 2020;5(2). doi: 10.1128/mSphere.00049-20.
445. Lin CJ, Grandis JR, Carey TE, Gollin SM, Whiteside TL, Koch WM, Ferris RL, Lai SY. Head and neck squamous cell carcinoma cell lines: established models and rationale for selection. Head Neck. 2007;29(2):163-88. doi: 10.1002/hed.20478.
446. Huang X, Gollin SM, Raja S, Godfrey TE. High-resolution mapping of the 11q13 amplicon and identification of a gene, TAOS1, that is amplified and overexpressed in oral cancer cells. Proc Natl Acad Sci U S A. 2002;99(17):11369-74. doi: 10.1073/pnas.172285799.
447. Britschgi A, Bill A, Brinkhaus H, Rothwell C, Clay I, Duss S, Rebhan M, Raman P, Guy CT, Wetzel K, George E, Popa MO, Lilley S, Choudhury H, Gosling M, Wang L, Fitzgerald S, Borawski J, Baffoe J, Labow M, Gaither LA, Bentires-Alj M. Calcium-activated chloride channel ANO1 promotes breast cancer progression by activating EGFR and CAMK signaling. Proc Natl Acad Sci U S A. 2013;110(11):E1026-34. doi: 10.1073/pnas.1217072110.
448. Bill A, Gutierrez A, Kulkarni S, Kemp C, Bonenfant D, Voshol H, Duvvuri U, Gaither LA. ANO1/TMEM16A interacts with EGFR and correlates with sensitivity to EGFR-targeting therapy in head and neck cancer. Oncotarget. 2015;6(11):9173-88. doi: 10.18632/oncotarget.3277.
449. Kulkarni S, Bill A, Godse NR, Khan NI, Kass JI, Steehler K, Kemp C, Davis K, Bertrand CA, Vyas AR, Holt DE, Grandis JR, Gaither LA, Duvvuri U. TMEM16A/ANO1 suppression improves response to antibody-mediated targeted therapy of EGFR and HER2/ERBB2. Genes Chromosomes Cancer. 2017;56(6):460-71. doi: 10.1002/gcc.22450.
450. Tang AL, Hauff SJ, Owen JH, Graham MP, Czerwinski MJ, Park JJ, Walline H, Papagerakis S, Stoerker J, McHugh JB, Chepeha DB, Bradford CR, Carey TE, Prince ME. UM-SCC-104: a new human papillomavirus-16-positive cancer stem cell-containing head and neck squamous cell carcinoma cell line. Head Neck. 2012;34(10):1480-91. doi: 10.1002/hed.21962.

451. Brenner JC, Graham MP, Kumar B, Saunders LM, Kupfer R, Lyons RH, Bradford CR, Carey TE. Genotyping of 73 UM-SCC head and neck squamous cell carcinoma cell lines. Head Neck. 2010;32(4):417-26. doi: 10.1002/hed.21198.
452. Sheppard DN, Welsh MJ. Effect of ATP-sensitive K+ channel regulators on cystic fibrosis transmembrane conductance regulator chloride currents. J Gen Physiol. 1992;100(4):573-91. doi: 10.1085/jgp.100.4.573.
453. Sheppard DN, Robinson KA. Mechanism of glibenclamide inhibition of cystic fibrosis transmembrane conductance regulator Cl- channels expressed in a murine cell line. J Physiol. 1997;503 (Pt 2):333-46. doi: 10.1111/j.1469-7793.1997.333bh.x.
454. Caci E, Caputo A, Hinzpeter A, Arous N, Fanen P, Sonawane N, Verkman AS, Ravazzolo R, Zegarra-Moran O, Galietta LJ. Evidence for direct CFTR inhibition by CFTR(inh)-172 based on Arg347 mutagenesis. Biochem J. 2008;413(1):135-42. doi: 10.1042/BJ20080029.
455. Ma T, Thiagarajah JR, Yang H, Sonawane ND, Folli C, Galietta LJ, Verkman AS. Thiazolidinone CFTR inhibitor identified by high-throughput screening blocks cholera toxin-induced intestinal fluid secretion. J Clin Invest. 2002;110(11):1651-8. doi: 10.1172/JCI16112.
456. Jin Y, Qin X. Integrated analysis of DNA methylation and mRNA expression profiles to identify key genes in head and neck squamous cell carcinoma. Biosci Rep. 2020;40(1). doi: 10.1042/BSR20193349.
457. Shin Y, Kim M, Won J, Kim J, Oh SB, Lee JH, Park K. Epigenetic Modification of CFTR in Head and Neck Cancer. J Clin Med. 2020;9(3). doi: 10.3390/jcm9030734.
458. Ramu Y, Xu Y, Lu Z. A novel high-affinity inhibitor against the human ATP-sensitive Kir6.2 channel. J Gen Physiol. 2018;150(7):969-76. doi: 10.1085/jgp.201812017.
459. Ramu Y, Lu Z. A family of orthologous proteins from centipede venoms inhibit the hKir6.2 channel. Sci Rep. 2019;9(1):14088. doi: 10.1038/s41598-019-50688-x.
460. Sies H, Jones DP. Reactive oxygen species (ROS) as pleiotropic physiological signalling agents. Nat Rev Mol Cell Biol. 2020;21(7):363-83. doi: 10.1038/s41580-020-0230-3.
461. Liou GY, Storz P. Reactive oxygen species in cancer. Free Radic Res. 2010;44(5):479-96. doi: 10.3109/10715761003667554.
462. Ogrunc M, Di Micco R, Liontos M, Bombardelli L, Mione M, Fumagalli M, Gorgoulis VG, d'Adda di Fagagna F. Oncogene-induced reactive oxygen species fuel hyperproliferation and DNA damage response activation. Cell Death Differ. 2014;21(6):998-1012. doi: 10.1038/cdd.2014.16.
463. Perillo B, Di Donato M, Pezone A, Di Zazzo E, Giovannelli P, Galasso G, Castoria G, Migliaccio A. ROS in cancer therapy: the bright side of the moon. Exp Mol Med. 2020;52(2):192-203. doi: 10.1038/s12276-020-0384-2.
464. Lander HM, Hajjar DP, Hempstead BL, Mirza UA, Chait BT, Campbell S, Quilliam LA. A molecular redox switch on p21(ras). Structural basis for the nitric oxide-p21(ras) interaction. J Biol Chem. 1997;272(7):4323-6. doi: 10.1074/jbc.272.7.4323.
465. Chan DW, Liu VW, Tsao GS, Yao KM, Furukawa T, Chan KK, Ngan HY. Loss of MKP3 mediated by oxidative stress enhances tumorigenicity and chemoresistance of ovarian cancer cells. Carcinogenesis. 2008;29(9):1742-50. doi: 10.1093/carcin/bgn167.

466. Guerra GR, Kong JC, Millen RM, Read M, Liu DS, Roth S, Sampurno S, Sia J, Bernardi MP, Chittleborough TJ, Behrenbruch CC, Teh J, Xu H, Haynes NM, Yu J, Lupat R, Hawkes D, Di Costanzo N, Tothill RW, Mitchell C, Ngan SY, Heriot AG, Ramsay RG, Phillips WA. Molecular and genomic characterisation of a panel of human anal cancer cell lines. Cell Death Dis. 2021;12(11):959. doi: 10.1038/s41419-021-04141-5.
467. Medeiros-Fonseca B, Cubilla A, Brito H, Martins T, Medeiros R, Oliveira P, Gil da Costa RM. Experimental Models for Studying HPV-Positive and HPV-Negative Penile Cancer: New Tools for An Old Disease. Cancers (Basel). 2021;13(3). doi: 10.3390/cancers13030460.
468. Zhou QH, Deng CZ, Li ZS, Chen JP, Yao K, Huang KB, Liu TY, Liu ZW, Qin ZK, Zhou FJ, Huang W, Han H, Liu RY. Molecular characterization and integrative genomic analysis of a panel of newly established penile cancer cell lines. Cell Death Dis. 2018;9(6):684. doi: 10.1038/s41419-018-0736-1.
469. Chen J, Yao K, Li Z, Deng C, Wang L, Yu X, Liang P, Xie Q, Chen P, Qin Z, Ye Y, Liu Z, Zhou F, Zhang Z, Han H. Establishment and characterization of a penile cancer cell line, penl1, with a deleterious TP53 mutation as a paradigm of HPV-negative penile carcinogenesis. Oncotarget. 2016;7(32):51687-98. doi: 10.18632/oncotarget.10098.
470. Rantanen V, Grenman S, Kurvinen K, Hietanen S, Raitanen M, Syrjanen S. p53 mutations and presence of HPV DNA do not correlate with radiosensitivity of gynecological cancer cell lines. Gynecol Oncol. 1998;71(3):352-8. doi: 10.1006/gyno.1998.5194.

Appendix

Table A.1 Plasmids used in this study.

Plasmid name	Backbone	Expression type	Resistance	Source
pcDNA3.1(+)	pcDNA3.1(+)	Transient	Ampicillin	Gift from Dr Martin Stacey (University of Leeds)
pcDNA3.1(+)-SUR1-HA	pcDNA3.1(+)	Transient	Ampicillin	Gift from Dr Jamel Mankouri (University of Leeds)
pcDNA3.1(+)-Kir6.2-HA	pcDNA3.1(+)	Transient	Ampicillin	Gift from Dr Jamel Mankouri (University of Leeds)
pcDNA3.1(+)-ΔJunD	pcDNA3.1(+)	Transient	Ampicillin	Gift from Prof Simon Arthur (University of Dundee)
pcDNA3.1(+)-FLAG-18E7	pcDNA3.1(+)	Transient	Ampicillin	Cloned from pcDNA3.1(+)-N-eGFP-18E7
pcDNA3.1(+)-N-eGFP	pcDNA3.1(+)-N-eGFP	Transient	Ampicillin	Genscript
pcDNA3.1(+)-N-eGFP-18E6	pcDNA3.1(+)-N-eGFP	Transient	Ampicillin	
pcDNA3.1(+)-N-eGFP-18E7	pcDNA3.1(+)-N-eGFP	Transient	Ampicillin	
pcDNA3.1(+)-N-eGFP-18E7 Δ24-27	pcDNA3.1(+)-N-eGFP	Transient	Ampicillin	Mutagenesis performed herein
pcDNA3.1(+)-N-eGFP-18E7 C27S	pcDNA3.1(+)-N-eGFP	Transient	Ampicillin	
pcDNA3.1(+)-N-eGFP-18E7 SS32/34AA	pcDNA3.1(+)-N-eGFP	Transient	Ampicillin	

Plasmid name	Backbone	Expression type	Resistance	Source
pcDNA3.1(+)-N-eGFP-18E7 L74R	pcDNA3.1(+)-N-eGFP	Transient	Ampicillin	
pcDNA3.1(+)-N-eGFP-18E7 C98S	pcDNA3.1(+)-N-eGFP	Transient	Ampicillin	
pCRV1-NLGP	pCRV1	2nd gen lentiviral	Ampicillin	Gift from Dr Sam Wilson (University of Glasgow)
pCMV-VSV-G	pCMV	2nd gen lentiviral	Ampicillin	Addgene #8454
pZIP-hEF1α-zsGreen-Puro-shNTC	pZIP-hEF1α-zsGreen-Puro	2nd gen lentiviral	Ampicillin	TransOMIC Technologies
pZIP-hEF1α-zsGreen-Puro-shSUR1 A	pZIP-hEF1α-zsGreen-Puro	2nd gen lentiviral	Ampicillin	
pZIP-hEF1α-zsGreen-Puro-shSUR1 B	pZIP-hEF1α-zsGreen-Puro	2nd gen lentiviral	Ampicillin	
pZIP-hEF1α-zsGreen-Puro-shSUR1 C	pZIP-hEF1α-zsGreen-Puro	2nd gen lentiviral	Ampicillin	
p18URRL	pBL	Transient	Ampicillin	Gift from Prof Felix Hoppe-Seyler (German Cancer Research Center)
pHPV16-LCR-luc	pGL3-Basic	Transient	Ampicillin	Gift from Dr Iain Morgan (Virginia Commonwealth University)
pAP1-luc	pGL3-Basic	Transient	Ampicillin	Cloned by Prof Andrew Macdonald

Plasmid name	Backbone	Expression type	Resistance	Source
				(University of Leeds)
pSUR1-luc WT	pGL3-Basic	Transient	Ampicillin	Gift from Prof J Marc Simard (University of Maryland)
pSUR1-luc ΔSP1 1	pGL3-Basic	Transient	Ampicillin	Mutagenesis performed herein
pSUR1-luc ΔSP1 2	pGL3-Basic	Transient	Ampicillin	
pSUR1-luc ΔSP1 3	pGL3-Basic	Transient	Ampicillin	
pSUR1-luc ΔSP1 4	pGL3-Basic	Transient	Ampicillin	
pRL-TK	pRL-TK	Transient	Ampicillin	Promega
pBSSK(-)-CMV-cJun S63/73D	pBSSK(-)-CMV	Transient	Ampicillin	Gift from Dr Hans van Dam (Leiden University Medical Centre)

Table A.2 Primers used in this study for site-directed mutagenesis.

Mutation	Forward primer (5'-3')	Reverse primer (5'-3')
18E7 Δ24-27	CACGAGCAGCTGTCTGAT	CACAGGGATCTCGTTCTG
18E7 C27S	GGACCTGCTGAGCCACGAGC AGC	ACAGGGATCTCGTTCTGGG GC
18E7 SS32/34 AA	TGCCGAGGAGGAGAACGACG AGATC	TCGGCCAGCTGCTCGTGGC ACAG
18E7 L74R	CCGCATCGAGCGGGTGGTGG AGA	GCCTCACACTTACAGCACA TGC
18E7 C98S	GTCCTTCGTGAGCCCCTGGT GTG	AGTGTATTCAGAAACAGCT GCTGG
SUR1-luc ΔSP11	GGTGAGGGAGGGGGAGGC	TGCTCCACCACCTGCGGG
SUR1-luc ΔSP12	GGCCCGGGGGGCGGGGGC	AGCCCCGCTGGCCTCCCC CTCC
SUR1-luc ΔSP13	GGGCCTGACGGCCGGGCC	CCCGGGCCCCGCCCAGCC
SUR1-luc ΔSP14	CGGAGCTGCAAGGGACAGAG GCTCG	GGCCCGGCCGTCAGGCCC

Table A.3 Mammalian cell lines used in this study.

Cells	Description	Source	Culture Media
C33A	Epithelial; derived from cervical carcinoma biopsy; HPV-	ATCC	DMEM + 10% FBS + 50 U/mL pen/strep
HeLa	Epithelial; derived from cervical adenocarcinoma; contains integrated HPV18 genome (10-50 copies/cell)	ATCC	
SiHa	Epithelial; established from primary cervical squamous cell carcinoma tissue sample; contains integrated HPV16 genome (1-2 copies/cell)	ATCC	
HEK293TT	Embryonic kidney cells; derived from HEK293 cells; expresses the SV40 small T and large T antigens	Gift from Dr Matthew Reeves (University College London)	
HN8	Derived from the lymph node metastasis of an oral cavity tumour; male patient; HPV-	Gift from Dr Iain Morgan (Virginia Commonwealth University)	
HN30	Obtained from the primary pharyngeal tumour of a male patient; HPV-		
SCC-61	Derived from a tongue squamous cell carcinoma of a male patient; HPV-		
UM-SCC-47	Isolated from a lateral tongue tumour; male patient; contains 18 copies of integrated HPV16	Sigma-Aldrich	
UM-SCC-104	Derived from a male patient with a recurrent oral cavity tumour; HPV16+	Gift from Dr Iain Morgan (Virginia	EMEM + 20% FBS + NEAA + 50 U/mL pen/strep

UPCI:SCC-152	Established from a male patient with a recurrent squamous cell carcinoma of the hypopharynx; contains integrated HPV16 genomes	Commonwealth University)	EMEM + 20% FBS + NEAA + 50 U/mL pen/strep
C33A HPV18 E6/E7 stable expression	As described, with stable overexpression of either HA-HPV18 E6 or HA-HPV18 E7	Viral transductions performed by Ms Molly Patterson	DMEM + 10% FBS + 50 U/mL pen/strep
HeLa shSP1 stable knockdown	As described, but stably expressing either non-targetting (shNEG) or SP1-specific shRNA (shSP1)		
HN8 HPV16 E6/E7 stable expression	As described, with stable overexpression of either HA-HPV16 E6 or HA-HPV16 E7	Viral transductions performed by Dr Yigen Li	
HN30 HPV16 E6/E7 stable expression	As described, with stable overexpression of either HA-HPV16 E6 or HA-HPV16 E7		

Table A.4 Information on siRNAs used in this study.

Target	5’-3’ Sequence (where custom made)	Source
HPV16 *E6*	N/A	SCBT (sc-156008)
HPV16 *E7*	N/A	SCBT (sc-270423)
HPV18 *E6*	CUAACACUGGGUUAUACAA CTAACTAACACTGGGTTAT	Dharmacon
HPV18 *E7*	CUCGUCGGGCUGGUAAAUGUU UAUUUCAUCGUUUUCUUCCUU	Dharmacon
ABCC8 (SUR1)	N/A	Qiagen (FlexiTube GeneSolution GS6833)
ABCC9 (SUR2)	N/A	Qiagen (FlexiTube GeneSolution GS10060)
KCNJ11 (Kir6.2)	N/A	Qiagen (FlexiTube GeneSolution GS3767)

Table A.5 Sequence information for shRNAs used in this study.

shRNA	Sense strand (5’-3’)	Loop	Antisense/guide strand (5’-3’)
ABCC8 A	ACAAGACCATCAAG TTTGTCAA	TAGTGAAGCC ACAGATGTA	TTGACAAACTTGATG GTCTTGG
ABCC8 B	CAGGGAAGATCCAG ATCCAGAA		TTCTGGATCTGGATC TTCCCTT
ABCC8 C	CCCGATCTACCGTC AAAGCTCA		TGAGCTTTGACGGT AGATCGGA
NTC	AAGGCAGAAGTATG CAAAGCAT		ATGCTTTGCATACTT CTGCCTG

Table A.6 List of primary and secondary antibodies used in this study. mAb, monoclonal antibody; pAb, polyclonal antibody. WB, western blot; ChIP, chromatin immunoprecipitation; IHC, immunohistochemistry.

Target	Manufacturer	Antibody type	Dilution
Anti-mouse	Stratech (115-035-174-JIR)	Goat HRP-conjugated	1:5000 (WB)
Anti-rabbit	Stratech (211-032-171-JIR)	Mouse HRP-conjugated	1:5000 (WB)
Caspase-3	CST (9662)	Rabbir pAb	1:1000 (WB)
cJun	CST (9165)	Rabbit mAb	1:1000 (WB), 1:100 (ChIP)
Cleaved caspase-3 (D175)	CST (9664)	Rabbit mAb	1:1000 (WB)
Cyclin A	SCBT (sc-271682)	Mouse mAb	1:100 (WB)
Cyclin B1	CST (12231)	Rabbit mAb	1:1000 (WB)
Cyclin D1	abcam (ab134175)	Rabbit mAb	1:1000 (WB)
Cyclin E1	CST (20808)	Rabbit mAb	1:1000 (WB)
ERK1/2	CST (9102)	Rabbit pAb	1:1000 (WB)
FLAG	Sigma-Aldrich (F1804)	Mouse mAb	1:1000 (WB)
GAPDH	SCBT (sc-365062)	Mouse mAb	1:5000 (WB)
GFP	SCBT (sc-9996)	Mouse mAb	1:2000 (WB)
HA	CST (3724)	Rabbit mAb	1:1000 (WB)
HPV16 E6	GeneTex, Inc. (GTX132686)	Rabbit pAb	1:500 (WB)
HPV16 E7	SCBT (sc-6981)	Mouse mAb	1:250 (WB)
HPV18 E6	SCBT (sc-365089)	Mouse mAb	1:500 (WB)
HPV18 E7	Abcam (ab100953)	Mouse mAb	1:1000 (WB)
JunD	CST (5000)	Rabbit mAb	1:1000 (WB)
Ki-67	Agilent (M724029-2)	Mouse mAb	1:100 (IHC)
Kir6.2	SCBT (sc-390104)	Mouse mAb	1:250 (WB)
PARP	CST (9542)	Rabbit pAb	1:1000 (WB)
p-cJun (S73)	CST (3270)	Rabbit mAb	1:1000 (WB)
pERK1/2 (T202/Y204)	CST (9101)	Rabbit pAb	1:1000 (WB)

Slug	CST (9585)	Rabbit mAb	1:1000 (WB)
Snail	CST (3879)	Rabbit mAb	1:1000 (WB)
SP1	CST (9389)	Rabbit mAb	1:1000 (WB) 1:100 (ChIP)
SUR1	Invitrogen (PA5-50836)	Rabbit pAb	1:100 (IHC)
Vimentin	CST (5741)	Rabbit mAb	1:1000 (WB)

Table A.7 Primers used in this study for RT-qPCR.

Gene	Forward primer (5'-3')	Reverse primer (5'-3')
HPV16 *E6*	CTGCAATGTTTCAGGACCCAC	GTTGTTTGCAGCTCTGTGCAT
HPV16 *E7*	ATTAAATGACAGCTCAGAGGA	GCTTTGTACGCACAACCGAAGC
HPV18 *E6*	TGGCGCGCTTTGAGGA	TGTTCAGTTCCGTGCACAGATC
HPV18 *E7*	GACCTAAGGCAACATTGCA	GCTCGTGACATAGAAGGTC
ABCC8	GGTGACCGAATCCCACCATC	CAGGGCAATTAGCAGCTTGG
ABCC9A	CTGGCTTTCTTCAGAATGGT	AAATACCCTCAGAAAAGACTAAAAC
ABCC9B	TGTGATGAAGCGAGGAAATA	TGACACTTCCATTCCTGAGAGA
KCNJ8	CTGGCTGCTCTTCGCTATC	AGAATCAAAACCGTGATGGC
KCNJ11	CCAAGAAAGGCAACTGCAACG	ATGCTTGCTGAAGATGAGGGT
GFP	ACGTAAACGGCCACAAGTTC	AAGTCGTGCTGCTTCATGTG
CCNA2	TGGAAAGCAAACAGTAAACAGCC	GGGCATCTTCACGCTCTATTT
CCNB1	AAGAGCTTTAAACTTTGGTCTGGG	CTTTGTAAGTCCTTGATTTACCATG
CCND1	CCGCTGGCCATGAACTACCT	ACGAAGGTCTGCGCGTGTT
CCNE1	GCCAGCCTTGGGACAATAATG	CTTGCACGTTGAGTTTGGGT
EGFR	CTCAGCCACCCATATGTACCATC	GAATTCGATGATCAACTCACGGAAC
SP1	TGGCAGCAGTACCAATGGC	CCAGGTAGTCCTGTCAGAACTT
SNAI1	TCGGAAGCCTAACTACAGCGA	AGATGAGCATTGGCAGCGAG
SNAI2	TGTTGCAGTGAGGGCAAGAA	GACCCTGGTTGCTTCAAGGA
TWIST1	GGACAAGCTGAGCAAGATTCAGA	TCTGGAGGACCTGGTAGAGGAA

ZEB1	GCACCTGAAGAGGACCAGAG	TGCATCTGGTGTTCCATTTT
VIM	GTTTCCCCTAAACCGCTAGG	AGCGAGAGTGGCAGAGGA
CDH2	TGCGGTACAGTGTAACTGGG	GAAACCGGGCTATCTGCTCG
FN1	CCGAGGGACCTGGAAGTT	ACTTGCTCCCAGGCACAG
MMP2	CTGATAACCTGGATGCAGTCGT	CCAGCCAGTCCGATTTGA
MMP9	TTGACAGCGACAAGAAGTGG	GCCATTCACGTCGTCCTTAT
TJP1	CGGTCCTCTGAGCCTGTAAG	GGATCTACATGCGACGACAA
U6	CTCGCTTCGGCAGCACA	AACGCTTCACGAATTTGCGT

Table A.8 Primers used in this study for ChIP-qPCR.

Locus	Forward primer (5'-3')	Reverse primer (5'-3')
ABCC8 promoter	CAAGCGTAGCAGGGCCG	GGGCTCAGCTGGCTCCG
HPV18 URR enhancer	CTTTTGGGCACTGCTCCTAC	CAATTGTTGTAGCGCACCTG
HPV18 URR promoter	GCTAATTGCATACTTGGCTTG	CCAACCTATTTCGGTTGCAT